Regulation of B cell responses during *Salmonella* Typhimurium infection

by

Ruth Elizabeth Coughlan

A thesis submitted to the University of Birmingham for the degree of DOCTOR OF PHILOSOPHY

School of Immunity and Infection
College of Medical and Dental Sciences
The University of Birmingham
September 2011

UNIVERSITY OF
BIRMINGHAM

University of Birmingham Research Archive

e-theses repository

This unpublished thesis/dissertation is copyright of the author and/or third parties. The intellectual property rights of the author or third parties in respect of this work are as defined by The Copyright Designs and Patents Act 1988 or as modified by any successor legislation.

Any use made of information contained in this thesis/dissertation must be in accordance with that legislation and must be properly acknowledged. Further distribution or reproduction in any format is prohibited without the permission of the copyright holder.

ABSTRACT

Immunity to *Salmonella* infection requires an integrated immune response, encompassing Th1 cell-mediated and humoral immunity at discrete stages of infection. Primary infection of mice with attenuated *Salmonella* Typhimurium (STm) drives an atypical B cell response, characterised by a rapid expansion of extrafollicular (EF) plasma cells which precedes germinal centre (GC) formation. This thesis examines elements of the GC and EF antibody response, and their regulation.

We show that the signalling, adhesion receptor CD31, the cytokines IL4, IL13 and IL6, and the transcription factor T-bet, have selective roles in regulating facets of the B cell response to STm. Antibody responses are severely impaired in $CD31^{-/-}$ mice during primary infection, as is protective immunity after subunit immunisation. The Th2-associated cytokines IL4, IL13 and IL6 promote optimal GC formation during STm infection, however only total loss of IL6 leads to defective class-switched antibody production. We further identify a B cell-intrinsic role for T-bet in IgG2a class-switching during STm infection, whilst T cell-intrinsic T-bet is completely dispensable for this response. In addition, a selective role for T-bet in GC responses to Th2 antigens is shown. These data identify some similarities and differences between the regulation of B cell responses to Th1 and Th2 antigens.

ACKNOWLEDGEMENTS

I would like to thanks numerous people for their help and support over the past three years. First and foremost, I would like to extend my gratitude to my three supervisors, Chris Buckley, Adam Cunningham and Ewan Ross, who have not only provided invaluable advice throughout my PhD, but have also helped me through the (occasional) nervous breakdown! Additionally, I am very grateful for the technical support that Ewan has offered during my time in Birmingham.

Many others have provided technical assistance during my time here; Mahmood Khan can only be described as the king of histology, and Jen Marshall is always my first port of call when B cell assistance is required. Thanks for all your help and encouragement. Thanks to all other members of the Cunningham group who have advised me on my work, provided technical support and fuelled my love of curry! The entire third floor team have provided a relaxed and fun atmosphere to work in, and indeed, have fuelled my love of beer! The Buckley group, past and present, have helped to advise me over the years, thank you for your time. The team at the animal house have also been superb, in particular Ian, Shaz and Karen, who have been patient and always helpful. I must also thank the Medical School at The University of Birmingham for providing my funding.

Last, but by no means least, I thank my long suffering family, who have felt every inch of my pain over the past three years. Mum, Dad, Nan, Kel and Fish, Bro-G and Em, Da and of course, my wonderful boyfriend Mathew. Thank you for your patience. I can't wait to come home.

TABLE OF CONTENTS

LIST OF FIGURES

LIST OF TABLES

LIST OF ABBREVIATIONS

The abbreviations given below denote both the singular and plural forms of the given word

ACK – ammonium chloride potassium
ADCC – antibody-dependent cellular cytotoxicity
AID – activation induced cytidine deaminase
ANA – anti-nuclear antibodies
AP – alkaline phosphatase
APC – antigen presenting cell
B cell – bone marrow-derived cell
Bcl-6 – B cell lymphoma-6
BCR – B cell receptor
BLIMP-1 – B lymphocyte-induced maturation protein-1
B.hermsii – Borrelia hermsii
B. pertussis – Bordetella pertussis
BMSU – biomedical services unit
BSA – bovine serum albumin
Bt - biotinylated
CD40L – CD40 ligand
CFU – colony forming units
CGG – chicken-γ-globulin
CIA – collagen-induced arthritis
CLP – common lymphoid progenitor
CpG – cytosine-phosphate-guanine
CR2 – complement receptor 2
CSR – class switch recombination
C_T – cycle threshold
D# – day of infection
D – diversity
DAB – deaminobenzidine tetrahydrochloride
DC – dendritic cell
DNP-KLH – dinitrophenol-keyhole limpet hemocyanin
EAE – experimental autoimmune encephalomyelitis
EB12 – Epstein-Barr virus-induced gene 2
EC – endothelial cells
EYFP – embryonic yellow fluorescent protein
EF – extrafollicular
ELISA – Enzyme-Linked Immunosorbent Assay
ES – embryonic stem
ETP – early thymic progenitor
Fab – fragment antigen binding
FACS – fluorescence activated cell sorting
Fc – fragment constant
FCS – foetal calf serum

FDC – follicular dendritic cell
GALT – gut-associated lymphoid tissue
GC – germinal centre
Grays - Gy
H – heavy
HEV – high endothelial venule
HRP – horseradish peroxidase
HSC – haematopoietic stem cell
i.p – intraperitoneal
i.v – intravenous
ICOS – inducible costimulator
Ig – immunoglobulin
ILT – Ig-like transcript
ITAM – immunoreceptor tyrosine activation motifs
ITIM – immunoreceptor tyrosine inhibitory motifs
J – joining
JAK – Janus kinase
LAIR – leucocyte-associated Ig-like receptor
LCMV – lymphocytic choriomeningitis virus
L – light
L – litre
L. major – *Leishmania* Major
L.B – Luria Bertani
LN – lymph node
LPS – lipopolysaccharide
MAC – membrane attack complex
MFI – median fluorescence intensity
MHC – major histocompatibility complex
MLN – mesenteric lymph nodes
MZ – marginal zone
ND – none detected
NFAT – nuclear factor of activated T cells
NK – natural killer
NHS – normal horse serum
NMS – normal mouse serum
NOD – nucleotide binding and oligomerisation domain
NP – 4-hydroxy-3-nitrophenyl acetyl
O.D – optical density
ON – overnight
OMP – outer membrane protein
OVA – ovalbumin
p.i – post infection
PALS – periarteriolar lymphatic sheath
PAMP – pathogen associated molecular pattern
PBMC – peripheral blood mononuclear cells
PBS – phosphate buffered saline
PD1 – programmed cell death 1
PEC – peritoneal exudate cells

PECAM-1/CD31 – platelet endothelial cell adhesion molecule 1
PIR-B – paired Ig-like receptor binding protein
PNA – peanut agglutinin
PP – peyers patches
ppt – precipitated protein
Pre - precursor
Pro – progenitor
PRR – pattern recognition receptor
PTP – protein tyrosine phosphatase
RPM – revolutions per minute
RNI – reactive nitrogen intermediates
ROI – reactive oxygen intermediates
RT-PCR – real-time polymerase chain reaction
S. Enteritidis – *Salmonella enterica* serovar enteritidis
sFliC – soluble flagella protein FliC
S.pneumoniae – Streptococcus pneumoniae
S. Typhi – *Salmonella enterica* serovar typhi
SAP – SLAM-associated protein
SCID – severe combined immunodeficiency
SH2 – Src homology 2
SHM – somatic hypermutation
SLC – surrogate light chain
SLE – systemic lupus erythematosus
SLO – secondary lymphoid organ
SPF – specific pathogen free
STAT – signal transducer and activator of transcription
STm – *Salmonella enterica* serovar Typhimurium
T cell – thymus-derived cell
T-B – T cell-B cell
TCR – T cell receptor
T-D – T cell-dependent
Tfh – T follicular helper
TGF- transforming growth factor
Th – T helper
T-I – T cell-independent
T-I 1 – T-independent type 1
T-I 2– T-independent type 2
TK – tyrosine kinase
TLR – toll-like receptor
TNF – tumour necrosis factor
V – variable
WT – wild type

CHAPTER 1: INTRODUCTION

1.1 Coordination of the Immune Response

Constant exposure to a plethora of antigenic material requires a robust and highly coordinated immune response. The rapid recruitment of innate immune cells into an infection site is critical for the early control of pathogen replication, but is not always sufficient for resolution. Under these circumstances, a delayed yet highly specific adaptive immune response must occur for complete pathogen elimination. As such, our immune system has evolved to encompass two distinct, yet not entirely autonomous, phases.

1.1.1 Linking innate and adaptive immunity

The innate immune system provides the rapid, non-specific first line of defence against foreign material and is comprised of multiple components. The skin and internal epithelial surfaces of the body provide an important physical barrier against the external environment, presenting the first challenge to the microorganisms attempting to breach it. As well as being a physical barrier, the epithelial surfaces contribute to innate immunity through the production and release of numerous antimicrobial substances, which can directly kill a number of pathogenic microbes, as well as stimulating cellular responses (1,2).

Cells of the innate immune system arise from progenitors in the bone marrow and include monocytes/macrophages, neutrophils, dendritic cells (DC) and natural killer (NK) cells (3). Microbes that penetrate the epithelial barriers and enter tissues encounter tissue resident macrophages, the mature form of blood monocytes, that are capable of ingesting pathogens by phagocytosis (4). Neutrophils can also engulf foreign material in this way, and are recruited into tissues in response to the pro-inflammatory environment created by macrophages (5). Following phagocytosis, macrophages and neutrophils release bactericidal agents that allow killing of the ingested pathogen (6).

Innate immune cells use a number of pattern recognition receptors (PRR) to identify pathogen-associated molecular patterns (PAMP) on the surface of microbes, through which they initiate their effector functions (7). Examples of PRR include acute phase proteins, mannose and scavenger receptors, nucleotide binding and oligomerisation domain (NOD)-like receptors and toll-like receptors (TLR) (3). Numerous TLR have now been identified on mammalian cells. Upon ligation, TLR signalling pathways can enhance phagocytosis and stimulate the release of pro-inflammatory cytokines (8). Another important feature of TLR is the activation of antigen presenting cells (APC) such as DC, a key requirement for priming the later, adaptive immune response (9). Thus, TLR can be seen as ‘bridging the gap’ between innate and adaptive immunity.

Other innate immune components link innate and adaptive immunity, such as the system of complement proteins. Activation of complement pathways can lead to the direct lysis of bacteria through the formation of a membrane attack complex (MAC), or to the opsonisation of microbes, marking them for uptake by phagocytes (10). The latter of these

functions is enhanced in the presence of antibody, which is produced by bone marrow-derived cells (B cells) and largely associated with the adaptive response. However, certain subsets of B cells, known as B1 cells, are able to produce antibody rapidly following antigen encounter and are also responsible for providing a pool of 'natural antibody,' which can be detected in the absence of exogenous antigen (11). Due to the rapid production and non-specific nature of such antibody, B1 cells are often described as innate-like B cells. However, some reports suggest a potential role for B1 cells during the adaptive response to infection (12-14).

Effector cells of the delayed, yet highly specific, adaptive response arise from a common lymphoid progenitor in the bone marrow. Despite this common origin, B lymphocytes (B cells) mature within the bone marrow whilst T lymphocytes (T cells) develop in the thymus. Throughout lymphocyte development, receptor gene rearrangement occurs, allowing for huge diversification within the lymphocyte pools and a high degree of specificity at an individual cell level (15). Following development in primary lymphoid tissue, T and B cells migrate to highly organised secondary lymphoid tissue, such as the lymph nodes (LN), white pulp areas of the spleen and peyers patches (PP). Here, multiple cellular interactions lead to the initiation of an adaptive immune response.

1.1.2 Organisation of secondary lymphoid organs

Secondary lymphoid organs (SLO) provide niches in which antigen presentation to lymphocytes and T cell-B cell (T-B) collaboration can occur, whilst also supplying survival signals (16). Figure 1.1 shows the organisation of T and B cells within the LN and

white pulp area of the spleen (17). Migration of lymphocytes to and within SLO is governed by adhesion molecules, chemokine receptors, and stromal-expressed chemokines. Mice that are deficient in the chemokine receptor CCR7 (18) or its ligands, CCL21 and CCL19 (19,20), exhibit defects in naive T cell homing to SLO and inappropriate localisation of T cells within these structures. Mice with a disruption in the gene encoding the chemokine receptor CXCR5 highlight the importance of this receptor for B cell homing to the follicles (21). The ligand for CXCR5, CXCL13, has been shown to direct B cells to follicles within SLO (22,23), and also directs trafficking of B cells across high endothelial venules (HEV) (24).

Entry of recirculating B cells into the follicular niche is required for B cell survival (25), via signals delivered by the follicular stroma such a B cell activation factor (BAFF). Following entry, B cells remain in the follicle for 12-24 hours before leaving and continuing the recirculation process between SLO, in search of foreign antigen. Those B cells that encounter antigen in the blood or marginal zone (MZ) interact with resident splenic T cells, whilst antigen encounter in the draining lymph nodes leads to interactions with T cells in the lymph node paracortex (26). The rarity of T and B cells possessing antigen receptors with compatible specificities provides an explanation for the delayed adaptive immune response during primary infection. However, the unique ability of T and B lymphocytes to acquire ‘immunological memory’ following antigen exposure, leads to the faster onset of an adaptive response upon pathogen re-encounter (27). Together, the innate and adaptive immune systems encompass multiple components, which must coordinate appropriately upon immunological challenge for successful pathogen clearance. B lymphocytes participate in both phases of the immune response, however variations in

development, function and anatomical location, provide individual B cell subsets with unique identities.

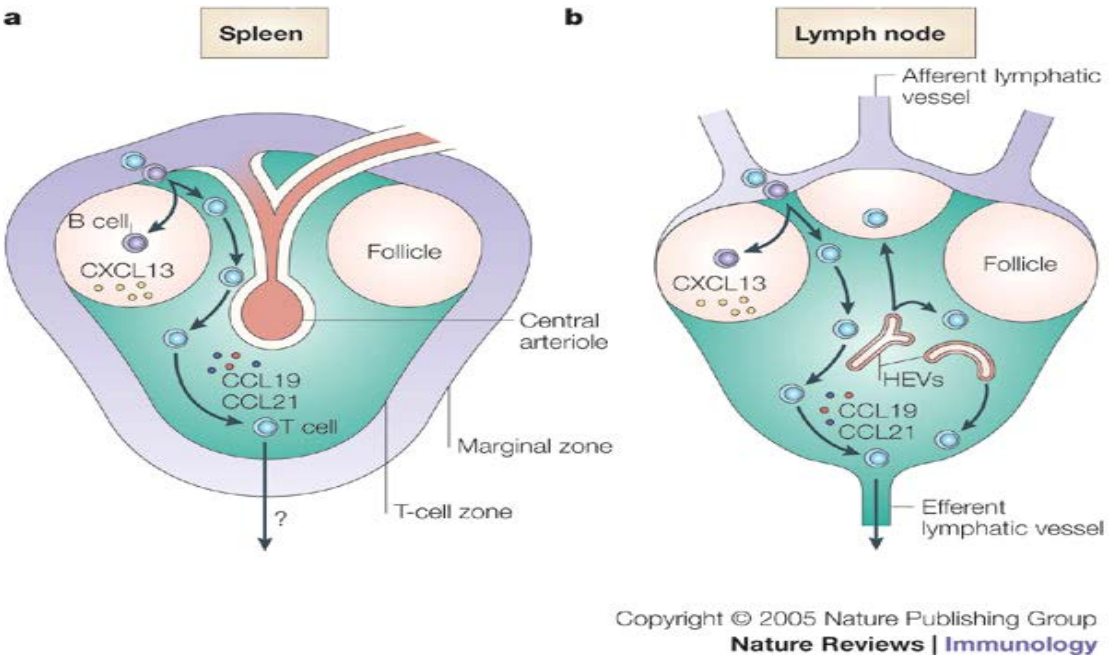

Figure 1.1 Structure and organisation of secondary lymphoid tissue. **a)** A white pulp area of murine spleen. The spleen is made up of red pulp interspersed with areas of lymphoid tissue known as the white pulp. Lymphocytes and antigen arrive in the white pulp via the blood, which drains into a central arteriole. Lymphocytes then pass into the marginal sinus, which is surrounded by the MZ. T cells migrate to the periarteriolar lymphoid sheath (PALS), shown as the T cell zone, via surface expressed CCR7 responding to chemokines CCL19 and CCL21. B cells that emigrate from the bone marrow follow the chemokine CXCL13, via surface expressed CXCR5, to the follicular areas of the white pulp. Separating the white pulp from the red pulp is the MZ, which contains a heterogeneous population of cells including MZ B cells and macrophages. **b)** The T and B cell areas of a lymph node, showing a similar organisation to the splenic white pulp. The main route of lymphocyte entry is through HEV, which perfuse the T cell-rich paracortex (green). B cells migrate to the follicles after entry through HEV or afferent lymph. Figure taken from Mebius and Kraal. *Nature Reviews Immunology*. 2005. **5(8):** 606 (17).

1.2 B Cell Development and Function

1.2.1 Developmental pathways of B cell subsets

Several peripheral B cell subsets have now been identified, however some are less well characterised than others. The greatest level of understanding surrounds the population of recirculating, follicular B2 cells, which form the most abundant B cell population in human and murine SLO (28). Arising from the same progenitor in the bone marrow is the MZ population of B2 cells, which are restricted to the spleen, although a population of B cells with a similar phenotype can be found residing in the medullary cords of LN (29). Less well understood is the developmental pathway of B1 cells, which make up the majority of B cells in the peritoneal and pleural cavities of the body, with a small number also being found in the spleen and lymph nodes.

1.2.1.1 B2 cell generation

The generation of B2 cells is a sequential process occurring in human and murine foetal liver and in foetal/adult bone marrow (30). As shown in figure 1.2 (31), different cell markers are expressed at each stage of development, with expression of a surface B cell receptor (BCR) of the immunoglobulin (Ig) μ (IgM) isotype occurring at the immature B cell stage. Expression of surface IgM is preceded by Ig heavy (H) and light (L) chain gene rearrangement which occurs throughout B cell development. Formation of a functional H chain involves rearrangement of the variable (V), diversity (D) and joining (J) gene segments, whilst L chain expression requires V and J gene rearrangement (32). Heavy chain rearrangement can be detected by the progenitor (pro)-B cell stage (33), whilst expression of the IgM H chain is evident within the cytoplasm of precursor (pre)-B cells.

Essential to the continuing development of B cells is the pairing of the μ H chain with a surrogate light chain (SLC) in pre-B cells, giving rise to the pre-BCR (34). This allows for the selection of successfully rearranged Ig H chains and expression of a functional BCR on the immature B cell. Subsequent B cell maturation in the periphery leads to co-expression of both surface IgM and IgD. Recirculating, follicular B2 cells can be identified as IgM^{lo} IgD^{hi} $CD19^{+}$ $B220^{+}$ $CD5^{-}$ $CD23^{hi}$ $CD21^{int}$, whilst MZ cells are IgM^{hi} IgD^{lo} $CD19^{+}$ $B220^{+}$ $CD5^{-}$ $CD23^{lo}$ $CD21^{hi}$. Stringent selection mechanisms are incorporated along the developmental continuum in the bone marrow and within the periphery, allowing for the elimination of autoreactive B cells (35).

1.2.1.2 B1 cell generation

In mice, B1 cells can be identified by their IgM^{hi} IgD^{lo} $CD19^{+}$ $B220^{lo}$ $CD23^{-}$ $CD21^{int/lo}$ phenotype, and can be further split into two populations based on the presence (B1a) or absence (B1b) of surface expressed CD5 (36,37). Expression of CD21 on B1 cells has been described as both intermediate and low in the literature (38-40). A possible reason for this discrepancy comes from data describing different levels of CD21 expression on $CD11b^{+}$ and $CD11b^{-}$ B1 cells in the peritoneum (41). Over half of the B1 cells present in the peritoneal cavity express CD11b, and these cells express the lowest amounts of CD21. Examination of the reconstitution potential of $CD11b^{-}$ B1 cells, suggested that this fraction may represent B1 cells at an earlier stage of development, rather than an entirely distinct population (41). As such, it is thought that the differentiation of B1 cells from $CD11b^{-}$ to $CD11b^{+}$ represents the differentiation of B1 cells into effector cells. In response to a protein antigen expressed on the surface of *Salmonella*, the B1 cells that expand in the peritoneal cavity are largely $CD11b^{+}$ and are also $CD21^{lo}$ (13). For this reason, B1 cells are

identified as CD21^{lo} throughout this thesis. Despite some controversy surrounding the existence of B1 cells in humans, a phenotypically distinct population of B cells, with functional characteristics akin to those of B1 cells in mice, has recently been identified in human umbilical cord and peripheral blood (42).

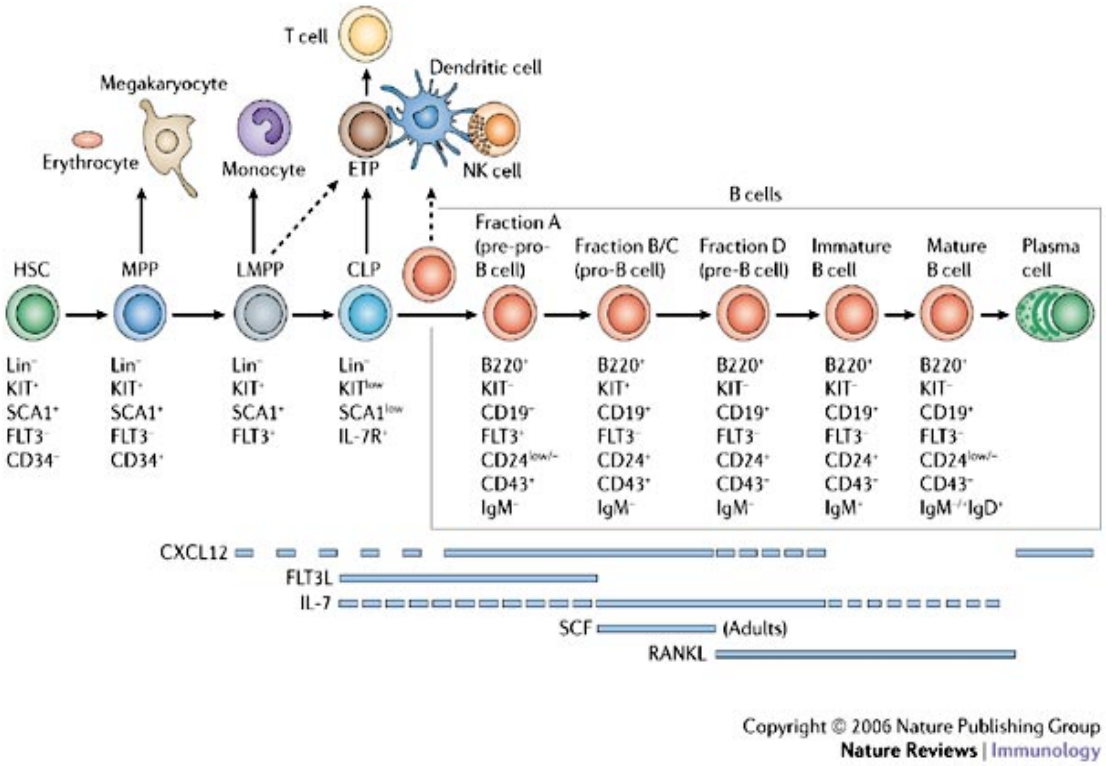

Figure 1.2 B2 cell development within the bone marrow and release into the periphery. Haematopoietic stem cells (HSC) within the bone marrow give rise to a common lymphoid progenitor (CLP), which has the capacity to differentiate into an early thymic progenitor (ETP) or an early pro-B cell (pre-pro B cell). The pre-pro B cell then passes through a pro-B and pre-B cell stage, before differentiating into an immature B cell expressing a functional BCR of the IgM isotype on the surface. Immature B cells then exit the bone marrow to continue the maturation process in secondary lymphoid tissue, where they further differentiate into follicular or MZ B2 cells (spleen) and have the capacity to become antibody-secreting plasma cells following antigenic challenge. Figure taken from Nagasawa, T. (2006) *Nature Reviews immunology*.**6:**107-116 (31).

Uncertainty surrounding the existence of a specific B1 cell progenitor has led to research into the developmental pathway of B1 cells. Suggestive of a distinct B1 progenitor cell is the observation that pro-B cells isolated from the foetal liver reconstitute the $CD5^{+}$ IgD^{lo} fraction of B cells in the spleen and peritoneal cavity after transfer into severe combined immunodeficiency (SCID) mice, whereas pro-B cells isolated from adult bone marrow repopulate the $CD5^{-}$ IgD^{hi} cells in the spleen and peritoneal cavity (28). A distinct population of pro-B cells with a $lineage^{-}$ $CD45R^{lo\text{-}neg}$ $CD19^{+}$ phenotype that are capable of reconstituting the $CD11b^{+}CD5^{+}$ and $CD11b^{+}CD5^{-}$ peritoneal B cell populations of Balb/c and SCID mice, but not the B2 cell populations of the spleen in the same mice, have also been identified in foetal and adult murine bone marrow (43). When isolated from foetal bone marrow, these progenitor cells were more effective at reconstituting the $CD11b^{+}CD5^{+}$ B1a cell population, whereas those from adult marrow effectively reconstituted $CD11b^{+}CD5^{-}$ B1b cells. This indicates that the different B1 cell populations may differ in their renewal potential and/or mechanisms during adult life. Despite the self-renewing capacity of B1 cells (44), one feature that sets them apart from B2 cells, recent evidence shows that B cells exiting the bone marrow can replenish the B1 cell pool of adult mice (45). Whilst the origin and development of murine B1 cells is beginning to be unravelled, the development of human B1 cells is less well characterized. The phenotypic characterisation of human B1 cells (42) will no doubt facilitate future investigation into this process.

1.2.2 B cell immunity

Whilst having numerous roles within the immune system, such as immunomodulation, cytokine secretion and antigen presentation, a major and possibly dominant effector function of the B cell is the secretion of Ig as antibody. Antibody offers important protection against both bacterial and viral pathogens, and is the basis of most vaccination programmes. Antibody protects against invading pathogens in a number of ways. Firstly, antibody can bind to the receptor binding domain of bacterial toxins or viruses, thereby preventing their entry into host cells (46,47). Alternatively, antibody can activate complement or directly opsonise pathogens for phagocytosis by macrophages, DC and neutrophils (48). NK cells can also eliminate antibody-bound pathogens via antibody dependent cellular cytotoxicity (ADCC). Here, NK cells bind antibody-antigen complexes via surface-expressed fragment constant (Fc) receptors, and release cytotoxic granules, directly killing the target (49).

B cells can be induced to differentiate into antibody-secreting plasma cells by both T cell-dependent (T-D) and T cell-independent (T-I) antigens, reflecting a flexible requirement for T cell help (50). Recirculating B2 cells rely upon T cell help during an immune response, whereas B1 cells responding to antigen have the capacity to secrete antibody in the absence of T cells (13). Whilst recirculating B2 cells can be recruited into germinal centre (GC) reactions, which require T cells for their maintenance, as well as extrafollicular (EF) reactions, B1 and MZ B cells responding to TI antigens are largely restricted to EF growth (26).

1.2.2.1 T-dependent antibody responses

1.2.2.1.1. B cell activation through the BCR

During T-D antibody responses, B cells must receive two separate activation signals before undergoing terminal differentiation into antibody-secreting plasma cells. Signal one is provided by the antigen itself, whilst the other is provided by T cell interaction. Antigen is recognised by the B cell through the fragment antigen binding (Fab) portion of its surface-expressed BCR, which can recognise both soluble and membrane bound antigen. However, it is now generally thought that much BCR triggering occurs via the recognition of antigen bound to APC such as DC (51,52). Ligation of the BCR leads to BCR cross linking and signal transduction into the cell, which is dependent upon the phosphorylation of immunoreceptor tyrosine activation motifs (ITAM) present in the Igα/β sheath that associates with the BCR (53). The subsequent formation of a signalosome, a signalling complex including a number of tyrosine kinases (TK) and adaptor molecules, allows for the initiation of downstream events associated with B cell activation (54). These include calcium (Ca^{2+}) mobilisation, gene expression and antigen internalisation, processing and presentation. It is this ability to present antigen that allows a B cell to receive a second critical signal, arising from T-B interaction (55).

1.2.2.1.2. T-B interaction

Prior to B cell differentiation, cognate interaction between T cells and B cells must occur at the T-B border in SLO (figure 1.3). To initiate T-B interaction, B cells migrate to the outer T-zone of SLO and present recently encountered antigen to T cells (56). Upon recognition of peptide bound in major histocompatibility complex (MHC) II molecules on the B cell,

activated T cells up-regulate CD40 ligand (CD40L) expression (57), allowing an interaction with B cell-expressed CD40 to take place. This engagement, along with interactions between T and B cell expressed co-stimulatory molecules, forms an essential part of the second signal delivered to B cells during a T-D immune response. During this initial interaction, germline switch transcripts of the Ig heavy chain constant region are produced in B cells (56). Following T-B communication, B cells are induced to proliferate either on follicular dendritic cell (FDC) stromal networks in the follicles where germinal centres (GC) are formed, or as plasmablasts in the EF areas of SLO (58) (figure 1.3). These responses are discussed in detail in later sections. A number of T cell subsets have now been identified within the immune system, including $CD8^+$ and $CD4^+$ T cells. It is the $CD4^+$ T-helper (Th) cells that provide critical signals to recirculating B2 cells during an immune response, an absence of which results in defective GC formation and antibody class switching *in vivo* (55).

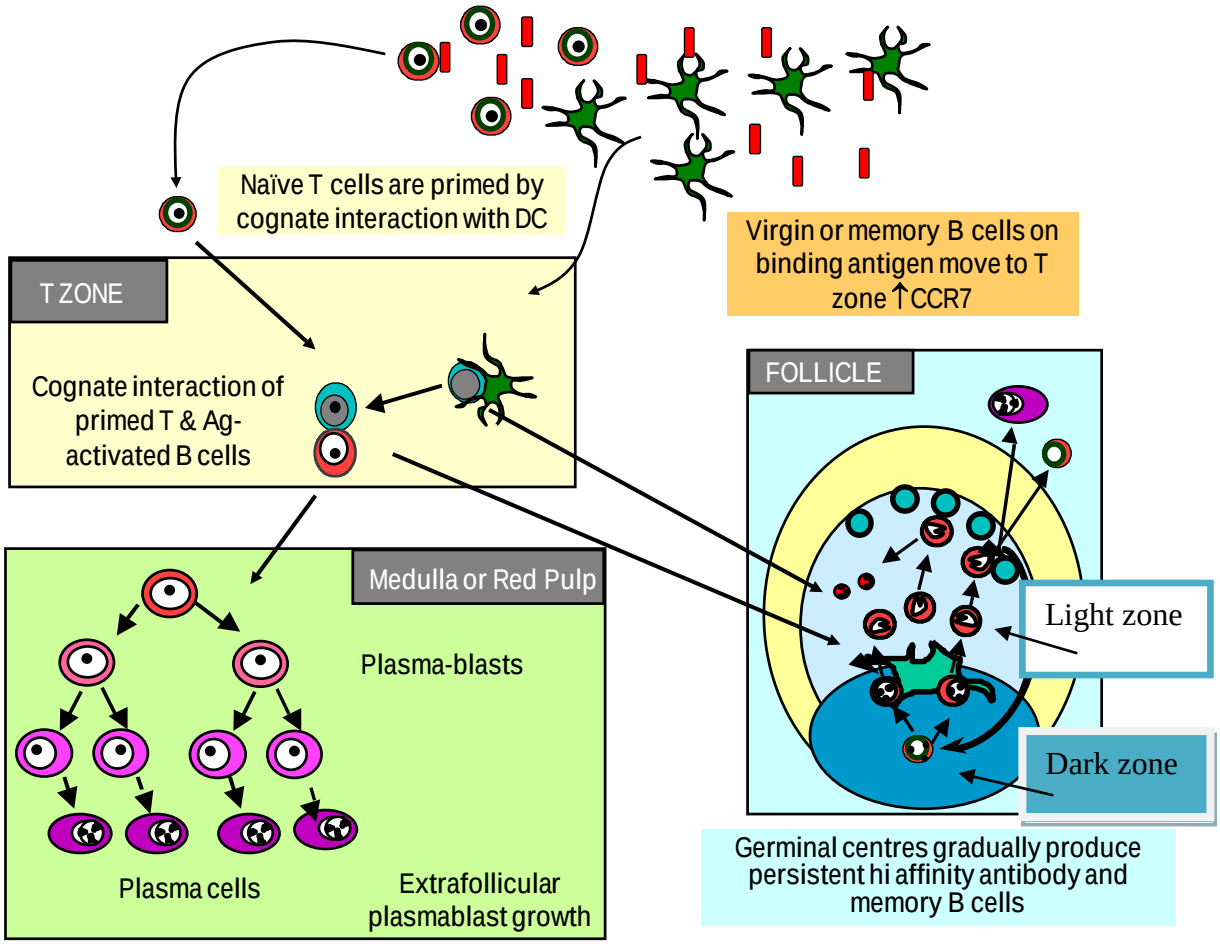

Figure 1.3 Development of T-D B cell responses. T-D antibody responses are initiated in SLO, when T cells that have been primed by antigen-loaded DC in the T zone migrate to the T-B border. Here, primed T cells interact with B cells that have recently encountered antigen through the BCR. Following cognate interaction at the T-B border, activated B cells follow one of two differentiation pathways. One pathway of expansion occurs when B cells migrate to the splenic red pulp areas bordering the white pulp (bridging channels), or to the medullary cords of lymph nodes, forming EF foci of dividing plasmablasts before undergoing full differentiation into short lived plasma cells. Alternatively, B cells proliferate within follicles where they form GC, which require further T cell help for their maintenance. Within GC, B cells undergo somatic hypermutation (SHM) in the dark zone and class-switch recombination (CSR) in the light zone, allowing for the generation of B cells with a high affinity for foreign antigen. Following selection by T cells and follicular dendritic cells (FDC), B cells can exit the GC and differentiate into long lived plasma cells or memory B cells. Alternatively, B cells return to the GC for further rounds of SHM. Those B cells that do not receive survival signals form T cells die in situ by apoptosis. Figure adapted from I.C.M MacLennan.

1.2.2.1.2.1 T-helper cells

As introduced above, $CD4^+$ Th cells recognise protein antigen presented by APC in the context of MHC class II molecules (59). APC include DC, macrophages and B cells, however DC are considered the most efficient and possibly exclusive cell for initial T cell priming *in vivo* (60,61). Upon antigen encounter in the tissues, DC mature and carry information to T cells in the T-zones of secondary lymphoid tissue (see figure 1.3). Here, interactions between APC and naïve T cells allow polarisation of Th cells along several different lineages (figure 1.4). Much like B cells, T cells must receive at least two signals before polarisation is initiated; the TCR must be engaged with antigen presented on MHC class II molecules and co-stimulation of CD28 on the T cell with CD80/86 on the APC must also occur (62). Co-stimulation up-regulates expression of CD40L on the T cell, which upon engagement of CD40 on the APC, reactivates the APC and drives the cytokine production necessary to allow T cell differentiation along the appropriate pathway (63,64).

The discovery that T cells could be separated into distinct lineages based upon the cytokines to which the T cells were exposed, gave rise to the Th1/Th2 paradigm (65). Th1 cells eliminate intracellular organisms, whilst Th2 cells fight extracellular pathogens and were originally considered the sole T cell subset promoting B cell secretion of antibody (66). It is now clear that both Th1 and Th2 cells can shape B cell responses, and the emergence of further T cell lineages has added considerably to our understanding of how B cell responses are regulated by T cells *in vivo.* Numerous Th cell lineages have now been identified, each polarised under different conditions, with cytokines being one of the most important determining factors (figure 1.4). These include, but are not limited to Th1, Th2, Tfh, Th17 and Th9 cells. In addition to Th cells, T regulatory (Treg) cells, that suppress T

cell activation subsequent autoimmune disease, have also been described (67,68). The Th cells that are discussed in the context of this thesis are Th1, Th2 and Tfh cells.

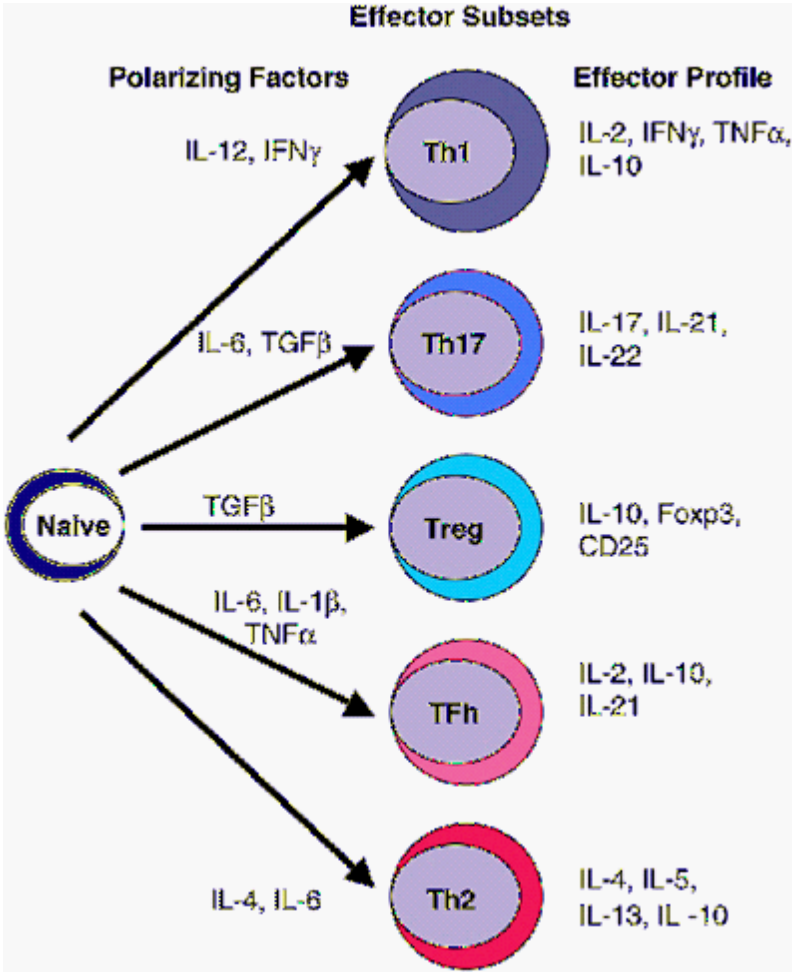

Figure 1.4 T cell polarisation and cytokine signature. Following interactions with DC, polarising cytokines induce naïve T cells to differentiate along one of at least five different pathways. The T helper cell subsets shown above that support B cell function include Th1, Th2, Th17 and T follicular helper (Tfh) cells, whilst regulatory T cells (Treg) are responsible for dampening Th cell responses and preventing excessive inflammation. Each T cell subset has a unique effector cytokine profile that shapes the subsequent immune response. Figure taken from Jelley-Gibbs, D et al. (2008) *Immunology and Cell Biology.* **86(4):** 343-352 (69).

Th1 cells

Infection with intracellular bacteria requires an immune response in which T cells differentiate to Th1, stimulating IFNγ production and the activation of macrophages. During Th1 responses in mice, antibody class-switching is dominated IgG2a and IgG2b (70,71). Key cytokines involved in the Th1 lineage decision are IL12 and IFNγ produced by APC, with IL18 having a later, less critical role in this process (62). Essential to Th1 lineage commitment is the expression of T-box transcription factor T-bet in the differentiating T cell (72), whose actions simultaneously repress the Th2 programme in the same cell (73). T-bet expression is induced in T cells via IFNγ signalling (74), leading to the activation of Janus kinase (JAK) 1 and 2 and subsequent phosphorylation of signal transducer and activator of transcription (STAT) 1 (75). T-bet directly transactivates the IFNγ gene, allowing IFNγ production and further Th1 differentiation via an autocrine loop (72,76). Reinforcement of the Th1 phenotype is also controlled by T-bet, which induces IL12Rβ2 expression on T cells (76), stimulating further IFNγ production via a JAK2/tyrosine kinase (TK)2-STAT 4-dependent pathway (77). Thus, T-bet$^{-/-}$ T cells are unable to secrete IFNγ *in vivo* (78) and T-bet$^{-/-}$ mice fail to mount Th1 responses to infections such as *Leishmania* Major (*L.* Major) (71) and *Salmonella enterica* serovar Typhimurium (STm) (79). On the other hand, a failure to induce Th1 inflammatory responses in the absence of T-bet is protective during autoimmune diseases such as colitis and crohn's disease (80).

Aside from a critical role in directing Th1 differentiation, T-bet deficient DC may also impair Th1 responses via inefficient T cell priming, which has been demonstrated in an *in vivo* model (81). An inability to mount Th1 responses further impacts upon antibody

production, as IFNγ directs Ig class-switching in B cells to IgG2a *in vitro* (82). In keeping with this, T-bet$^{-/-}$ mice infected with STm for 14 days failed to induce antibody class switching to IgG2a, however IgG2b responses were not apparent in either WT or T-bet$^{-/-}$ mice (79). The lack of IgG2a production was considered an effect of T-bet absence and subsequent IFNγ loss in Th1 cells, however *in vitro* studies have shown that T-bet$^{-/-}$ B cells fail to complete class switch recombination (CSR) to IgG2a (83). Thus, this defect may have been controlled in a B cell intrinsic manner. Considering these data, as well as the expansion in our understanding of other Th subsets, the role of Th1 cells in directing B cell class-switching *in vivo* may require some re-appraisal. One aim of this thesis was to examine the role of T-bet in T cells and B cells for antibody class-switching during STm infection.

Th2 cells

Th2 cells are effective in controlling host defence against extracellular organisms and parasites (66), but are also generated during the immune response to model protein antigens, such as alum-precipitated (alum-ppt) protein (84). Following Th2 differentiation, the cytokines released by these cells include IL4, IL5, IL9, IL10 and IL13, which help to shape the subsequent immune response (85). One classic feature of such responses is antibody production by B cells, with sequential class-switching to IgG1 and then IgE (86). As T-bet is able to suppress the Th2 programme (73) T-bet$^{-/-}$ mice have been reported to produce higher levels of these antibody isotypes (83).

Early *in vitro* studies describe IL4 as the main cytokine driving Th2 differentiation (87), through a JAK1/3-STAT 6-mediated pathway (88). This pathway leads to the expression

of the zinc finger transcription factor GATA-3 and a concomitant suppression of the Th1 programme (89). IL4 and IL13 signal via a receptor with a common subunit, the IL4Rα chain (90), and as such have some overlapping functions *in vivo* (91). *In vitro* studies have demonstrated impaired development of cells with a Th2 profile in the absence of IL13 (92). However, *in vivo* studies have since shown that an absence of IL4, IL13 or the IL4Rα chain, does not impede the development of Th2 cells *in vivo* (93,94), or the initiation of Th2 antibody responses following immunisation with non-viable protein antigen (93). However, IL4 is essential for the maintenance of the Th2 clones *in vivo* (95) and for optimal IgE and IgG1 antibody production during late primary and memory responses to Th2-associated antigens (91,95,96). Furthermore, mice double deficient in IL4 and IL13, or the IL4Rα exhibit defects in GC size at a point when B cells are selected by T cells in GC (93,94).

Other soluble mediators shown to influence Th2 cell differentiation include IL10 and IL6, which unlike IL4 and IL13 can be produced by DC (97,98). Human studies have shown that production of IL10 by DC inhibits IL12 synthesis, down-regulating the IL12βR2 and inhibiting Th1 development (98). IL6 has long been recognised as a differentiation factor for plasma cells and a growth factor for myeloma cells (99), but has since been shown to drive Th2 differentiation in three ways, two of which involve autocrine production of IL4 to promote the Th2 phenotype. One of the IL4-dependent pathways requires nuclear factor of activated T cells (NFAT)c2 up-regulation (100), whilst the other promotes IL4 expression via a STAT 3-c-*maf* dependent mechanism (101). An indirect, IL4-independent pathway also exists, in which IL6 suppresses IFNγ signalling and subsequent Th1 differentiation, thus skewing the balance in favour of Th2 development (102). Following

immunisation with model protein antigens, impaired GC and class-switched antibody responses have been reported in $IL6^{-/-}$ mice (103,104). However, the defect in antibody production is not limited to Th2-related isotypes, highlighting a possible role for IL6 in GC reactions and class-switched antibody production to a range of antigenic stimuli. The cytokines referred to here are studied in the context of B cell responses to STm in this thesis, and are therefore discussed in more detail in the relevant results chapter.

Tfh cells

In addition to the classic Th cell lineages described above, a subset of $CD4^+$ T cells that migrate to follicles during T-D immune responses and provide help to GC B cells, has recently been described as a unique T cell lineage; T follicular helper (Tfh) cells (105). Exactly when in ontogeny T cells commit to this lineage is a matter of ongoing debate, and some controversy still surrounds the exact differentiation pathway and phenotype of Tfh cells. This is further compounded by the probable existence of numerous Tfh subsets that interact with B cells at different locations within SLO (106). It is now generally accepted that the Tfh cells that interact with B cells in the GC differ, at least phenotypically, from pre-GC T cells that provide B cells with signals at the T-B border (107), or those that provide B cell help in EF areas of the tissue (108). There is evidence to suggest that full differentiation into a GC Tfh cell, and subsequent T cell entry into the GC reaction, relies upon sustained T-B interaction (109). Probably the most accurate description of a bona-fide Tfh cell at present is one that is located within GC, expressing high levels of some signature markers. A number of groups have now shown that expression of the transcriptional repressor B cell lymphoma-6 (Bcl-6) is essential for Tfh cell lineage commitment (110-112). This in turn drives expression of CXCR5, which is highly

expressed by GC Tfh cells and allows movement into the B cell follicle (113-115). Other phenotypic markers include programmed cell death-1 (PD1) (116) and inducible costimulator (ICOS) (105), which are expressed at higher levels by Tfh cells when compared to other Th cells. ICOS is crucially important to the development and function of Tfh cells, ligation of which initiates a PI3K signalling pathway, culminating in IL21 and IL4 expression via the actions of transcriptions factors NFAT and c-Maf (117). The importance of the PI3K signalling pathway in Tfh cells is highlighted by the reduced number of GC B cells, Tfh cells and impaired memory antibody responses that occur in its absence (118). The adaptor molecule SLAM-associated protein (SAP) is also essential for Tfh cell function, as it allows stable contacts to form between Tfh cells and GC B cells (119). The downstream signalling of pathway of SAP is not yet clearly defined and warrants further investigation.

Cytokines also have a role in Tfh cell development, the primary candidates being IL6 and IL21. Tfh cells can develop when either of these cytokines are absent in isolation (120,121), commensurate with their shared ability to activate STAT 3 (60,122,123). However, a loss of both cytokines impairs, but does not eliminate, Tfh cell differentiation (124). These findings indicate a redundant role for IL6 and IL21 in Tfh cell formation, but also highlight the existence of numerous signalling pathways that facilitate Tfh cell differentiation. A number of groups have attempted to dissect the cytokine signature of Tfh cells, with IL21, IL4, IFNγ and IL17 being amongst those reported (112,125,126). However, it is again important to consider differences between GC Tfh cells and pre-GC Tfh cells in this regard. IL21 is consistently reported at high levels in $CXCR5^{hi}$ T cells, and IL4 is often present at substantial levels in these cells (112,125). Whilst IFNγ can be

expressed by GC Tfh cells (126), it is often expressed at higher levels by $CXCR5^{int}$ T cells in areas outside the follicle, as is the case with IL17. What seems likely, is that the cytokine profile of the Tfh cell is dictated by the nature of the immune response.

1.2.2.1.3 B cell differentiation pathways

Following cognate interaction with T cells, B cells expand either in follicles where GC are formed, or as plasmablasts in the EF areas of SLO (58) (figure 1.3). Whilst the signals that determine the route of B cell differentiation are not fully understood, the expression of certain transcriptional repressors by B cells can be used as an indicator of cell fate. B cells that express Bcl-6 after T-B communication migrate to B cell follicles and generate GC (127). In accordance, mice deficient in Bcl-6 fail to form GC to T-D antigens (128). Bcl-6 acts by repressing B lymphocyte-induced maturation protein 1 (BLIMP-1) (129), a transcriptional repressor essential for the terminal differentiation of plasma cells (130). Thus, Blimp-1 expression signifies B cells that follow a pathway of EF growth, however plasma cells that form as a result of the GC reaction will also eventually express Blimp-1. Expression of Epstein-Barr virus-induced gene 2 (EB12) in B cells is also crucial to the formation of normal EF plasma cell responses to T-D antigens (131).

The Germinal Centre Response

Germinal centres are areas of intense, antigen-driven B cell proliferation and selection, in which B cells somatically mutate their Ig variable region genes and undergo Ig class switching (132). Two compartments known as the dark zone and the light zone exist within the GC, (see figure 1.3) the segregation of which involves the chemokine receptor CXCR4, which is preferentially expressed by B cells that migrate to the dark zone (133,134).

According to classical models of GC dynamics, proliferation of B blasts, known as centroblasts, occurs within the dark zone, whilst their non-dividing progeny, centrocytes, undergo selection within the light zone (132,135,136). Despite the recent advent of several modified interpretations of GC events (137-140), the fundamental features of the original model remain remarkably intact two decades-on.

In the dark zone, centroblasts down regulate their germline encoded BCR and undergo massive clonal expansion and somatic hypermutation. This programmed mutation process, driven by activation-induced cytidine deaminase (AID) (141,142), promotes BCR diversification and the selection of centrocytes bearing a BCR with a high affinity for antigen within the light zone (143). Both FDC and Tfh cells are involved in the selection process. FDC form a stromal network within the GC light zone, where they capture antigen-bound antibody, known as immune complexes, and present them to the centrocytes that migrate here (144). This interaction is highly dependent upon complement-derived ligands held on FDC and their contact with B cell-expressed CD21 (145). Centrocytes that pass this initial checkpoint are able to process the captured antigen and present it to Tfh cells, forming a second checkpoint in the GC B cell fate decision. Survival of centrocytes relies heavily upon the proliferation, survival and differentiation signals provided by Tfh cells (143) through CD40L (146) and cytokines. Whilst Tfh cells will rescue a minority of centrocytes from apoptosis in this way, the unsuccessful majority of centrocytes will either undergo programmed cell death or, according to traditional interpretations, return to the dark zone for further gene rearrangement (132).

More recently, imaging experiments have visualised cell division taking place in both zones, suggesting that proliferation may not be limited to the dark zone and that further somatic hypermutation may not require dark zone re-entry (147). Intravital microscopy has allowed the movement of GC B cells to be tracked in real time and their directional motility assessed (138). The paucity of GC B cells visualised crossing the dark zone-light zone border suggests that this is a rare event during the GC reaction, challenging original models in which frequent trafficking of B cells between the zones is required. Other models support a random walk theory of B cell movement within the GC (137,140) which contrasts to the chemokine-driven directionality of B cells as described by the classical cyclic re-entry model (133).

Whilst the intricacies of GC dynamics remain a topic of debate, the fundamental purpose of the GC reaction is clear: it allows for the selection of class switched, high affinity B cells into the long lived plasma and memory B cell repertoire. This said, the generation of such cells does not come without limitations. The somatic hypermutation that occurs within GC provides an opportunity for the production of autoreactive B cells. As such, a central function served by Tfh cells is the elimination of these cells, highlighting their importance in the control of peripheral B cell tolerance (143).

The Extrafollicular Response

An alternative differentiation pathway for B cells during T-D responses arises from EF growth. Following T cell help, B cells migrate to the splenic red pulp areas bordering the white pulp (bridging channels), or to the medullary cords of lymph nodes, and form EF

foci of dividing plasmablasts (26). Migration to these areas is thought to be governed by plasmablast-expressed CXCR4, responding to chemokine CXCL12 (148). Following a period of growth, some of these plasmablasts will differentiate into non-dividing plasma cells, an event dependent upon association with $CD11c^{high}$ dendritic cells (149). There is also some evidence to suggest that plasmablasts make contact with T cells in EF areas of the tissue, however these cells differ from those Tfh cells found within the GC and may only be relevant in autoimmune settings (150). Most of the plasma cells generated via EF growth following exposure to T-D antigens are short lived, dying by apoptosis *in situ* after about three days (151). Whilst Ig class switching can occur during EF responses, plasma cells generated in this way do not classically mutate their Ig V region genes, resulting in lower affinity antibody production when compared to GC-derived plasma cells (26). However, manipulating certain parameters such as antigen type, antigen persistence and antigen concentration, has lead to high affinity, class switched antibody production in mice that lack GC (152,153). These findings indicate that GC presence is not an unqualified requirement for affinity maturation in individual cells.

Of all the B cells that are recruited into follicular and EF reactions, a proportion will become non-dividing, long-lived plasma cells. These cells enter certain niches in the bone marrow (154), splenic red pulp (155) and gut lamina propria (156), where interaction with the stroma supports their prolonged survival.

1.2.2.2 T-independent antibody responses

Unlike recirculating, follicular B2 cells, B1 cells and MZ B cells confer protection against a range of antigens in the absence of T cell help (157). As such, these responses do not

induce sustainable GC reactions (158), although a role for MZ cells in T-D antibody responses has been described previously, along with an ability to participate in GC reactions (159). As outlined in earlier sections **(1.2.1.2)**, B1 cells are comprised of B1a and B1b cells and provide an immediate source of antibody towards invading pathogens (160). B1a cells produce a source of 'natural IgM antibody,' which can be detected in the blood in the absence of exogenous antigenic stimuli (161). The repertoire of antigens recognised by B1a cells include a number of common bacterial components, such as lipopolysaccharide (LPS) (162) and phosphorycholine (163) which are collectively known as T-I type 1 (T-I 1) antigens. Upon stimulation, B1a cells can migrate from the peritoneal cavity to the mesenteric lymph nodes (MLN), spleen and gut-associated lymphoid tissue (GALT), where they differentiate into antibody-secreting plasma cells (164). As the main constituent of the B cell pool during infancy (28), B1a cells provide crucial protection against bacterial infection in neonates.

B1b cells also confer early protection against a range of bacterial antigens, however these antibodies are thought to arise primarily after antigen exposure (14). B1b and MZ cells collectively form the main line of defence against T-I type 2 (T-I 2) antigens, characterised by high molecular weight and repeating epitopes (14). Examples of these are bacterial polysaccharides, present in the capsules of *Streptococcus pneumoniae,*(*S. pneumoniae*) *Neisseria meningitidis and Haemophilus influenzae* (165). Antibody towards such antigens is not produced early in ontogeny, resulting in frequent infant death by diseases such as meningitis and pneumonia (166). As well as these typical T-I 2 antigens, B1b cells can be recruited into antibody responses to *Borrelia hermsii* (*B.*hermsii) (167). A novel finding was the discovery that B1b cells can produce protective antibody responses to *B. Hermsii*

(12), a finding that has since been extended to other bacterial infections, including *S. pneumoniae* (14) and a protein from the outer membrane of STm, which is effective at protecting against subsequent STm infection (13). It is also possible that the anatomical location of MZ cells (see figure 1.1) allows them to form antibody responses to protein antigens on blood borne pathogens (168).

An antigen for studying the kinetics of T-I 2 antibody responses can be created by haptenating the polysaccharide Ficoll with (4-hydroxy-3-nitrophenyl) acetyl (NP) (NP-Ficoll). Despite not requiring specific T cell help, B cells responding to NP-Ficoll have been shown to migrate to the T-zone following antigen recognition (165). It was suggested that the responding B cells may require alternative signals, provided within the T-zone, for their progression into plasma cells. Typically, immunisation of mice with T-I 2 antigens results in an early wave of EF plasma cells and IgM antibody production, followed by class switching to IgG3 after a week of infection (14,165). Further studies have shown that the early EF plasmablasts seen in the spleen following immunisation with blood borne particulate T-I antigen arise from both MZ and B1 cells (169). In contrast to T-D EF responses, T-I 2 responses are also characterised by their longevity, as NP-specific plasmablasts have been detected in the spleen several months following NP-Ficoll immunisation, which may relate to the slow degradability of T-I 2 antigens *in vivo* (170).

1.2.3 Regulation of B cell activation by inhibitory receptors

The efficient initiation of an immune response is critical to the timely clearance of invading pathogens. Of equal importance, however, is the cessation of the response upon

resolution, a failure of which leads to persistent inflammation and autoimmune disease. A number of inhibitory receptors, that negatively regulate B cell activation, have now been identified. Many of these receptors belong to the Ig-superfamily, including FcγRIIb, PD-1, CD22, paired Ig-like receptor binding protein (PIR-B), Ig-like transcript (ILT)-2, CD5, leucocyte-associated Ig-like receptor (LAIR)1, CD66a and platelet-endothelial cell adhesion molecule 1 (CD31) (171,172). Each of these receptors has an extracellular portion made up of Ig-like domains, as well as a cytoplasmic tail containing immunoreceptor tyrosine inhibitory motifs (ITIM). Tyrosine phosphorylation of ITIM by the TK lyn, allows for the recruitment of Src-homology 2 (SH2) domain-containing phosphatases to the cytoplasmic tail. Subsequent binding and activation of these phosphatases, which include protein tyrosine phosphatases (PTP) SHP-1 and SHP-2 and phosphoinositol phosphatases SHIP and SHIP2, activates various downstream signalling pathways that mediate cellular inhibition (172). Gene-targeting in mice has established a role for these receptors in B cell survival (173), regulation of B cell activation (173,174) and autoimmune disease (175-177).

1.2.3.1 CD31

CD31 was originally classified as an adhesion molecule, through homophilic binding of its extracellular domains on opposing cells (178-180). Further analysis of the cytoplasmic tail revealed two ITIM surrounding amino acid residues Y_{663} and Y_{686} (181), suggesting that CD31 may also have inhibitory role within the immune system. However, further comparisons with the consensus sequence for ITAM revealed that CD31 also conforms to an ITAM signature (182). It has since become clear that CD31 is a dual function molecule, able to activate and inhibit a range of cellular processes.

Expression of CD31 is not limited to lymphocytes, but extends to all other haematopoietic cells, endothelial cells and platelets (183,184). The role of CD31 on non-lymphocytes has been extensively investigated. CD31 is known to support the transendothelial cell migration of non-lymphocytes (185-187), the migration of leucocytes into inflammatory milieu (188) and megakaryocyte (MK) migration within the bone marrow (189). An ability to regulate apoptosis has also been demonstrated in endothelial cells (EC) (190) and transmigrating peripheral blood mononuclear cells (PBMC), via homophilic CD31:CD31 interactions (191). The clinical importance of this anti-apoptotic role is highlighted by the high levels of CD31 expression in many human malignancies, including haematopoietic and vascular cell cancers (192), and the resistance to chemotherapy-induced apoptosis conferred by it (193).

The role of CD31 on lymphocytes has been less well characterised, with the majority of research carried out *in vitro*. These studies show that CD31 can regulate β1 integrin-mediated adhesion on T cells (194,195) and prevent T cell apoptosis (196) (197). Further *in vitro* studies suggest that CD31 can negatively regulate lymphocyte signalling. During the transition from a naïve to a memory T cell (194), CD31 expression is down-regulated and it can also dampen T cell receptor (TCR) signalling in a SHP-2-dependent manner (198). Furthermore, Zap-70 phosphorylation following CD3 ligation is partially inhibited by CD31 triggering (197). Similar inhibitory effects have been reported in B cells. Crosslinking of the BCR in parallel with PECAM-1 inhibits the release of Ca^{2+} and subsequent NFAT activity that is induced by BCR crosslinking alone (199). This inhibitory activity requires phosphorylation of tyrosine residues Y_{663}/ Y_{686} and involves PTP SHP-1 and SHP-2.

The expression of CD31 on diverse leucocyte populations and its proposed role in regulating processes such as adhesion, migration, apoptosis and lymphocyte activation, suggested this molecule as a potential candidate for regulating multiple facets of the immune and inflammatory response. This is supported by studies in $CD31^{-/-}$ mice, that despite a near normal resting phenotype (184), undergo excessive anaphylactic responses (200) and have a heightened susceptibility to LPS-induced endotoxic shock (201). The potential role for CD31 as an inhibitory receptor is further reflected in models of autoimmunity, such as experimental autoimmune encephalomyelitis (EAE) (176) and collagen-induced arthritis (CIA) (177), to which $CD31^{-/-}$ mice display a greater susceptibility. An autoimmune B cell phenotype (202) and a failure to induce tolerance in a model of T cell-mediated allograft rejection (197) have also been reported in $CD31^{-/-}$ mice.

These results indicate that CD31 deficiency enhances susceptibility to autoimmune disease and results in a poorer prognosis when placed under immunological stress, however the contribution of CD31 to a normal resolving infection had not been addressed. As such, we investigated the role of CD31 in immunity to STm, clearance of which depends upon the effector functions of $CD4^{+}$ T cells. Following infection with STm, T cell homeostasis was impaired in $CD31^{-/-}$ mice, resulting in a failure to effectively resolve infection (203). During these studies we noticed a high frequency of GC and lower numbers of follicular B cells in the spleens of uninfected $CD31^{-/-}$ mice. These data form a prelude to the first chapter of my PhD project, which focuses upon the contribution of CD31 to B cell immunity during STm infection.

1.3 Salmonella

The *Salmonella* genus consists of three species: *Salmonella enterica, Salmonella bongori* and *Salmonella subterranean,* with *Salmonella enterica* being accountable for the vast majority of significant human *Salmonella* infections worldwide (204). *Salmonella enterica* are gram-negative, intracellular bacteria that cause a range of diseases, depending upon the serovar and strain encountered (205). Millions of cases of typhoid fever caused by *Salmonella enterica* serovar Typhi (*S.* Typhi) occur each year, resulting in hundreds of thousands of deaths. Other strains, such as STm and *Salmonella enterica* serovar enteritidis (*S.* Enteritidis) can be transmitted from animals to humans or humans to humans, and may cause fever, diarrhoea and/or a fatal bacteraemia (206). Apart from being a problem for the food industry, these illnesses are a major concern in developing countries where a high incidence of infant mortality is reported. Immunity to *Salmonella* encompasses aspects of innate, cell-mediated and humoral immunity (207), making this a good model to dissect interactions between these three arms of the immune system.

1.3.1 Immunity to *Salmonella*

1.3.1.1 Innate immunity to *Salmonella*

Following oral infection with *Salmonella,* bacteria cross the intestinal epithelial barrier by invading M cells in the peyers patches (208), or via DC that use their processes to breach the epithelium and capture bacteria from the gut lumen (209). The subsequent release of IL-8 by epithelial cells and attraction of neutrophils to the gut, is dependent upon the ligation of epithelial-expressed TLR5 by bacterial flagellin and signalling via the

NFkappaB pathway (210). Signalling through this pathway results in the release of numerous pro-inflammatory cytokines, including IL-18, IL-12, IFNγ and TNFα.

These initial events and bacterial dissemination stimulate the recruitment neutrophils, macrophages, DC and NK cells into bacteria-harbouring tissues (211). These include the spleen, liver, MLN and PP, where the majority of bacteria are found residing within macrophages (205). During these early stages of the murine innate response, bacterial replication in the tissues is controlled by the *Nramp1* gene of resistant mice, which is expressed in macrophages and granulocytes. *Nramp1* encodes for a membrane phosphoglycoprotein that is recruited to the bacteria-containing phagosome and functions as a divalent metal ion pump (212). Susceptibility to STm infection in mice is associated with a natural Gly-Asp mutation at amino acid 169 of *Nramp1* (213), leading to the rapid replication of bacteria in reticuloendothelial organs.

In the murine spleen, absolute neutrophil and macrophage numbers increase substantially by day 5 following oral administration of virulent *Salmonella* and appear to provide the main source of tumour necrosis factor (TNF)α and IFNγ at early stages of the response (214). Cytokine production by phagocytes is instrumental in controlling early bacterial replication, as they stimulate the production of highly bactericidal reactive oxygen intermediates (ROI) and later reactive nitrogen intermediates (RNI) (205). Uncontrollable spread of infection throughout the host is further prevented by the formation of pathological lesions by phagocytes, a process governed by the cytokines TNFα, IFNγ, IL18 and IL12 (206). Thus, the release of pro-inflammatory cytokines has a number of

important functions during the innate response to *Salmonella* infection, whilst also prompting the Th1-driven adaptive response

1.3.1.2 The role of T cells in immunity to STm

The importance of $CD4^+$ Th1 cells in clearance of primary STm is demonstrated in mice deficient in MHC class II molecules, the TCR β chain, or the IFNγ receptor. These mice have a severe defect in their ability to clear bacteria from the spleen and liver compared to heterozygous littermates (215). Furthermore, mice deficient in T-bet are unable to produce IFNγ-secreting T cells in response to attenuated *Salmonella* immunisation, resulting in increased splenic bacterial burdens and a higher mortality rate (79). A failure of activated $CD4^+$ T cells to survive in $OX40^{-/-}CD30^{-/-}$ mice (216) mice, or a failure to maintain $CD4^+$ T homeostasis during infection of $CD31^{-/-}$ mice, also results in a marked failure to resolve infection (203). Conversely, mice deficient in surface MHC class I molecules do not display defects in bacterial clearance from the spleen and liver, providing evidence against a crucial role for $CD8^+$ T cells in the clearance of primary *Salmonella* infection (217). Human studies supporting a $CD4^+$ Th1-mediated clearance include reports of enhanced susceptibility to *Salmonella* in individuals with IL-12 receptor (218,219) or IFN-γ receptor (219) signalling deficiencies.

1.3.1.3 The role of B cells in immunity to STm

As an intracellular pathogen, a role for B cells in *Salmonella* resolution has long been debated. B cell-deficient mice to not succumb to infection with attenuated *Salmonella* (220), which is in stark contrast to the mortality observed in T cell-deficient mice. However, a role for B cells has been demonstrated in B cell-deficient mice following oral

infection with virulent *Salmonella* (221), and vaccination of adults against typhoid with purified polysaccharide Vi antigen from *S.* Typhi is sufficient to protect against invasive disease (222,223).

It is also clear that B cells are recruited into the immune response to STm, as evidenced by the strong, EF plasma cell response that occurs within three days of immunisation with attenuated STm (70). This response is dominated first by IgM and later by IgG2a and IgG2b. Although this early IgM response is T-independent, class switching relies on the presence of T cells (13). The production of class-switched IgG2a during STm is reportedly dependent upon B cell-intrinsic MyD88 signals, an absence of which attenuates IFNγ production by $CD4^+$ T cells (224). High titres of class-switched antibody production coincides with the later appearance of GC, which do not appear until around a month into infection with STm, when bacterial infection has largely resolved (70). However the splenic bacterial load resolves at similar rates in WT and CD40L-deficient mice that lack GC, demonstrating that high affinity antibody production is not required for the resolution of primary infection (70). Although antibody cannot prevent the progress of infection in the tissues, antibody can reduce bacteraemia during the primary response to STm in the mouse (70). This observation is strengthened by the association between bacteraemia and antibody-absence in Malawian children. Bacteraemia from non-typhoidal strains of *Salmonella* is most prevalent amongst children aged 4 months-2 years, a period when maternal antibody is lost and host anti-NTS antibodies have not yet developed (225).

A crucial role for B cells during secondary responses to *Salmonella* infection has also been reported. B cell-deficient mice fail to survive after STm vaccination and oral rechallenge

with virulent *Salmonella,* whereas WT mice are effectively protected by the vaccination (226). Immune serum transfer experiments have provided varied results. Early experiments show that protection against oral challenge with virulent *Salmonella* requires the transfer of both immune serum and immune cells, including antigen-experienced T cells (227). Later experiments failed to restore protection in immunised B cell-deficient mice with the transfer of immune serum prior to rechallenge with virulent organisms. This occurred despite the presence of functional, antigen experienced T cells, (226) leading to the suggestion that alternative B cell functions, such as antigen presentation and cytokine production, contribute to the protective nature of B cells following *Salmonella* rechallenge. In line with this, a role for B cells in antigen presentation and effective development of memory T cell responses during STm has been described recently (228). On the other hand, the different antigen doses used for rechallenge in these studies may explain some of the discrepancies observed.

An interesting recent observation comes from within our laboratory, where antibody produced towards the outer membrane protein (Omp) D of STm confers protection against attenuated and virulent *Salmonella* (13). At least a proportion of this antibody arose from B1b cells, highlighting a novel role for these cells in protective antibody responses to *Salmonella*.

1.3.2 STm as a model of infection

Despite causing typhoid fever in humans, *S.* Typhi does not cause typhoid fever in many other mammals, aside from some higher primates. However, infection of innately

susceptible mice with STm causes a systemic, typhoid-like disease with bacterial dissemination to the spleen, liver and bone-marrow (229). As such, this model is commonly used to study the development of innate and acquired immunity to typhoid fever. Common infection routes using this model include oral, intravenous (i.v) and intraperitoneal (i.p) administration of bacteria. Virulent *Salmonella,* when given i.v or i.p, are lethal at doses as low as 1 organism (230). Whilst higher oral doses of virulent STm can be administered to susceptible mouse strains, the infection is always lethal (227), limiting the study potential of this strain. Furthermore live, attenuated STm, when delivered orally, fails colonise effectively. On the other hand, i.p or i.v infection of susceptible mouse strains with attenuated STm provides a model that retains many features of disseminated infection, such as induction of a low grade bacteraemia. Whilst i.v infection is not reduced by the presence of immune sera, i.p infection is, enabling the role of antibody in protection to be assessed. Thus, the i.p route of infection is used throughout.

When administered i.p into WT mice, live, attenuated STm, strain SL3261, results in a slowly resolving infection, characterized by a high splenic bacterial burden and severe splenomegally (70) (figure 1.5). Large numbers of bacteria are also recovered from the liver and bone marrow. Bacterial loads in the tissues fall gradually over the course of infection, reaching low levels from day 35 post-infection (p.i) onwards. Typically, the infection is cleared completely within two months (231). Splenomegally gradually increases after the initial infection, peaking at day 20 when bacterial loads are already falling, then reducing greatly by day 35 (figure 1.5). Thus, i.p. infection with STm elicits an antigen-specific inflammatory immune response, which has both an induction and resolution phase. This provides an excellent model for studying the innate and adaptive T

and B cell response to a normal, resolving infection. In the current study, live, attenuated STm, strain SL3261 *aro*A, was used throughout.

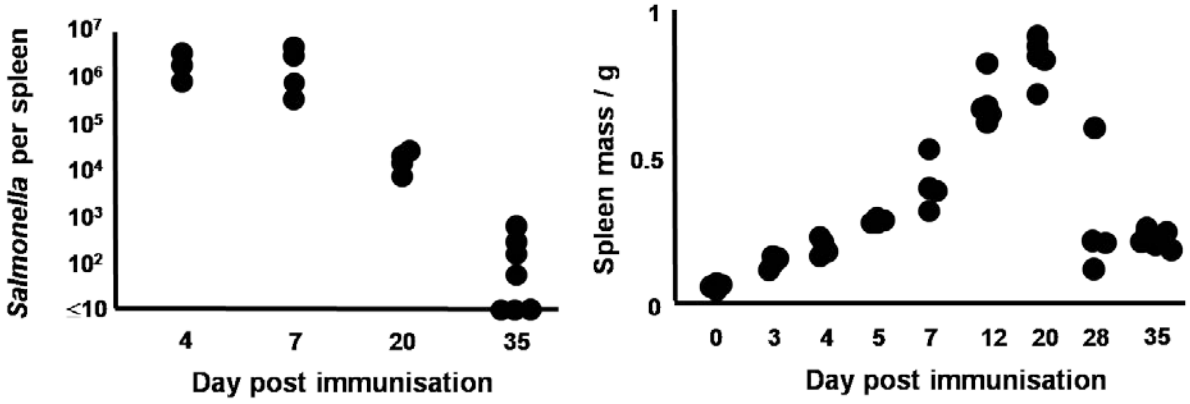

Figure 1.5 Splenic bacterial burden and spleen weight in WT mice before throughout STm infection. Following immunisation with STm, the number of bacteria in the spleen remains high throughout the first week p.i., when the innate system controls the infection (left panel). Bacterial numbers are falling by day 20 p.i. and reach low or undetectable levels by day 35 p.i. Alongside this, splenomegally increases gradually until a peak at day 20 p.i, after which spleen mass begins to recover. By day 35, the spleen weight has not completely recovered, despite only low levels bacteria remaining in the spleen. Figure taken from Cunningham, A.F et al, (2007) *J. Immunol.* **178**: 6200-6207 (70).

1.4 Study Rationale

Extensive use of the mouse typhoid model has significantly advanced our understanding of host-pathogen interactions during *Salmonella* infection, identifying a critical role for $CD4^+$ Th1 cells in the clearance of primary infection (79,217). The role of B cells in *Salmonella* immunity has received increasing attention over the years, not least because of their essential role in protective immunity (226,227). However, primary *Salmonella* infection resolves in the absence of B cells (220), which is somewhat surprising given their active

recruitment and persistent nature during this phase of the response (70,226,227). Furthermore, as discussed previously, the splenic EF and GC response to STm is rather atypical (70). Following infection, a rapid, massive, EF plasma cell response develops in the absence of a concomitant GC response, which is delayed until a month into the infection. This response contrasts with that to typical Th2 antigens, such as alum-ppt protein, where EF and GC responses develop in parallel (70). Whilst a number of model antigen systems are used to study the B cell response to Th2 antigens, antibody responses to Th1 antigens are relatively under-studied and less well understood. Furthermore, whilst model antigens have been instrumental to our understanding of B cell responses *in vivo,* they are limited by their inability to mimic an infection scenario where B cell responses develop within an inflammatory milieu. Thus, understanding the factors that regulate the B cell response during primary *Salmonella* infection will not only further our understanding of protective antibody generation, but also provides an excellent tool for dissecting the B cell response to a viable, Th1 antigen, both within an inflammatory setting and when natural resolution of the infection occurs.

1.4.1 Aims and objectives

The original focus of this project was to establish the role of CD31 in B cell immunity to STm, an area we were keen to pursue following our finding that T cell homeostasis and immunity to STm is severely impaired in $CD31^{-/-}$ mice (203). Unfortunately, we were unable to take the CD31 B cell project as far as anticipated, due to some unforeseen problems with the CD31 colony (discussed in chapter 3). As such, the first results chapter

included here presents data from the CD31 project. Thereafter, we maintained a focus on STm and antibody responses, but broadened the scope of the study to include other factors.

Thus, the overall aim of this thesis was to address the following key question:

How are Th1 GC and EF B cell responses, induced by STm, regulated, and how do they differ from classic, Th2 B cell responses?

In addressing the above question, the realigned objectives of this project were to:

A) Investigate the role of CD31 in B cell responses to STm

B) Investigate the role of classic Th2 cytokines in Th1 antibody responses to STm

C) Investigate the role of the transcription factor T-bet in antibody class-switching during STm infection

CHAPTER 2: MATERIALS AND METHODS

A list of the media and buffers used throughout can be seen in appendix 1. All reagents used were purchased from Sigma-Aldrich (Poole, UK), unless otherwise specified.

2.1 Mice

Mice used for animal studies were age- and sex-matched and were 6-12 weeks old at the beginning of each procedure. Wild type (WT) C57BL6/J mice were obtained from HO Harlan OLAC Ltd. (Bicester, U.K.) and wild type Balb/C mice were sourced from colonies maintained at the Biomedical Services Unit (BMSU) at The University of Birmingham. Genetically modified mice were obtained from colonies bred and maintained under specific pathogen free (SPF) conditions at the BMSU. Generation of $CD31^{-/-}$ (184), $T\text{-}bet^{-/-}$ (71), $IgHkappa^{-/-}$ (232), TCRβδ (233) $IL6^{-/-}$ (234), $IL4^{-/-}$ (235), $IL4R\alpha^{-/-}$ (90), $IL13^{-/-}$ (92), SM1 (236) and EYFP (237) mice have been described previously. Brief descriptions and the original sources are detailed in table 2.1. All experiments were performed with approval from the UK ethics committee.

Table 2.1. Genetically modified mice used herein

Mouse Strain	Description	Source
CD31$^{-/-}$ (C57BL6/J background)	Disruption of the CD31 gene by homologous recombination.	Dr. Susan Nourshargh Imperial College London
T-bet$^{-/-}$ (C57BL6/J background)	Disruption of the T-bet gene by homologous recombination.	Jackson Laboratory
IL6$^{-/-}$ (C57BL6/J background)	Disruption of the IL6 gene by homologous recombination	Charles River Laboratories
IL4$^{-/-}$ (BALB/c background)	Disruption of the IL4 gene by homologous recombination	Professor Manfred Kopf Basel Institute for Immunology
IL4Rα$^{-/-}$ (BALB/c background)	Impaired IL4 and IL-13 signalling by deficiency of the IL-4 receptor alpha chain following Cre-mediated recombination of the IL4-receptor alpha allele through the cre/loxP system.	Professor James Alexander University of Strathclyde
IL13$^{-/-}$ (BALB/c background)	Disruption of the IL13 gene by homologous recombination.	Dr. Andrew McKenzie MRC Laboratory of Molecular Biology, Cambridge
IgH$^{-/-}$kappa$^{-/-}$ (C57BL6/J background)	B-cell deficient. Generated by breeding out the QM IgH transgene from QM mice, which have the other IgH locus inactivated.	Dr. Kai Toellner The University of Birmingham
TCRβδ$^{-/-}$ (C57BL6/J background)	Absent γδ and αβ T cells through targeted deletion of beta and delta TCR genes.	Jackson Laboratory
SM1 (RAG2-deficient, C57BL6/J background)	αβTCR transgenic specific for STm flagellin peptide residues 427-441 bred to Rag-2 deficient mice.	Professor Paul Garside University of Strathclyde.
EYFP (C57BL6/J background	EYFP inserted into the ROSA26 locus preceded by a loxP-flanked stop sequence. Crossing with a Cre transgenic mouse leads to constitutive EYFP expression	Professor Graham Anderson University of Birmingham

2.2 Immunisation Procedures

2.2.1 *Salmonella* Typhimurium (STm)

For infection studies, $5x10^5$ or 10^5 STm strain SL3261 (238) was used throughout. Primary infection was for 7, 20, 35, 42 or 55 days, whilst for vaccination experiments, STm was given as a 4 day infection following primary immunisation with porins, as described in **2.2.4**. STm was prepared by growing a bacterial colony overnight (ON) in sterile L.B medium with shaking (180 revolutions per minute (rpm)) at 37ºC. Bacteria were harvested in mid-exponential phase (optical density (O.D) λ600nm of 0.8-1.0) by centrifugation at 6000 x g for 5 minutes. The bacteria were then washed twice in 1ml sterile PBS with spinning at 6000 x g for 5 minutes, resuspended in sterile PBS (Sigma) and the O.Dλ600nm re-assessed. The O.Dλ600nm was used to quantify the number of bacteria/ml using a growth curve for SL3261. *Salmonella* were then diluted to the desired volume and administered via i.p injection in a volume of 200µl/mouse. At the stated time points p.i, mice were sacrificed and tissues removed for various analyses as indicated in the text.

2.2.2 Soluble FliC (sFliC)

Primary immunisation with 25µg soluble flagella protein FliC (sFliC) was for 7 or 14 days. Secondary boost experiments were performed by giving 25µg sFliC for 35days, followed by a 20µg boost for 4 days. sFliC was routinely prepared by Jessica Hitchcock or Charlotte Cook in conjunction with Dr. Margaret Goodall and has been previously described (239). A detailed protocol can be seen in appendix 2. The resultant antigen was stored at -20ºC. Before use, the antigen was thawed, diluted in sterile PBS and administered i.p in a volume

of 200µl. At the appropriate time point p.i, mice were sacrificed and tissues removed for analysis as indicated in the text.

2.2.3 Alum precipitated protein (alum-protein)

Primary immunisation with 25µg alum-precipitated chicken-γ-globulin (CGG) (Jackson ImmunoResearch Laboratories, Newmarket, UK) (alum-CGG) was for 7 or 14 days. Memory responses to alum-CGG were assessed by an initial immunisation of 25µg alum-CGG for 35 days followed by 20µg soluble NP-CGG for 4 days. Conjugation of NP (Biosearch Technologies, Novato, USA) to CGG was performed by Chandra Raykundalia and has been previously described (240). A detailed description of this methodology can be seen in appendix 3. Alum-CGG was prepared by mixing 150µl of CGG at 5mg/ml with 150µl 9% Alu-Gel-S (alum) (Serva Electrophoresis, Heidelberg, Germany). The pH was adjusted to ≥ 6.5 by adding 6.7-8.3µl of 10M NaOH. The preparation was kept in the dark at room temperature for 30 minutes, with gentle spinning to mix. After incubation, the protein was washed twice with sterile PBS pH 7.4 with spinning at 250 x g for 5 minutes. Protein was then resuspended in sterile PBS to give the desired concentration and administered via i.p injection in a volume of 200µl/mouse. At the stated time points p.i, mice were sacrificed and tissues removed for analysis as indicated in the text.

2.2.4 Porins

Vaccination experiments were carried out by immunising with 20µg porins from STm for 21days, followed by $5x10^5$ STm for 4 or 5 days. In some experiments, porins were given twice, with the second immunisation taking place on day 21 for 14 days, followed by

$5x10^5$ STm for 4 days. Porins were kindly provided by Constantino Lopez Macias (Medical Research Unit on Immunochemistry; Mexico) and prepared by Dr. Cristina Gil as described (13). A detailed protocol is provided in appendix 4. Before use, porins were thawed and kept at 37ºC for 1 hour, before being diluted in sterile PBS and administered i.p in a volume of 200µl/mouse. At the relevant time point p.i, mice were sacrificed tissues removed for the indicated analyses.

2.3 Bone Marrow Chimeras

2.3.1 IL-6 chimeras

Bone marrow chimeras were constructed in which mice lacked IL6 on either radiation-resistant cells or haematopoietic cells. Recipient WT, WT-enhanced yellow fluorescent protein (EYFP) or $IL6^{-/-}$ mice received 9 Grays (Gy) of γ-radiation over 2 doses of 450rads. Donor WT, WT-EYFP or $IL6^{-/-}$ total BM cells were then transferred i.v into recipient mice to make four groups of (donor – recipient) chimeras (WT(EYFP) – WT), (WT(EYFP) – $IL6^{-/-}$), ($IL6^{-/-}$ - WT(EYFP) and ($IL6^{-/-}$ - $IL6^{-/-}$). BM cells were prepared under sterile conditions by flushing the femur and tibia from each leg in 10mls sterile RPMI_1640 media (Sigma). Cells were then centrifuged at 350 x g, resuspended in sterile full culture medium and counted using a haemocytometer. After spinning, cells were washed twice in sterile PBS and resuspended to $5x10^7$/ml. Cells were then administered via i.v injection to recipient mice in a volume of 200µl sterile PBS, giving 10^7 cells/mouse. Tail bleeds were taken from all chimeras at 8 weeks post-transfer, to assess for the elimination of host cells by flow cytometry through the presence or absence of EYFP cells in the blood. After 12

weeks of reconstitution the mice were infected with 10^5 STm. At day 35 p.i, mice were sacrificed and tissues removed for the indicated analyses.

2.3.2 Mixed bone marrow chimeras

Mice lacking T-bet in either T cells (T-bet$^{-/-Tcell}$) or B cells (T-bet$^{-/-Bcell}$) alone were created using a mixed bone marrow chimera system (241). For T-bet$^{-/-Tcell}$ chimeras, TCRβδ$^{-/-}$ mice that lack all T cells were used as recipients, whilst donor BM consisted of 80% TCRβδ$^{-/-}$ BM mixed with 20% T-bet$^{-/-}$ BM. The same principle was applied to the T-bet$^{-/-Bcell}$ chimeras, using IgH$^{-/-}$kappa$^{-/-}$ mice that lack B cells as recipients and IgH$^{-/-}$kappa$^{-/-}$ mice and T-bet$^{-/-}$ mice as donors. The resultant mice therefore lacked T-bet in all T cells or B cells whilst the remainder of the cells were largely T-bet sufficient. For all experiments, control mice were constructed by substituting the T-bet$^{-/-}$ BM with WT BM. Donor BM cells were prepared as described in **2.3.1**. Once prepared, cells from the TCRβδ$^{-/-}$ or IgHkappa$^{-/-}$ suspension were mixed with cells from either the WT or T-bet$^{-/-}$ suspension at a ratio of 80:20. A total of 10^7 cells were then administered i.v to recipient mice that had received 8 Gy of γ-radiation over 2 doses of 400rads, in a volume of 200µl sterile PBS. Tail bleeds were taken from all chimeras at 6 weeks post cell transfer, to assess for reconstitution by flow cytometry. Mice were infected with 10^5 STm at 10 weeks post transfer or remained uninfected as controls. At day 7 or 35 p.i, mice were sacrificed and spleens were removed for various analyses as outlined in the text.

2.4 SM1 T Cell Transfer

SM1 T cell transfer experiments were carried out, in order to enhance the number of antigen specific T cells in WT and T-bet$^{-/-}$ mice prior to immunisation with sFliC (2.2.2). Spleens were removed from SM1 mice and prepared for fluorescence activated cell sorting (FACS) under sterile conditions. Spleen cells were obtained by teasing the tissue through a 70µm pore cell strainer and rinsing the filter through with 5mls of full culture medium. Cells were then centrifuged at 350 x g for 10 minutes and the red blood cells lysed using ACK buffer. Following centrifugation at 350 x g for 10 min, cells were resuspended in blocking buffer, and kept on ice for 30 minutes. After centrifugation, antibodies targeting non-T cells were added to the sample at the desired dilution (table 2.2) in 2% BSA/PBS. The antibody targets were Gr1, F480, CD11c, CD11b, NK1.1. This was done to eliminate as many non-T cells as possible (SM1 do not have B cells-see table 2.1) during sorting, thus enriching the T cell population without directly labelling the cells with antibody. After incubation on ice for 30 minutes, unlabelled antibody was removed by washing twice with sterile PBS and centrifugation at 350 x g for 10 minutes. Cells were then resuspended in 300µl RPMI_1640 supplemented with 10% FCS and filtered to remove clumps. Unlabelled cells were collected by Roger Bird using a MoFlo high speed cell sorter (Dako, Ely, UK). After sorting, cells were washed x 2 in sterile PBS with centrifugation at 350 x g. Cells were then resuspended in sterile PBS to give $1.5x10^6$ cells/200µl, and transferred i.v into WT or T-bet$^{-/-}$ recipients. Subsequent staining of the sorted cell population revealed that ≥ 96% of the transferred cells were T cells. 24hr post-transfer, mice that had received cells were immunised with 25µg sFliC (2.2.2), alongside a second group of control WT and T-bet$^{-/-}$ mice that had not received cells. At 14d p.i, all mice were sacrificed and blood was collected for measurement of serum antibody.

2.5 Bacterial Culture

Upon sacrifice of STm infected mice, spleens were removed and weighed and a portion was used to enumerate the total number of bacteria per spleen. This was achieved by teasing the portion of spleen through a 70µm pore cell strainer (BD Biosciences, Oxford, UK), rinsing the filter through with 1ml sterile RPMI (Sigma) and diluting appropriately. 100µl of the culture was then transferred onto an agar plate and spread until dry. The plates were incubated ON at 37ºC and bacterial colonies per plate were counted. Numbers were adjusted to the dilution and the spleen weight to give the total colony forming units (CFU) per spleen.

2.6 Flow Cytometry

Single cell suspensions from the spleen and peritoneal cavity were prepared for flow cytometry. Peritoneal exudate cells were collected from mice by peritoneal lavage in 5mls PBS and diluted in 5mls RPMI_1640. Spleen cells were obtained by teasing the tissue through a 70µm pore cell strainer and rinsing the filter through with 5mls RPMI_1640. Cells were then centrifuged at 350 x g for 10 minutes, the red blood cells lysed where appropriate using ACK buffer and counted using a haemocytometer. Cells were resuspended to $1x10^7$/ml in RPMI_1640 and 10^6 cells/sample added to FCS-coated 96-well flexie-plates (BD Biosciences, Oxford, UK). Plates were centrifuged at 350 x g for 10 minutes and blocked in blocking buffer for 30 minutes on ice. After centrifugation and where necessary, biotinylated antibodies were diluted appropriately (table 2.2) in 2% BSA/PBS and added to the cells for 30 minutes on ice. Following incubation, cells were washed twice in cold PBS and secondary and directly conjugated antibodies were added

(table 2.2) at the appropriate dilution for 30 minutes on ice. Cells were then washed twice in cold PBS with centrifugation at 350 x g for 4 minutes and resuspended in 100µl of 2% BSA/PBS. Cells were added to FCS-coated FACS tubes containing 200µl of 2% BSA/PBS and analysed using a CyAn ADP flow cytometer (Dako, Ely, UK).

Table 2.2. Primary, secondary and directly conjugated antibodies for flow cytometry

Target	Fluorochrome	Supplier and clone.	Stock concentration	Dilution
Mouse CD31	Biotin	AbD Serotec (Oxford, UK) ER-MP12	0.1mg/ml	1:100
Biotin	Streptavidin PE-Texas Red	BD Biosciences (Oxford, UK)	0.2mg/ml	1:1000
Mouse CD21	APC	BD Biosciences 7G6	0.2mg/ml	1:300
Mouse CD23	PE	BD Biosciences B3B4	0.2mg/ml	1:200
Mouse CD5	FITC	eBioscience (Hatfield, UK) 53-7.3	0.5mg/ml	1:100
Mouse IgM	PECy7	e-Bioscience II/41	0.2mg/ml	1:100
Mouse B220	efluor 450	eBioscience RA3-6B2	0.2mg/ml	1:100
Mouse B220	FITC	eBioscience RA3-6B2	0.5mg/ml	1:100
Mouse CD19	APC	BD Biosciences ID3	0.2mg/ml	1:300
Mouse CD19	APC-Cy7	BD biosciences ID3	0.2mg/ml	1:300
Mouse CD8	FITC	eBioscience	0.5mg/ml	1:100

		53-6.7		
Mouse CD62L	PE	eBioscience MEL14	0.2mg/ml	1:300
Mouse CD3	APC	eBioscience 145-2C11	0.2mg/ml	1:100
Mouse CD4	eFluor 450	eBioscience RM4-5	0.2mg/ml	1:100
Mouse Gr1	FITC	eBioscience RB6-8C5	0.5mg/ml	1:100
Mouse F480	FITC	eBioscience BM8	0.5mg/ml	1:100
Mouse NK1.1	FITC	eBioscience PK136	0.5mg/ml	1:100
Mouse CD11b	FITC	eBioscience M1/70	0.5mg/ml	1:100
Mouse CD11c	FITC	eBioscience N418	0.5mg/ml	1:100

2.7 Immunohistochemistry

2.7.1 Sectioning

Spleens for sectioning were snap frozen in liquid nitrogen following removal and stored at -80ºC. Frozen spleens were cut using a cryostat. Spleens were mounted in O.C.T. compound (Sakura Finetek, Zoeterwoude, NL) and trimmed at 25µm until the white pulp area was clearly visible. 5µm sections were cut from the spleen and mounted onto 4-spot slides (Hendley, Essex, UK). Sections were left to dry for 30 minutes, fixed in cold acetone for 20 minutes and air dried for 10 minutes. Slides were then stored at -20ºC until further use.

2.7.2 Staining

Prior to staining, slides were defrosted at room temperature and washed in Tris buffer pH 7.6. Primary antibodies were then added at 75µl/section at the appropriate dilutions (table 2.3). Of note, C57BL/6 mice express the IgG2c allotype as opposed to IgG2a. The anti-mouse IgG2a antibody used for histology staining (table 2.3) was raised against a mixture of IgG2a and IgG2c antibodies, and is therefore appropriate for the detection of both the IgG2a and IgG2c allotypes (see product technical data sheet). Slides were incubated for 1h in a moist chamber and then washed twice in Tris buffer pH 7.6. Normal mouse serum (NMS) was diluted 1:10 in Tris buffer 7.6 and absorbed with secondary antibodies where appropriate (table 2.4), specific to the species of the primary antibody. Secondary antibodies were either biotinylated (bt) or horseradish peroxidase (HRP)-linked. These were added at 75µl/section, incubated for 45 minutes in a moist chamber and then washed in Tris buffer pH 7.6. When staining for FliC positive cells only, an additional step was included in between the primary and secondary antibody stage; 75µl of sheep anti-biotin was added to the sections, diluted 1/800 in Tris buffer 7.6, for 45 min. The AP complex (ABComplex, Vector Laboratories) was made by adding 10µl of avidin and 10µl bt AP to 1ml Tris buffer 7.6 and allowing to mix for 30 minutes. The complex was added at 75µl/section, followed by a 40 minute incubation in a moist chamber. Slides were then washed twice in Tris buffer pH 7.6 and developed using peroxidise and AP substrates (see appendix 1) to give brown and blue staining respectively. The peroxidise substrate was added first, until the desired positivity was obtained. Slides were then washed in Tris buffer pH 7.6 before addition of the AP substrate. Once developed, slides were washed in Tris buffer pH 7.6, rinsed in dH_2O and air-dried at room temperature before mounting using immunomount (Thermo Electron Corporation, Pittsburgh).

2.7.3 Quantification of cell numbers and densities

GC areas were quantified using a point counting method (242), in which all intersections of a $1cm^2$ graticule occupied by GC and/or by follicle were counted, except for the farthest right and bottom intersections. This was repeated in several fields of view, covering the whole tissue section. The proportion of follicle occupied by GC was calculated based on these counts. To quantify total GC volume, the average number of intersections occupied by GC in each field of view was calculated and adjusted for magnification, giving the fraction of tissue occupied by GC. The percentage per mm^2 occupied by the tissue was then calculated and applied to the total spleen. The spleen weight was converted into a volume, based upon the assumption that 1g of tissue is equal to $1cm^3$. The proportion of spleen occupied by GC could then be expressed as a volume.

Cell numbers were quantified by counting all positive cells within the $1cm^2$ graticule. This was repeated in several fields of view, covering the whole tissue section. The mean number of cells per mm^2 was then calculated, based upon the magnification used.. Counts were adjusted to spleen weight by multiplying the number of cells/cm^3 by the spleen weight, based upon the assumption that 1g is equal to $1cm^3$. Published data from our laboratory has shown that the quantification of class- switched plasma cells by intracellular IgG flow cytometry staining, returns similar numbers to those produced using the histological counting method (243).

Table 2.3. Primary and directly conjugated antibodies used for immunohistology

Antibody Target	Species	Dilution	Source and clone
IgM	Rat	1/600	AbD Serotec LO-MM-9
IgD	Sheep	1/1000	Abcam (Cambridge, UK) Polyclonal
IgG1	Rat	1/300	AbD Serotec LO-MG1-2
IgG2a	Rat	1/200	BD Biosciences R11-89
IgG2b	Rat	1/200	AbD Serotec LO-MG2b-2
Biotinylated peanut agglutinin (PNA)	Goat	1/200	Vector Laboratories (Peterborough, UK)
Biotinylated sFliC	STm	1/400	The University of Birmingham
Biotinylated CGG	Chicken	1/300	Biotinylated at The University of Birmingham
NP	Conjugated to sheep IgG	1/2500	Conjugated to sheep IgG at the University of Birmingham

Table 2.4. Secondary antibodies used for immunohistology staining

Antibody	Species	Dilution	Source
Anti-sheep (Px)	Donkey	1/100	The Binding Site (Birmingham, UK)
Anti-sheep (Bt)	Donkey	1/100	The Binding site
Anti-rat (Bt)	Rabbit	1/600	Dako
Anti-rat (Px)	Rabbit	1/80	Dako

2.8 Confocal Microscopy

The presence of Tfh cells in the spleens of uninfected and *Salmonella* infected mice was assessed by confocal microscopy. Tissues were sectioned as described in **2.7.1** and frozen at -20ºC until further use. Before staining, slides were defrosted at room temperature and rehydrated in PBS for 10 minutes. All subsequent steps were carried out in a moist

chamber protected from the light, at room temperature. Slides were first blocked in 75µl/spot of 10% normal horse serum (NHS)/PBS for 10 minutes. Slides were then washed 2x in PBS for 5 minutes before addition of the primary antibody for 1hr, diluted to the optimal concentration (see table 2.5) in 10%NHS/PBS. After washing a further 2 times in PBS, the appropriate secondary antibodies (see table 2.6) were added to the slides for 1hr, followed by washing x 2. All spots then received 75µl of anti-FITC 488 (Invitrogen) at a dilution of 1/200 was then added to the slides for 30 mins before washing x 2 in PBS. Slides were then incubated in Hoescht 33258 nuclear counterstain (Sigma) for 2 minutes, washed, and mounted with a coverslip using glycerol containing anti-fade reagent DABCO (Sigma). Slides were then wrapped in aluminium foil and stored at -20ºC until analysis. Staining was visualised on an LSM510 confocal microscope (Zeiss, Germany) and images taken using Zeiss LSM image software (Zeiss).

Table 2.5 Primary antibodies used for confocal microscopy staining

Target	Species	Concentration	Dilution	Source and clone
Mouse CD3	Armenian hamster	0.5mg/ml	1:200	BD biosciences 145-2C11
Mouse PD1	Rat	0.5mg/ml	1:200	Biolegend (Cambridge, UK) RMP1-14
Mouse Bcl6	Rabbit	0.2mg/ml	1:30	SantaCruz (Heidelberg, Germany) N3
-	Armenian hamster IgG	0.5mg/ml	1:200	eBioscience
-	Rat IgG2a	0.5mg/ml	1:200	Biolegend
-	Rabbit IgG	0.5mg/ml	1:30	Cambridge Bioscience (Cambridge, UK)

Table 2.6 Secondary antibodies used for confocal microscopy staining

Target	Species	Concentration	Dilution	Source
Rabbit	Donkey (FITC)	1.2mg/ml	1/300	Jackson Laboratories
Armenian hamster	Goat (Cy5)	1mg/ml	1/100	Jackson Laboratories
Rat	Donkey (Cy3)	1mg/ml	1/150	Jackson Laboratories

2.9 Enzyme-Linked Immunosorbent Assay (ELISA)

Relative antigen-specific serum antibody titres were assessed by ELISA. Peripheral blood was obtained by cardiac puncture from WT and gene knockout mice at various days after infection or immunisation with the antigens described. Blood was allowed to clot at room temperature and serum was separated from blood cells by spinning at 6500 x g for 10 minutes. Serum was aliquoted and frozen at -80 ºC until further use. To assess for STm-specific antibody, an outer membrane protein (OMP) preparation was used to coat ELISA plates (MaxiSorp plates, Nunc) at 5µg/ml coating buffer. The OMP preparation was prepared by Jessica Hitchcock or Charlotte Cook and has been described (244). For a detailed description of this preparation see appendix 5. Soluble FliC (**2.2.2)** was used to coat ELISA plates at 5µg/ml coating buffer. Detection of anti-CGG and anti-NP antibody was achieved by coating plates with 5µg/ml CGG or NP_{15}BSA. After an overnight incubation at 4°C, plates were washed x 3 in PBS and blocked for 1h at 37°C in 100µl 1% BSA/PBS to prevent non-specific binding. After incubation, plates were washed x3 in PBS. Sera were diluted in PBS/1% BSA/0.05%Tween 20 and added to each row in four-fold serial dilutions. Plates were then incubated for 1h at 37°C followed by washing x3. AP-linked goat anti-mouse IgM, IgG2a, IgG2b, or IgG1 (all from Southern Biotechnology

Associates, Birmingham, USA) were added to the appropriate wells, diluted in PBS/1% BSA/0.05%Tween 20 at 1:1000 and incubated for 1h at 37°. Plates were then washed x3 and antibodies detected using 100µl/well Sigma fast p-Nitrophenyl phosphate solution. Plates were incubated at 37°C to develop the colour reaction and O.D were read at 405nm using the softmax Pro programme. Relative antibody titres were determined by plotting the dilution against the O.D values and taking the dilution of each sample at a constant O.D value, set in the mid-exponential phase of the curve.

2.10 Real-Time Reverse Transcriptase Polymerase Chain Reaction (RT-PCR)

2.10.1 RNA Extraction and generation of a cDNA template

Cell sorting of purified cells for RNA extraction were obtained by FACS, which was kindly carried out by Roger Bird. Cells were prepared for sorting as described in **2.5**. From the mixed bone marrow chimeras, $2x10^5$ $CD19^+$ $B220^+$ B cells and $2x10^5$ $CD3^+$ T cells were isolated from each chimera. For $IL6^{-/-}$ mice at day 30 and 42 p.i, $2x10^5$ $CD19^+$ $B220^+$ B cells and $2x10^5$ $CD3^+$ $CD4^+$ T cells were isolated from each mouse. Following isolation, cells were pelleted, washed and immediately lysed in buffer RLT from the Qiagen RNeasy mini kit (Qiagen UK). Cell lysates were stored at -80ºC until further use. Prior to RNA extraction, lysates were thawed and RNA extracted using the RNeasy micro kit as per the manufacturer's instructions. RNA was eluted in H_2O and immediately reverse transcribed

to yield a cDNA template. Reverse transcription was carried out using the Superscript Vilo cDNA synthesis kit (Invitrogen) according to the manufacturer's guidelines. Reverse transcription was carried out on Techne 312 Thermal Cycler PCR machine using the following conditions: 25ºC for 10 min, 42ºC for 120 min, 85ºC for 5 min. The concentration of cDNA in each sample was measured on a Nanodrop 100 spectrophotometer (Thermo Scientific, Wilmington, USA) and the template was subsequently diluted to a concentration of 100ng/µl, before storing at -80ºC.

2.10.2 RT-PCR

Relative expression of the gene of interest to β-actin message was quantified by TaqMan RT-PCR. Reactions were carried out in a 96-well optical reaction PCR plate in a final volume of 20µl. The reaction mix contained a forward primer, a reverse primer and a probe, specific to both the gene of interest and the housekeeping gene (β-actin). These were diluted to their optimal pre-determined working concentrations. Probes for the house-keeping and target gene were labelled with VIC and FAM, respectively. 10µl of 2 x ABI PCR master mix (Applied Biosystems, Warrington, U.K) was also added to each reaction, along with 2µl of cDNA template and the volume was made up to 20µl using RNase free H_2O (Qiagen, UK). Primer sequences can be viewed in table 2.7. TaqMan probes and primers were designed using Primer Express computer software (Applied Biosystems, Warrington, U.K) and synthesised by Eurogentec. Before running the reaction, the plate was sealed using a MicroAmp™ Clear Adhesive Film and centrifuged for 1 min at 350 x g. The reaction was run using standard TaqMan PCR conditions on a 7900 qPCR machine (Applied Biosystems, Warrington, U.K). Relative quantification of signal per cell or tissue

was achieved as described (93). Briefly, fluorescent thresholds were set within the logarithmic phase of the PCR for the house-keeping gene and the target gene, and the cycle number at which the threshold was reached (C_T) was determined. The C_T for the target gene was subtracted from the C_T for the house-keeping gene to give ΔC_T. The ΔC_T of a fixed sample was then subtracted from all ΔC_T within the experiment to give $\Delta\Delta C_T$. The relative amount was calculated as $2^{-\Delta\Delta CT}$.

Table 2.7 Primer and probe sequences for RT-PCR

Gene	Forward Primer	Reverse Primer	Probe
B-actin	CGTGAAAAGATGACCCAGATCA	TGGTACGACCAGAGGCATACAG	TCAACACCCCAGCCATGTACGTAGCC
IFNγ	TCTTCTTGGATATCTGGAGGAACTG	GAGATAATCTGGCTCTGCAGGATT	TTCATGTCACCATCCTT
γ2a germline-switch transcripts	GGAACACTAAAGCTGCTGACACAT	AACCCTTGACCAGGCATCCT	AGCCCCATCGGTCTATCCACTGGC
Bcl-6	GCCAGGCAAGTCCCTAATGA	CGAGTAGATGTTGCTGTGACACAA	CCAGCCATGGAGGTGTCCCCC
AID	GTCCGGCTAACCAGACAACTTC	GCTTTCAAAATCCCAACATACGA	TGCATCTCGCAAGTCATCGACTTCGT

2.11 Statistical Analysis

Differences between the medians of two groups were calculated using the two-tailed, non-parametric Mann-Whitney sum of ranks test. All p values were calculated using the statistics programme included in GraphPad Prism version 4.0, and p values of ≤ 0.05 were accepted as significant. The majority of experiments were performed at least twice, to check for consistency in results. Where experiments were not repeated, this is indicated in the figure legend.

CHAPTER 3: B CELL IMMUNITY TO STM IN CD31$^{-/-}$ MICE

3.1 Introduction

The adhesion, signalling receptor CD31 is involved in numerous immune processes, including adhesion, migration, apoptosis regulation and the regulation of lymphocyte activation. As a multi-functional molecule and negative regulator of cellular processes, a role for CD31 in controlling the balance between appropriate and excessive immune activation, has previously been considered. Taken together, these studies conclude that CD31 deficiency results in a poorer prognosis when placed under conditions of immunological stress (200,201) or autoimmunity (176,177,197,200,201,245). Despite a clear role in regulating inflammation and lymphocyte activation, no studies had assessed the contribution of CD31 to a normal resolving infection, such as STm. Immunity to STm infection involves complex interactions between innate and adaptive immune cells, as well as the proliferation and survival of effectors, within a highly inflammatory environment. Clearance of primary STm infection is dependent upon $CD4^+$ T cells, whilst B cells are rapidly recruited to the primary response and are essential for protective immunity. Such a model allows the role of CD31 in multiple elements of the immune response to be assessed.

CD31 was first identified on the surface of B cells almost 20 years ago (246) and later identified as a negative regulator of B cell signalling (202,247). An autoimmune B cell phenotype has now been described in CD31$^{-/-}$ mice, including fewer peripheral B2 cells,

elevated numbers of peritoneal B1a cells, high titres of anti-nuclear antibodies (ANAs) and a systemic lupus erythematosus (SLE)-like disease with age (202). This phenotype reflects that of other B cell-inhibitory receptor knock-out mice (248). A breakdown of B cell tolerance within the periphery (245) has also been reported in $CD31^{-/-}$ mice.

During my MSc degree, we began to assess the role of CD31 in T cell immunity to STm (203). The ability of $CD31^{-/-}$ mice to resolve STm infection was assessed by quantifying the bacterial load in the spleen at various time points p.i. Strikingly, $CD31^{-/-}$ mice were unable to effectively resolve infection, the defect being consistent with times when $CD4^{+}$ T cells contribute to bacterial clearance. T cell-depletion studies revealed that a loss of CD31 on $CD4^{+}$ T cells was accountable, in the large part, for this failure to resolve. The T cells from $CD31^{-/-}$ mice had a heightened proliferative capacity, coupled with a greater propensity to undergo apoptosis, resulting in defective accumulation in the spleen during infection. We therefore concluded that CD31 on T cells regulates T cell homeostasis during STm infection, allowing for effective coordination of T cell immunity (203).

During these studies it became apparent that CD31 loss also affected B cell homeostasis both before and during infection. The *in vivo* data addressing normal B cell immunity in $CD31^{-/-}$ mice is limited. One study measured antibody responses to a model Th2 antigen, reporting no defect in IgM production or isotype switching in $CD31^{-/-}$ mice (202), however B cell responses during a resolving infection have not been studied. Thus, the aim of this chapter is to assess the role of CD31 in primary B cell responses to STm infection, as well as in protective immunity.

3.2 Results

3.2.1 Defective bacterial clearance in CD31$^{-/-}$ mice

The defect in bacterial clearance in CD31$^{-/-}$ mice (203) is shown in figure 3.1. WT and CD31$^{-/-}$ mice were infected with $5x10^5$ STm and splenic bacterial burden was assessed at various time points p.i. From one week after infection, splenic bacterial numbers began to fall in WT mice, and infection had largely resolved by day 42 p.i. In contrast, there was a severe delay in bacterial clearance in CD31$^{-/-}$ mice, so that at day 20, 35 and 42 p.i, the bacterial burden was significantly greater than that of WT mice ($p \leq 0.05$).

3.2.2 Uninfected CD31$^{-/-}$ mice have altered splenic B cell numbers

Whilst investigating the T cell responses to STm, immunohistological staining of spleen sections revealed some B cell abnormalities in resting CD31$^{-/-}$ mice. These included reduced numbers of follicular B2 cells, a near absence of MZ B2 cells (figure 3.2A) and an increased frequency of GC within the B cell follicles (figure 3.2B). These observations led us to study the impact of infection upon B cell-expressed CD31, and the effect of its loss upon B cell homeostasis during infection and following vaccination.

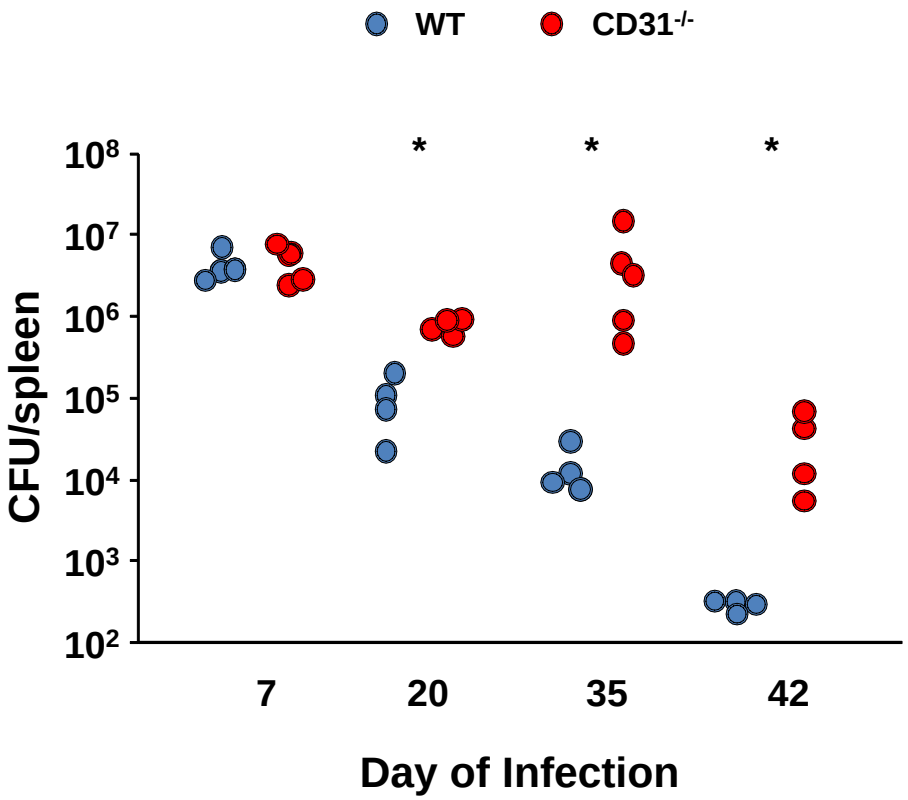

Figure 3.1. Bacterial burden in WT and CD31$^{-/-}$ mice during infection with STm. WT and CD31$^{-/-}$ mice were infected with 5x10^5 STm and the number of colony forming units (CFU) per spleen were quantified at various days p.i. Data are representative of ≥ three experiments giving similar results. * $p \leq 0.05$.

A.

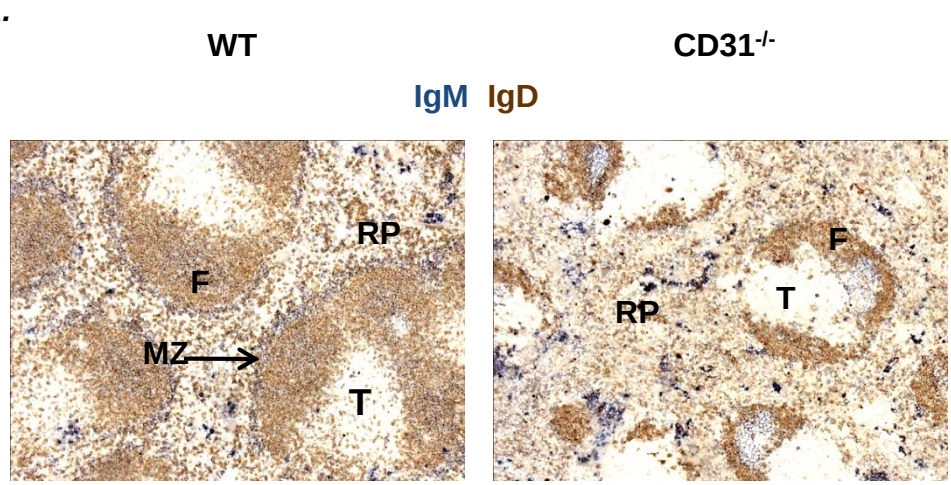

B.

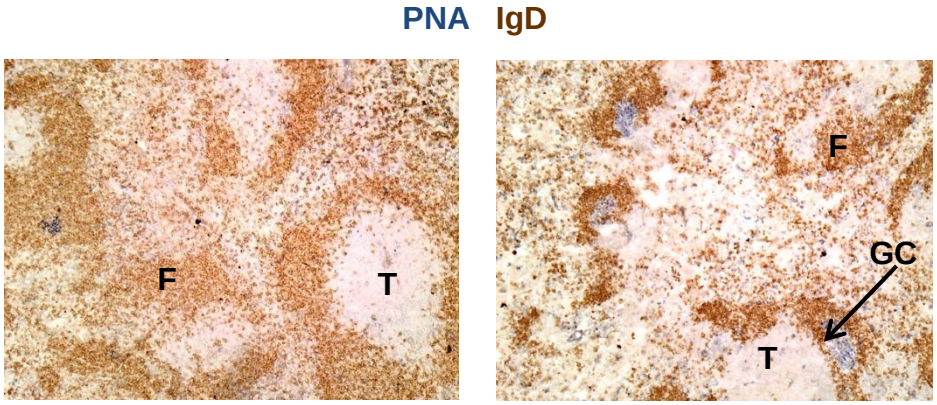

Figure 3.2 Splenic architecture and organisation in resting WT and CD31$^{-/-}$ mice. Uninfected mice were sacrificed and spleen sections were stained with ***A*****,** IgM (blue) to identify MZ cells and IgM^{+} plasma cells and IgD (brown) to identify mature B cells ***B,*** PNA (blue) to identify GC and IgD (brown) to identify mature B cells. Photos are representative of at least 8 mice per time point. GC = germinal centre; T = T cell zone; F = B cell follicle; RP = Red pulp; MZ = marginal zone.

3.2.3 CD31 is expressed on all B cell subsets before and during STm

Before assessing the B cell response to infection in $CD31^{-/-}$ mice, CD31 expression was measured on WT B cells by flow cytometry. CD31 expression has previously been reported on all murine peripheral B cells (202), however subset-specific differences and the impact of infection upon expression levels have not been addressed. As the spleen and peritoneal cavity are important sites of B1 and B2 cell responses during STm infection, CD31 expression on B cells from these sites was assessed. Recirculating B2 cells were identified by their $IgM^{+}CD19^{+}B220^{+}CD5^{-}CD23^{+}CD21^{int/lo}$ phenotype, whilst splenic MZ cells were identified as $IgM^{+}CD19^{+}B220^{+}CD5^{-}CD23^{lo}CD21^{hi}$ (figure 3.3A). By day 7 of infection, there was a peak in CD31 expression on recirculating B2 cells from the spleen, and peritoneal cavity (figure 3.3B left panel). In the spleen, CD31 expression remained higher than uninfected levels at all time points studied p.i, whilst it returned to background levels after day 7 p.i on recirculating cells in the peritoneal cavity (figure 3.3B left panel). As with recirculating B cells in the spleen, CD31 expression increased on MZ B cells by day 7 of infection, remaining elevated thereafter (figure 3.3B right panel). Thus, the overall pattern of CD31 expression on B2 cells was a tendency to increase after infection.

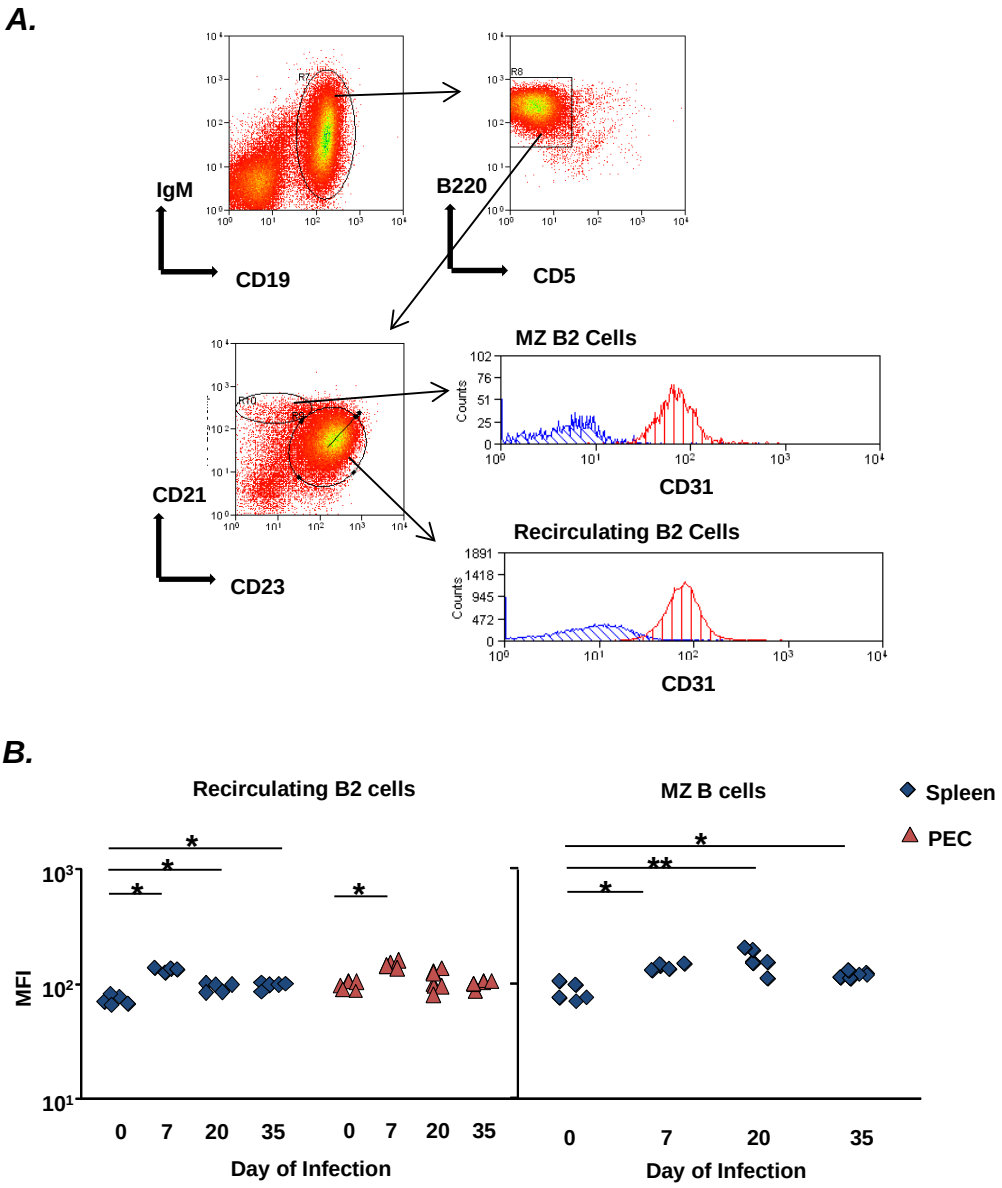

Figure 3.3. CD31 expression on recirculating and MZ B2 cells before and after STm infection. ***A.*** Representative flow cytometry staining of WT splenocytes, showing the gating procedure for recirculating B2 cells, identified as $IgM^{+}CD19^{+}B220^{+}CD5^{-}CD23^{hi}CD21^{int}$ and MZ B2 cells, identified as $IgM^{+}CD19^{+}B220^{+}CD5^{-}CD23^{lo}CD21^{hi}$. CD31 expression on each population is shown (red) alongside the isotype control (blue). ***B.*** CD31 expression on recirculating B2 cells (left panel) and MZ B2 cells (right panel) before and at the indicated time points after infection. CD31 expression data are from 2 experiments per time point. One point represents one mouse. MFI = median fluorescence intensity. PEC = peritoneal exudate cells. * $p \leq 0.05$; ** $p \leq 0.01$

B1a and B1b cells were identified as $IgM^{+}CD19^{+}CD23^{lo}CD21^{lo}B220^{int}CD5^{hi}$ and $IgM^{+}CD19^{+}CD23^{lo}CD21^{lo}B220^{lo}CD5^{lo}$ respectively. An example of the gating strategy for the identification of B1 cells in the peritoneal cavity is shown in figure 3.4A. CD31 expression increased on B1a cells from the spleen and peritoneal cavity by day 7, fell again by day 20 p.i and increased by day 35 (figure 3.4B left panel). CD31 expression pattern on B1b cells in the peritoneal cavity was higher than background levels at day 7, but similar to uninfected levels at day 20 and 35 p.i. (figure 3.4B right panel). Thus, there was a tendency to increase CD31 expression on all B1 cells during the early stages of infection, and aside from a dip in expression on B1a cells at day 20 p.i, expression was otherwise similar to background levels. Overall, CD31 expression was maintained on all B cell subsets during infection. We next assessed the impact of CD31 loss upon B cell numbers before and during STm infection.

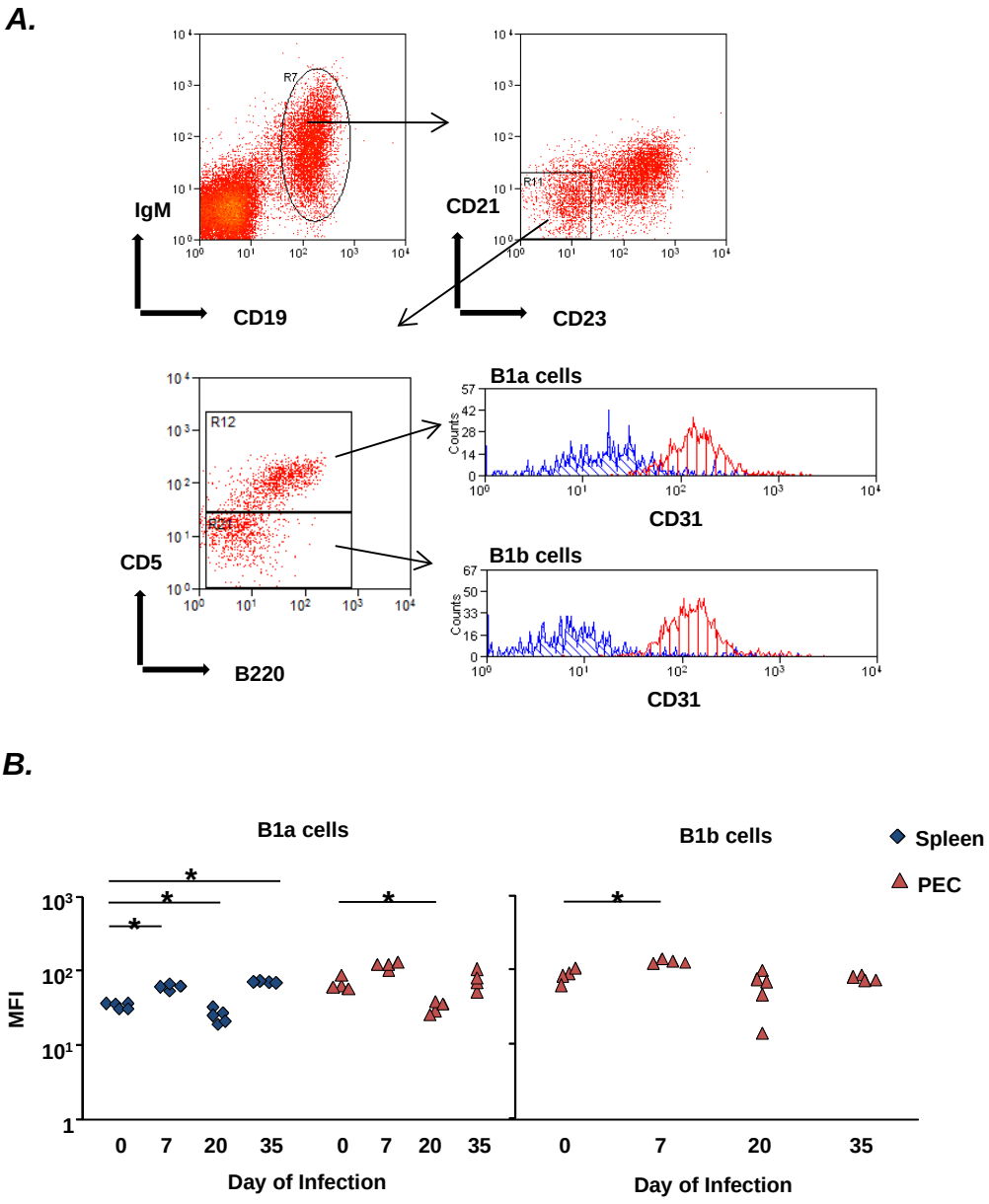

Figure 3.4. CD31 expression on B1 cells before and during STm infection. ***A.*** Representative flow cytometry staining of WT PEC cells showing the gating procedure for B1a cells, identified as IgM^{+}CD19^{+}CD23^{lo}CD21^{lo}B220^{int}CD5^{hi}, and B1b cells, identified as IgM^{+}CD19^{+}CD23^{lo}CD21^{lo}B220^{lo}CD5^{lo}. CD31 expression on each population is shown (red) alongside the isotype control (blue). ***B.*** CD31 expression on splenic and peritoneal exudate B1a cells (left panel) and peritoneal exudate B1b cells (right panel) before and at the indicated time points after infection. Expression data are from 2 experiments per time point. One point represents one mouse. *p ≤0.05

3.2.4 Loss of CD31 negatively impacts upon B2 but not B1 cell numbers.

The individual B cell subsets were identified by flow cytometry according to the staining protocols shown figures 3.3 and 3.4. Consistent with our earlier observations (figure 3.2), fewer recirculating B2 cells were observed in the spleen ($p \leq 0.05$) and peritoneal cavity ($p \leq 0.05$) of resting $CD31^{-/-}$ mice when compared to WT mice (figure 3.5A and Bi). Prior to infection, splenic MZ B cell numbers were also markedly impaired in $CD31^{-/-}$ mice, the reduction compared to WT mice being almost 100-fold ($p \leq 0.05$) (figure 3.5A and Bii).

During infection, the proportion of recirculating B2 cells in the spleen reduced dramatically in WT and $CD31^{-/-}$ mice (figure 3.5A). However, the massive expansion in spleen size allowed overall numbers to remain fairly consistent over the time-course in WT mice, although there may have been an increase in numbers between day 35 and 42 p.i (figure 3.5Bi). A similar pattern was observed in $CD31^{-/-}$ mice, aside from a dip at day 35 p.i, which had recovered by day 42 p.i. At each time point, $CD31^{-/-}$ mice had significantly lower numbers of recirculating B2 cells in the spleen when compared to WT mice ($p \leq 0.05$) (figure 3.5Bi). Splenic MZ B cell numbers were less consistent in WT mice throughout infection, with a ten-fold reduction in cell numbers occurring by day 20 p.i (figure 3.5A and Bi). MZ B cell numbers remained low on day 35 p.i but had recovered to pre-infection levels in WT mice by day 42 p.i (figure 3.5Bii). In contrast, the reduced numbers of MZ B cells in resting $CD31^{-/-}$ spleens persisted throughout infection (figure 3.5A and Bii), being significantly lower than in WT mice at day 7 and 42 p.i ($p \leq 0.05$) (figure 3.5Bii).

Numbers of recirculating peritoneal B2 cells did not alter markedly in WT mice over the time course, however a slight increase in numbers was observed once the infection had resolved (figure 3.5Biii). A different pattern was observed in $CD31^{-/-}$ mice, where an increase in cell number was observed between day 0 and 7. After this, cell numbers fell again and were significantly reduced below WT numbers at day 20 and 35 pi ($p \leq 0.05$). Similar to WT mice, there was an increase in cell number between day 20 and 42 p.i. It is noteworthy that the accuracy of B cell number quantification in the peritoneal cavity is hampered somewhat by the technicalities of obtaining peritoneal washes, which may account for some of the variability in B cell numbers in $CD31^{-/-}$ mice. Overall however, defects in B2 cell numbers were seen consistently in $CD31^{-/-}$ mice in the two sites before and during STm infection.

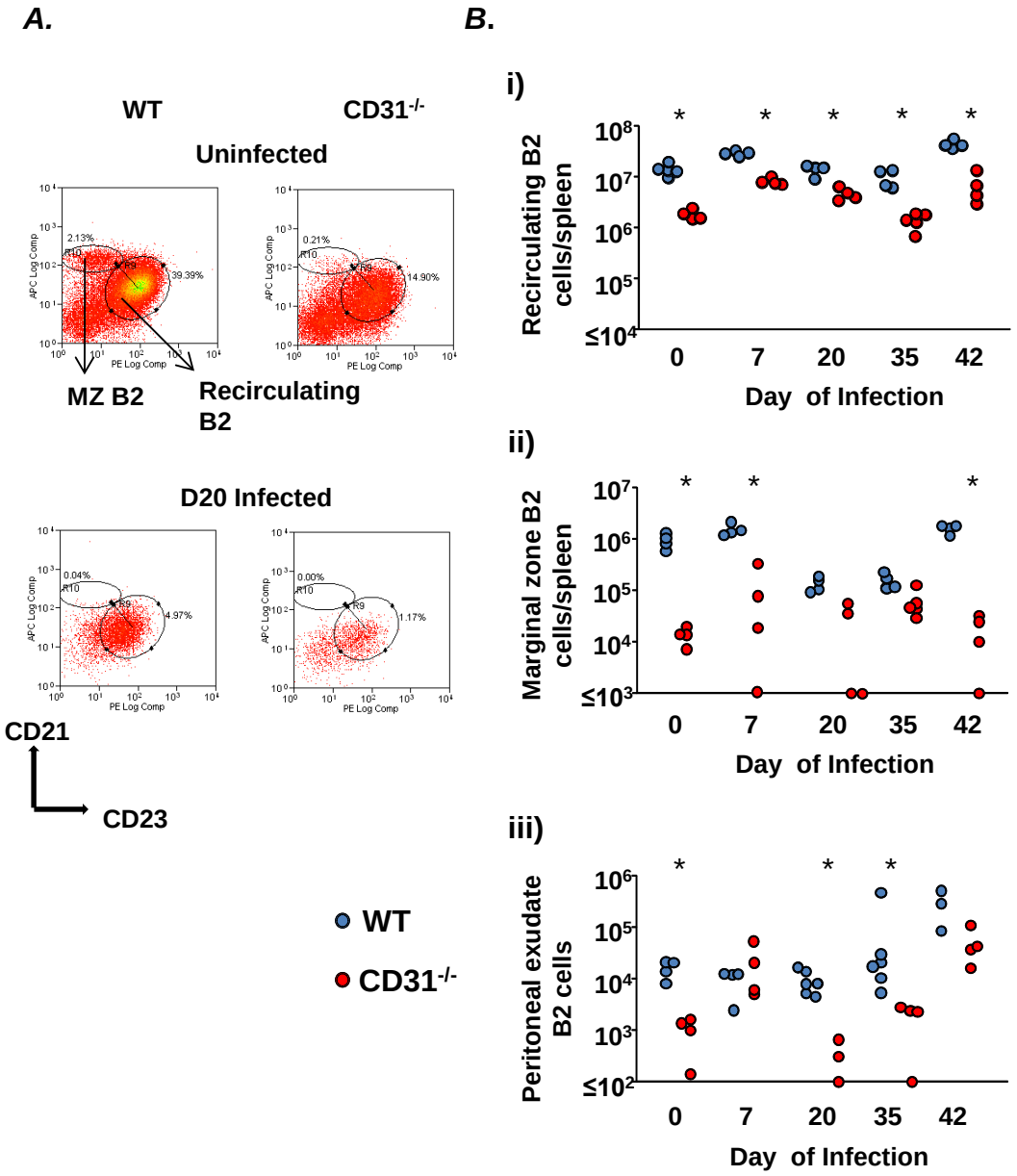

Figure 3.5. Splenic and peritoneal B2 cells in WT and CD31$^{-/-}$ mice before and after STm infection. WT and CD31$^{-/-}$ mice were infected with 5x10^5 STm or remained uninfected as controls. ***A.*** Representative flow cytometry plots gated on IgM$^+$ CD19$^+$B220$^+$CD5$^-$ splenic B cells as shown in figure 3.3. Plots show splenic recirculating B2 (CD23$^+$ CD21$^{int/lo}$) and MZ (CD23^{lo} CD21^{hi}) B2 cells in WT and CD31$^{-/-}$ mice before and at day 20 of infection. Percentages denote cell populations as a proportion of total splenocytes. ***B.*** total number of **i)** splenic recirculating B2 cells **ii)** splenic MZ B2 cells and **iii)** peritoneal recirculating B2 cells in WT and CD31$^{-/-}$ mice before and at the indicated time points after infection. Data are representative of ≥ 2 experiments giving similar results. One point represents one mouse. D = day. * $p \leq 0.05$.

In contrast, B1a and B1b cell numbers were similar in WT and CD31$^{-/-}$ mice at the majority of time points studied (figure 3.6). In the spleen of WT mice, B1a cell numbers were unchanged throughout infection (figure 3.6Bi), although a slight increase was observed to day 20, after which the numbers returned to resting levels. A similar kinetic was observed in CD31$^{-/-}$ spleens. Although CD31$^{-/-}$ mice had fewer splenic B1a cells than WT mice at day 0 ($p \leq 0.05$), cell numbers were similar to WT mice throughout infection. Enhanced numbers of B1a and B1b cells were observed in the peritoneal cavity of resting CD31$^{-/-}$ mice when compared to WT mice ($p \leq 0.05$) (figure 3.6A, Bii and Biii). B1a cell numbers remained constant in WT mice throughout infection, however a loss of cells was apparent in CD31$^{-/-}$ mice between day 0 and day 20. Thus, whilst CD31$^{-/-}$ B1a cell numbers in the peritoneal cavity were similar to WT mice for the majority of the infection, at day 20 they were significantly lower ($p \leq 0.05$) (figure 6A, Bii). B1b cells from the peritoneal cavity were also largely unchanged in WT mice throughout infection, aside from a slight increase during the late infection. CD31$^{-/-}$ B1b cell numbers in the lavage fluid did not alter throughout infection and were generally similar to WT numbers, apart from at day 20 p.i when a reduction was apparent ($p \leq 0.05$). Overall, the effect of CD31 loss on B1 cell numbers was marginal, however large differences were apparent in B2 cell numbers at all time points studied. We therefore questioned whether the paucity of B2 cells in CD31$^{-/-}$ mice had functional implications during STm infection.

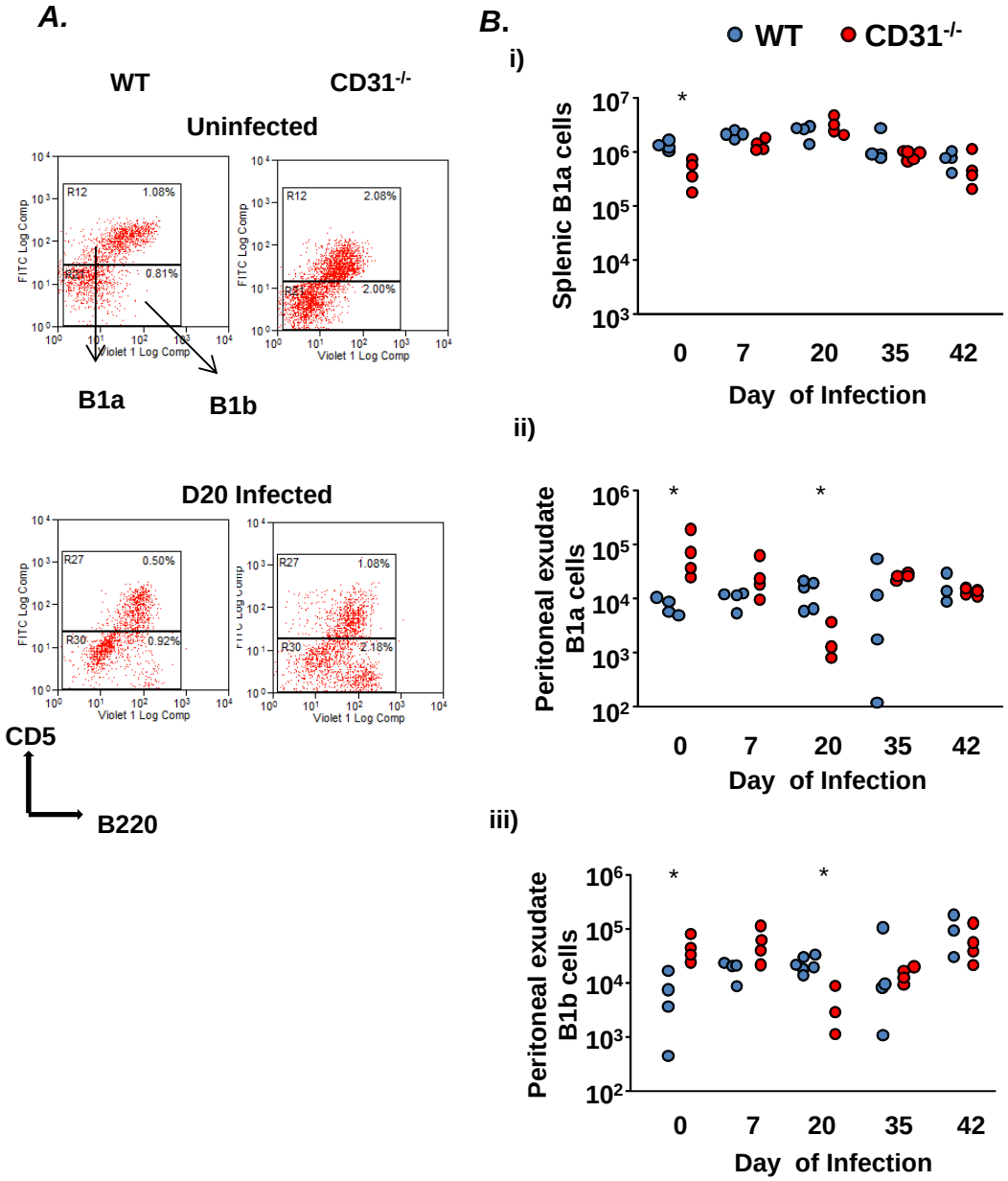

Figure 3.6. Splenic and peritoneal B1 cells in WT and CD31$^{-/-}$ mice before and during STm infection. WT and CD31$^{-/-}$ mice were infected with 5x10^5 STm or remained uninfected as controls. ***A.*** Representative flow cytometry plots gated on IgM$^+$ CD19$^+$CD21^{lo}CD23^{lo} peritoneal B cells as shown in figure 3.4. Plots show splenic B1a (CD5^{hi} B220^{int}) and B1b (CD5^{lo} B220^{lo}) cells in WT and CD31$^{-/-}$ mice before and at day 20 of infection. Percentages denote cell populations as a proportion of total PEC. ***B.*** Total number of **i)** splenic B1a cells **ii)** peritoneal exudate B1a cells and **iii)** peritoneal B1b cells in WT and CD31$^{-/-}$ mice before and at the indicated time points after infection. Data are representative of ≥2 experiments giving similar results. One point represents one mouse. * $p \leq 0.05$.

3.2.5 The EF plasma cell response is maintained in CD31$^{-/-}$ mice

Recent evidence suggests that B1b cells contribute significantly to the early EF plasma cell response to STm (13,70). Later in the infection, plasma cells may arise from B1 or B2 cells, or both. Given the different effects of CD31 loss on B1 and B2 cell numbers, the EF plasma cell response was examined in WT and CD31$^{-/-}$ mice before and during STm infection. At all time points studied, WT and CD31$^{-/-}$ mice had comparable numbers of IgM^{+} plasmacytoid cells in the spleen (figure 3.7A and 3.8A), as determined by immunohistochemistry staining (figure 3.7A) and cell counting (figure 3.8A). Consistent with the study that originally classified this model (70), a 10-fold induction of IgM^{+} plasma cells was seen by day 7 p.i in both groups. A very gradual decline in IgM^{+} plasma cell numbers followed in WT mice, however numbers remained elevated above background levels at day 42 p.i. After the initial increase, IgM^{+} plasma cell numbers remained elevated in CD31$^{-/-}$ mice throughout the infection.

The switched, IgG2a^{+} plasma cell response was also similar in the two groups (figure 3.7B and 3.8B). As expected (70), an early, large induction of IgG2a^{+} plasma cells occurred in WT mice, and this was also evident in CD31$^{-/-}$ mice. Despite the similar response kinetics, there was a tendency towards lower numbers of switched cells in CD31$^{-/-}$ mice during the latter stages of infection, with a significant difference apparent at day 35 p.i ($p \leq 0.05$). However, aside from these relatively modest defects, the EF plasma cell response to STm remained intact in CD31$^{-/-}$ mice. A second avenue of antibody production is the GC; we therefore compared the development of GC in WT and CD31$^{-/-}$ mice throughout infection.

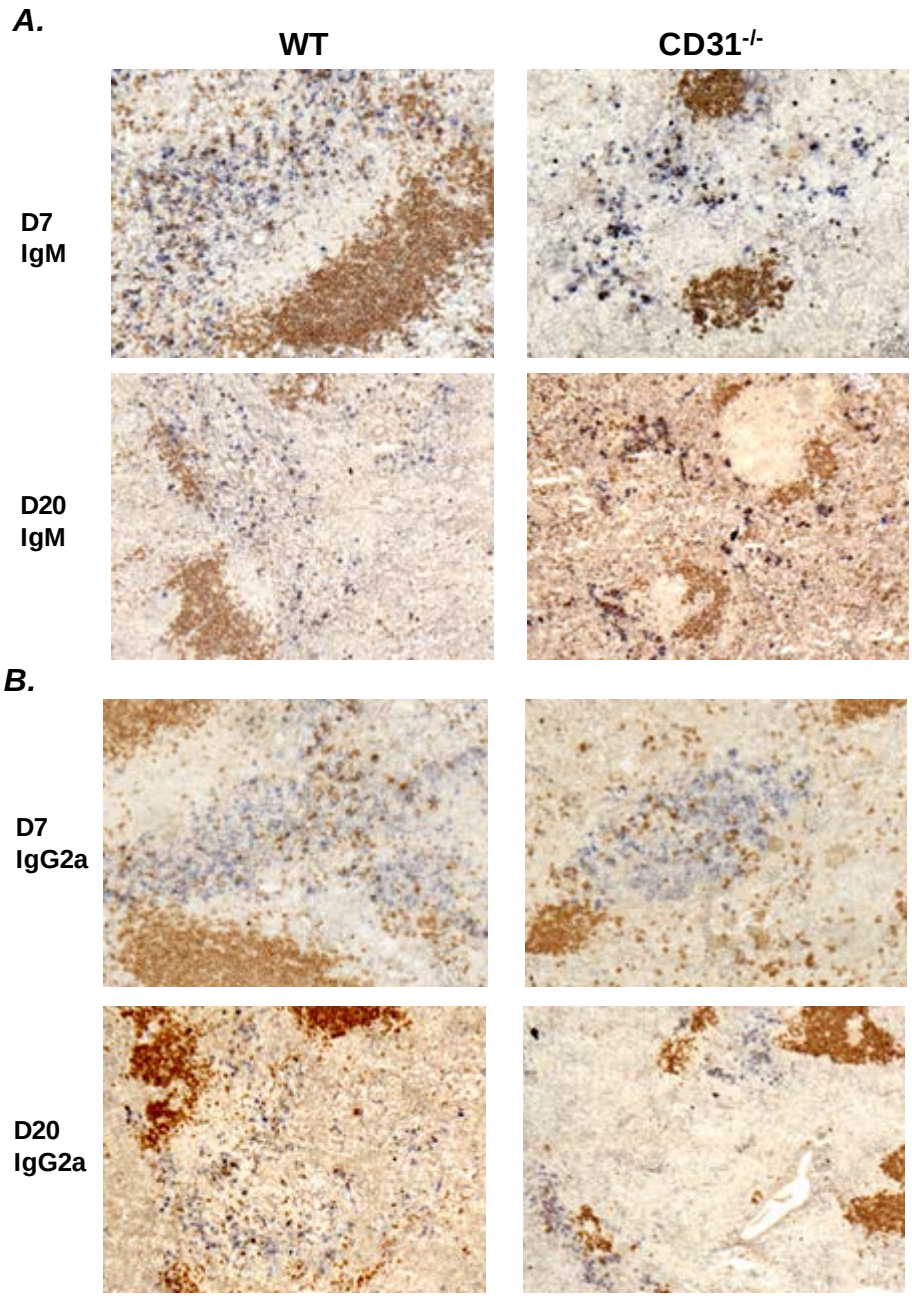

Figure 3.7 Splenic EF IgM^+ and $IgG2a^+$ plasma cells in WT and $CD31^{-/-}$ mice during STm infection. WT and $CD31^{-/-}$ mice were infected with $5x10^5$ STm or remained uninfected as controls. Spleens were stained for ***A.*** IgM (blue) and IgD (brown) to detect non-switched plasmacytoid cells and ***B*****,** IgG2a (blue) and IgD (brown) to detect class-switched plasmacytoid cells in the extrafollicular areas of the spleen. Representative photographs from at least 8 WT and $CD31^{-/-}$ mice are shown, at day 7 and 20 of infection.

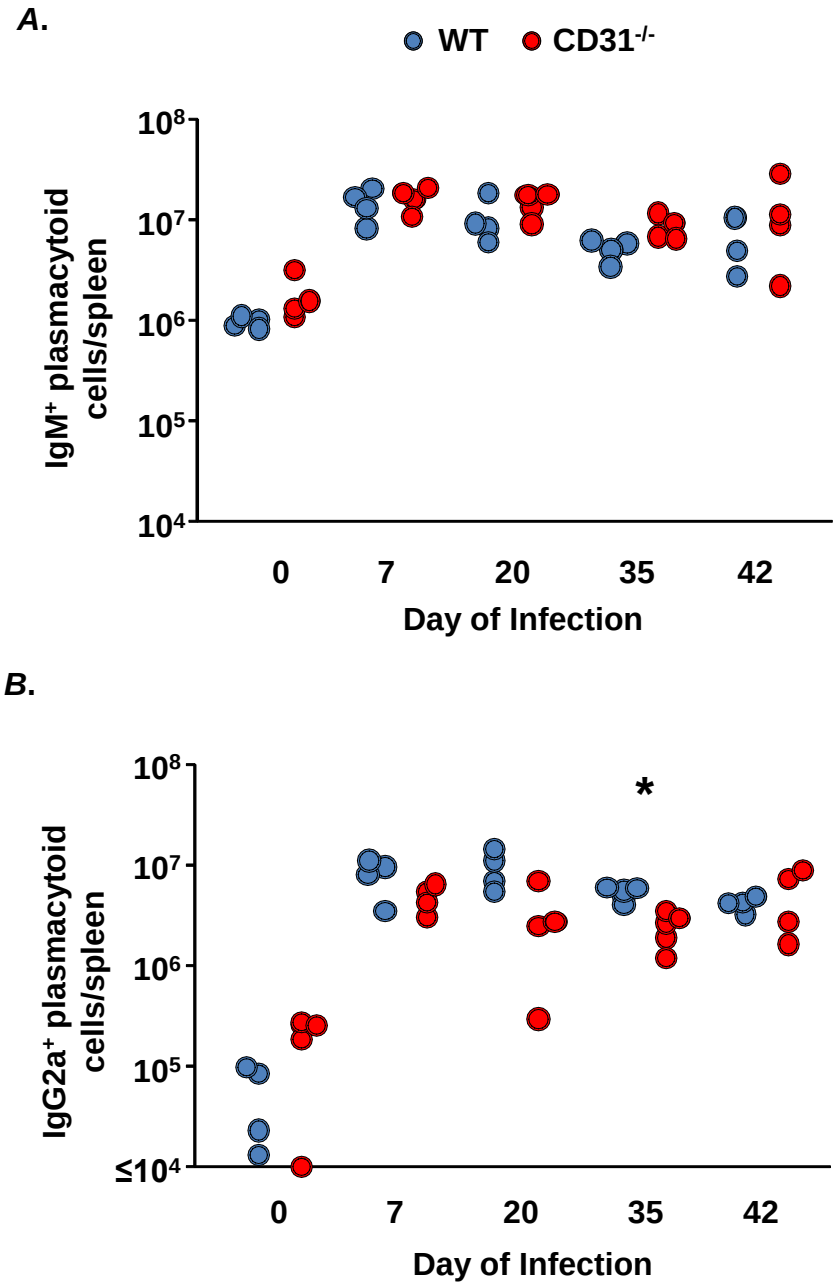

Figure 3.8. Splenic EF IgM$^+$ and IgG2a$^+$ plasma cell numbers in WT and CD31$^{-/-}$ mice before and after STm infection. WT and CD31$^{-/-}$ mice were infected with 5x10^5 STm or remained uninfected as controls. The total number of ***A*****,** IgM$^+$ and ***B*****,** IgG2a$^+$ plasmacytoid cells in the extrafollicular areas of the spleen were quantified by counting before and at the indicated time points after infection. Data are representative of ≥ 2 experiments giving similar results. One point represents one mouse. * $p \leq 0.05$.

3.2.6 Germinal centres are present in CD31-/- mice throughout STm infection.

One of our initial observations was the presence of GC in the spleens of uninfected $CD31^{-/-}$ mice (figure 3.2). Consistent with this, the overall volume and proportion of follicle occupied by GC was significantly higher in resting $CD31^{-/-}$ spleens when compared to WT mice ($p \leq 0.05$) (figure 3.9B). Throughout infection, GC were present in $CD31^{-/-}$ spleens and were more abundant than in WT mice until day 35 p.i, when the first expansion in WT GC was observed (figure 3.9A and B). In WT mice, GC expand only once the infection is waning (70), coinciding with a recovery in splenic B cell proportions. GC take up less of the total follicular area in WT mice when compared to $CD31^{-/-}$ mice, which have consistently lower numbers of follicular B cells throughout infection (figure 3.5A). Histological analysis of spleen sections at day 20 revealed a huge expansion of the red pulp in $CD31^{-/-}$ mice and a relative paucity of white pulp areas (figure 3.9A). Thus, whilst the histology suggests a suppression of GC in $CD31^{-/-}$ mice at this time point, the rare follicles were usually occupied by GC, leading to an overall increase in GC as a proportion of total follicle (figure 3.9B).

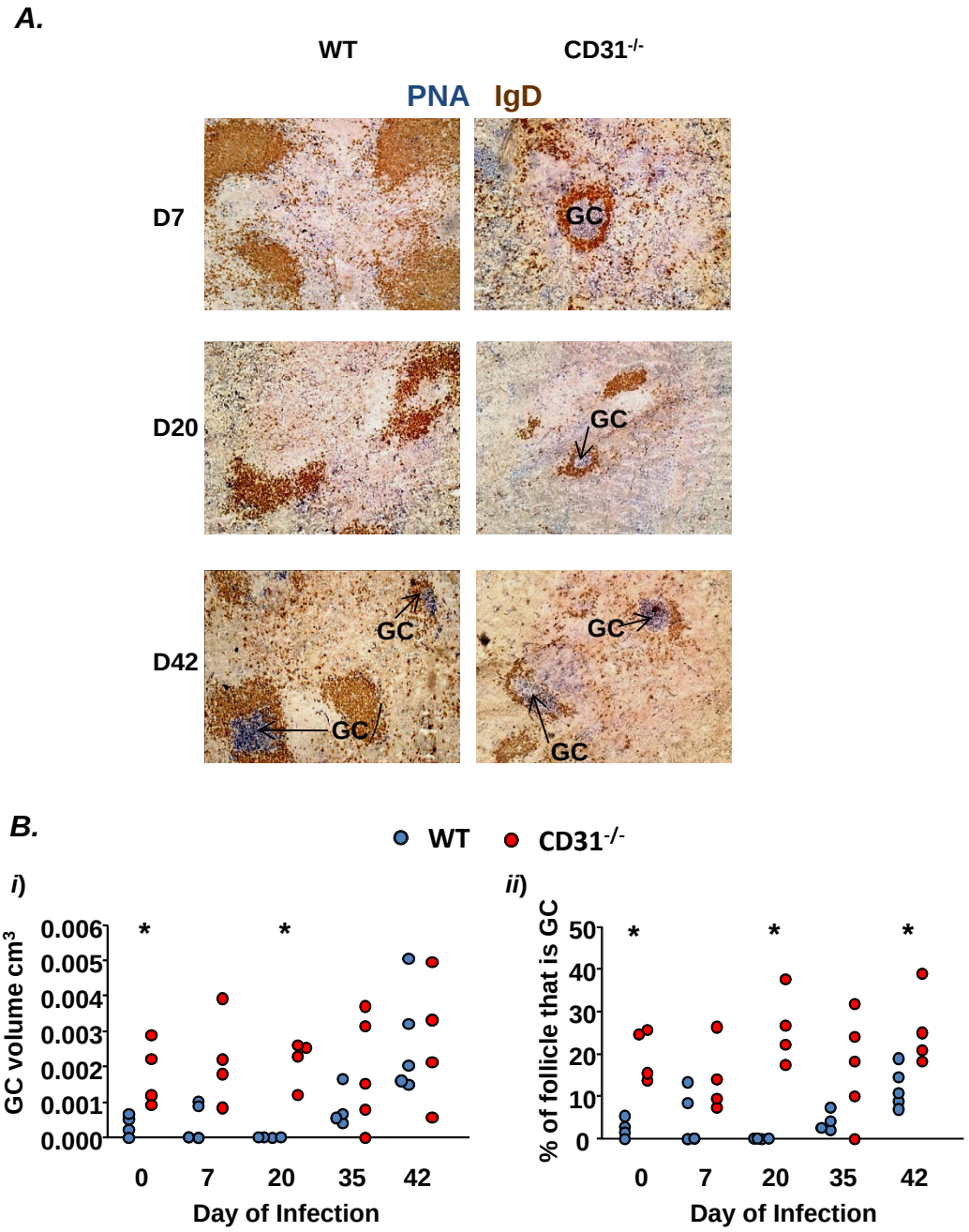

Figure 3.9 Splenic GC in WT and CD31$^{-/-}$ mice before and during STm infection. WT and CD31$^{-/-}$ mice were infected with 5x10^5 STm. ***A.*** Spleens were removed and stained with PNA (blue) to identify GC and IgD (brown) to identify mature B cells. The photos are taken from representative points in the early infection (D7), at the peak of infection (D20) and during the late infection (D42). ***B.*** **i)** The volume of GC per spleen and **ii)** the proportion of follicle that is GC, was quantified by histology before and at the indicated time points during infection. Data are representative of ≥2 experiments giving similar results. * = $p \leq 0.05$. Photos are representative of at least 8 mice per time point.

3.2.7 Striking defects in Salmonella-specific, class-switched antibody production by CD31-/- mice

A large proportion of antibody produced in the early stages of STm infection arises from B1 cells (160). High affinity, class-switched antibody is produced after day 35 p.i in WT mice (70), consistent with high affinity antibody arising from GC. As EF and GC responses were present in $CD31^{-/-}$ mice, we predicted that antibody production would also be intact. Serum antibody titres, specific to an OMP preparation from STm, were measured over the course of infection (figure 3.10). Heightened background levels of IgM antibody were detected in the sera of $CD31^{-/-}$ mice when compared to WT mice (figure 3.10A), whereas no class-switched antibody was detected in either group before infection (figure 3.10B and C). An increase in anti-OMP IgM occurred in WT mice over the first three weeks of infection, reaching a plateau thereafter. Whilst $CD31^{-/-}$ mice maintained a steady level of anti-OMP IgM antibody over the first week of infection, this had reduced by day 20 p.i and was almost absent at day 35 and 42 p.i. When compared to WT mice, IgM was significantly reduced at day 20 and 35 pi ($p \leq 0.05$). A more striking observation was the complete lack of switched IgG2b and IgG2a antibody in $CD31^{-/-}$ sera at all time-points p.i. (figure 3.10B and C). Class-switched antibody began to appear in WT mice after 2-3 weeks of infection, whilst $CD31^{-/-}$ mice had virtually undetectable titres of switched antibody throughout infection. Statistical analysis showed these reductions to be significant at day 20, 35 and 42 p.i (IgG2b) and at day 35 and 42 p.i (IgG2a) (all $p \leq 0.05$). Thus, despite the presence of GC and EF plasma cells throughout infection, no class-switched antibody was produced by $CD31^{-/-}$ mice.

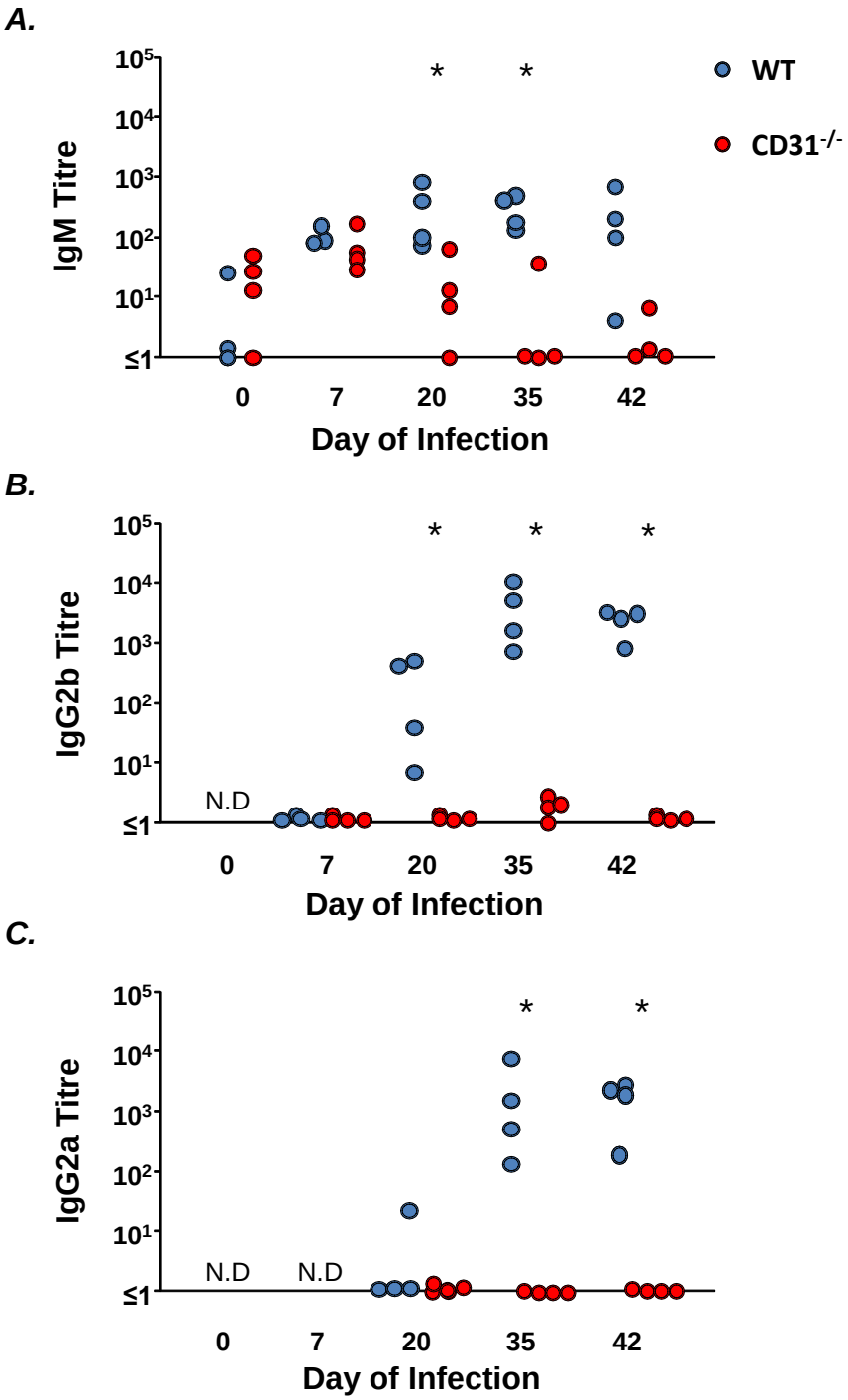

Figure 3.10. OMP-specific antibody titres in WT and CD31$^{-/-}$ mice throughout STm infection. WT and CD31$^{-/-}$ mice were infected with 5x10^5 STm or remained uninfected as controls. OMP-specific ***A*****,** IgM ***B*****,** IgG2b and ***C*****,** IgG2a serum antibody was quantified in WT and CD31$^{-/-}$ mice before and at the indicated time points after infection. Data are representative of ≥ 3 experiments giving similar results. * = $p \leq 0.05$; N.D = None detected

3.2.8 A single vaccination with porins from STm offers reduced levels of protection against *Salmonella* rechallenge in CD31$^{-/-}$ mice.

Recently published data shows that immunisation of WT mice with OMP from STm offers good, antibody-dependent protection against rechallenge with attenuated and virulent STm (13). Specifically, the porin OMPD was identified as the protein target of the antibody required to restrict bacterial growth. As protection was conferred largely by class-switched antibody, we predicted that CD31$^{-/-}$ mice would not be protected by vaccination with purified porins.

In the absence of vaccination, WT and CD31$^{-/-}$ mice had similar, high levels of bacteria present in the spleen at day 4 p.i (figure 3.11A). Following a three week vaccination and subsequent challenge with attenuated STm for 4 days, both groups displayed a significant reduction in splenic bacterial load ($p \leq 0.05$). However, the median splenic bacterial burden was ≥10-fold higher in CD31$^{-/-}$ mice when compared to WT mice ($p \leq 0.05$). When 2 porin vaccinations were given, the degree of protection against subsequent STm infection was enhanced further in CD31$^{-/-}$ mice ($p \leq 0.05$), and the splenic bacterial burden was now similar in WT and CD31$^{-/-}$ mice.

Protection conferred by porins is antibody-mediated. As such, serum antibody titres were assessed. As expected, infecting the mice with STm for 4 days induced an IgM response in both groups, whilst switched antibody production was absent (figure 3.11B). Upon vaccination, a significant increase in OMP-specific IgM antibody was apparent in WT sera ($p \leq 0.05$), whilst the increase observed in CD31$^{-/-}$ mice was far less marked. Some class-switched antibody was now detected in WT and CD31$^{-/-}$ mice, however a notable

difference was observed in IgG2b titres, which were significantly higher in WT mice when compared to CD31$^{-/-}$ mice after one vaccination ($p \leq 0.05$). This observation was consistent across two experiments. Following two vaccinations, antibody titres of each subclass were similar in WT and CD31$^{-/-}$ mice. These data indicate that antibody-mediated protection against attenuated STm is less effective in CD31$^{-/-}$ mice, however this protection can be restored after boosting with porins. Therefore, CD31$^{-/-}$ mice have a defect in class-switched antibody production during infection, but this is not necessarily recapitulated following immunisation with protein antigens.

Having made these interesting observations, we were next keen to investigate the mechanism behind the defects in antibody production. Unfortunately, at this point we were experiencing some severe breeding problems with our CD31 colony. In order to recover the line, we decided to refresh our mice with some CD31$^{-/-}$ mice from Prof. Sussan Nourshargh's group in London (186), who had originally provided us with this strain. Upon arrival in Birmingham, the mice underwent the required rederivation process before experimentation could continue. Following this, we carried out a phenotypic assessment of the mice, comparing them to our original CD31 colony. For clarity, the new, rederived CD31$^{-/-}$ colony was named PECAM$^{-/-}$, whilst the original colony remained as CD31$^{-/-}$.

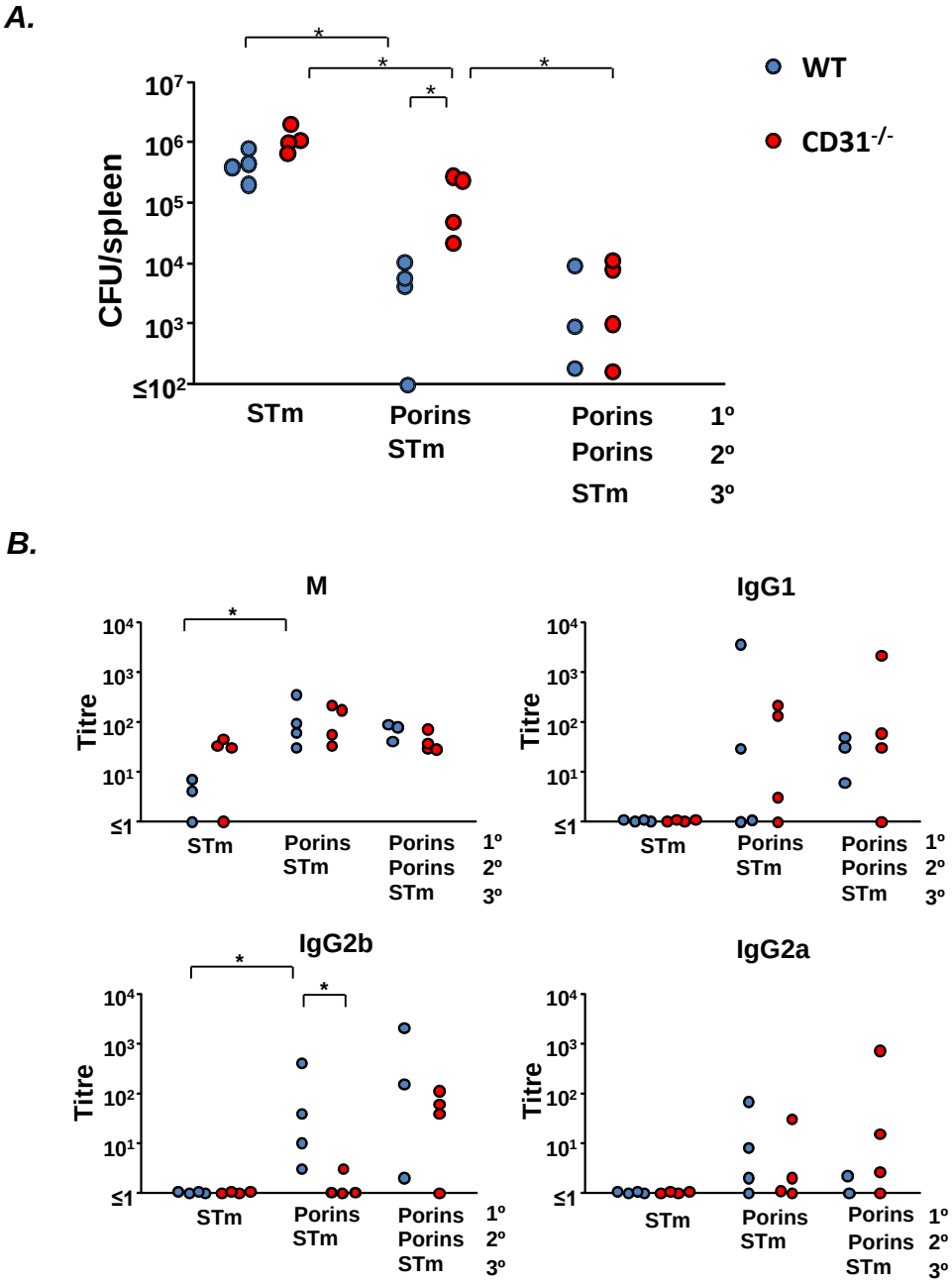

Figure 3.11. Bacterial burden and antibody production before and after immunisation against STm. WT and CD31$^{-/-}$ mice were either infected with STm for 4 days, or immunised once or twice with porins from STm before subsequent challenge with 5x10^5 STm for 4 days. Immunisation one was for 21 days and vaccination two was for 14 days. ***A.*** The number of CFU in the spleen of WT and CD31$^{-/-}$ mice following infection with STm for 4 days, in the presence or absence of porin immunisation. ***B.*** Serum anti-OMP IgM (top left), IgG1 (top right), IgG2b (bottom left) and IgG2a (bottom right) antibody titres in WT and CD31$^{-/-}$ mice following STm infection for 4 days in the presence or absence of porin vaccination. Data are representative of ≥ 2 experiments giving similar results. One point represents one mouse. * $p \leq 0.05$.

3.2.9 Resting PECAM-/- mice have no defect in splenic B2 cell numbers

Following rederivation, PCR analysis was carried out on PECAM$^{-/-}$ tissue to confirm the presence of the disrupted CD31 gene. Homozygous CD31 deficiency was confirmed in all PECAM$^{-/-}$ mice, by the presence of 1500bp fragment, corresponding to the disrupted gene (data not shown). These mice were used as breeders for all future experiments. . Subsequent flow cytometry cell surface staining for CD31 revealed a complete absence of CD31 expression on total splenocytes from PECAM$^{-/-}$ mice (figure 3.12). This staining was carried out on all mice used, with WT and CD31$^{-/-}$ mice stained alongside for comparison. Despite confirmed CD31 deficiency in PECAM$^{-/-}$ mice, assessment of PECAM$^{-/-}$ spleens revealed that the defect in B cell numbers was not apparent. Both histological (figure 3.13A) and flow cytometric (figure 3.13B) analysis revealed near normal proportions of follicular B2 and normal proportions of MZ B cells in the spleens of resting PECAM$^{-/-}$ mice. This observation was made in several mice. Furthermore, whilst initial experiments showed the GC phenotype to be retained in the PECAM$^{-/-}$ mice, over time this phenotype disappeared (figure 3.13Aii). It was therefore clear that these mice were phenotypically different from the CD31$^{-/-}$ mice we had been working on thus far. Having made these observations, we infected the PECAM$^{-/-}$ mice alongside the original CD31$^{-/-}$ mice, to assess whether infection would cause a diminution of B cell numbers.

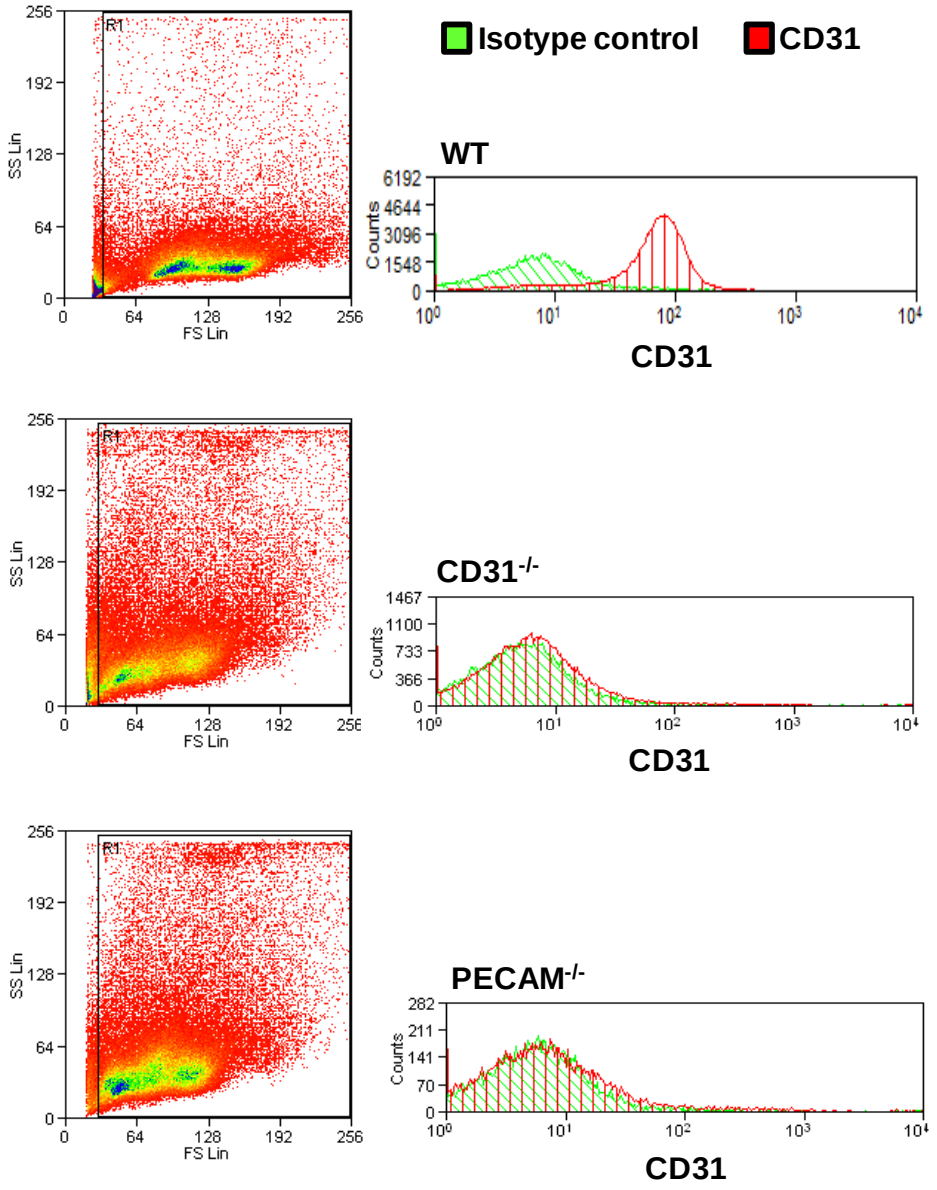

Figure 3.12. Total splenocytes from PECAM$^{-/-}$ mice lack surface CD31 expression. Total splenocytes from WT, CD31$^{-/-}$ and PECAM$^{-/-}$ mice were stained by flow cytometry for cell surface expression of CD31. Histogram overlays show CD31 expression in red and isotype control staining in green. Histograms are representative of at least 15 mice per group giving the same result.

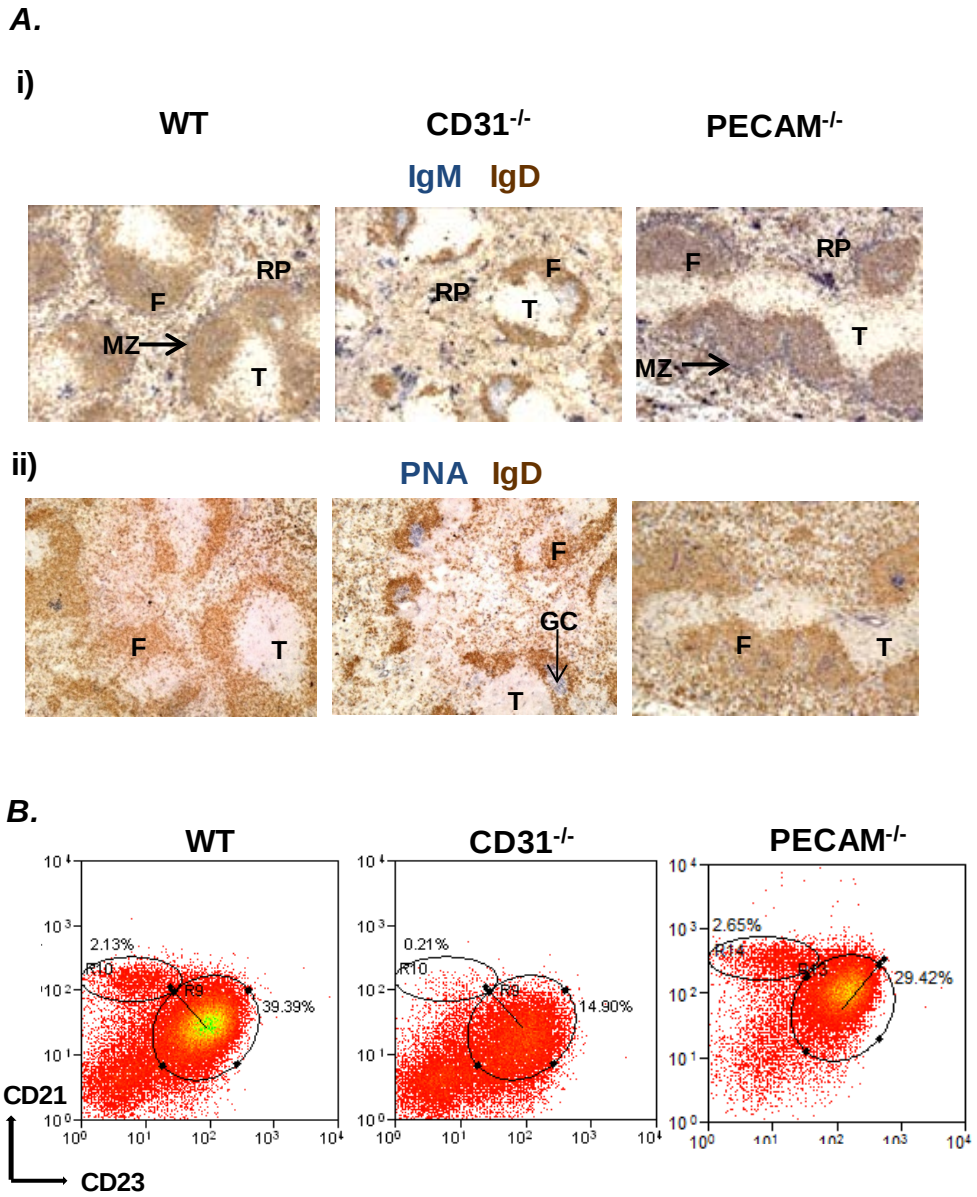

Figure 3.13 Follicular and MZ B cells in resting WT, CD31$^{-/-}$ and PECAM$^{-/-}$ mice. Uninfected WT, CD31$^{-/-}$ and PECAM$^{-/-}$ mice were sacrificed and the spleens removed for analysis by histology and flow cytometry. ***A.*** Representative photographs showing staining for **i)** IgM (blue) to identify MZ cells and IgM^{+} plasma cells and IgD (brown) to identify mature B cells and **ii)** PNA (blue) to identify GC and IgD (brown) to identify mature B cells. ***B.*** Representative flow cytometry plots showing follicular B2 and MZ B2 cells in uninfected spleens. Percentages denote follicular and MZ cells as a proportion of total splenocytes. Cells were identified as shown in figure 3.3 Photos are representative of 8 mice per group. Flow cytometry plots are representative of at least 4 mice per group.

3.2.10 B cell numbers in PECAM$^{-/-}$ mice are similar to WT mice throughout STm infection

Quantification of total B2 cell numbers before infection confirmed the histological analysis, revealing normal total numbers of follicular (figure 3.14A) and MZ (figure 3.14B) B2 cell numbers in the spleens of PECAM$^{-/-}$ mice. Infection of PECAM$^{-/-}$ mice with STm for 7, 20 and 42 days did not impact upon B cell numbers, so that unlike CD31$^{-/-}$ mice, numbers of follicular (figure 3.14A) and MZ (figure 3.14B) B2 cells were similar to WT numbers at all stages of infection. Splenic B1a cell numbers were also comparable to WT mice (figure 3.13C), however this was not unexpected. As there appeared to be no impact of CD31 loss upon B cell numbers, we assessed B cell function by measuring antibody titres in the serum at the various stages of infection.

3.1.11 STm-specific antibody production is similar in WT and PECAM$^{-/-}$ mice

Unfortunately, upon assessment of antibody responses to STm in PECAM$^{-/-}$ mice, findings were also inconsistent with our previous data (figure 3.15). Anti-OMP IgM, IgG2b and IgG2a titres in PECAM$^{-/-}$ mice were comparable to WT mice throughout infection. As expected, with the exception of IgM titres at day 7 p.i, CD31$^{-/-}$ mice produced little or no anti-OMP antibody during the infection. As the B cell results from our new PECAM$^{-/-}$ colony were inconsistent with the data already produced, we were left with no choice but to terminate this part of the project. As such, we maintained a focus upon B cell responses during STm infection, but expanded the project to focus specifically upon the factors that regulate GC responses and antibody class-switching in this model.

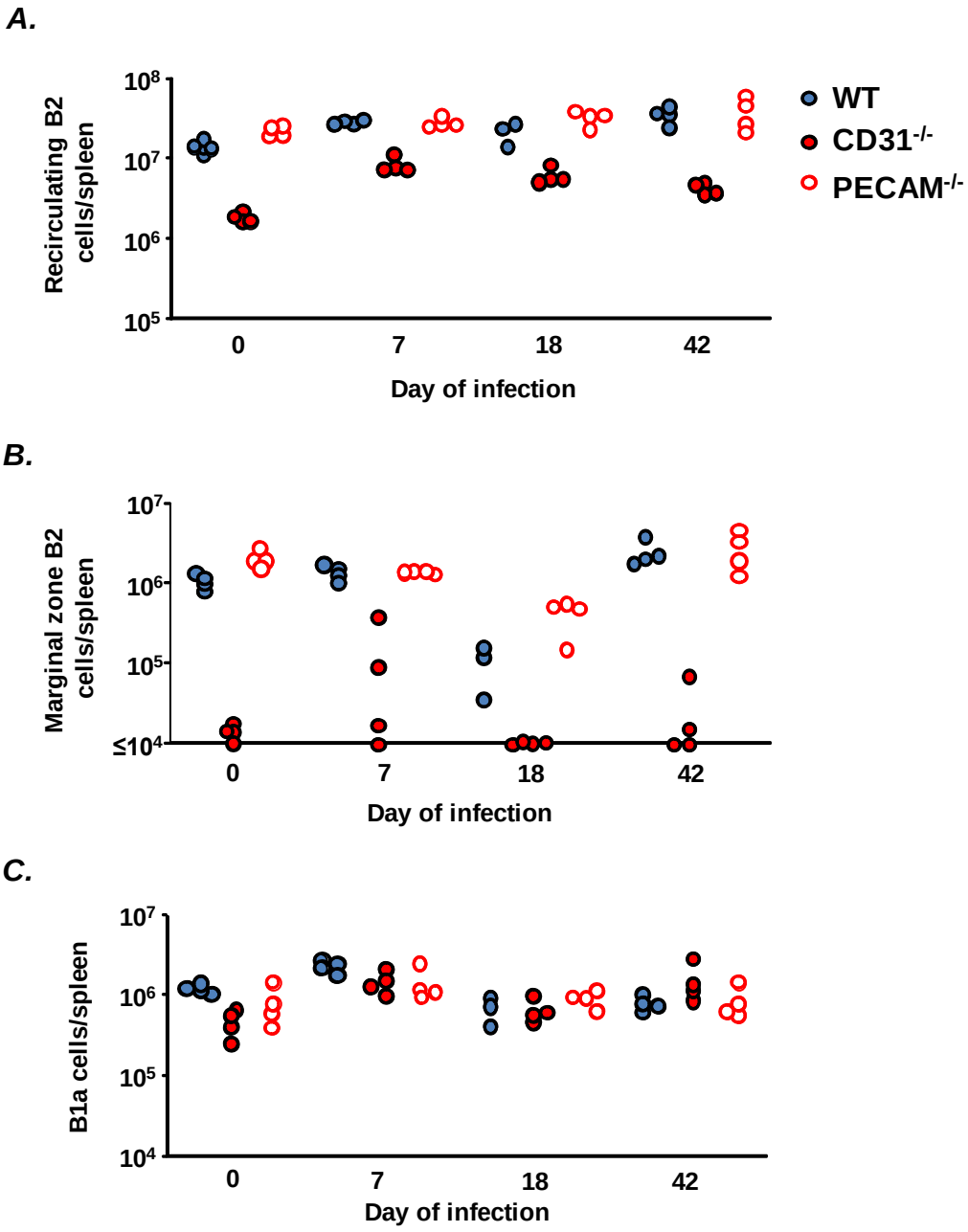

Figure 3.14 Splenic B2 cells in WT, CD31$^{-/-}$ and PECAM$^{-/-}$ mice before and after STm infection. WT, CD31$^{-/-}$ and PECAM$^{-/-}$ mice were infected with 5x10^5 STm and spleens removed for flow cytometry analysis at the time points indicated. The total number of ***A,*** splenic recirculating B2 cells, ***B,*** MZ B2 cells and ***C,*** B1a cells in WT, CD31$^{-/-}$ and PECAM$^{-/-}$ mice is shown. Cell populations were determined as shown in figure 3.3 and 3.4. Data are from 1-2 experiments per time point. One point represents one mouse.

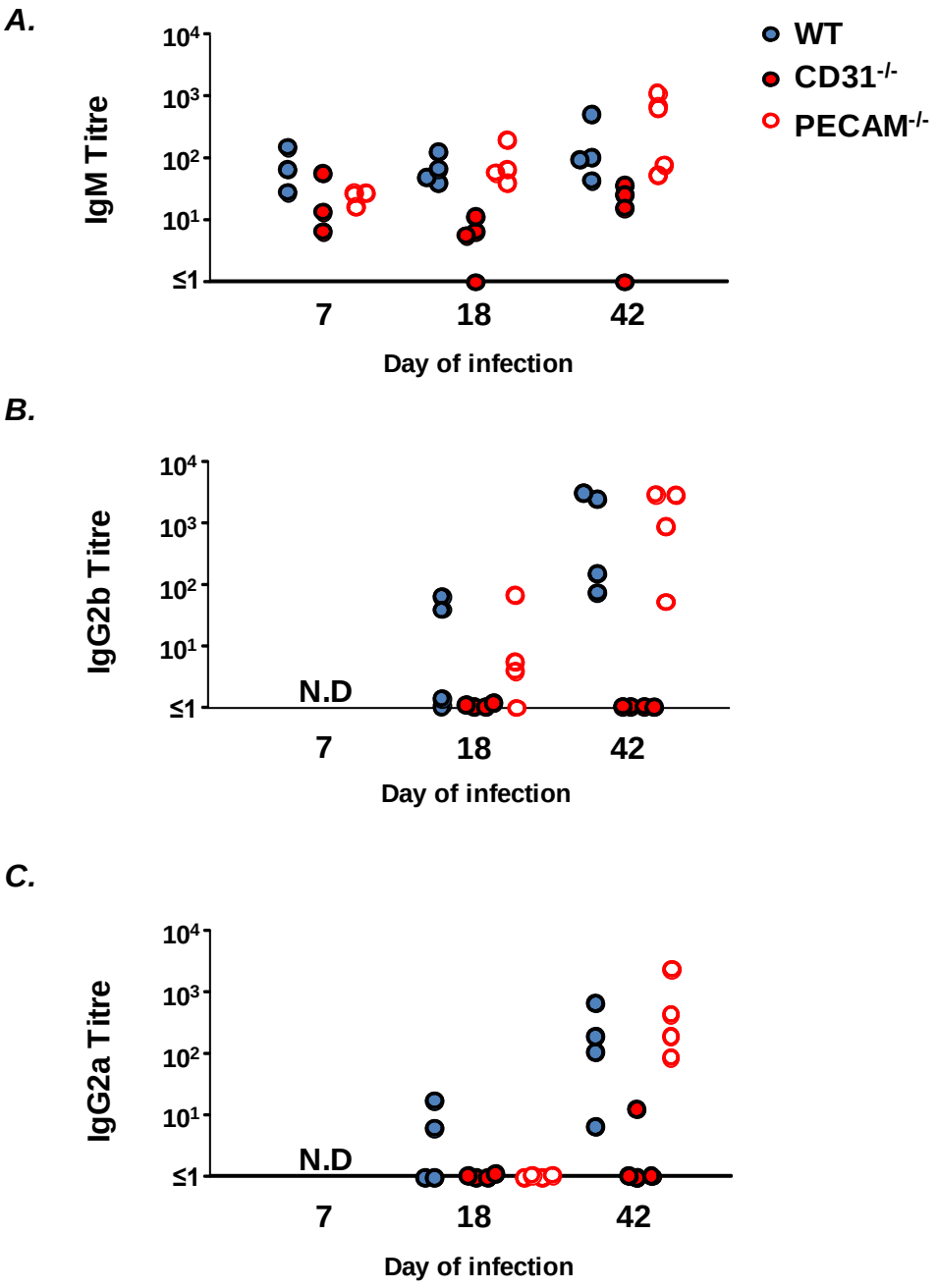

Figure 3.15. OMP-specific antibody titres throughout STm infection in WT, CD31$^{-/-}$ and PECAM$^{-/-}$ mice. Mice were infected with 5x10^5 STm and OMP-specific ***A,*** IgM**,** ***B,*** IgG2b, and ***C,*** IgG2a (bottom panel) serum antibody was quantified at the indicated time points after infection. Data are representative of 2 experiments giving similar results.

3.3 Discussion

Clearance of primary STm infection requires an efficient, Th1-driven adaptive immune response (79,217), whilst B cells can prevent bacteraemia (70,217) and are essential for subsequent protective immunity (226). CD31 is expressed on multiple immune cells, including T and B lymphocytes, and has been implicated in numerous immune processes. We therefore examined the immune response to STm in $CD31^{-/-}$ mice, revealing a striking defect in the ability of $CD31^{-/-}$ mice to clear bacteria from the spleen (203). This defect was shown to be largely T cell-dependent and was confirmed when $CD31^{-/-}$ mice were backcrossed onto green fluorescent protein (GFP) mice, as well as in the rederived $PECAM^{-/-}$ strain. Our published data also detailed the down-regulation of CD31 expression on $CD4^{+}$ T cells after activation, which correlates with $CD4^{+}$ T cell proliferation. A loss of CD31 on T cells resulted in increased cell death after activation, consistent with CD31 playing a regulatory role in infection (203). These data are in agreement with the purported role for CD31 as a negative regulator of T cell signalling (197,198).

During this work, histological analysis of spleen sections revealed a marked loss of follicular and MZ B2 cells in the resting $CD31^{-/-}$ mouse. Since CD31 expression on T cells was dependent upon activation status, we assessed whether CD31 expression on WT B cells changed during infection. Consistent with previous reports (184,202), we observed CD31 expression by flow cytometry on all peripheral B cells in resting mice. As CD31 has been reported to inhibit B cell signalling (199) and hyperproliferation (202), we anticipated seeing a reduction in CD31 expression on B cells during infection. However, CD31 was consistently expressed on all B2 and B1 cells throughout infection, only falling on B1 cells in the peritoneum between day 7 and 20 p.i. An increase in CD31 expression was observed

on all B cells early in the infection, suggesting that a loss of CD31 is not required for B cell activation. One potential caveat when interpreting this finding is that B cell activation was not directly assessed. However, little spread was observed in the CD31 expression peaks throughout infection, suggesting uniform expression within subsets. It may have been more informative, however, to assess CD31 expression on plasmablasts during the response, which could be achieved using intracellular IgG and surface CD31 staining.

As a functionally diverse molecule, CD31 may serve an alternative function on B cells, such as facilitating B cell recruitment. It is known that CD31 supports the migratory activity of leucocytes and modulates chemokine receptor polarisation (186,187,199,249), and this may account for the lower numbers of splenic, but higher numbers of PEC, B1a cells in resting $CD31^{-/-}$ mice when compared to resting WT mice. However, in our current work, B2 and B1 cell numbers increased in the spleens of $CD31^{-/-}$ mice at day 7 p.i and B2 cell numbers increased in the peritoneum. This suggests that CD31 is not essential for B cell recruitment, although this could be masked by a hyperproliferative response, which has previously been reported in $CD31^{-/-}$ mice (202).

An alternative function for CD31 on B cells could be a pro-survival one. CD31 has been implicated in the regulation of B cell activation (199) and CD31-expressing cells are purportedly more resistant to apoptosis (190,193,196), which could explain the lack of B cells in $CD31^{-/-}$ mice. On the other hand, MZ B cells are severely depleted in WT mice after STm infection, despite the maintenance of CD31 expression on the remaining cells. It is plausible however, that only the surviving cells retain CD31 expression, or that the observed decline in MZ B cells represents their recruitment into the EF plasma cell

response, rather than their demise. Recent evidence suggests this early response to be T-independent and involve B1b cells (13,70), but may also involve MZ B cells. Indeed, MZ cells have been shown to unite with B1b cells in early antibody responses to T-I 2 antigens (169) and may also respond to protein antigens on blood borne bacteria (250).

As WT B cells express CD31 throughout infection, we assessed how a loss of this molecule would affect B cell responses to STm in $CD31^{-/-}$ mice. Our initial data were very interesting, highlighting clear defects in B cell function in $CD31^{-/-}$ mice. Most notably, the antibody response to STm infection was severely attenuated, despite the presence of EF plasma cells and GC in the spleen throughout infection. Moreover, the antibody-mediated protection to STm conferred by porins (13) was limited in $CD31^{-/-}$ mice. Having made these observations we were keen to assess the cellular basis for these defects. Unfortunately, due to the inconsistent responses revealed in the $PECAM^{-/-}$ strain upon rederivation, we were unable to progress further with this work. The phenotype reversal in $PECAM^{-/-}$ mice was B cell specific, with the T cell features remaining consistent, albeit to a lesser degree. It is unclear which B cell phenotype is most representative of CD31 deficiency. Placing our findings into context with the published CD31 literature is likely to be informative in this regard.

Although less marked than shown here, a previous study reported a deficiency in peripheral B2 cells and an elevation in peritoneal B1a cells in resting $CD31^{-/-}$ mice (202). These and our data may relate to the purported inhibitory role of CD31 on B cells (199). A loss of B cell inhibitory receptors results in B cell survival defects (173) and an inability to effectively regulate B cell activation, which can result in an autoimmune phenotype

(173,174). The lack of peripheral B2 cells observed in CD31$^{-/-}$ mice here suggests a possible survival defect, whilst the abundance of GC in the spleen prior to antigenic challenge is suggestive of an autoimmune phenotype. Studies supporting a survival defect include adoptive transfer experiments, in which transferred CD31$^{-/-}$ B cells failed to survive over time (202). We attempted to assess antibody responses in CD31$^{-/-}$ mice following total splenocyte transfer into RAG1$^{-/-}$ hosts, which have no T cells or B cells, however CD31$^{-/-}$ B cells were unable to reconstitute the spleen (data not shown), which could further indicate a survival defect. Previous reports also show that CD31$^{-/-}$ B cells are more susceptible to tolerance breakdown (245) and CD31$^{-/-}$ mice are more likely to develop B cell (202) and T cell driven (176,177) autoimmune conditions. An over-production of autoreactive B cells could itself explain the lack of recirculating B2 cells in CD31$^{-/-}$ mice. Entry into secondary lymphoid tissue is required for follicular B cell survival, however this space cannot accommodate the huge numbers of B cells that leave the bone marrow each day (25,177). As such, fierce competition exists for follicular entry and self-reactive B cells are eliminated from the B cell pool (25).

An alternative reason for the lack of B2 cells could relate to a developmental defect within the bone marrow. Wilkinson and colleagues (202) reported a maturational block in B2 cells between the immature and mature B cell stage in CD31$^{-/-}$ mice. Our observation, that B2 cells are diminished in the absence of CD31 whilst B1 cells are not, suggests a relationship with B cell ontogeny and a possible defect at the progenitor stage within the bone marrow. This has not been addressed in detail here, however some preliminary flow cytometry data suggests that B cell numbers at each maturational stage in the bone marrow are similar in WT and CD31$^{-/-}$ mice (data not shown). More extensive analyses would be required to

confirm this. A developmental failure could also occur in the spleen, where immature B cells mature into either MZ cells or follicular B2 cells. This lineage decision is thought to involve a signal strength model, in which strong signalling through the BCR favours follicular B cell development and vice versa (250). Mice deficient in CD22, a negative regulator of B cell signalling, receive mainly strong signals through the BCR, resulting in fewer MZ cells (173). As a negative regulator of B cell signalling, a similar scenario may also occur in $CD31^{-/-}$ mice, although no concomitant increase in follicular B cells is observed.

The above outlines some research that supports our original $CD31^{-/-}$ B cell phenotype data. With regard to B cell function, we observed a severe defect in class-switched antibody production during primary infection with STm, which is in stark contrast to the normal antibody responses to the T-D antigen alum-precipitated dinitrophenol-keyhole limpet hemocyanin (DNP-KLH), reported by Wilkinson and colleagues (202). These incongruent findings may relate to the different antigens used. Alum-ppt protein drives a Th2 response with antibody class-switching to IgG1 (94), and hyper-responsive Th2 cells have previously been reported in mice lacking B cell-inhibitory receptors (174). Thus, $CD31^{-/-}$ mice may produce IgG1 more efficiently than IgG2a or IgG2b. A second consideration is that during STm infection, high titres of switched antibody become detectable only once splenic GC form, which coincides with bacteria in the spleen falling to below 10^4 CFU (70). The defect in bacterial clearance and the high number of background GC in $CD31^{-/-}$ spleens, suggest that the GC observed throughout infection are not STm specific. As such, the reduction in antibody titres may be partly due to the inability of $CD31^{-/-}$ mice to resolve infection, rather than an inherent inability to produce class-switched antibody. In support

of this, WT and CD31$^{-/-}$ mice produced equal levels of class-switched OMP-specific antibody after two porin immunisations and challenge with STm, demonstrating that CD31$^{-/-}$ mice can form productive GC and mount memory B cell responses, albeit with delayed kinetics. It is however surprising that despite the largely intact EF plasma cell response during primary infection, no antibody was detectable throughout.

A second finding from Wilkinson and colleagues (202) was heightened T-I antibody responses to alum-precipitated DNP-ficoll in CD31$^{-/-}$ mice. We observed higher background levels of natural anti-OMP IgM in CD31$^{-/-}$ sera and B1a cells are a likely source of this antibody (161). B1a cells were elevated in the peritoneal cavity of CD31$^{-/-}$ mice in this work and that of Wilkinson and colleagues, consistent with the heightened natural antibody titres. Furthermore, in the current study, IgM^{+} and IgG2a^{+} plasma cell numbers and IgM antibody titres were similar in WT and CD31$^{-/-}$ mice at day 7 p.i, and B1b cells are thought to contribute significantly to this response (13,70). Taken together, these data indicate that B1 cell function remains intact in CD31$^{-/-}$ mice.

Thus, whilst B cell function has not previously been extensively investigated in CD31$^{-/-}$ mice, much of the available evidence supports the data produced using our original CD31$^{-/-}$ colony. Furthermore, other B cell-inhibitory receptor knockout mice have a similar phenotype to that observed here, suggesting that our original CD31$^{-/-}$ colony may be more representative of this strain than the rederived PECAM$^{-/-}$ colony. What factors may have contributed to the dramatic change in phenotype observed in the rederived PECAM$^{-/-}$ strain? The CD31$^{-/-}$ and PECAM$^{-/-}$ colonies were housed in separate institutions for some time, were initially bred and maintained in different rooms within the animal facility at the

University of Birmingham and underwent different patterns of rederivation, breeding and backcrossing. These factors, as well as an absence of inter-colony phenotypic variation, make it impossible to ascribe these variations to stochastic events. Variations in autoantibody production in genetically identical mice have previously been described in this way, however all other potential confounders were controlled for (251).

Environmental factors may influence phenotypes, especially in autoimmune-susceptible strains. The PECAM$^{-/-}$ mice were rederived and bred in isolators for some time upon arrival in Birmingham. As such, these mice were not exposed to the same environmental antigens as the CD31$^{-/-}$ mice. The autoimmune-like phenotype observed in the CD31$^{-/-}$ mice, such as reduced B2 cells and large numbers of splenic GC, may have been driven by exposure to environmental antigens in the animal facility. Susceptibility to autoimmunity is well described in these mice, which could explain why WT mice bred under the same conditions do not have a similar phenotype.

Changes in the gut flora have also been described in genetically identical rodents housed in different rooms within the same animal facility, resulting in alterations to metabolic phenotype (252,253). Changes in the composition of gut microflora and subsequent metabolic profile can significantly alter the response of the host to newly introduced substances (254). Whilst most applicable to mucosal immunity and responses to orally administered drugs, these data highlight how seemingly small differences in husbandry can have a significant impact upon biological data.

Genetic background is also able to influence mouse phenotypes, due to epistatic modifiers. Of note, genetic background is often the difference between a healthy and an autoimmune phenotype. Alterations in autoimmune susceptibility have been reported when B cell-inhibitory receptor knockout mice, such as the FcγRIIB$^{-/-}$, are backcrossed onto different genetic backgrounds (175). Although the CD31$^{-/-}$ and PECAM$^{-/-}$ strains were both on a C57BL/6 background, the original generation of CD31$^{-/-}$ mice involved disruption of the CD31 gene in 129 embryonic stem (ES) cells and injection into C57BL/6 blastocysts (184). Despite being an efficient and widely utilised approach, this method of gene disruption has received some criticism (255,256). Even with extensive backcrossing onto the desired genetic background (in this case C57BL/6), the area proximal to the targeted gene will always reflect the genetic background of the ES cell strain (257). As such, researchers have questioned whether the phenotype of mice produced in this way is influenced by the closely surrounding genes of the 129 background, rather than by disruption of the targeted gene (255). It is therefore plausible that the remaining 129 region in the CD31$^{-/-}$ mice gives rise to the observed B cell phenotype. As the new PECAM$^{-/-}$ colony had undergone rederivation in London, further rounds of backcrossing and rederivation again in Birmingham, perhaps such effects of the 129 background had been substantially reduced.

Without extensive investigation, it is impossible to attribute these phenotypic changes to an individual factor. PCR analysis of CD31$^{-/-}$ and PECAM$^{-/-}$ tissue, to assess for remaining 129 genes, may be informative in this regard. To provide more concrete answers however, microarray analysis would need to be carried out on the original and rederived strain, to assess for differences in gene expression that might contribute to alterations in phenotype.

Analysing gut flora in the two strains and pinpointing any phenotypic changes occurring as a result could also add to our understanding of this problem. All of these approaches were beyond the scope of this project, and as such, these findings can be considered a cautionary tale for investigators using genetically modified animals to answer research questions. These data also highlight the importance of collaborative efforts between institutions for data validation purposes.

Despite the termination of the $CD31^{-/-}$ project, some interesting B cell observations, consistent with the published literature, were made. The $CD31^{-/-}$ model was complex, emphasising the need to address the fundamental factors regulating B cell responses during STm infection. Germinal centre responses and antibody class-switching during T-dependent responses to non-viable model antigens are now well characterised, however the control of B cell responses to viable Th1 antigens is less well understood. The remainder of this project focused specifically upon investigating the factors that regulate GC formation and antibody class-switching during systemic infection with STm. We first addressed whether cytokines with known involvement in GC responses to protein antigens, can also influence GC development and function in this model.

CHAPTER 4: CYTOKINE REGULATION OF GERMINAL CENTRE RESPONSES DURING STM INFECTION

4.1 Introduction

During T-D antibody responses to viable or non-viable antigen, EF and GC responses can develop simultaneously (93) or distinctly (70). Cytokines have an important role in the development and maintenance of EF and GC reactions and in shaping the antibody repertoire. The cytokine-mediated control of Th2 GC responses is now understood in some detail, however those that regulate GC reactions during the immune response to viable, Th1 antigens, are less well characterised.

Immunisation with model protein antigens gives rise to IL4, IL5 and IL13-expressing Th2 cells, with antibody class-switching dominated by IgG1 and IgE (93,96,258). Early studies using $IL4^{-/-}$ mice show this cytokine to be essential for the maintenance of the Th2 clones *in vivo* (95) and for optimal IgE and IgG1 antibody production in late primary and memory responses to Th2-associated antigens (91,95,96). Closer analysis of $IL4^{-/-}$ and $IL13^{-/-}$ mice reveal that the early features of Th2 B cell response are retained in these mice, such as the initial induction of γ1 germline switch transcripts and antigen specific $IgG1^{+}$ plasma cell induction. Whilst $IL4^{-/-}$ and $IL13^{-/-}$ mice also form GC normally in response to NP-CGG and *Bordetella pertussis*, (*B. pertussis*) $IL4^{-/-}IL13^{-/-}$ double-deficient mice have a smaller GC area than WT mice or single cytokine deficient mice at day 7 of this response (93). In

agreement with this, mice deficient in the IL4-receptor alpha chain (IL4Rα$^{-/-}$) have smaller GC and lower levels of γ1 and ε germline switch transcript expression in B cells at day 7 of the response to alum-ppt protein, a point at which B cell selection by T cells is occurring in the GC (94). Double deficiency in IL4 and IL13 (91) or IL4 alone (91,95), also leads to diminished IgG1 and augmented IgG2a and IgG2b responses during recall responses to alum-ppt protein (91). These data collectively show that the initiation of the Th2 responses can occur in the absence of IL4 and IL13 signalling, however these cytokines are important for the maintenance of Th2 responses and recall responses to such antigens.

The importance of IL4 signalling within the GC may relate to the ability of Tfh cells to express (114,126,259) and produce this cytokine (126,260). B cells interacting with IL4^{+} Tfh cells up-regulate expression of γ1 switch transcripts following infection with *Leishmania* Major (*L.* Major), whilst those that communicate with IFNγ^{+} Tfh cells produce γ2a switch-transcripts (126). These data further illustrate how cytokines within the GC can influence the direction of Ig class-switching.

Cytokines involved in Tfh development can also promote GC development and subsequent antibody responses. IL6 and IL21 operate in a redundant fashion to promote Tfh cell differentiation (124) however, a loss of IL6 (103,104) or IL21 (120,121,124,261) alone can significantly impair GC development and subsequent antibody responses. Whilst GC defects are seen consistently in IL21-deficient mice (120,121,124,261), the data linking IL6-deficiency with GC and antibody defects are more varied. IL6 has long been known to promote B cell growth and support the generation of antibody secreting plasma cells (99). A role for IL6 in optimal GC formation has also been reported in response to model protein

antigens *in vivo* (103,104). Radiation chimeras demonstrated that FDC-derived IL6 was essential for this process and for the promotion of somatic hypermutation (SHM) *in vitro* (104). In these studies, sub-optimal IgG responses were linked to the GC defects. On the other hand, infection models have produced varied results. Some early studies support a role for IL6 in IgA production (262), whilst others suggest that IL6 is dispensable for optimal IgA and IgG production (263). More recently, GC B cell development was not impaired and plasma cell development only modestly impacted during acute lymphocytic choriomeningitis virus (LCMV) infection of $IL6^{-/-}$ mice, despite a marked reduction in viral IgG titres. Thus, a role for IL6 in the regulation of GC reactions and EF responses is likely to be antigen dependent and remains to be fully defined.

Cytokines are instrumental in promoting effective class-switched antibody responses, however the role of cytokines in the B cell response to STm has not been dissected. Using a number of gene-deficient mouse strains, this chapter addresses the cytokine dependency of GC development, EF plasma cell responses and antibody class-switching during STm infection. Specifically, we question whether the cytokines that facilitate antibody responses to model, protein antigens, such as IL4, IL13, and IL6, can also influence GC and EF responses during infection with a live, Th1-dominant antigen.

4.2 Results

4.2.1 IL4 and IL13 promote optimal GC formation during STm infection

The cytokines IL4 and IL13 regulate GC responses to protein antigens (93). To assess whether these cytokines can influence GC development during a Th1-dominated response, WT, IL4$^{-/-}$, IL13$^{-/-}$ and IL4Rα$^{-/-}$ mice were infected with STm and sacrificed at day 42 p.i, when the GC reaction is established in WT mice. The ability of these mice to resolve infection was assessed by quantifying the CFU per spleen at day 42 p.i, revealing no difference in bacterial burden between the four groups (figure 4.1A). To assess whether GC form optimally in the absence of IL4, IL13 and IL4Rα, spleens were stained with PNA and IgD before infection (staining not shown) and at day 42 p.i, to identify GC within the B cell follicles (figure 4.1B I). Examination of spleen sections prior to infection revealed low levels of background GC in WT, IL4$^{-/-}$ and IL4Rα$^{-/-}$ spleens, whilst IL13$^{-/-}$ mice had significantly higher numbers of background GC in the spleen when compared to WT mice ($p \leq 0.05$) (figure 4.1B II and III). By day 42 p.i, splenic GC were present in abundance in all four groups of mice (figure 4.1B I), however closer analysis revealed that the total GC volume (figure 4.1B II) and the proportion of follicle occupied by GC (figure 4.1B III), had a tendency to be lower in IL4$^{-/-}$, IL13$^{-/-}$ and IL4Rα$^{-/-}$ mice when compared to WT mice. The reduction in GC size and volume below that of WT mice was very similar in all three groups of gene-deficient mice, however statistical analysis showed these differences to be borderline significant.

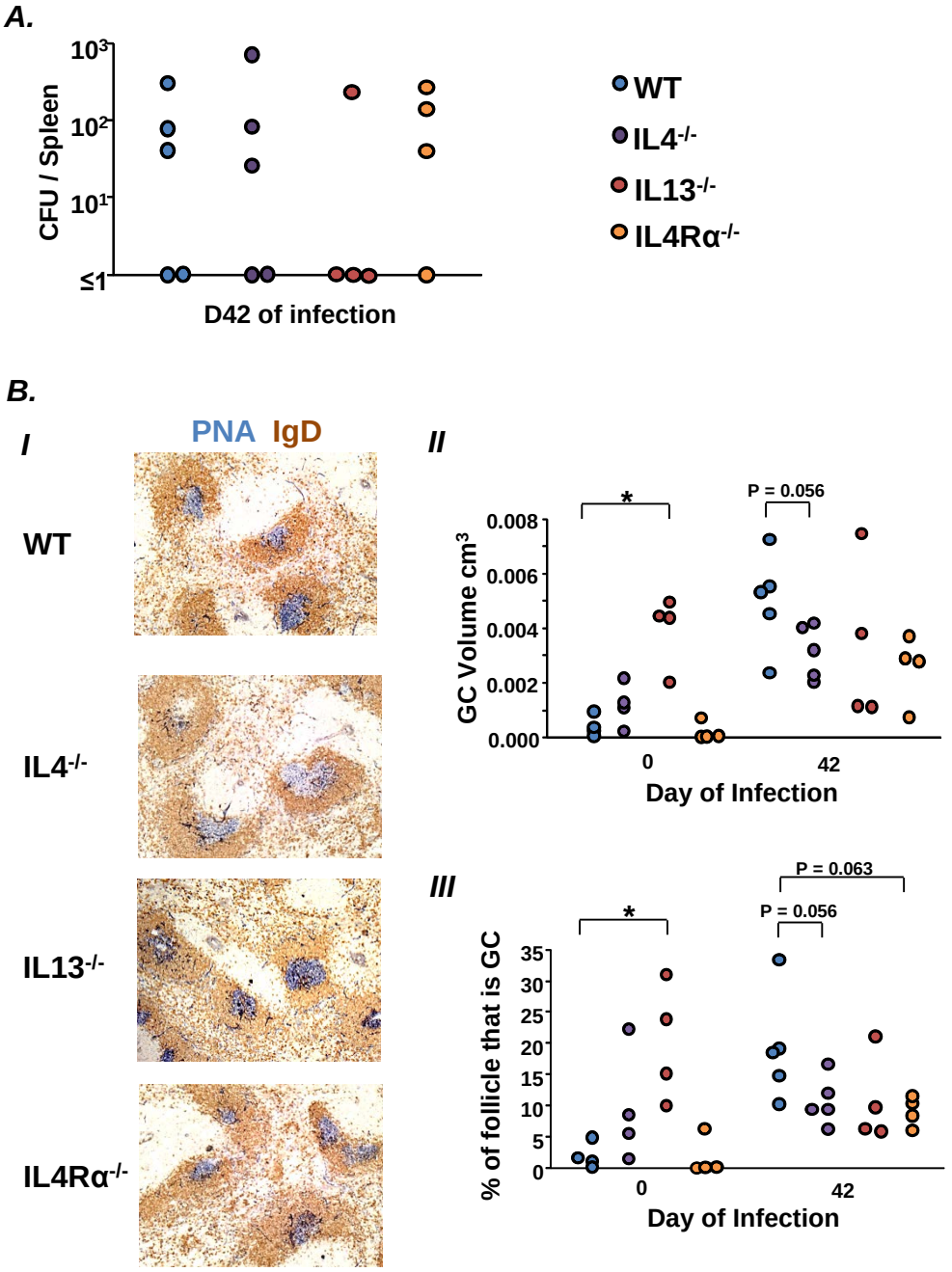

Figure 4.1. GC development in WT, IL4$^{-/-}$, IL4rα$^{-/-}$ and IL13$^{-/-}$ mice following STm infection. WT and gene-deficient mice were infected with 5x10^5 STm for 42 days and ***A,*** the total CFU per spleen were quantified; ***B,*** spleens were removed and stained with PNA (blue) to identify GC and IgD (brown) to identify mature B cells. GC ***II*** volume and ***III*** size were quantified by histology before infection and at D42 p.i. Photos show a representative example of splenic GC at day 42 p.i, from at least 4 mice per group. Data are from one experiment. One point represents one mouse. * p ≤ 0.05.

4.2.2 Class switching to IgG2a is not enhanced in IL4$^{-/-}$, IL13$^{-/-}$ and IL4Rα$^{-/-}$ mice

Previous studies report that class-switching to IgG2a can be enhanced in the absence of IL4 (91,95). Having noticed a modest impairment in GC development, we next addressed whether the plasma cell response and direction of class-switching in IL4-, IL13- and IL4Rα-deficient mice at this point reflects that of WT mice. Before and at day 42 of infection, spleen sections were stained for IgM^{+} and IgG2a^{+} plasma cells by histology and cell numbers were quantified by counting. Prior to infection, all groups had high numbers of background IgM^{+} plasma cells in the spleen, however no differences in cell number were observed between WT mice and the gene-deficient mice (figure 4.2A). Similarly, at day 42 p.i, IgM^{+} plasma cell numbers were comparable in all four groups of mice. Staining for IgG2a^{+} plasma cells (figure 4.2B) revealed a high frequency of these cells in uninfected IL13$^{-/-}$ spleens (figure 4.2B II), consistent with the elevated GC volume shown in figure 4.1. WT, IL4$^{-/-}$ and IL4Rα$^{-/-}$ spleens contained similar numbers of background IgG2a^{+} plasma cells and at day 42 of infection, IgG2a^{+} cell numbers had increased 10-100-fold in these three groups. An increase in IgG2a^{+} plasma cell numbers was also observed in IL13$^{-/-}$ mice, however this was masked substantially by the high numbers of switched cells in uninfected IL13$^{-/-}$ spleens. When compared to WT mice, all of the gene-deficient mice produced similar numbers of IgG2a^{+}, class-switched plasma cells in response to STm infection. Thus, the marginal aberrations in GC development caused by an absence of IL4, IL13 and IL4Rα were not paralleled by a defect in IgG2a^{+} plasma cell formation.

A.

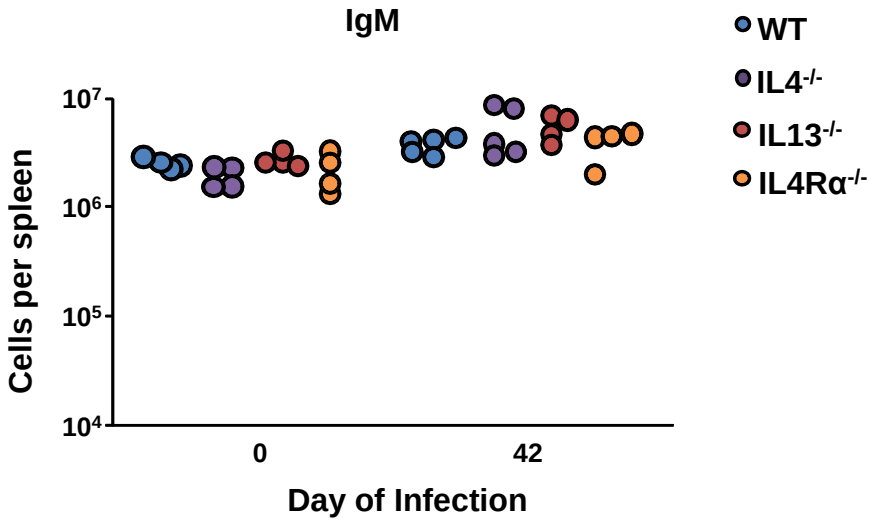

B.

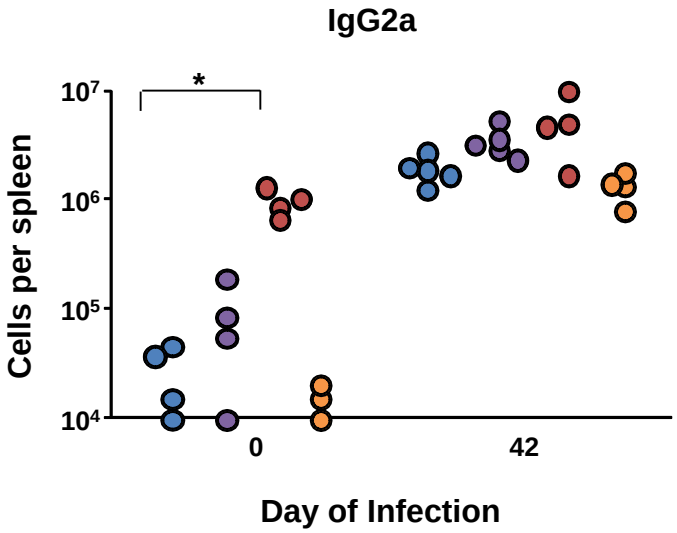

Figure 4.2. EF plasma cell numbers in WT, IL4$^{-/-}$, IL4rα$^{-/-}$ and IL13$^{-/-}$ mice at day 42 of STm infection. WT and gene-deficient mice were infected with 5x10^5 STm for 42 days or remained uninfected as controls. Spleens were removed and stained for IgM and IgD to identify non-switched plasma cells and IgG2a and IgD to identify class-switched plasma cells. Graphs show total number of ***A.*** IgM$^+$ and ***B.*** IgG2a$^+$ plasma cells in the spleens of uninfected and infected WT and gene deficient mice, as quantified by histology. Photographs are representative of at least 4 mice per group. One point represents one mouse.

4.2.3 WT, IL4$^{-/-}$, IL13 and IL4Rα$^{-/-}$ mice show a similar serum antibody profile at day 42 of infection

To assess whether the defect in GC development impacted upon antibody secretion, OMP-specific serum antibody titres were quantified by ELISA in WT, IL4$^{-/-}$, IL13 and IL4Rα$^{-/-}$ mice before and at day 42 p.i. Before infection, low levels of OMP-specific IgM were detected in some mice, but class-switched IgG2b and IgG2a antibody was completely absent in all groups. At day 42 p.i, anti-OMP IgM (figure 4.3A), IgG2b (figure 4.3B) and IgG2a (figure 4.3C) titres were comparable in all four groups of mice. Thus IL4$^{-/-}$, IL13$^{-/-}$ and IL4Rα$^{-/-}$ mice produced similar levels of Th1-associated Ig subclasses to WT mice in response to STm infection. These data indicate that both IL4 and IL13 can optimise GC formation during STm infection, however a loss of these cytokines does not affect antigen-specific antibody production in this model. We therefore investigated the role of IL6 in antibody responses to STm infection, as this cytokine is important for optimal GC formation, antibody class-switching and B cell affinity maturation following immunisation with model Th2 antigens (103,104).

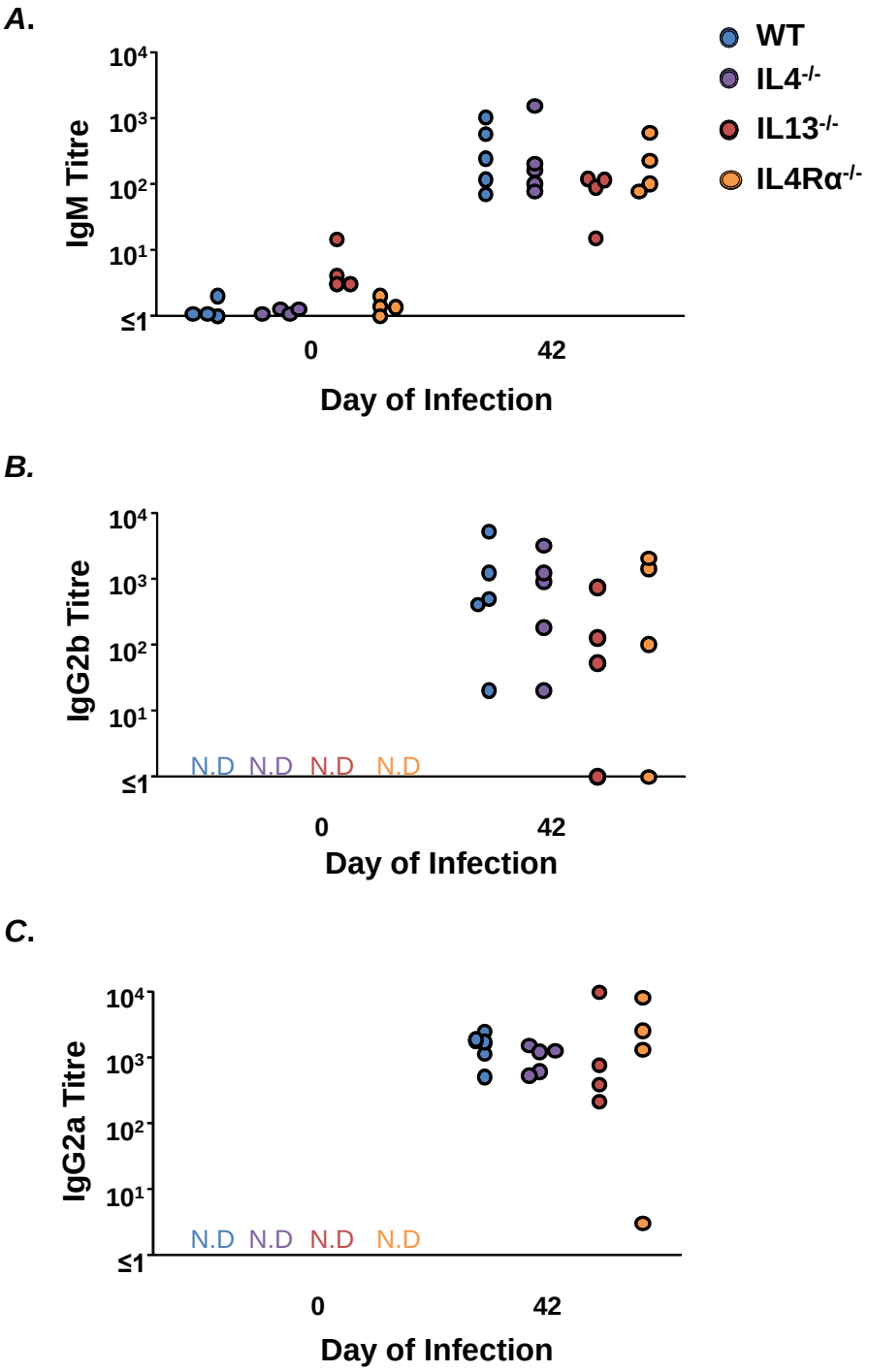

Figure 4.3. OMP-specific antibody titres before and at day 42 of STm infection. WT, IL4$^{-/-}$, IL4rα$^{-/-}$ and IL13$^{-/-}$ mice were infected with 5x10^5 STm or remained uninfected as controls. OMP-specific ***A*****,** IgM ***B*****,** IgG2b and ***C,*** IgG2a serum antibody was quantified by ELISA in all mice before and at day 42 p.i. One point represents one mouse. Data are from one experiment.

4.2.4 IL6$^{-/-}$ mice resolve STm infection effectively but have delayed GC development

Germinal centres do not form in WT mice until infection is largely resolved (70). To compare the rate of bacterial clearance in the two groups, splenic bacterial load was quantified in WT and IL6$^{-/-}$ mice from two weeks after infection. Whilst higher numbers of bacteria have previously been observed in IL6$^{-/-}$ spleens at day 7 of infection (our own unpublished observations), similar numbers of bacteria were recovered from the spleens of WT and IL6$^{-/-}$ mice at day 18, 42 and 55 p.i, revealing no defect in bacterial clearance in IL6$^{-/-}$ mice (figure 4.4A). We next assessed GC formation in the spleen by histological analysis. Spleen sections from uninfected mice revealed low numbers of background GC in WT and IL6$^{-/-}$ mice (figure 4.4 B) and these remained largely absent at day 18 p.i. By day 42 p.i, GC were abundant in WT mice, however there were markedly fewer in the spleens of IL6$^{-/-}$ mice (figure 4.4B) ($p \leq 0.05$). By day 55 p.i, GC appeared to be physically smaller in IL6$^{-/-}$ mice when compared to WT mice (figure 4.4BI), however their abundance resulted in a similar total GC volume to WT mice (figure 4.4BII). Thus, IL6 deficiency resulted in a delay in GC development during STm infection. To assess whether antibody class-switching remained intact in IL6$^{-/-}$ mice, the EF plasma cell response was assessed at each time point.

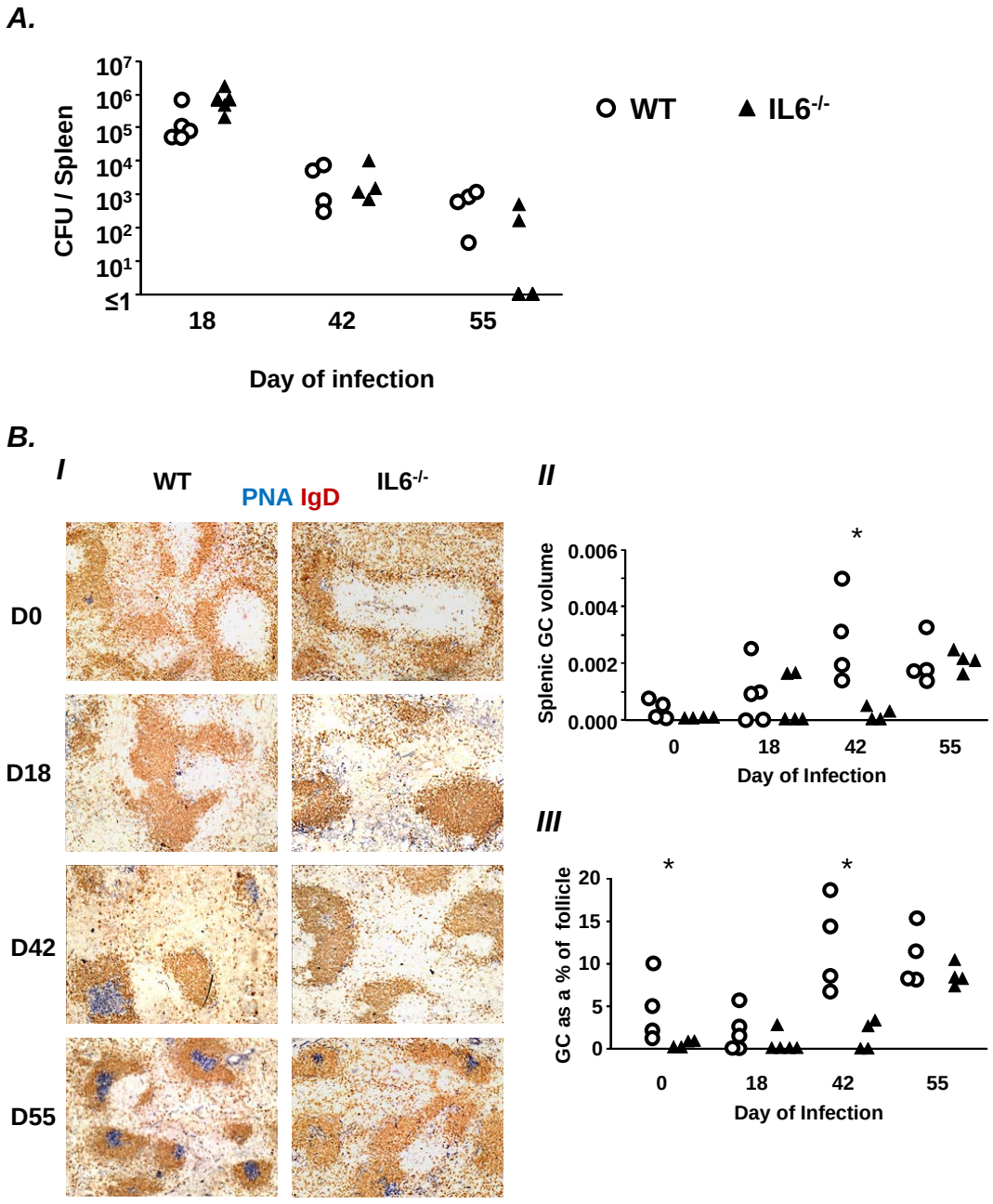

Figure 4.4 Splenic germinal centres in WT and IL6$^{-/-}$ mice before and during STm infection. WT and IL6$^{-/-}$ mice were infected with 5x10^5 STm, or remained uninfected as controls. Spleens were removed and ***A,*** the CFU per spleen were quantified at various days p.i. and ***B I*** stained with PNA (blue) to identify GC and IgD (brown) to identify mature B cells at the time points specified. The total ***II*** GC volume and ***III*** GC as a proportion of total follicle was quantified by histology. Photos are representative of at least 7 mice in each group per time point. Data are representative of ≥ 2 experiments. * p ≤0.05.

4.2.5 Class-switched EF plasma cell responses are maintained in IL6$^{-/-}$ mice

A defect in class-switching to IgG2a and IgG2b has previously been reported in IL6$^{-/-}$ mice in response to protein antigens (103), and conflicting data exists on the necessity of IL6 for IgA production (262,263). WT and IL6$^{-/-}$ spleens were stained by histology for IgM^{+} (staining not shown), IgA^{+}, IgG2b^{+} and IgG2a^{+} plasmacytoid cells (figure 4.5) and numbers were subsequently quantified by counting (figure 4.6). Staining demonstrated that IL6$^{-/-}$ mice can develop a strong, non-switched (not shown) and class-switched EF plasma cell response during STm infection (figure 4.5). Quantification of total cell numbers revealed that prior to infection, similar background numbers of all plasma cell isotypes were present in the spleens of WT and IL6$^{-/-}$ mice (figure 4.6 A-D), with the exception of IgA^{+} plasma cells, which were observed in higher frequencies in IL6$^{-/-}$ mice (figure 4.6B). After infection, the IgM^{+} plasma cell response developed with similar kinetics in WT and IL6$^{-/-}$ mice (figure 6A). There was a tendency for IgA^{+} (figure 4.6B) and IgG2b^{+} (figure 4.6C) plasma cell numbers to be lower in IL6$^{-/-}$ mice than in WT mice throughout infection, however at no point were these differences statistically significant. There was no observed defect in the IgG2a EF plasma cell response in IL6$^{-/-}$ mice, aside from a slight reduction in cell number at day 18 p.i. (figure 4.6D). As GC development was impaired in IL6$^{-/-}$ mice, but the EF plasma cell response was largely maintained, we addressed the impact of this upon antigen specific antibody production.

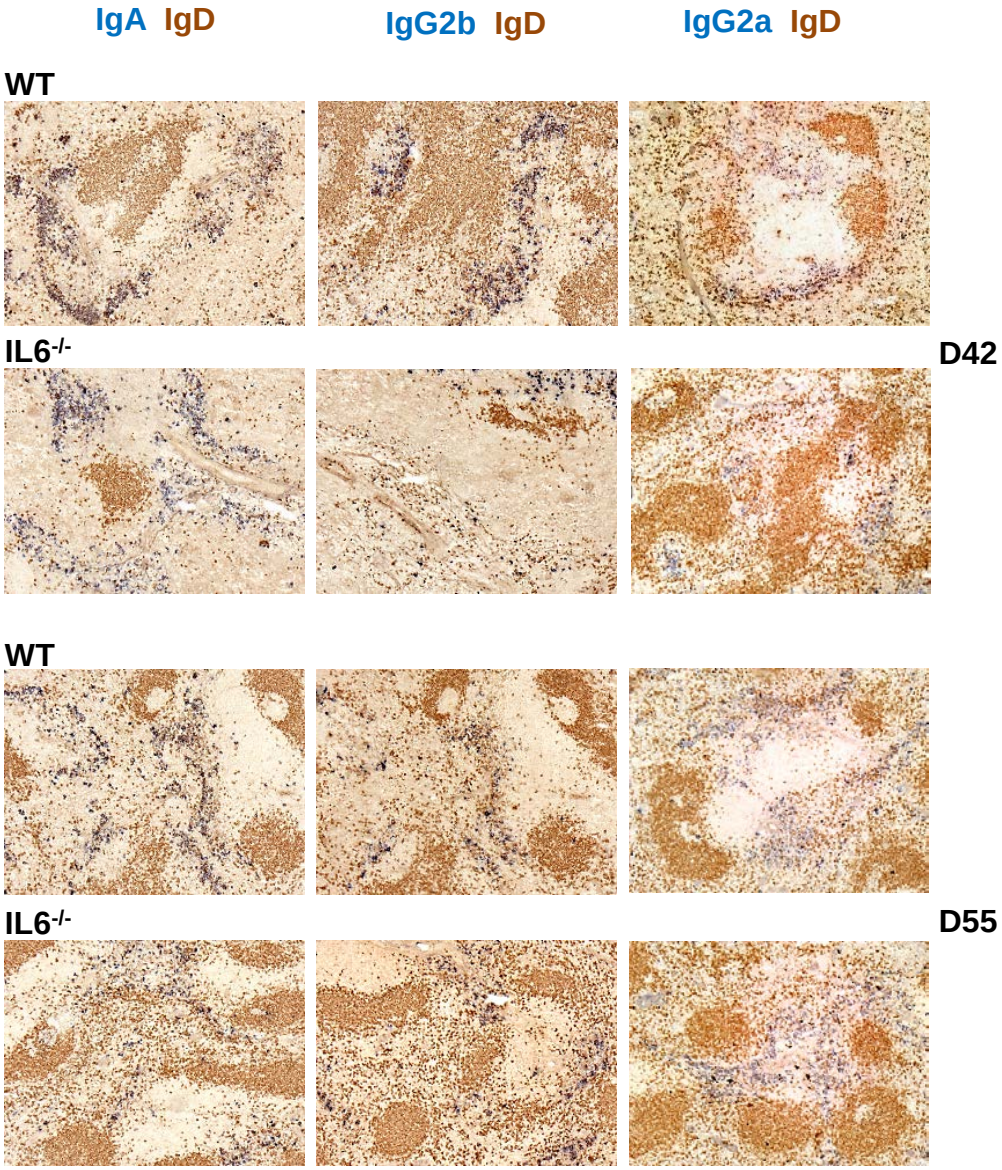

Figure 4.5. Splenic EF class-switched plasma cells in WT and IL6$^{-/-}$ mice at the late stages of STm infection. WT and IL6$^{-/-}$ mice were infected with 5x10^5 STm. Spleens were removed at the specified time points after infection and stained for IgM (not shown) IgA (left panels) IgG2b (middle panels) and IgG2a (right panels) (all blue) to detect class switched plasmacytoid cells and IgD (brown) to detect mature B cells. Photos are representative of at least 7 mice per group at each timepoint.

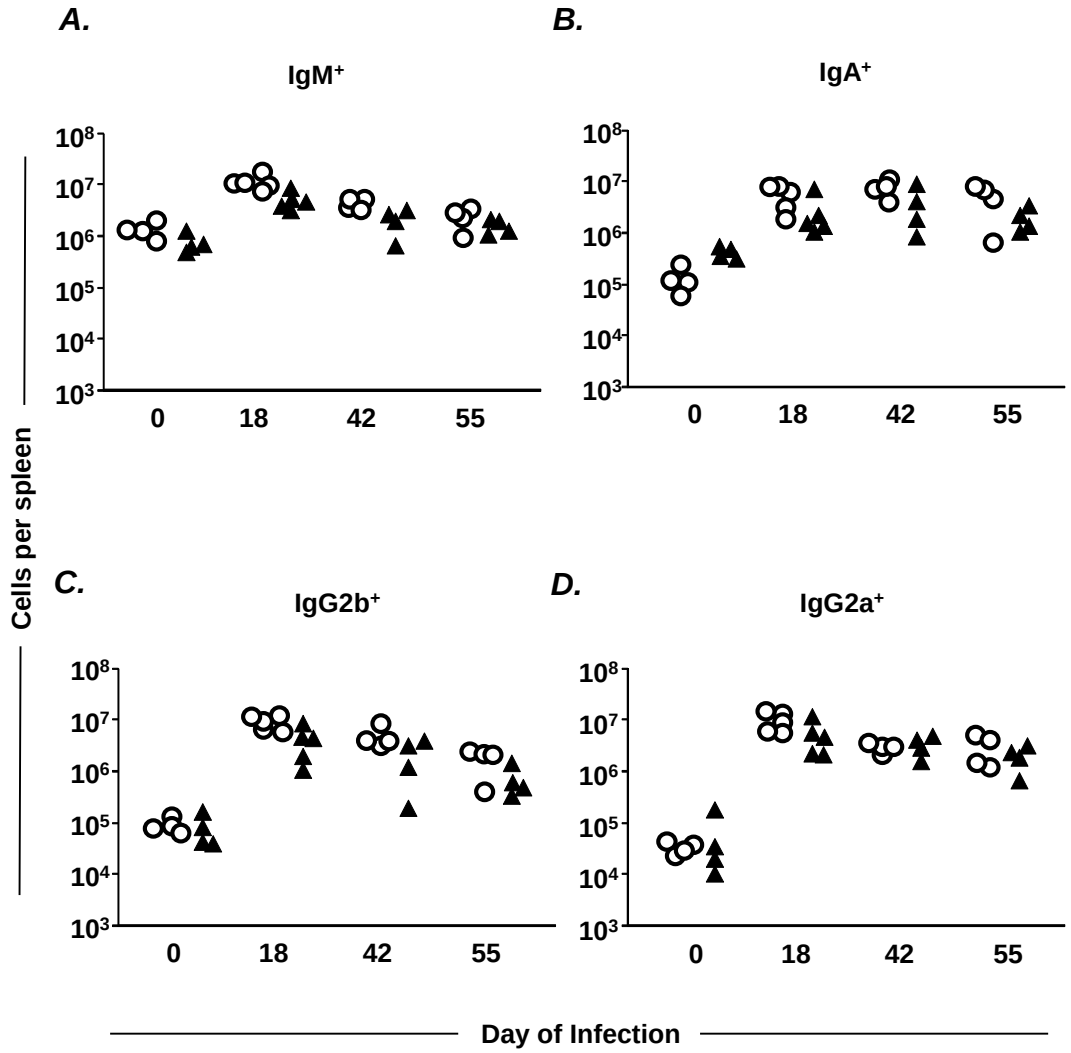

Figure 4.6. Splenic EF plasma cell numbers in WT and IL6$^{-/-}$ mice during STm infection. WT and IL6$^{-/-}$ mice were infected with 5x10^5 STm or remained uninfected as controls. Spleens were removed at the specified time points and the number of ***A,*** IgM$^+$ ***B,*** IgA$^+$ ***C,*** IgG2b$^+$ and ***D,*** IgG2a$^+$ plasmacytoid cells were quantified by histology. One point represents one mouse. Data are representative of ≥ 2 experiments giving similar results.

4.2.6 IL6$^{-/-}$ mice have sub-optimal antibody responses during STm infection

During STm infection of WT mice, the appearance of GC coincides with enhanced titres of class-switched antibody in the serum (70). As GC development was impaired in IL6$^{-/-}$ mice, whilst the EF plasma cell response remained largely intact, OMP-specific serum antibody titres were quantified in WT and IL6$^{-/-}$ mice by ELISA, before and during STm infection. Prior to infection, low levels of anti-OMP IgM were detected in the sera of some WT and IL6$^{-/-}$ mice, however switched OMP-specific antibody was undetectable in both groups (figure 4.7). At each time point p.i, titres of serum IgM were similar between the two groups, with the exception of day 18 when IgM antibody titres were significantly lower in IL6$^{-/-}$ mice compared to WT mice ($p \leq 0.05$) (figure 4.7A). As expected, by day 42 p.i, WT mice had high levels of switched IgA, IgG2b and IgG2a OMP-specific antibody in the serum (figure 4.7 B-D). In contrast, IL6$^{-/-}$ mice had decreased levels of each of these subclasses when compared to WT mice (all $p \leq 0.05$), however antibody titres had recovered by day 55 p.i. Thus, the delay in GC formation in IL6$^{-/-}$ mice coincides with a delay in class-switched antibody production, whilst EF plasma cell development is only modestly impacted by a loss of IL6.

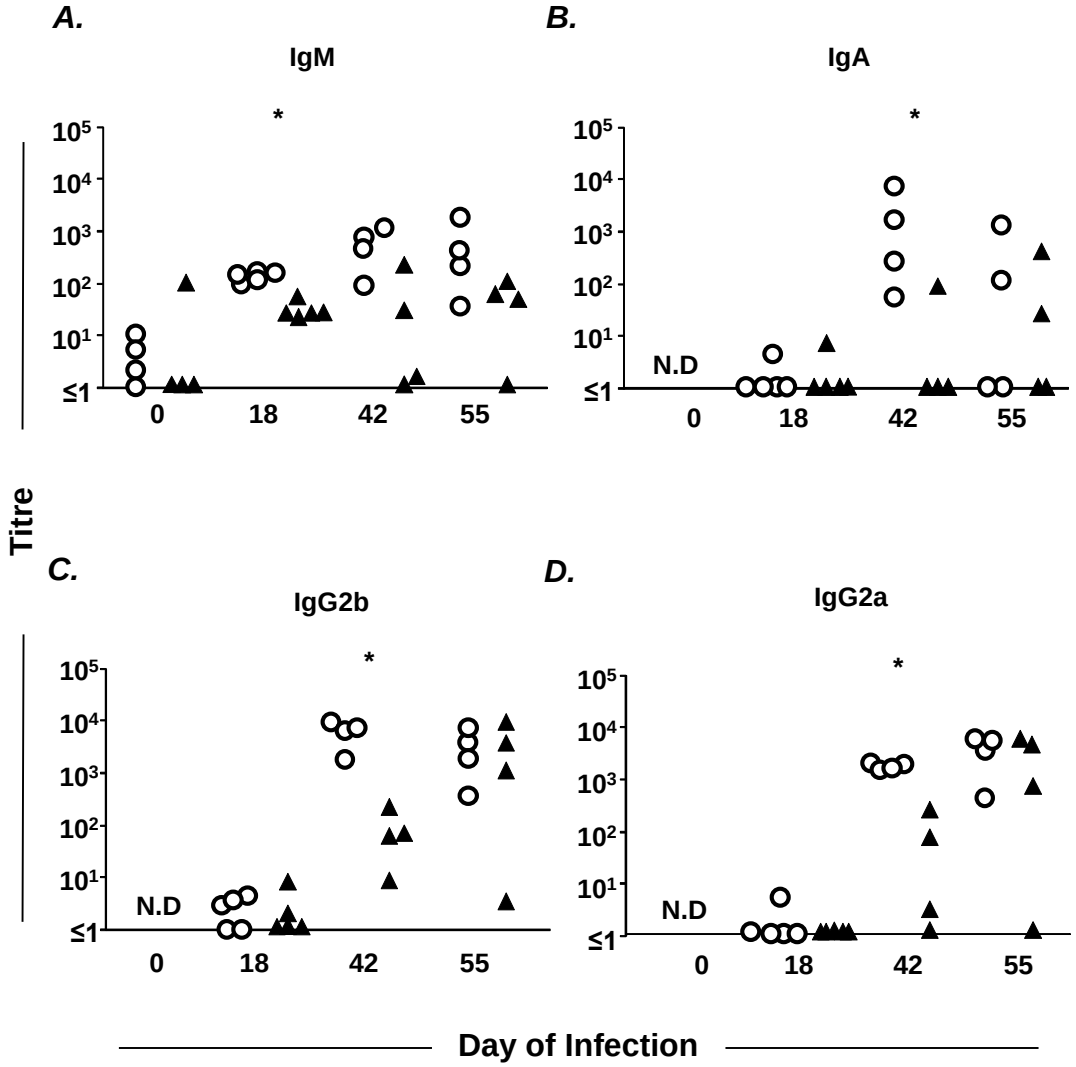

Figure 4.7. OMP-specific antibody titres in WT and IL6$^{-/-}$ mice throughout STm infection. WT and IL6$^{-/-}$ mice were infected with 5x10^5 STm or remained uninfected as controls. Anti-OMP ***A,*** IgM$^+$, ***B,*** IgA$^+$, ***C,*** IgG2b$^+$ and ***D,*** IgG2a$^+$ serum antibody was quantified in WT and IL6$^{-/-}$ mice before and at the indicated time points after infection. One point represents one mouse. Data are representative of ≥ 2 experiments giving similar results. * $p \leq 0.05$.

4.2.7 Selective defects in mRNA gene expression in STm-exposed IL6$^{-/-}$ B cells

During T-D antibody responses, class-switching in B cells is initiated during the initial cognate T-B interaction at the T-B border in SLO, at which point, germline switch-transcripts are up-regulated in B cells (56). Given the presence of a class-switched EF response, we hypothesised that T-B interaction in the spleen and switch transcript induction would remain intact in IL6$^{-/-}$ B cells. To test this B220^{+} CD19^{+} splenic B cells were FACS sorted from WT and IL6$^{-/-}$ mice that had been exposed to STm for either 30 days or 42 days, for gene expression analysis by RT-PCR. Unpublished data from our laboratory shows that two peaks in γ2a-germline switch transcript-expression occurs during STm infection, one at day 4 and day 35 p.i, whilst at day 7 and 21, expression is at uninfected levels. Consistent with this, at day 30 p.i, some of the WT and IL6$^{-/-}$ mice analysed here expressed very low levels of γ2a-germline switch transcript mRNA, whilst by day 42 p.i, expression levels had increased in both groups (figure 4.8A). Importantly, there was no difference in expression between WT and IL6$^{-/-}$ mice at either time point, indicating that T-B interactions were probably taking place in the spleens of IL6$^{-/-}$ mice.

The processes of CSR and SHM in B cells both require AID (141,142), and as such, this enzyme is highly expressed in GC B cells. As GC development and optimal class-switching is defective in IL6$^{-/-}$ mice, we assessed AID expression in CD19^{+}B220^{+} B cells at day 30 and 42 p.i. Consistent with this, mRNA expression of AID was significantly lower in IL6$^{-/-}$ B cells than in WT B cells at day 30 p.i ($p \leq 0.05$), but had reached expression levels that were similar to WT by day 42 p.i (figure 4.8B). B cells that enter GC reactions also up-regulate Bcl6 (127), as do the specialized subset of Tfh cells that facilitate GC

reactions (111,112,121). IL6 has been shown to influence Tfh development and as such, mRNA expression of Bcl6 was measured in FACS sorted $B220^+$ $CD19^+$ B cells and $CD3^+$ $CD4^+$ T cells from STm-exposed WT and $IL6^{-/-}$ mice by RT-PCR. This analysis revealed that IL6-loss did not affect BCL6 expression in T cells and B cells at day 30 or 42 p.i. (figure 4.8C). We therefore sought to determine whether Tfh cells could be detected in the spleens of STm infected $IL6^{-/-}$ mice.

4.2.8 Tfh cells are largely absent from the spleens of $IL6^{-/-}$ mice until day 55 p.i

Spleen sections were stained by confocal microscopy, using the markers CD3, PD1 and Bcl6 to identify Tfh cells, as described previously (107). At day 18 of infection, no cells of this phenotype could be detected in the spleens of WT or $IL6^{-/-}$ mice (data not shown). By day 42 p.i, numerous Tfh cells of this phenotype were detectable in WT GC, however these cells were only sporadic in $IL6^{-/-}$ spleens (figure 4.9). By day 55 however, when $IL6^{-/-}$ mice had formed GC, Tfh cells could be observed at higher frequencies within these structures. Thus, these data may infer that a loss of IL6 impairs GC-Tfh development during STm infection. However, it is difficult to determine whether the lack of Tfh cells is due to the paucity of GC, or whether GC do not develop as a consequence of Tfh absence. To help us determine the cellular source of the IL6 that drives optimal GC responses during STm infection, we created radiation chimeras in which IL6 was absent in either haematopoietic cells, or in radiation-resistant cells. Cells of both origins are able to secrete IL6 and may therefore have a role in mediating effective antibody responses during STm infection.

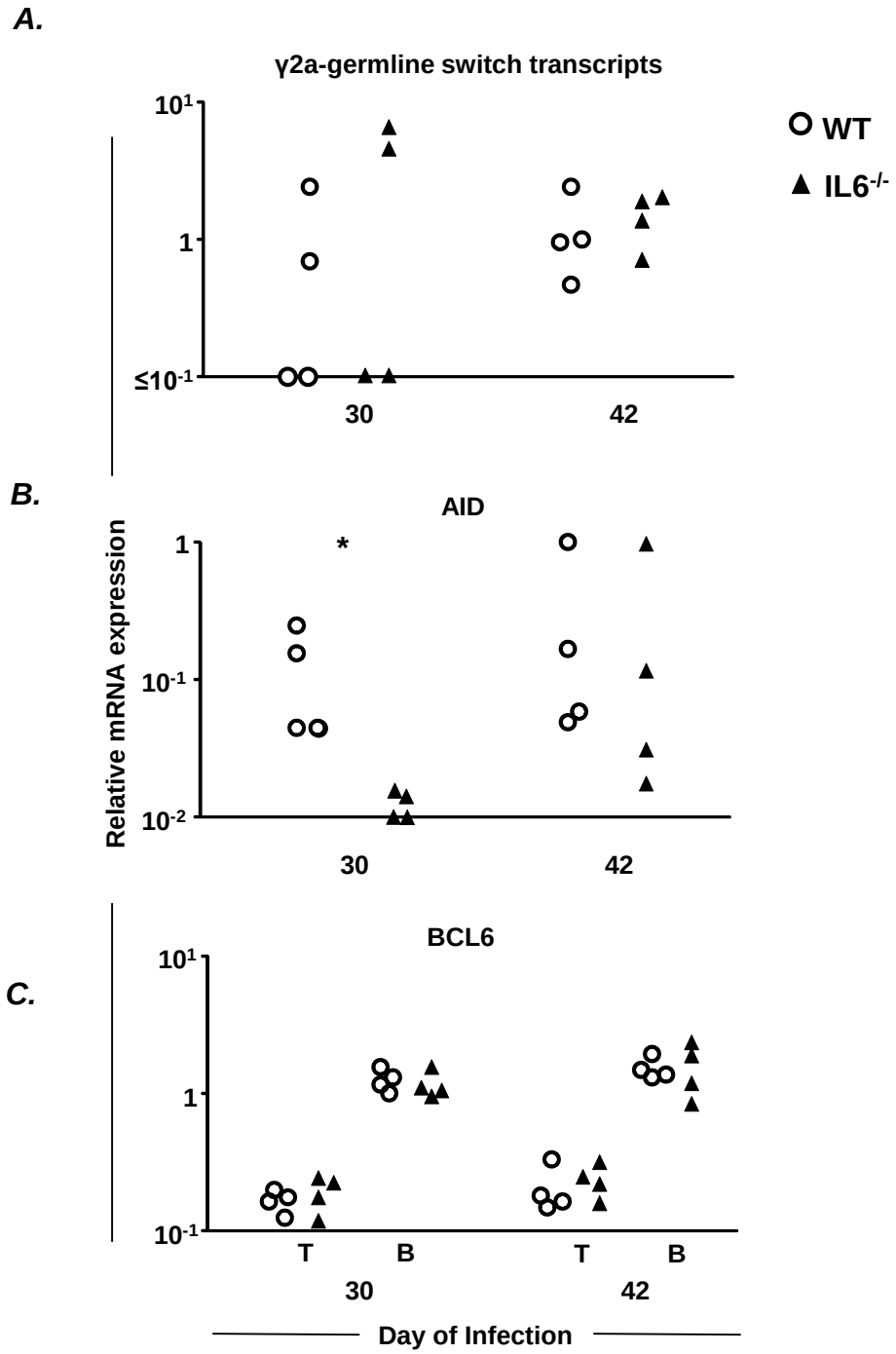

Figure 4.8. Relative γ2a-germline switch transcript, AID and Bcl-6 expression in WT and IL6$^{-/-}$ cells during the late stages of STm infection. WT and IL6$^{-/-}$ mice were infected with 5x10^5 STm and at the specified time points, splenic CD19$^+$B220$^+$ B cells and CD3$^+$CD4$^+$ T cells were sorted by FACS. Relative mRNA gene expression of ***A,*** γ2a germline-switch transcripts in B cells ***B,*** AID expression in B cells and **C,** Bcl6 in T cells and B cells was quantified by RT-PCR. Samples were normalized to β-actin. One point represents one mouse. Data are from one experiment. * $p \leq 0.05$.

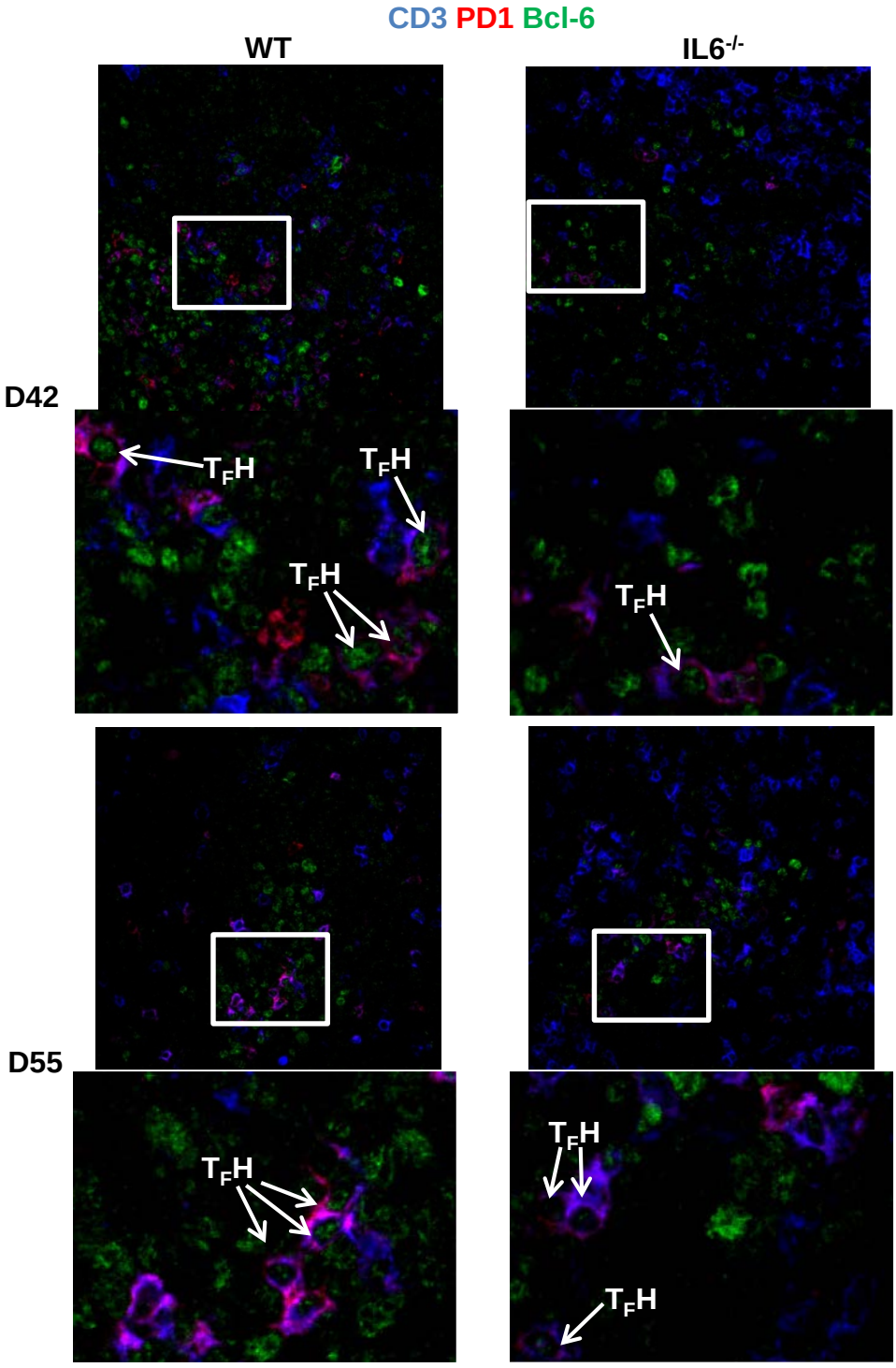

Figure 4.9. Tfh cells in WT and IL6$^{-/-}$ mice during the late stages of STm infection. WT and IL6$^{-/-}$ mice were infected with 5x10^5 STm and at the specified time points, spleens were removed and stained for CD3$^+$(blue) PD1$^+$(red) Bcl6$^+$(green) Tfh cells by confocal microscopy. White squares represent enlarged areas shown below. Photos are representative of at least 7 mice per group.

4.2.9 Bone-marrow chimeras with selective deficiency in IL6 resolve STm infection comparatively

WT and IL6$^{-/-}$ mice were lethally irradiated (recipient) and reconstituted with WT or IL6$^{-/-}$ bone marrow cells (donor). Where possible, EYFP WT mice were used either as donors or recipients, in order to assess reconstitution by flow cytometry. Four groups of donor>recipient chimeric mice were created as follows: WT(EYFP)>WT, WT(EYFP)>IL6$^{-/-}$, IL6$^{-/-}$>WT(EYFP) and IL6$^{-/-}$>IL6$^{-/-}$ (figure 4.10) resulting in mice that were IL6 sufficient in all cells, haematopoietic cells alone, radiation-resistant cells alone or no cells respectively. In the WT(EYFP)>WT and WT(EYFP)>IL6$^{-/-}$ mice, 100% of the haematopoietic cells were expected to be EYFP^{+}, whilst in the IL6$^{-/-}$>WT(EYFP) mice, 0% of the haematopoietic cells should be EYFP^{+}. For clarity, the EYFP denotations will no longer be referred to in the text. Flow cytometric analysis revealed that CD3^{+}CD4^{+} T cells and CD19^{+}IgM^{+} B cells reconstituted the spleen at the expected frequency (data not shown). Staining of total splenocytes by flow cytometry revealed that the vast majority of host cells had been replaced by the donor population (figure 4.11A). Typically, ≥ 90% of B cells and T cells in the spleen were of donor BM origin (figure 4.11B). Elimination of host cells and replacement by donor BM cells was consistently more effective in the IL6$^{-/-}$>WT group when compared to the other chimeras. This suggests that some of the non-EYFP cells found in the WT>WT and WT>IL6$^{-/-}$ groups may arise from the small population of non-EYFP cells that, in our experience, are found in EYFP mice. Following reconstitution, chimeric mice were infected with 10^5 STm for 35 days, a point at which the GC response would be established if bacterial infection had largely resolved. As expected, quantification of splenic bacteria found all chimeras to have similar bacterial burdens at day 35 p.i (figure 4.12), demonstrating an equal capacity to resolve the infection across groups.

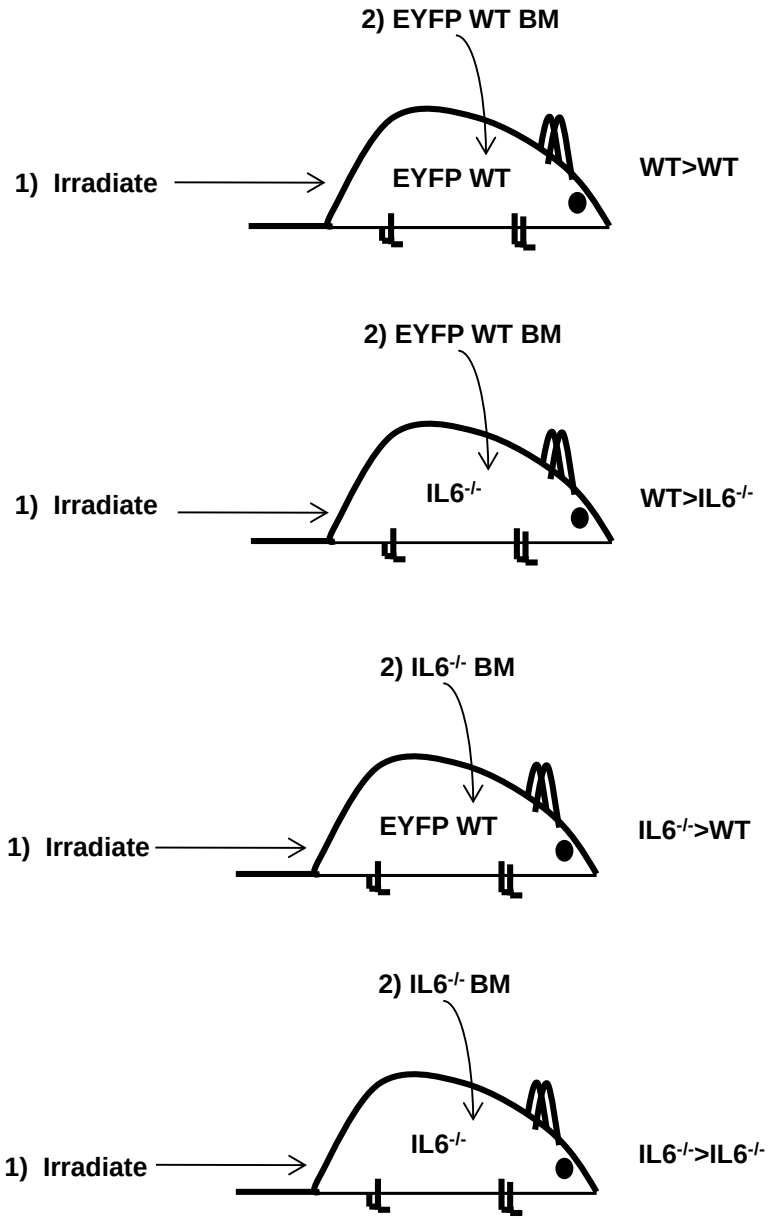

Figure 4.10. Creation of BM chimeras with selective deficiency in IL6. EYFP WT or IL6$^{-/-}$ mice were lethally irradiated (9Gys) (recipient, labelled on the cartoon) and then reconstituted with EYFP WT or IL6$^{-/-}$ total bone marrow cells (donor, shown above the cartoon). Four groups of doner>recipient mice were created as follows: WT>WT, WT>IL6$^{-/-}$, IL6$^{-/-}$>WT and IL6$^{-/-}$>IL6$^{-/-}$. Following reconstitution, chimeric mice were infected with 10^5 STm for 35 days.

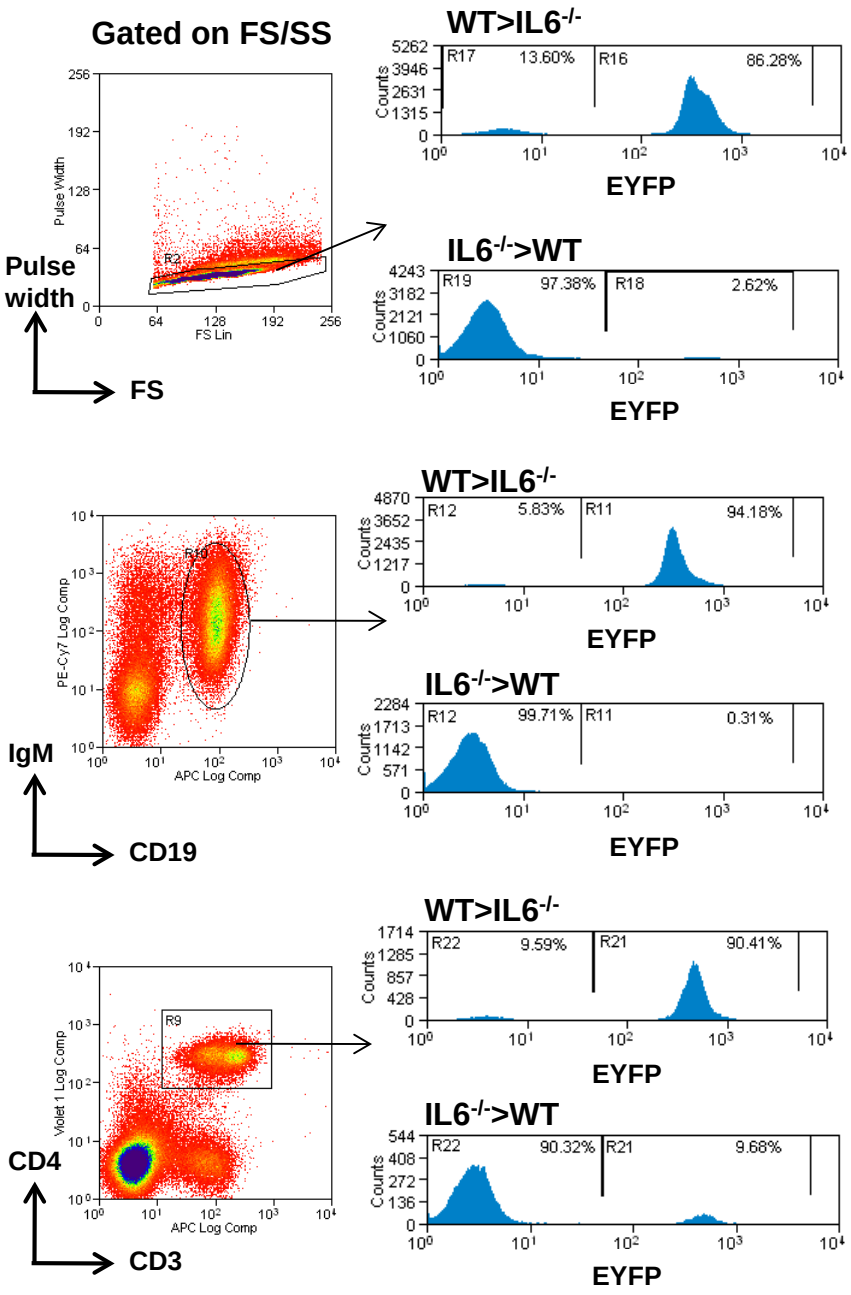

Figure 4.11. Splenic reconstitution of BM chimeras at day 35 of infection with STm. WT and IL6$^{-/-}$ mice were lethally irradiated and reconstituted with WT or IL6$^{-/-}$ total bone marrow cells. Following reconstitution, chimeric mice were infected with 10^5 STm for 35 days and splenocytes were stained for the presence of EYFP$^+$ cells in WT>WT (not shown) and WT>IL6 mice and for the absence of EYFP cells in Il6>WT mice. EYFP presence/absence is shown on total splenocytes (top histograms), B cells (middle histograms) and CD4$^+$ T cells (bottom histograms). Plots are representative of 8 mice in each group. FS = forward scatter; SS = side scatter.

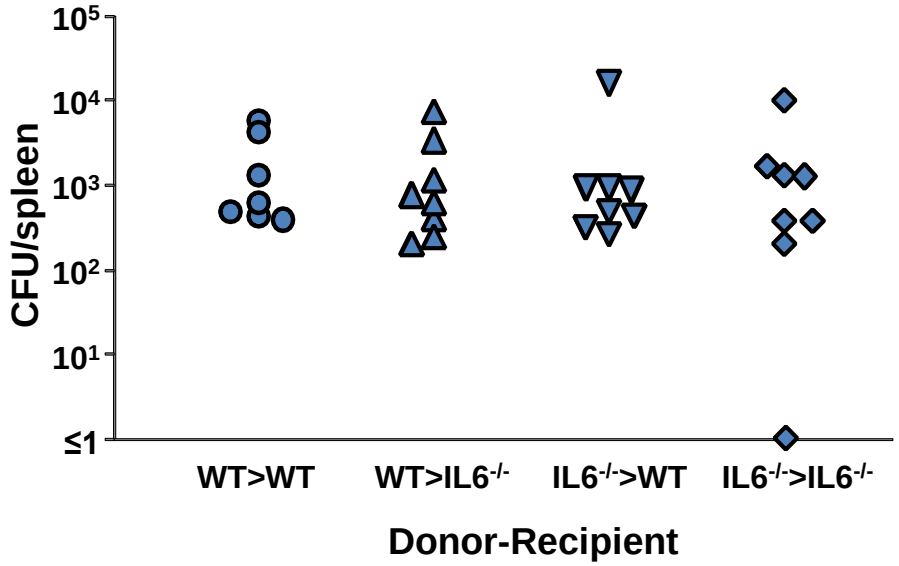

Figure 4.12. Number of bacteria per spleen in bone marrow chimeras at day 35 of infection with STm. WT and IL6$^{-/-}$ mice were lethally irradiated and reconstituted with WT or IL6$^{-/-}$ total bone marrow cells. Following reconstitution, chimeric mice were infected with 10^5 STm for 35 days and the number of CFU per spleen were quantified. One point represents one mouse . Data are pooled from 3 individual experiments.

4.2.10 IL6 produced by either haematopoietic or radiation-resistant cells is sufficient to restore normal B cell responses during STm infection

To help determine the origin of the IL6 required for optimal GC formation and antibody production during STm infection, splenic GCs were quantified by histology in the four groups of chimeric mice. Staining of spleen sections revealed that, as expected, GC development was impaired in the $IL6^{-/-}$>$IL6^{-/-}$ chimeras when compared to the WT>WT chimeras ($p \leq 0.05$) at day 35 of infection (figure 4.13). Surprisingly however, both the WT>$IL6^{-/-}$ and $IL6^{-/-}$>WT chimeras had a similar GC volume and proportion of follicle occupied by GC to WT>WT mice (figure 4.13BI). Furthermore, examination of the splenic EF plasma cell response revealed that whilst $IL6^{-/-}$>$IL6^{-/-}$ mice had fewer IgM^+, $IgG2b^+$ and $IgG2a^+$ plasma cells than WT>WT mice ($p \leq 0.05$), plasma cell numbers in WT>$IL6^{-/-}$ and $IL6^{-/-}$>WT mice were comparable to WT>WT mice (figure 4.14). Antigen-specific antibody responses were next measured by ELISA, revealing that IgM production was similar in all groups (figure 4.15 A). Analysis of class-switched IgG2b and IgG2a antibody identified a clear defect in class-switched antibody production by $IL6^{-/-}$>$IL6^{-/-}$ mice, whereas no difference in antibody titres was observed in WT>$IL6^{-/-}$ and $IL6^{-/-}$>WT mice when compared to WT>WT mice (figure 4.15B and C). Thus, the provision of IL6 from either haematopoietic or radiation resistant cells was sufficient to restore GC development and antibody class-switching during STm infection. Thus, IL6 can be considered an important cytokine in the regulation of B cell responses during STm infection, however redundancy in the cellular source of IL6 that promotes these functions are apparent in this model.

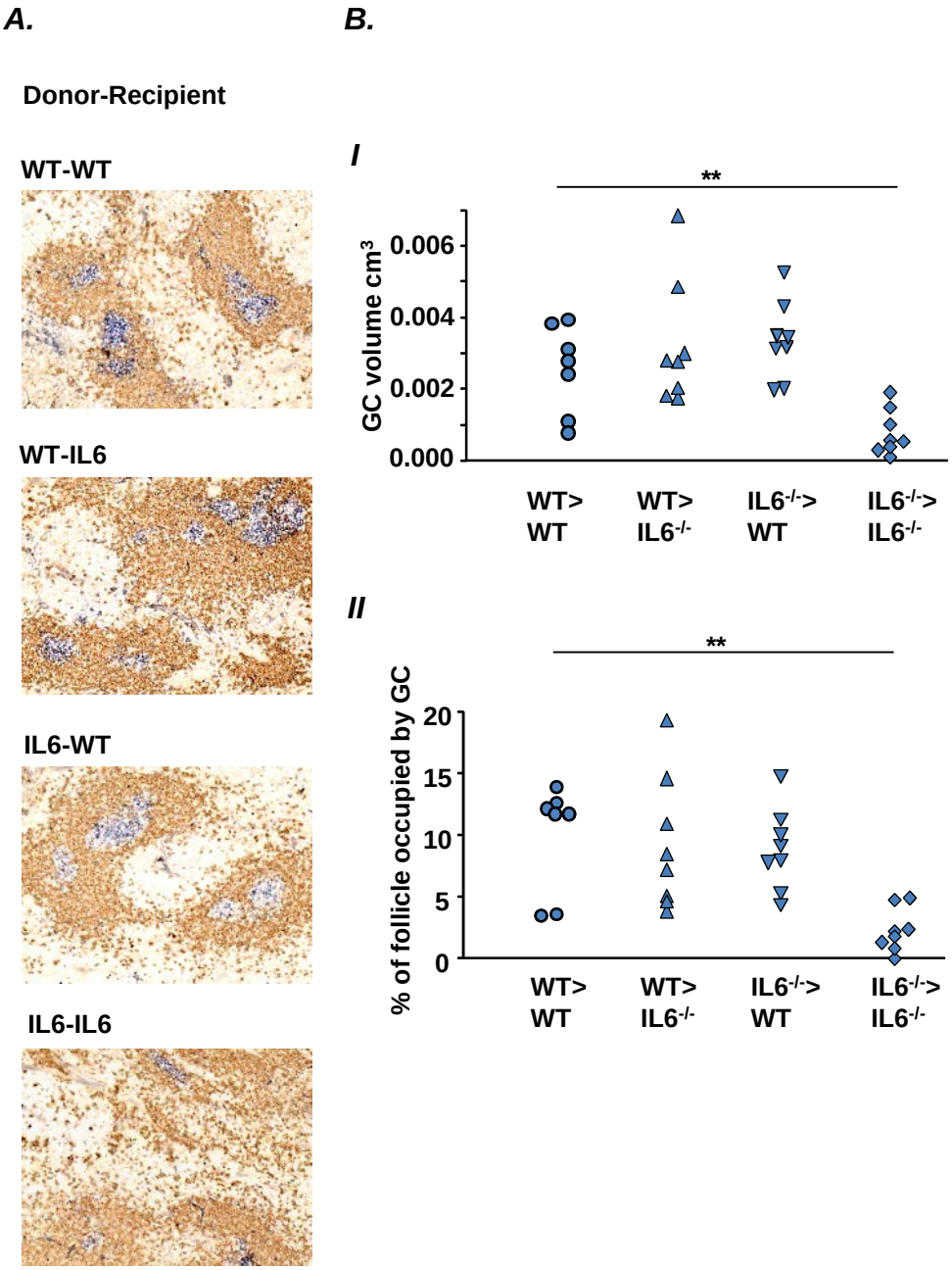

Figure 4.13. GC development in bone marrow chimeras at day 35 of infection with STm. WT and IL6$^{-/-}$ mice were lethally irradiated and reconstituted with WT or IL6$^{-/-}$ total bone marrow cells. Following reconstitution, chimeric mice were infected with 10^5 STm for 35 days. ***A.*** Spleens were stained for PNA (blue) to identify GC and IgD (brown) to identify follicular B cells. ***B. II*** total GC volume and ***III*** the proportion of follicle occupied by GC was quantified by histology. Photos are representative of 7-8 mice per group. One point represents one mouse. Data are combined from three individual experiments. ** $p \leq 0.01$

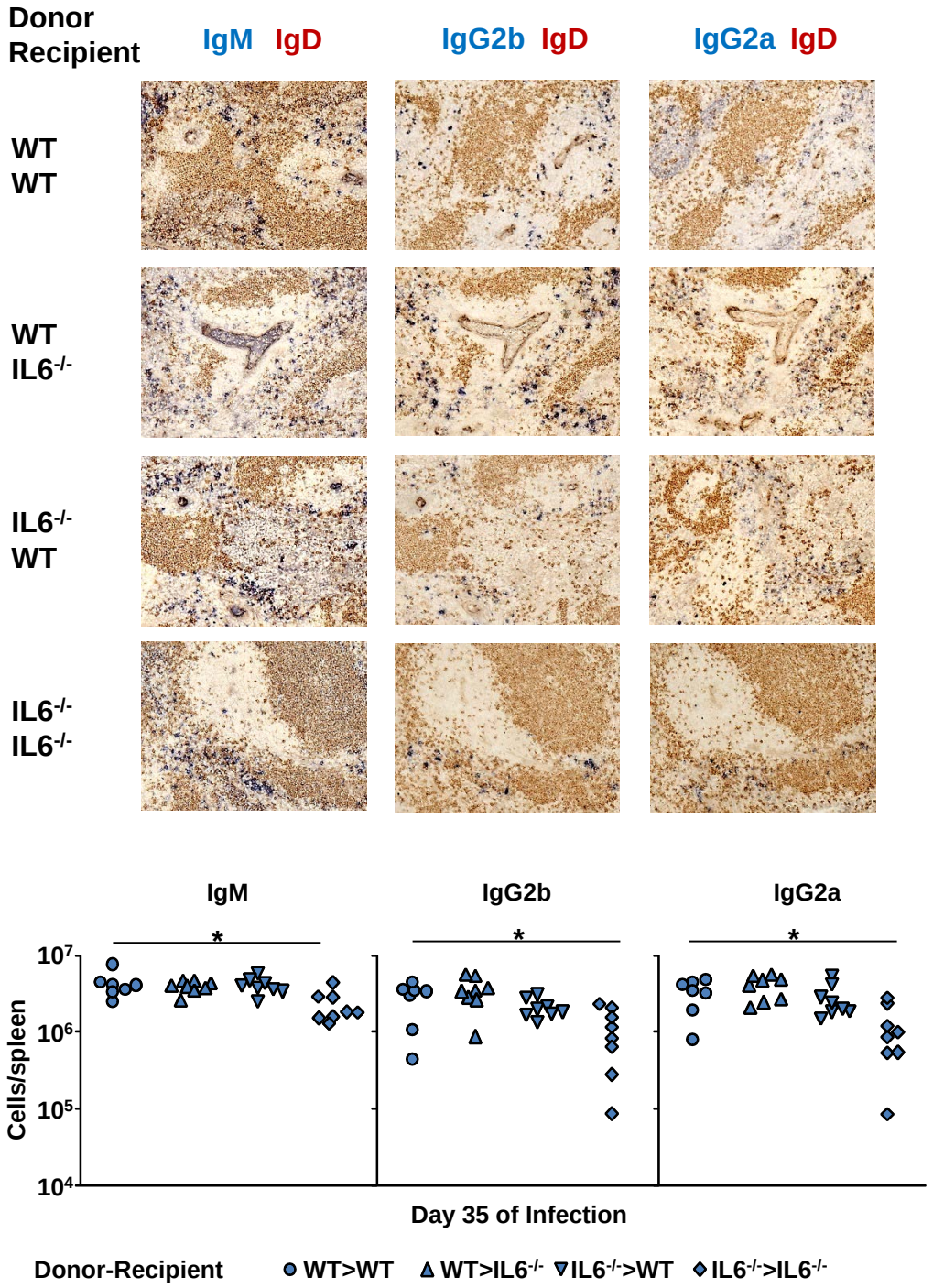

Figure 4.14. GC development in bone marrow chimeras at day 35 of infection with STm. WT and IL6$^{-/-}$ mice were lethally irradiated and reconstituted with WT or IL6$^{-/-}$ total bone marrow cells. Following reconstitution, chimeric mice were infected with 10^5 STm for 35 days. Spleens were stained for IgM (left panels), IgG2b (middle panels) and IgG2a (right panels) to identify non-switched and switched EF plasma cells Photos are representative of 7-8 mice per group. One point represents one mouse. Data are combined from three individual experiments. * $p \leq 0.05$

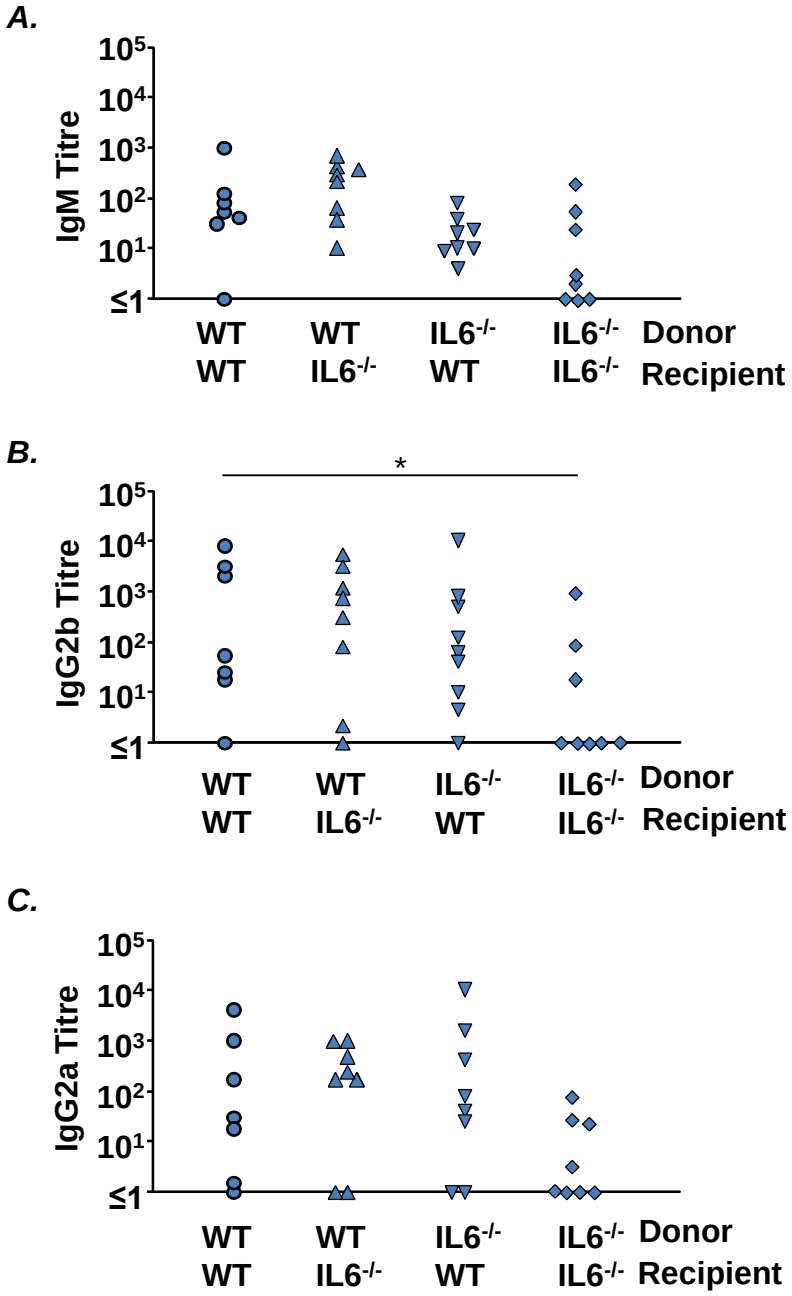

Figure 4.15. OMP-specific serum antibody titres in bone marrow chimeras at day 35 of infection with STm. WT and IL6$^{-/-}$ mice were lethally irradiated and reconstituted with WT or IL6$^{-/-}$ total bone marrow cells. Following reconstitution, chimeric mice were infected with 10^5 STm for 35 days. Anti-OMP serum ***A,*** IgM, ***B,*** IgG2b and ***C,*** IgG2a antibody titres were quantified by ELISA. One point represents one mouse. Data are combined from three individual experiments. * $p \leq 0.05$

4.3 Discussion

Cytokines have an important role in driving and regulating GC responses and antibody class-switching following immunisation with protein antigens. This chapter assessed the contribution of IL4, IL13 and IL6 to GC and EF antibody responses during STm infection. Whilst EF plasma cell development was maintained in IL4$^{-/-}$, IL13$^{-/-}$ and IL4Rα$^{-/-}$ mice, GC development was somewhat attenuated in each of these groups. These aberrations did not affect antibody output, as antigen-specific serum antibody titres were comparable to WT mice at the time point studied. Furthermore, a loss of IL4 and/or IL13 signalling did not result in enhanced levels of serum IgG2a or IgG2b in response to STm, as might be expected based on previous data (91,94,95). Conversely, IL6$^{-/-}$ mice were unable to mount effective antibody responses to STm, with GC development and optimal class-switched antibody production delayed until day 55 p.i. Smaller defects were apparent in the EF pathway of B cell differentiation into class-switched plasma cells, although differences between WT and IL6$^{-/-}$ mice may have been masked by small group numbers. Surprisingly, the provision of IL6 from either radiation-resistant or haematopoietic cells was sufficient to restore the GC response and antibody class-switching following STm infection. Thus, this work reveals some similarities and some differences in the way that Th1 and Th2 GC responses develop and are maintained.

4.3.1 Regulation of GC formation and antibody class switching by IL4 and IL13

Infection of IL4$^{-/-}$, IL13$^{-/-}$ and IL4Rα$^{-/-}$ mice show these cytokines to be dispensable for bacterial clearance. These findings contradict those that describe IL4 as detrimental to the

resolution of *Salmonella* infection (264), as the elimination of this cytokine did not accelerate recovery. The absence of IL13 did appear to accelerate clearance, however further unpublished data from our laboratory did not confirm this. As bacterial clearance was efficient in all groups of mice, any observed defect in GC development could not be attributed to a failure to resolve infection. Whilst numerous GC were present in the spleens of $IL4^{-/-}$, $IL13^{-/-}$ and $IL4R\alpha^{-/-}$ mice following STm infection, there was a diminution in the total GC volume and proportion of follicle occupied by GC in each of these groups at day 42 p.i. Furthermore, the extent of the defect was remarkably similar in all groups, which taken together, suggests a probable role for IL4 and IL13 in optimising GC development in during STm infection. These data further imply some overlap in IL4 and IL13 function in this model. One confounding factor is the high number of background GC observed in the spleens of uninfected $IL13^{-/-}$ mice. The median volume of GC in the spleen actually reduced in this group following infection, making the data more difficult to interpret. However, this finding is consistent with the ability of STm to suppress GC development (70), and the high titres of class-switched antibody in the sera of $IL13^{-/-}$ mice at day 42 p.i confirm the antigen specificity of these GC.

In response to model protein antigens, neither IL4 nor IL13 deficiency alone alters GC formation, however double deficiency in IL4 and IL13, or an inability to respond to these cytokines via the IL4Rα, does cause a reduction in GC size at a point when B cells are being selected in GC (93) (94). The data from the current study suggest that IL4 and IL13 do not operate in a redundant fashion to promote GC development, however this could explain the data from experiments using non-viable protein antigens, as the presence of either IL4 or IL13 is sufficient to restore the defect that occurs when both cytokines or the

receptor alpha-chain is absent. Thus, IL4 and IL13 may have a generic role in GC formation, highlighting an ability for GC to Th1 and Th2 antigens to develop in the same way. One cell that may be important in this regard is the Tfh cell, as they can express (114,126,259) and produce IL4 (126,260), although IL13 expression has not been reported in these cells. It could be argued that IL4 from Tfh cells supports GC reactions *per se*, rather than having a bias for Th2 responses. Arguing against this is the finding that Tfh cells can also secrete IFNγ (126) and the Ig isotype produced by B cells that have entered GC reactions is dependent upon the cytokine expression profile of the interacting Tfh cell (126). Thus, during STm infection, where production of IgG2a and Igg2b is dominant, one would assume that Tfh cells secrete IFNγ and that IL4 is dispensable. Indeed, no defect in IgG2a or IgG2b switched antibody was observed in $IL4^{-/-}$, $IL13^{-/-}$ or $IL4R\alpha^{-/-}$ mice at this time point. Perhaps in the absence of these cytokines, the capacity for B cells to switch to Th1-related isotypes is enhanced, and the less abundant GC actually mask this effect. Previously, enhanced Th1 activity, including higher levels of T-bet and γ2a-switch transcript expression, was reported in spleens from $IL4R\alpha^{-/-}$ mice following immunisation with alum-ppt protein (94). Others report enhanced IgG2a secretion in $IL4^{-/-}$ mice (95), and enhanced IgG2a and IgG2b in IL4 and $IL4^{-/-}IL13^{-/-}$ double deficient mice (91) during recall responses to *N*. brasiliensis and alum ppt-protein.

Given the presence of antigen-specific, class-switched antibody in $IL4^{-/-}$, $IL13^{-/-}$ and $IL4R\alpha^{-/-}$ mice during infection, the reduced GC volume in these mice is unlikely to impact upon primary antibody responses to STm. Switched IgG1 antibody, which is associated with Th2 responses that induce IL4 ad IL13 production, is not secreted during primary responses in this model. However, this sub-class of antibody can be detected in the sera of

WT mice following *Salmonella* infection and rechallenge (79). It would therefore be interesting to ascertain whether IL4 and/or IL13 have a role in protective immunity to STm. Furthermore, enhanced IgG2a production may only become apparent during recall responses, as seen previously in IL4 or $IL4^{-/-}IL13^{-/-}$ double deficient mice (91,95).

4.3.2 Regulation of GC formation and antibody class switching by IL6

Infection of $IL6^{-/-}$ mice with STm revealed that IL6 is not required for bacterial clearance, although heightened bacterial burdens have previously been shown in $IL6^{-/-}$ mice during the early infection (our unpublished observations). Here we show that optimal GC formation and class-switched antibody production is dependent upon IL6, a cytokine that has long been recognised as a growth factor for B cells (265) and is known for its role in plasmablast proliferation and survival (266). Consistent with this, several studies report impaired antibody responses in the absence of IL6 (103,104,267). During T-D B cell responses, antibody can arise from either EF- or GC-derived plasma cells. In the current study, the production of class-switched EF plasma cells was marginally affected by IL6 loss, whilst optimal GC development and class-switched antibody secretion was markedly impaired. These findings suggest that the GC pathway of antibody production is impaired in $IL6^{-/-}$ mice, with the low titres of class-switched antibody present in the sera of $IL6^{-/-}$ at day 42 p.i arising from the EF pathway of plasma cell growth. These data are inconsistent with others that attribute defects in antibody production in $IL6^{-/-}$ mice to defects in EF plasma cell secretion (121,124). A recent study reported marked defects in anti-viral antibody responses following IL6 blockade in C57BL6 mice, which coincided with a modest reduction in EF plasma cells numbers but no reduction in GC B cell numbers

(124). Others have reported significantly reduced IgG titres in $IL6^{-/-}$ mice infected with LCMV for 8 days, despite no diminution in GC B cell numbers. These titres recovered by day 15, suggesting a defect in the earlier-onset EF plasma cell response (121). Whilst our data also show a delay in optimal antibody production, this is likely to reflect a GC defect, as GC development is also impaired and a high proportion of the antibody secreted into the sera at day 42 p.i arises from the GC (70).

In support of our data, GC defects have been reported in $IL6^{-/-}$ mice immunised with model protein antigens. A reduction in GC volume was observed in $IL6^{-/-}$ mice at day 9 after immunisation with DNP-OVA, despite the normal formation of GC by day 7 (103). These data suggest a defect in GC maintenance, rather than GC induction, which differs from our data, although GC persistence was not directly assessed here. Other studies have reported defective GC formation in $IL6^{-/-}$ mice in a dose-dependent manner; whilst GC formation was impaired following a low dose of alum-ppt protein, they developed independently of IL6 at higher antigen doses (104). Importantly, these defects in GC formation were linked to impaired IgG2a and IgG2b (103) or total IgG (104) antibody production, findings that are consistent with our data.

Whilst a number of studies support a role for IL6 in Ig class-switching, some infection models disagree with this requirement. Mice deficient in IL6 were shown to produce enhanced levels of antigen specific IgG2a in response to infection with *Candida.* albicans, despite producing lower levels of IFNγ and higher levels of IL4 than WT mice (268). Other conflicting results from $IL6^{-/-}$ mice relate to IgA production. Whilst some research supports a role for IL6 in local IgA production (262), others find IL6 to be dispensable for

local intestinal GC formation, lavage-fluid IgA and serum IgG production, in response to infectious antigens (263). Release of IgA at mucosal surfaces is likely to have a role during STm infection and IL6 is released by intestinal epithelial cells during the response (269). Our data clearly demonstrate that IgA^+ EF plasma cells can form in the spleens of $IL6^{-/-}$ mice, however titres of serum IgA are impaired at day 42p.i. Incongruent research findings may relate to the different antigens used to stimulate the antibody response, however antigen dose may also be a contributory factor. IL6 is thought to regulate the production of complement component C3 (103), and the disruption of C3 ligation to CD21 (complement receptor 2; CR2) was linked to attenuated antibody responses and GC formation in response to DNP-OVA (103). Other studies have shown that blocking CR2 ablates IgG antibody responses only at suboptimal concentrations of antigen (270), suggesting that at high antigen doses, the need for IL6-mediated binding of C3 to CR2, may be overcome. Since GC development coincides with a dramatic reduction in bacterial burden during STm infection, IL6 may be important for complement-mediated, GC derived antibody production in this system.

An alternative explanation is that antibody defects arise from a loss of IL6 signalling in lymphocytes. A previous report, analysing the cytokines present in different areas of the lymph node during T-D antibody responses, revealed that IL6 is expressed at the highest level within the T cell zone and that $CD11c^+$ DC are the main source of this cytokine (271). As such, IL6 may be important for T cell priming and subsequent interactions with B cells may be delayed in its absence. In support of this, $IL6^{-/-}$ DC pulsed with keyhole limpet hemocyanin (KLH) antigen were unable to induce antigen-specific IgG1 or IgG2a antibody following injection into WT mice (122). This suggests that IL6 can act on T cells

to induce antibody production by B cells. In agreement, IL6 has been shown to up-regulate IL21 in T cells when stimulated *in vitro* or *ex vivo*, which in turn stimulates B cells to produce class-switched antibody (267). An IL6-mediated increase in class-switched antibody production via IL21 was also demonstrated *in vivo,* using inactive influenza vaccination in conjunction with IL6 (267). Thus, IL6 can promote antibody production by B cells via indirect, T cell mediated mechanisms, suggesting that T-B interactions may be negatively affected in the absence of IL6. Numerous factors induce AID expression in B cells, one of these being CD40-CD40L engagement in combination with cytokine stimulation (272,273). The induction of AID was delayed in $IL6^{-/-}$ mice, which may reflect aberrant T-B communication prior to GC or EF growth. A loss of CD40-CD40L signals could also explain defects in GC formation, as these structures do not form adequately in the absence of these molecules (55,274). On the other hand, mRNA expression of γ2a-germline switch transcripts was not compromised in $IL6^{-/-}$ mice at day 30 or 42 of STm infection, implying that T-B interactions did occur in $IL6^{-/-}$ mice at these times (56). Although AID expression was defective in $IL6^{-/-}$ B cells it was not completely absent, which may reflect a lack of the integrated signalling required to optimise AID expression. This in turn would explain why optimal CSR is not apparent until later in $IL6^{-/-}$ mice.

The expansion of B cells in EF, rather than follicular sites, suggests a possible defect in B cell or T cell GC entry. This could not be attributed to a failure of $IL6^{-/-}$ B cells or T cells to express Bcl-6, as expression levels were equivalent to WT B cells. A requirement for B cells and Tfh cell movement into follicles is the expression of CXCR5. Blocking T helper cell activation inhibits CXCR5 expression by T cells and GC reactions are subsequently impaired (275). IL6 has not been reported to modulate CXCR5 expression, or the

migration of T and B cells into follicles, however a closer analysis of chemokines and chemokine receptors within various areas of IL6 deficient spleens would help to address this issue.

A second, critical point of T-B interaction occurs once B cells enter the GC reaction. Much recent interest has surrounded the signals that govern T cell differentiation into Tfh cells, for which IL6 and IL21 are both primary candidates. Whilst both of these cytokines can contribute to Tfh development, mice lacking either of these cytokines in isolation are able to generate Tfh cells *in vivo* (120,121). In agreement, recent data highlights a redundant role for IL6 and IL21 in Tfh development (124), commensurate with their shared ability to signal through STAT-3 (276). As such, we were not surprised to see Bcl6 expressed at similar levels in WT and $IL6^{-/-}$ T cells during STm infection, data that is in agreement with others (121). However, Bcl-6 alone cannot identify Tfh cells. The Tfh cells that are found within GC are phenotypically distinct from those pre-GC-Tfh cells that interact with pre-GC B cells at the T-B border, however both express Bcl-6 (107). Staining for Tfh cells by confocal revealed a near absence of $CD3^{+}PD1^{+}Bcl\text{-}6^{+}$ cells in $IL6^{-/-}$ mice at day 42 p.i, a time at which numerous cells of this phenotype were detected in the spleens of WT mice, localised within GC. By day 55 p.i, when GC had developed in $IL6^{-/-}$ mice, these cells were now visible in the spleen. The presence of Tfh within GC is essential for the maintenance of GC reactions, as highlighted by the GC that develop during T-I immune responses, which collapse once T cell help becomes necessary (158). Thus, it is tempting to speculate that defects in GC development in $IL6^{-/-}$ mice are due to a lack of GC-Tfh cell development, however it is important to consider cause and effect. The T-I GC data (158) suggest that GC Tfh cells are not necessary for the initial induction of GC reactions, but

rather for their maintenance. Recent data shows that effective contact time between pre-GC Tfh cells and pre-GC B cells is required for Tfh cells to enter and sustain a forming GC reaction (109), showing that Tfh cells maintain but do not initiate GC reactions. It seems likely that in the current study, GC do not form for another reason and the absence of GC Tfh cells is a consequence of this. Thus, the inability to form GC in $IL6^{-/-}$ mice may be attributable to a failure B cells to migrate to, or expand within, the follicles following T-B interaction. Defective expansion of GC B cells in the follicles may explain why GC were smaller in $IL6^{-/-}$ mice at day 55 p.i.

In an attempt to identify the source of the IL6 that drives GC reactions, we created BM chimeras in which IL6 was deficient either in haematopoietic cells or in radiation-resistant cells. Numerous cells produce IL6, including T cells (277), B cells (278), macrophages (277), dendritic cells (271), endothelial cells (279), follicular dendritic cells (FDC) (104) and fibroblasts (280). Unpublished data generated during my MSc degree shows that most of the IL6 expressed at day 18 and 35 of STm infection comes from non-T, non-B cells. Whilst T cells express some IL6 at day 35, B cells express very little at either time point. Thus, an alternative candidate is likely to provide the IL6 that optimises GC responses in this system. The role of IL6 in T cell priming by DC has already been discussed. Alternatively, radiation-resistant cells may be the source of the IL6 that promotes effective GC responses. It has been reported that FDC, which are stromal in origin, are the sole source of IL6 in the GC and this facilitates class switch recombination and SHM in B cells (103,104). Surprisingly, we found that IL6 provided by either haematopoietic or radiation-resistant cells was able to correct the defect in GC development and antibody class switching seen in $IL6^{-/-}$ and $IL6^{-/-}$>$IL6^{-/-}$ chimeras. The WT-WT chimeras did display a

lower than expected antibody response to STm, when compared to a normal infection of C57BL6 mice, which masked the differences between WT>WT and $IL6^{-/-}$>$IL6^{-/-}$ mice somewhat. However, the ability to form GC and class-switched antibody responses were clearly diminished in IL6>IL6 mice.

Thus, these studies have produced a novel finding, showing that haematopoietic and radiation resistant cells can act in a redundant fashion to provide the IL6 necessary to support optimal humoral responses to STm infection. Identifying the cells that respond to IL6 in this system will be key to understanding how this compensatory mechanism operates. It would be intriguing in this regard, to identify those cells that up-regulate or acquire the IL6R during the later stages of STm infection, when IL6 becomes important for initiating GC responses. IL6 signalling is initiated when IL6 binds to a receptor complex, consisting of the specific IL6R and a second, common signalling component, gp130 (281). Whilst a number of cells express the membrane bound IL6R, a soluble form of the IL6R (sIL6R) also exists, allowing cells that express gp130, but not the IL6R, to become responsive to IL6 during an immune response (276). This signalling mechanism may also enhance the repertoire of cells from which the responsive cells can acquire IL6 signals, helping to explain the bone-marrow chimera data. As such, the regulation of antibody responses in this model may not require IL6 production by one specific cell type and its effects are likely to be multifaceted. Overall, the data presented in this chapter show that there are some, previously unappreciated similarities in the way that GC and class-switched antibody responses develop during immune responses to Th1 and Th2 antigens. We next focused specifically upon the control of antibody class-switching during infection, by defining the role of the transcription factor T-bet in antibody responses to STm.

CHAPTER 5: THE ROLE OF T-BET IN ANTIBODY CLASS-SWITCHING DURING STM INFECTION

5.1 Introduction

The T-box transcription factor T-bet is essential for Th1 lineage commitment (72). As such, $CD4^+$ T cell-expressed T-bet and (79) subsequent IFNγ production (217) are critical for the control of numerous intracellular infections, including STm. Cytokines such as IL4 (264) and IL10 (282) are not associated with protection against STm infection due to their anti-inflammatory properties and suppression of IFNγ (264,282). To this end, mice deficient in T-bet produce higher levels of IL-10 during infection with *Mycobacterium* Tuberculosis (283) and splenocytes from $T\text{-}bet^{-/-}$, STm infected mice secrete more IL10 than those isolated from WT mice (79). Thus, T-bet controls infection with intracellular bacteria by stimulating IFNγ production and suppressing the anti-inflammatory cytokine IL10.

T-bet is widely recognised as the global regulator of Th1 differentiation, however the literature suggests multiple additional roles for T-bet within the immune system. T-bet has been proposed to regulate the migration of $CD4^+$ T cells (284), Tregs (285) mast cells (286) and cytotoxic T lymphocytes (287). Furthermore, T-bet deficiency in DC can lead to sub-optimal $CD4^+$ T cell priming (81,288), and the cytotoxic function of $CD8^+$ T cells is impaired in the absence of T-bet (289). Deficiency of T-bet in NK and NKT cells results in

developmental, survival and functional defects, including reduced IFNγ production during infection responses (290).

Of particular interest here, is the association of T-bet with CSR to IgG2a in B cells. Whilst T-bet independent pathways of IgG2a production do exist (83), a number of studies have highlighted an important role for T-bet in this process (79,83,291,292). *In vitro* assays show that T-bet$^{-/-}$ B cells cannot produce IgG2a under a variety of stimulation conditions and IgG2a germline and post-switch transcripts are absent in these cells following stimulation with IFNγ and LPS (83). Furthermore, TLR9 stimulation of B cells with cytosine-phosphate-guanine (CpG) DNA can upregulate T-bet expression in B cells (293), as well as γ2a-switch transcript induction and antibody secretion (293,294). *In vivo,* pathogenic IgG2a production is severely depleted when T-bet$^{-/-}$ mice are intercrossed with the lupus-prone mouse strain MRL/MpJ-Fas$^{lpr/lpr}$, whilst the Th2-related antibody isotypes, IgG1 and IgE, are elevated (83). IgG2a antibody is also absent in the sera of T-bet deficient mice at day 14 of infection with STm (79), in which class switching is T cell dependent (70). Contrary to this, T-bet$^{-/-}$ mice immunised with non-viable T-D antigens purportedly produce normal levels of IgG2a, whilst failing to produce this subclass when immunised with TI antigens (291). Thus, conflicting data in the literature may reflect an antigen and context specific role for T-bet in controlling CSR to IgG2a.

Whilst *in vivo* data support a role for T-bet in the IgG2a response to viable T-D antigens, it is not clear whether this response is regulated by T cell- or B cell-intrinsic T-bet expression, or indeed both. Recent work has shown that IFNγ produced by CD8 T cells can skew antibody class-switching from IgG1 to IgG2a or IgG2b, in response to immunisation

with alum-precipitated ovalbumin (OVA) (292). The switch to IgG2a required T-bet expression in B cells, but not T cells or non-lymphocytes, whilst the production of IgG2b in this system was T-bet independent. Whether T cell-intrinsic T-bet becomes important for guiding switching to IgG2a during a Th1 infection response is unclear. During STm infection, class-switching is almost entirely T cell-dependent (70) and IgG2a production is T-bet dependent (79), suggesting that T cell intrinsic T-bet may be important in guiding this response. On the other hand, whilst some studies show expression of T-bet in specialized Tfh cells (295), others report its absence (105), suggesting that T-bet expression in T cells may be dispensable for class-switching.

This chapter addresses the cellular basis for T-bet dependent class switching to IgG2a during STm infection, and examines whether class-switching to IgG2b is T-bet dependent in this system. We were also interested in the purported ability of T-bet deficient mice to produce enhanced titres of the Th2-related antibody subclass IgG1 (83). STm drives class-switching to IgG2a, however immunisation with certain protein components of the bacterium, such as sFliC, induces a Th2 immune response with antibody class-switching to IgG1 (239). As such, two separate hypotheses are investigated here; firstly we examine the hypothesis that class-switching to IgG2a during STm infection is dependent upon both T cell-intrinsic and B cell-intrinsic T-bet, whilst class-switching to IgG2b is T-bet-independent. The second half of this chapter investigates the hypothesis that antibody responses are enhanced in T-bet$^{-/-}$ mice following immunisation with sFliC.

5.2 Results

5.2.1 T-bet-mediated control of class-switching during STm infection

5.2.1.1 T-Bet$^{-/-}$ mice fail to clear STm infection despite normal levels of CD4^{+} T cell activation

During the first week of STm infection, bacterial replication is controlled by the innate immune system, however clearance requires IFNγ production by Th1 cells (79). T-bet is the global transcriptional regulator of Th1 cells and in its absence, mice fail to control infection with STm (79). To confirm these data, we infected T-bet$^{-/-}$ mice with STm and quantified the CFU per spleen at day 7 and 35 p.i. As expected, similar numbers of bacteria were recovered from the spleens of WT and T-bet$^{-/-}$ mice at day 7 p.i. (figure 5.1). Bacterial numbers had fallen substantially in WT spleens by day 35 of infection, however T-bet$^{-/-}$ mice were unable to resolve the infection, with the CFU being ≥ 100-fold greater than in WT spleens ($p \leq 0.05$).

As CD4^{+} T cells are required for bacterial clearance, splenic CD4^{+} T cell numbers were quantified and their activation status assessed by flow cytometry. Both before and during the infection, no difference was observed in the total numbers of CD4^{+} T cells in WT and T-bet$^{-/-}$ spleens (figure 5.2B I). Using CD62L loss as a marker of T cell activation, we observed that T-bet deficient T cells were able to activate during the infection (figure 5.2A and BII). The proportion of activated splenic T cells was similar in WT and T-bet$^{-/-}$ mice prior to infection and at day 7 p.i. However, at day 35p.i, a significantly greater proportion of T cells remained activated in T-bet$^{-/-}$ spleens ($p \leq 0.05$).

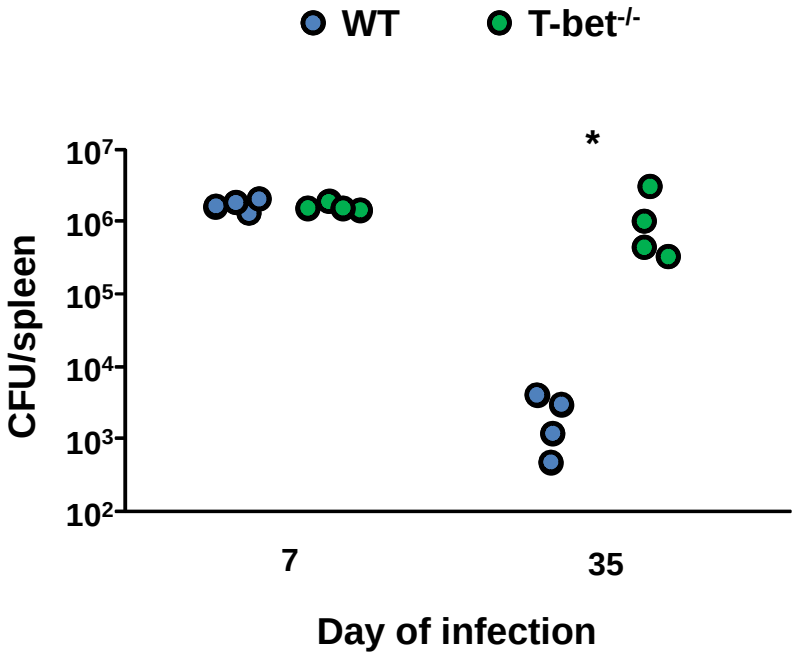

Figure 5.1. Bacterial burden in WT and T-bet$^{-/-}$ mice during STm infection. WT and T-bet$^{-/-}$ mice were infected with 10^5 STm and the number of CFU per spleen were quantified at day 7 and day 35 p.i. One point represents one mouse. Data are representative of ≥ 2 individual experiments giving similar results. * $p \leq 0.05$

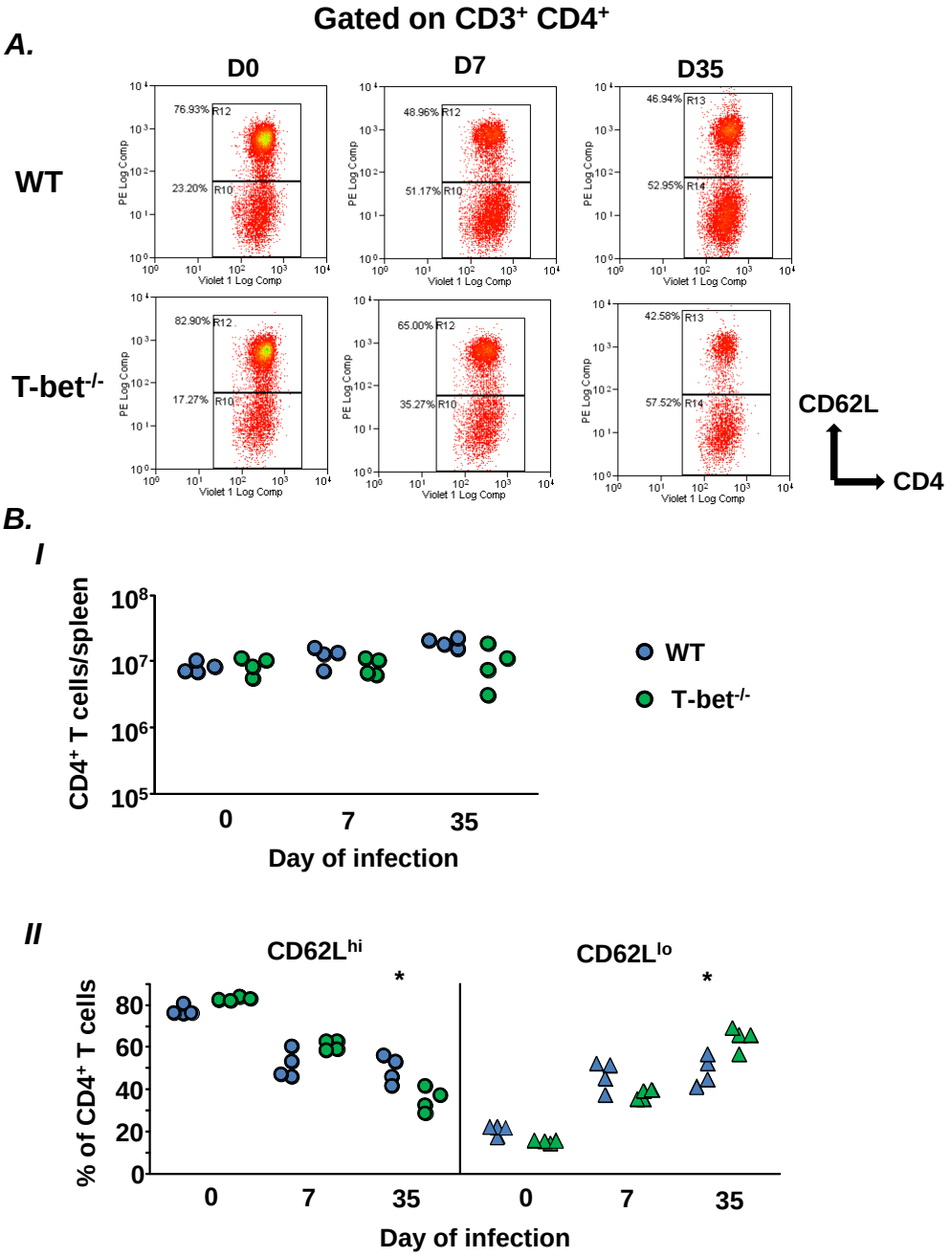

Figure 5.2. Splenic T cell numbers in WT and T-bet$^{-/-}$ mice before and during STm infection. WT and T-bet$^{-/-}$ mice were infected with 10^5 STm or remained uninfected as controls. At the specified time points, mice were sacrificed and splenic T cell numbers were quantified by flow cytometry. ***A.*** Representative flow cytometry plots showing the activation status of CD3$^+$CD4$^+$ splenocytes from WT and T-bet$^{-/-}$ mice, based upon CD62L staining. Percentages denote the proportion of total CD4$^+$ T cells that are activated (CD62L^{lo}) and naive (CD62L^{hi}). ***B. I*** Total number of splenic CD4$^+$ T cells in WT and T-bet$^{-/-}$ spleens before and during infection with STm. ***II*** Proportion of splenic CD4$^+$ T cells that are naive (dots) and activated (triangles) in WT and T-bet$^{-/-}$ mice before and after infection. Each point represents one mouse. Data are representative of ≥ 2 experiments giving similar results. * $p \leq 0.05$.

5.2.1.2 T-bet-/- mice have normal numbers of follicular B2 cells but fewer splenic MZ cells than WT mice

As we were interested in assessing the antibody response to infection, we next examined whether splenic B cell numbers were similar in WT and T-bet$^{-/-}$ mice. Using flow cytometry, the total number of splenic recirculating and MZ B2 cells were quantified in WT and T-bet$^{-/-}$ mice before and during infection. Cells were identified as previously described (see figure 3.3). Before infection, T-bet$^{-/-}$ mice had similar numbers of splenic follicular B cells but fewer MZ B cells when compared to WT mice (figure 5.3A and B). During the infection, the proportion of follicular B cells was lower in T-bet$^{-/-}$ mice (figure 5.3A), however the exaggerated splenomegally resulted in similar total numbers of follicular B cells when compared to WT mice (figure 5.3BI). Marginal zone B cells remained significantly lower in T-bet mice at day 7 and 35 p.i ($p \leq 0.05$). The dramatic difference between WT and T-bet$^{-/-}$ MZ cell numbers at day 35p.i. presumably reflects the presence of an active infection in T-bet$^{-/-}$ mice at this point. Having quantified B cell numbers, we next sought to define the role of T-bet in antibody class-switching to IgG2a and IgG2b during STm infection.

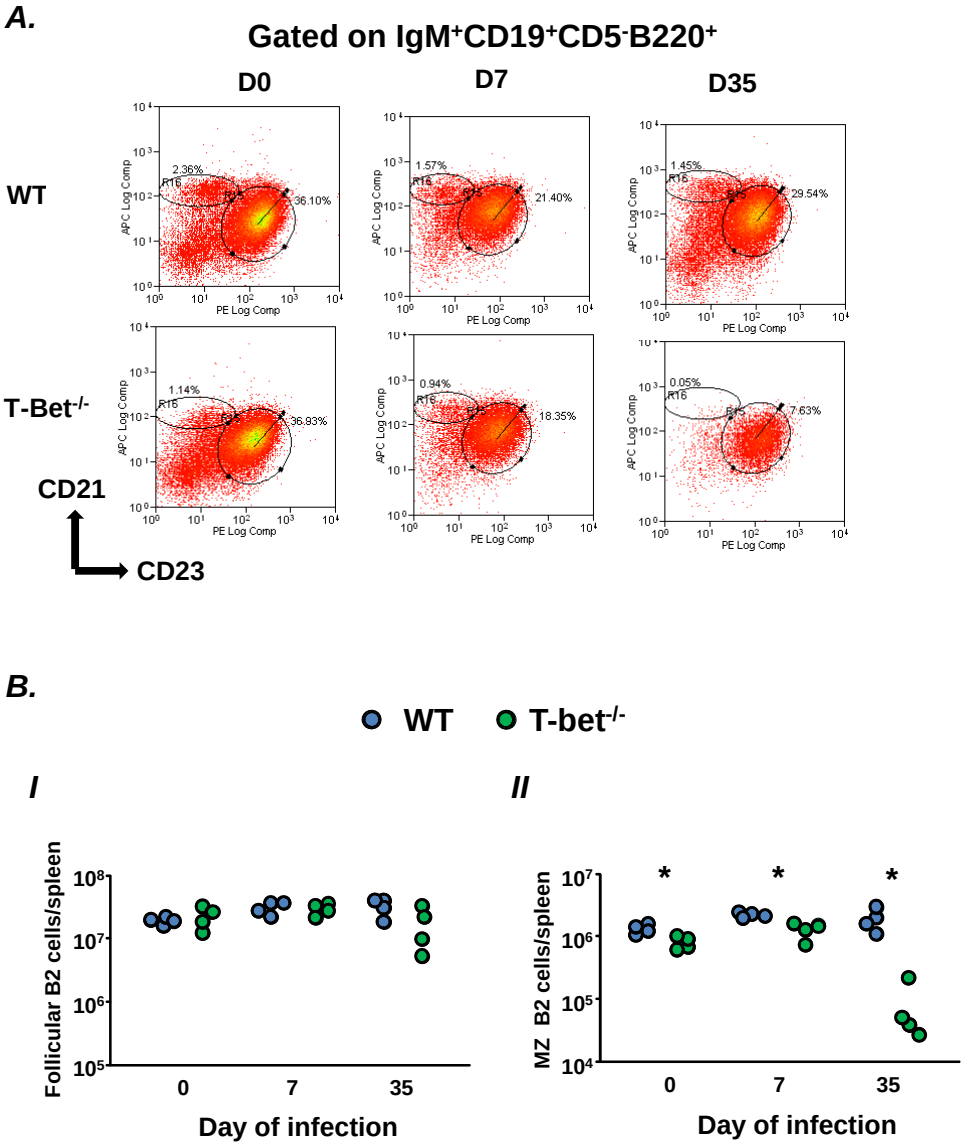

Figure 5.3. Splenic B cell numbers in WT and T-bet$^{-/-}$ mice before and during STm infection. WT and T-bet$^{-/-}$ mice were infected with 10^5 STm or remained uninfected as controls. At the specified time points, mice were sacrificed and splenic B cell numbers were quantified by flow cytometry. ***A.*** Representative flow cytometry plots showing recirculating follicular and MZ B cell staining of WT and T-bet$^{-/-}$ splenocytes, before and during STm infection. Percentages denote MZ or recirculating B2 cells as a proportion of total splenocytes. ***B. I*** Total number of splenic recirculating B cells in WT and T-bet$^{-/-}$ spleens before and during infection. ***II*** Total number of splenic MZ B cells in WT and T-bet$^{-/-}$ spleens before and during infection. Each point represents one mouse. Data are representative of ≥ 2 experiments giving similar results. * $p \leq 0.05$.

5.2.1.3 T-Bet is required for class- switching to IgG2a but not IgG2b during STm infection

The dominant isotypes of switched-antibody produced during primary STm infection are IgG2a and IgG2b. To compare the role of T-bet in switching to these isotypes, spleen sections from WT and T-bet$^{-/-}$ mice were examined for the presence of non-switched and class-switched EF plasma cells during the early and late infection. As shown in figure 5.4, IgM^{+} and class-switched IgG2b^{+} plasma cells were clearly present in the spleens of WT and T-bet$^{-/-}$ mice at both stages of infection. However, whilst large numbers of IgG2a^{+} plasma cells were detected in WT spleens, this response was not evident in T-bet$^{-/-}$ spleens (figure 5.4). Consistent with these observations, anti-OMP IgM (figure 5.5A) and IgG2b (figure 5.5B) antibody production was normal in T-bet$^{-/-}$ mice, whilst IgG2a secretion was completely absent (figure 5.5C). These data indicate that T-bet independent mechanisms control class-switching to IgG2b, whilst switching to IgG2a is T-bet-dependent. Anti-OMP IgG1 was undetectable in WT sera and the majority of T-bet$^{-/-}$ sera throughout infection (figure 5.5D). Those T-bet$^{-/-}$ mice that produced some IgG1 antibody did so at very low titres, indicating that T-bet$^{-/-}$ mice do not compensate for a lack of IgG2a by reverting to a Th2 pathway of antibody production.

As antibody class-switching during STm infection is T cell-dependent (70) and IgG2a class-switching is T-bet dependent, we hypothesised that T cell-intrinsic T-bet would be necessary for CSR to IgG2a. To test this we used an established, mixed bone marrow chimera model (241) in which mice containing a T-bet-deficient T cell compartment (T-bet$^{-/-TCELL}$) were generated alongside mice whose T cell compartment was T-bet sufficient (T-bet$^{+/+TCELL}$).

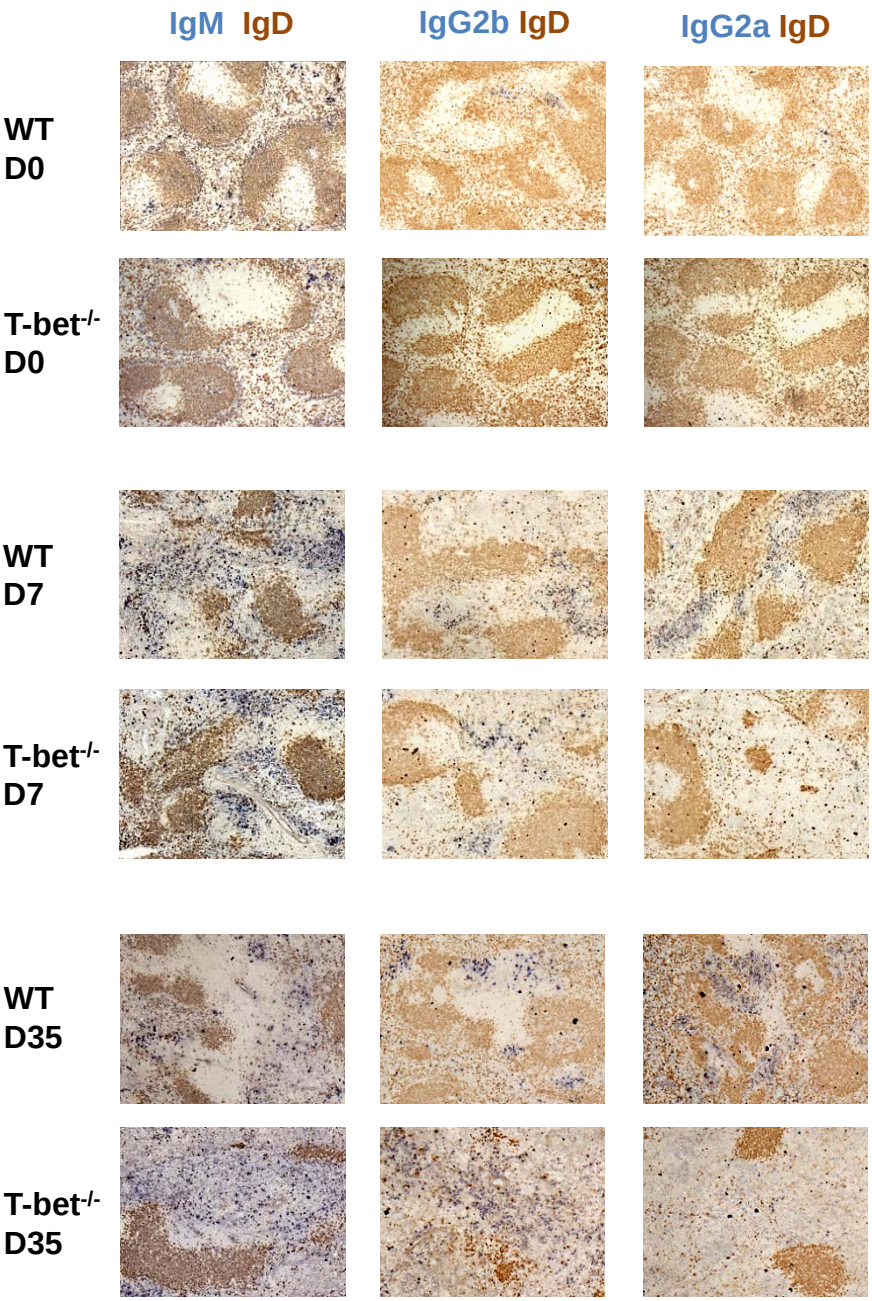

Figure 5.4. Staining of EF plasma cells in WT and T-bet$^{-/-}$ mice before and during STm infection. WT and T-bet$^{-/-}$ mice were infected with 10^5 STm or remained uninfected as controls. At the specified time points, mice were sacrificed and the spleens were stained with left panels; IgM (blue) and IgD (brown) to detect non-switched EF plasma cells, middle panel; IgG2b (blue) and IgD brown and right panels IgG2a (blue) and IgD (brown) to detect class-switched EF plasma cells. Experiments were performed at least twice and photographs are representative of ≥ 8 mice per group at each time point.

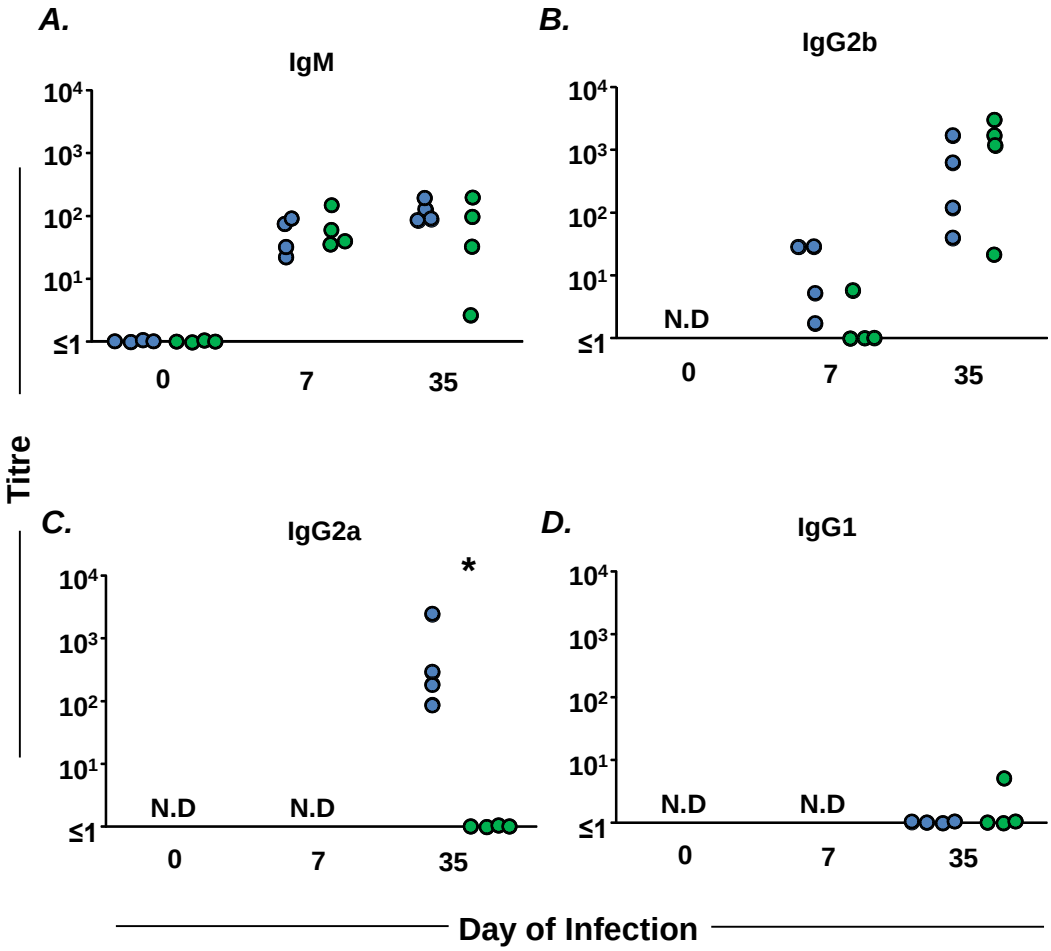

Figure 5.5. Antibody titres in WT and T-bet$^{-/-}$ mice before and during STm infection. WT and T-bet$^{-/-}$ mice were infected with 10^5 STm or remained uninfected as controls. At the specified timepoints, mice were sacrificed and ***A,*** IgM, ***B,*** IgG2b, ***C,*** IgG2a and ***D,*** IgG1 serum antibody titres were measured by ELISA. One point represents one mouse. Data are representative of ≥ 2 experiments giving similar findings. * $p \leq 0.05$

5.2.1.4 T-bet$^{-/-}$ T cells activate during STm infection but fail to promote bacterial clearance

Following reconstitution, T cell chimeras were infected with STm for 7 or 32 days. All mice satisfactorily reconstituted the splenic T and B cell compartments and these data are discussed below. At day 7 and 35 of infection the splenic bacterial burden was assessed in the chimeras. At day 7 p.i, the CFU per spleen was similar in T-bet$^{+/+TCELL}$ and T-bet$^{-/-TCELL}$ mice (figure 5.6), reflecting the innate control of bacterial replication at this point. As expected, at day 32 p.i, T-bet$^{-/-TCELL}$ mice had failed to resolve the infection, with the median CFU being almost 1000-fold higher when compared to T-bet$^{+/+TCELL}$ mice ($p \leq 0.001$).

Flow cytometric analysis revealed normal splenic CD4^{+} T cell reconstitution in both T-bet$^{+/+TCELL}$ and T-bet$^{-/-TCELL}$ mice, although fewer CD4^{+} T cells were detected in T-bet$^{-/-TCELL}$ spleens during infection ($p \leq 0.05$) (figure 5.7A and BI). Consistent with our earlier data, we observed that T cells from T-bet$^{-/-TCELL}$ mice were able to activate during the infection, as the proportion of CD4^{+} T cells that were also CD62L^{lo} increased over the time course (figure 5.7A and BII). However, we previously observed a higher proportion of activated T cells in T-bet$^{-/-}$ mice at day 35 of infection when compared to WT mice, whilst here the proportion of activated CD4^{+} T cells was significantly lower in T-bet$^{-/-TCELL}$ mice ($p \leq 0.001$) at both stages of infection. Although not pursued, perhaps this reflects a suppression of T-bet$^{-/-}$ T cell activation by T-bet$^{+/+}$ B cells or other cells.

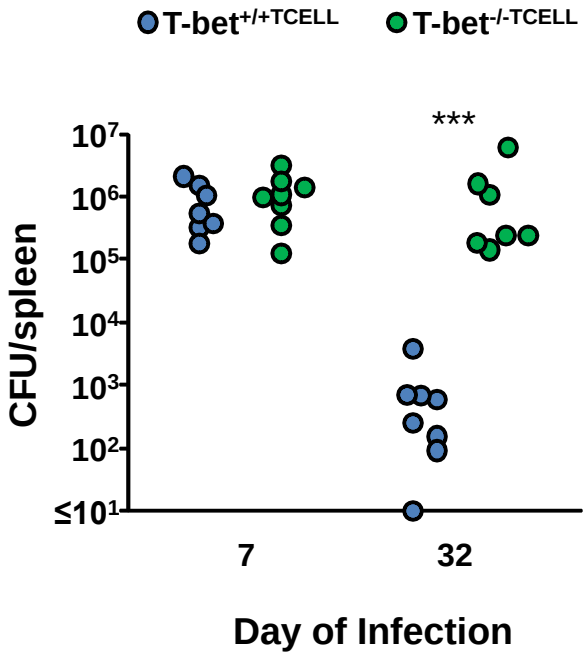

Figure 5.6. Bacterial burden in chimeric mice with either T-bet-sufficient or T-bet-deficient T cells. Chimeras were infected with 10^5 STm and the number of CFU per spleen were quantified at day 7 and day 35 p.i One point represents one mouse. Data are pooled from 2 individual experiments. *** $p \leq 0.001$

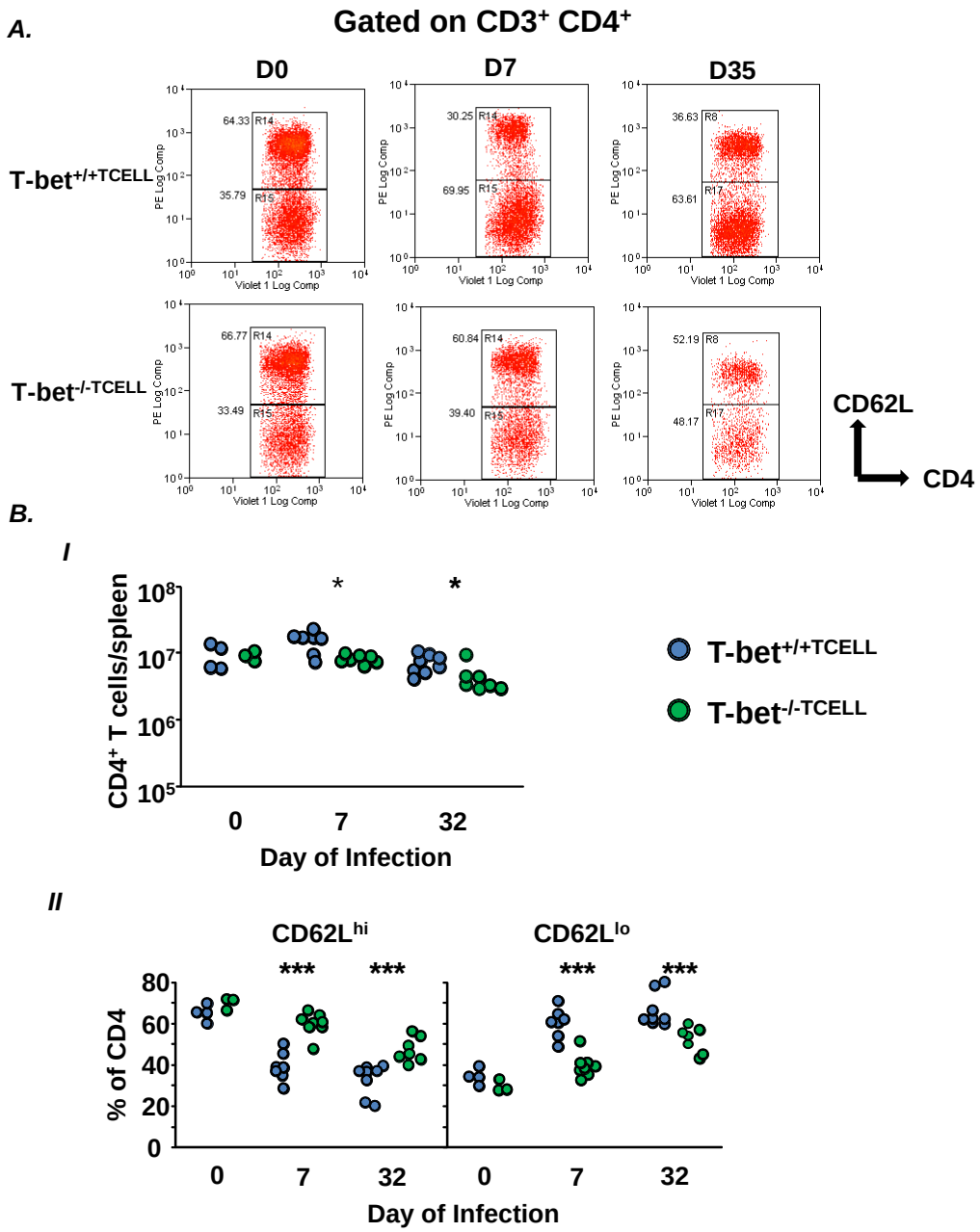

Figure 5.7. Splenic T cell numbers in chimeric mice with either T-bet-sufficient or T-bet-deficient T cells before and during STm infection. Chimeras were infected with 10^5 STm or remained uninfected as controls. At the specified time points p.i, mice were sacrificed and splenic T cell numbers were quantified by flow cytometry. ***A.*** Representative flow cytometry plots showing the activation status of $CD3^+CD4^+$ splenocytes from from T-bet$^{+/+TCELL}$ and T-bet$^{-/-TCELL}$ mice, based on CD62L staining. Numbers on histograms denote the proportion of total $CD4^+$ T cells that are activated ($CD62L^{lo}$) and naive ($CD62L^{hi}$). ***B. I*** Total number of splenic $CD4^+$ T cells in T-bet$^{+/+TCELL}$ and T-bet$^{-/-TCELL}$ spleens before and during infection. ***II*** Proportion of splenic $CD4^+$ T cells that are $CD62L^{hi}$ and $CD62L^{lo}$ in T-bet$^{+/+TCELL}$ and T-bet$^{-/-TCELL}$ mice before and after infection. Each point represents one mouse. Data are pooled from 2 individual experiments. * $p \leq 0.05$; *** $p \leq 0.001$.

5.2.1.5 B cell numbers are similar in T-bet$^{+/+TCELL}$ and T-bet$^{-/-TCELL}$ mice throughout infection

To assess B cell reconstitution in the T cell chimeras, flow cytometric analysis of splenic recirculating and MZ B cells was carried out on T-bet$^{+/+TCELL}$ and T-bet$^{-/-TCELL}$ mice before and during infection. The numbers of these B cells in uninfected T-bet$^{+/+TCELL}$ and T-bet$^{-/-TCELL}$ mice were similar to those seen in uninfected WT C57BL6 and T-bet$^{-/-}$ mice and no differences were observed between the two groups of chimeras (figure 5.8). Throughout infection, recirculating B cell numbers were also similar in T-bet$^{+/+TCELL}$ and T-bet$^{-/-TCELL}$ mice (figure 5.8BI). Unlike our observations in T-bet$^{-/-}$ mice, MZ B cell numbers were similar in T-bet$^{+/+TCELL}$ and T-bet$^{-/-TCELL}$ mice throughout infection, despite the T-bet$^{-/-TCELL}$ mice remaining heavily infected at day 32 p.i. This partly reflects the less efficient recovery of MZ B cell numbers in T-bet$^{+/+TCELL}$ mice when compared to WT mice. Overall, the T cell chimeras were able to reconstitute the splenic B cell compartment effectively and we next assessed the ability of these B cells to undergo CSR to IgG2a and IgG2b during infection.

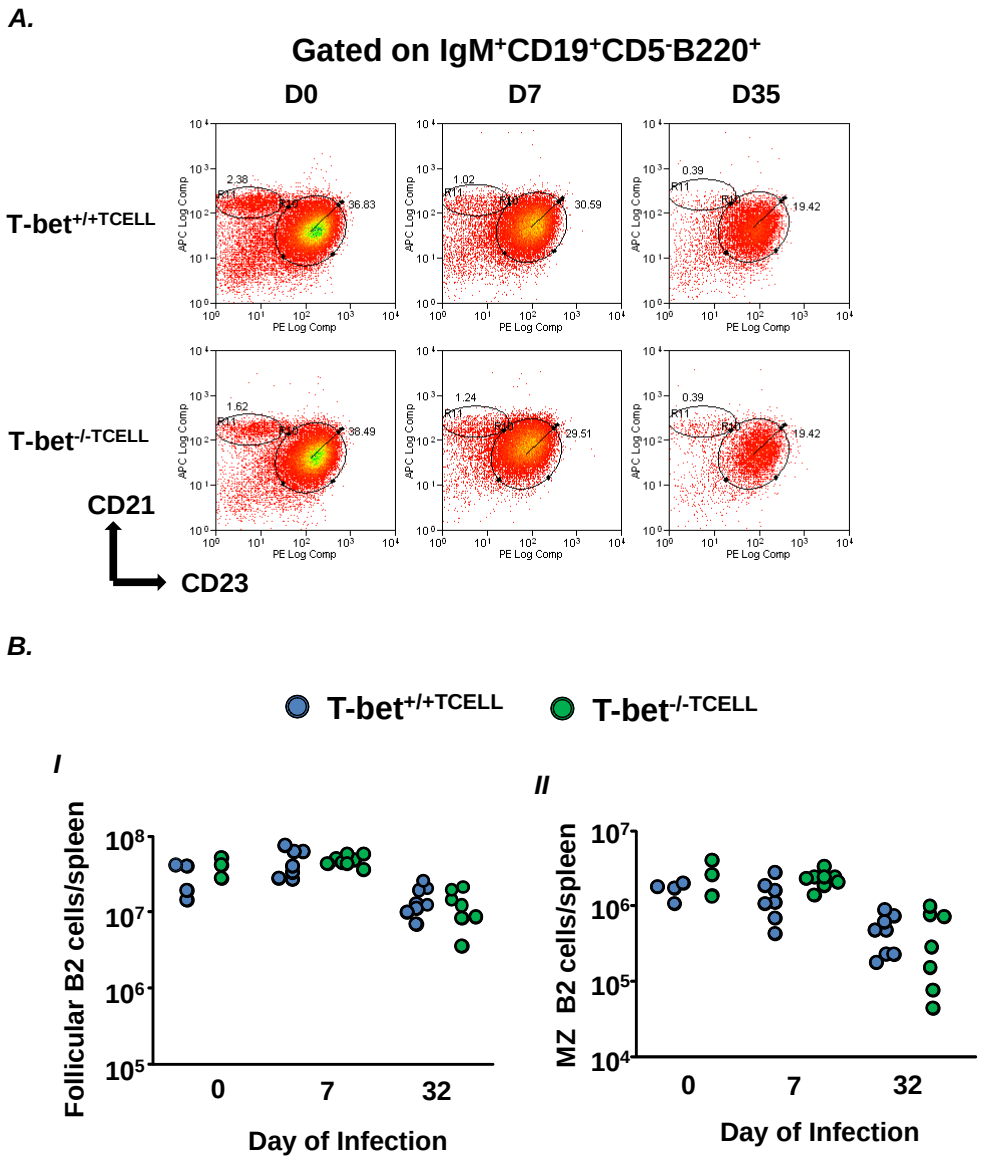

Figure 5.8. Splenic B cell numbers in chimeric mice with either T-bet-sufficient- or T-bet-deficient T cells before and during STm infection. Chimeras were infected with 10^5 STm or remained uninfected as controls. At the specified timepoints, mice were sacrificed and splenic B cell numbers were quantified by flow cytometry ***A.*** Representative flow cytometry plots showing recirculating follicular and MZ B cell staining of splenocytes from T-bet$^{+/+TCELL}$ and T-bet$^{-/-TCELL}$ mice. Numbers denote MZ or recirculating B2 cells as a proportion of total splenocytes. ***B. I*** Total number of splenic recirculating B cells in T-bet$^{+/+TCELL}$ and T-bet$^{-/-TCELL}$ spleens before and during infection. ***II*** Total number of splenic MZ B cells in T-bet$^{+/+TCELL}$ and T-bet$^{-/-TCELL}$ spleens before and during infection. Each point represents one mouse. Data are pooled from 2 experiments.

5.2.1.6 T-bet expression in T cells is dispensable for CSR to IgG2a during STm infection

To assess the class-switched plasma cell response in the chimeras, spleen sections were stained for IgM^+, $IgG2b^+$ and $IgG2a^+$ plasma cells, which were subsequently quantified by counting. Consistent with our earlier data, comparable numbers of IgM^+ and $IgG2b^+$ plasma cells were detected in the spleens of T-$bet^{+/+TCELL}$ and T-$bet^{-/-TCELL}$ mice before and during infection (figure 5.9 and 5.10A and B). Surprisingly, the two groups of mice also formed similar numbers of $IgG2a^+$ plasma cells at each stage of infection (figure 5.9A and 5.10C). The low numbers of class-switched plasma cells in uninfected T-$bet^{-/-TCELL}$ mice strongly suggested this response to be antigen specific. To assess this further, OMP-specific serum antibody titres were measured by ELISA, confirming that T-bet expression in T cells is not required for the secretion of antigen-specific IgM, IgG2b or IgG2a antibody (figure 5.11). Thus, the signals delivered to B cells by T cells during STm infection allow antibody class switching to IgG2a in the absence of T cell-intrinsic T-bet. As such, we used the same chimera system to assess whether B cell-intrinsic T-bet is necessary for this response, following which we carried out RT-PCR analysis on T cells and B cells from both sets of chimeric mice.

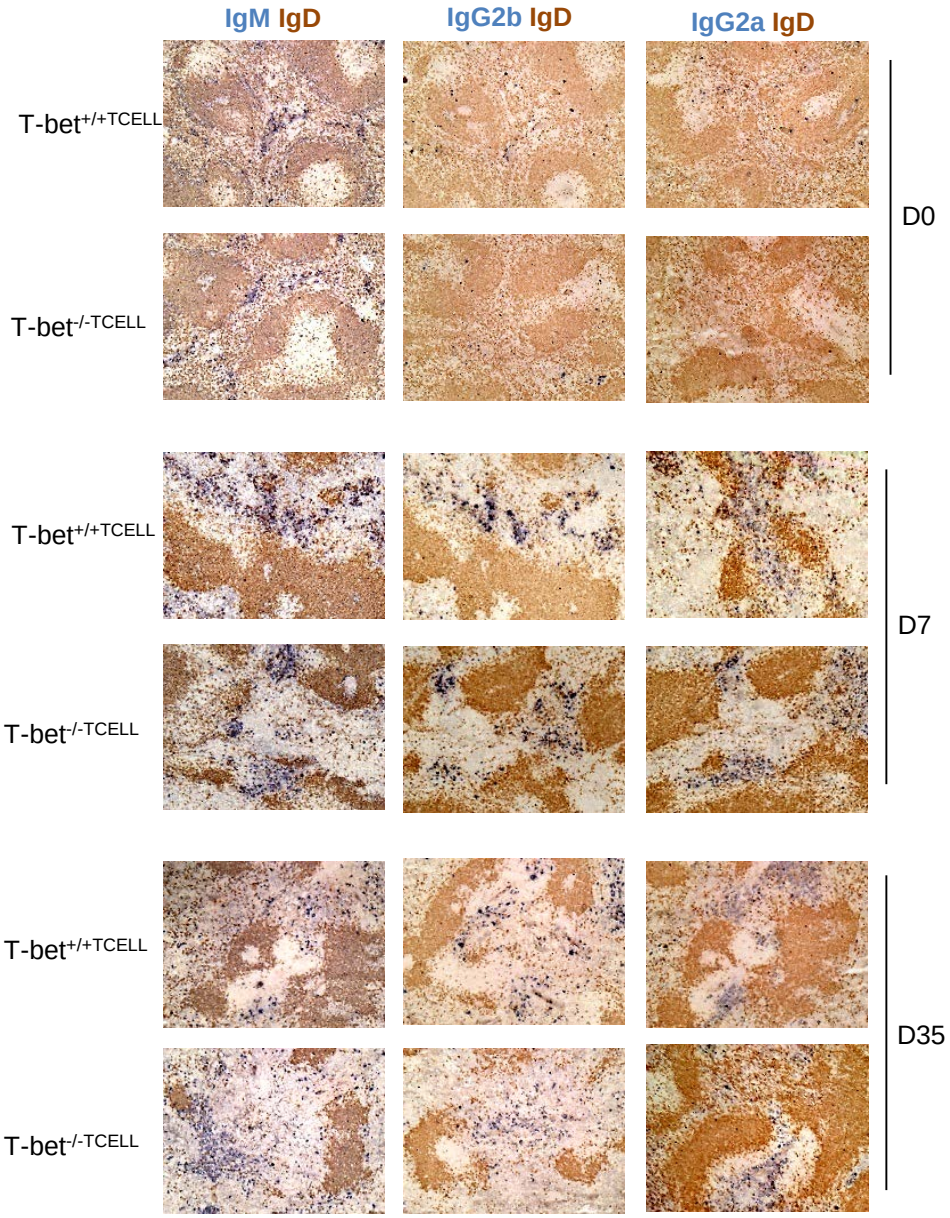

Figure 5.9. Staining of EF plasma cells in chimeric mice with either T-bet-sufficient or T-bet-deficient T cells before and during STm infection. Chimeras were infected with 10^5 STm or remained uninfected as controls. At the specified time points, mice were sacrificed and the spleens were stained for EF plasma cells. Representative photographs from T-bet$^{+/+TCELL}$ and T-bet$^{-/-TCELL}$ spleens stained with ***left panels*** IgM (blue) and IgD (brown) to detect non-switched EF plasma cells, ***middle panels*** IgG2b (blue) and IgD brown and ***right panels*** IgG2a (blue) and IgD (brown) to detect class-switched EF plasma cells. Photographs are representative of at least 7 mice per groups at day 7 and 35 and at least 3 mice at day 0.

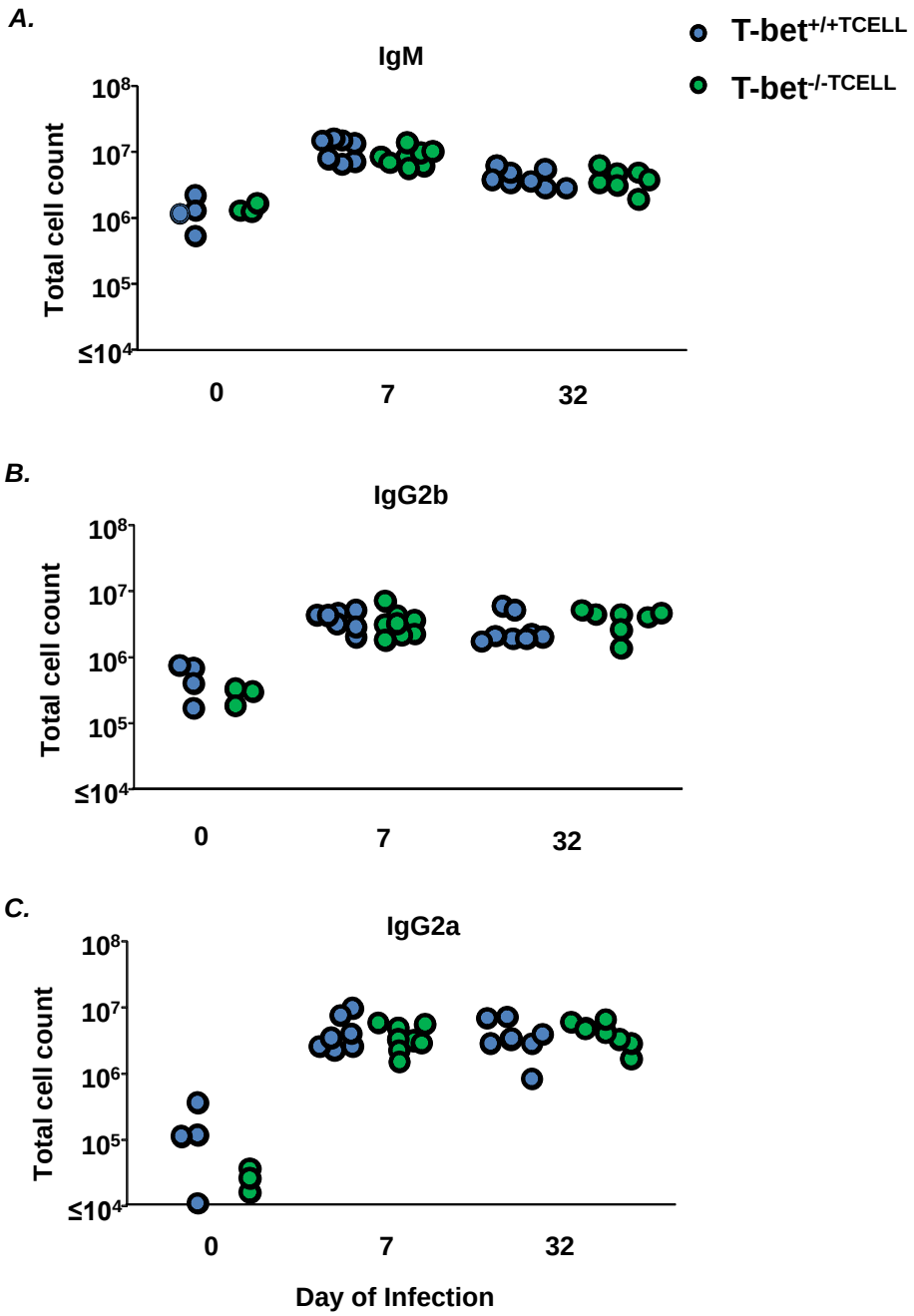

Figure 5.10. EF plasma cell numbers in chimeric mice with either T-bet-sufficient or T-bet-deficient T cells before and during STm infection. Chimeras were infected with 10^5 STm or remained uninfected as controls. At the specified time points, mice were sacrificed and the spleens were stained for EF plasma cells. Graphs show the total number of splenic ***A,*** IgM^+, ***B,*** $IgG2b^+$ and ***C,*** $IgG2a^+$ plasma cells in T-$bet^{+/+TCELL}$ and T-$bet^{-/-TCELL}$ mice at the specified time points, as determined by histology. One point represents one mouse. Data are pooled from 2 individual experiments.

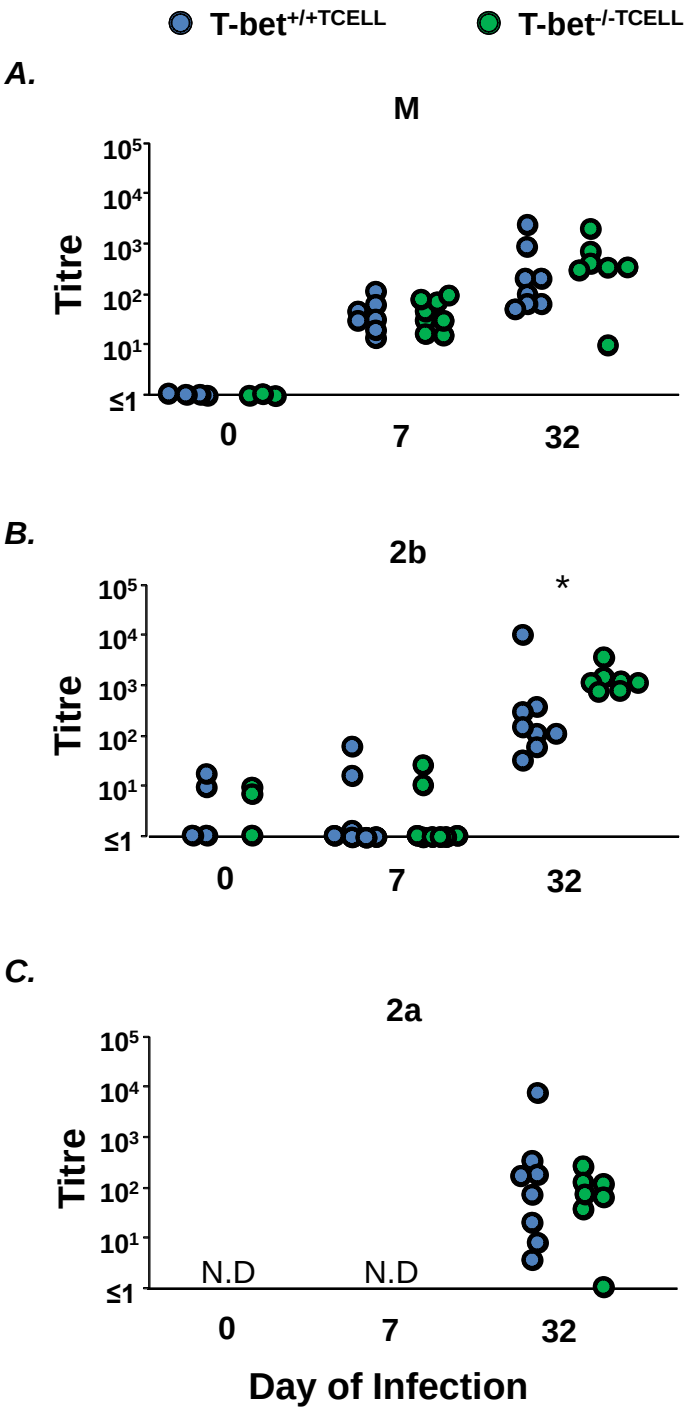

Figure 5.11. OMP-specific antibody titres in chimeric mice with either T-bet-sufficient or T-bet-deficient T cells before and during STm infection. Chimeras were infected with 10^5 STm or remained uninfected as controls. At the specified time points, mice were sacrificed and ***A,*** IgM, ***B,*** IgG2b and ***C,*** IgG2a serum antibody titres were measured by ELISA. One point represents one mouse. Data are pooled from 2 individual experiments. * $p \leq 0.05$

5.2.1.7 B cell-intrinsic T-bet expression is not required for clearance of STm infection or splenic T cell activation

Since T-bet in T cells is not required for IgG2a class-switching, chimeric mice lacking T-bet in all B cells (T-bet$^{-/-BCELL}$) were generated alongside T-bet-sufficient B cell chimeras (T-bet$^{+/+BCELL}$), and mice were infected with STm for 7 or 35 days. As discussed below, reconstitution of the T and B cell compartments in these mice was normal. Clearance of primary STm infection does not require B cells (220), however modified B cell compartments can alter clearance kinetics (228). Nevertheless, a loss of T-bet in B cells did not affect infection resolution, as no difference in bacterial burden was observed between T-bet$^{+/+BCELL}$ and T-bet$^{-/-BCELL}$ mice at day 7 or 35 p.i (figure 5.12).

Splenic CD4^{+} T cell numbers were quantified next, showing comparable total numbers in T-bet$^{+/+BCELL}$ and T-bet$^{-/-BCELL}$ mice before and throughout infection (figure 5.13B I). The proportion of activated CD4^{+} T cells in resting T-bet$^{+/+BCELL}$ and T-bet$^{-/-BCELL}$ mice was higher than expected prior to infection (figure 5.13A and BII), as was the case in the T-bet$^{-/-TCELL}$ chimeras, albeit to a lesser extent. This masked the infection-mediated activation of CD4^{+} T cells somewhat, however the proportion of activated CD4^{+} T cells was increased above background in both groups of mice during the infection. Furthermore, the equal capacity of T-bet$^{+/+BCELL}$ and T-bet$^{-/-BCELL}$ mice to resolve infection demonstrates appropriate CD4^{+} T cell effector function in both groups of mice.

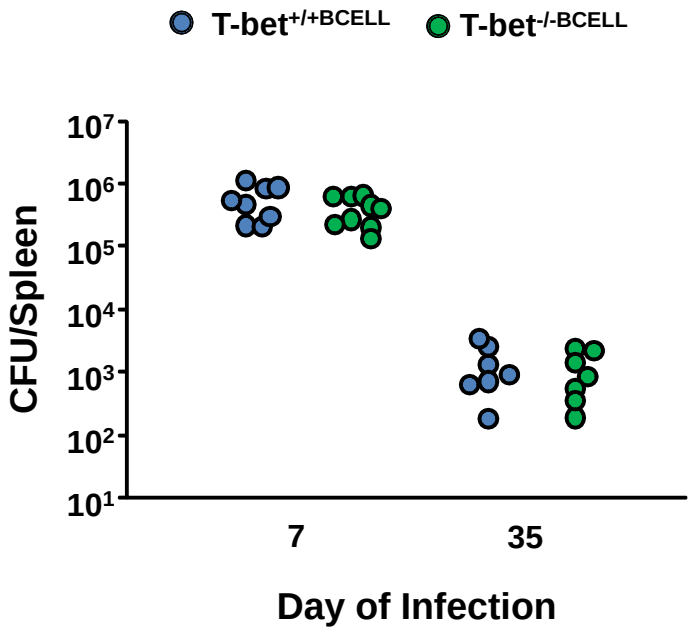

Figure 5.12. Bacterial burden in chimeric mice with either T-bet-sufficient or T-bet-deficient B cells. Chimeras were infected with 10^5 STm and the number of CFU per spleen were quantified at day 7 and day 35 p.i. One point represents one mouse. Data are pooled from 2-3 individual experiments.

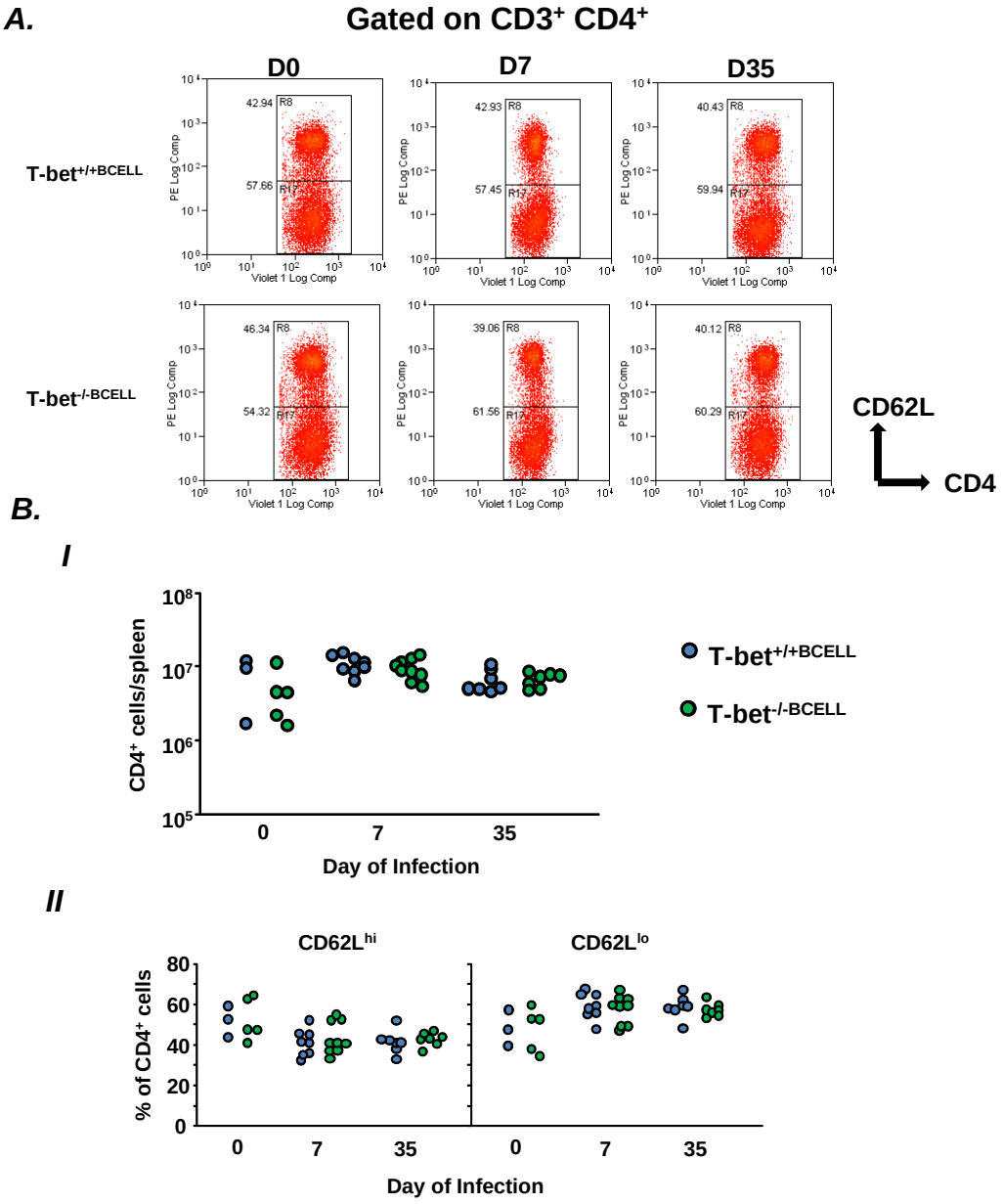

Figure 5.13. Splenic T cell numbers in chimeric mice with either T-bet-sufficient or T-bet-deficient B cells before and during STm infection. Chimeras were infected with 10^5 STm or remained uninfected as controls. At the specified time points, mice were sacrificed and splenic T cell numbers were quantified by flow cytometry. ***A.*** Representative flow cytometry plots showing the activation status of $CD4^+$ T cells from T-$bet^{+/+BCELL}$ and T-$bet^{-/-BCELL}$ mice, based on CD62L staining. Numbers in the histograms denote the proportion of total $CD4^+$ T cells that are activated ($CD62L^{lo}$) and naive ($CD62L^{hi}$). ***B. I*** Total number of splenic $CD4^+$ T cells in T-$bet^{+/+BCELL}$ and T-$bet^{-/-BCELL}$ spleens before and during infection with STm. ***II*** Proportion of splenic $CD4^+$ T cells that are naive and activated in T-$bet^{+/+BCELL}$ and T-$bet^{-/-BCELL}$ mice before and after infection with STm. Each point represents one mouse. Data are pooled from 2-3 experiments.

5.2.1.8 Splenic B cell reconstitution is not affected by the absence of T-bet in B cells

In order to assess the capacity of T-bet-deficient B cells to reconstitute the splenic B cell compartment, recirculating and MZ B cells were quantified by flow cytometry before and during infection. Equal numbers of recirculating B cells were identified in the spleens of T-bet$^{+/+BCELL}$ and T-bet$^{-/-BCELL}$ mice before and during infection, although there was a tendency towards lower total numbers in T-bet$^{-/-BCELL}$ mice (figure 5.14A and BI). Marginal zone B cell numbers were similar in uninfected T-bet$^{+/+BCELL}$ and T-bet$^{-/-BCELL}$ spleens (figure 5.14A and BII). During infection, there was a large amount of spread in MZ B cell numbers in both groups, however overall numbers were similar in both groups of mice at this time point, as well as at day 35 p.i (figure 5.14 BII). As B cell reconstitution was effective in the chimeric mice, we next assessed antibody class-switching in response to STm infection.

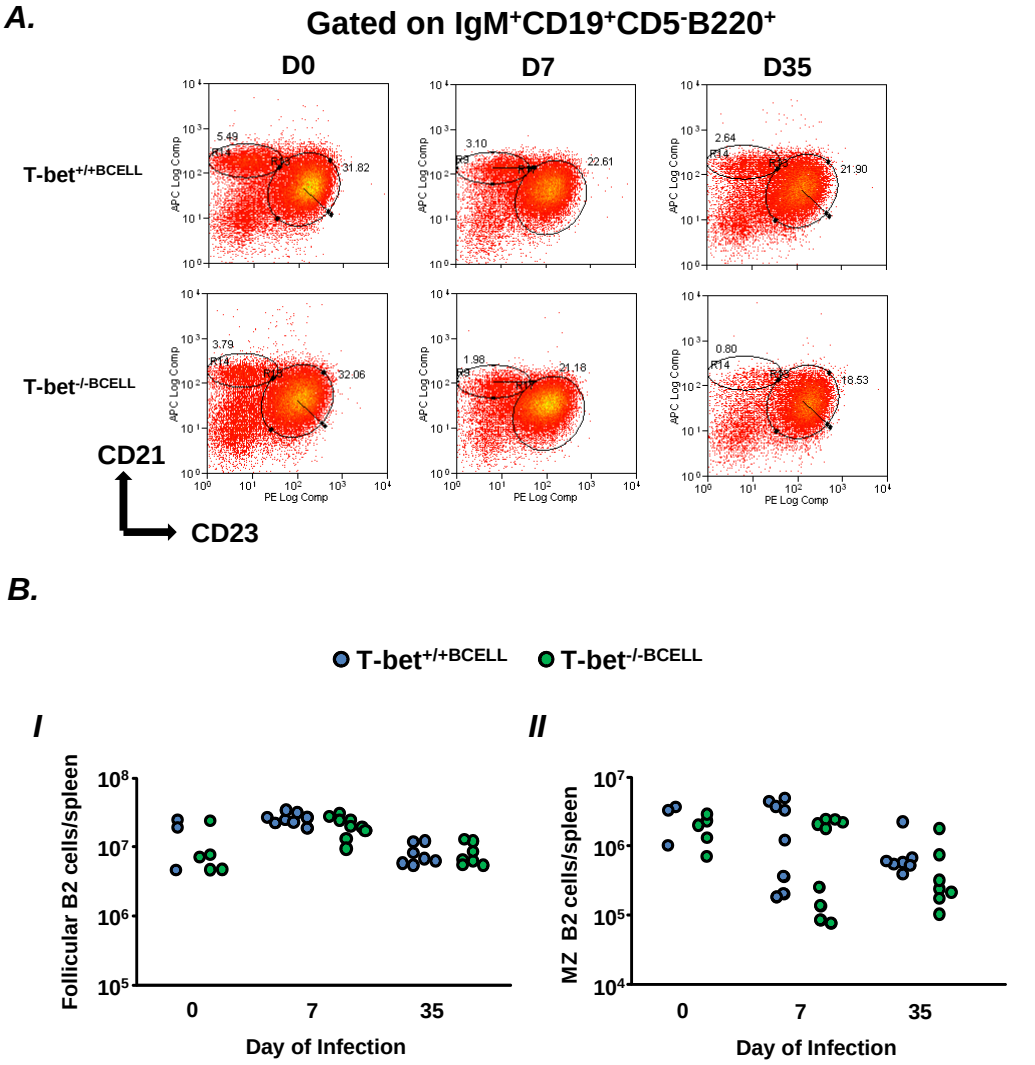

Figure 5.14. Splenic B cell numbers in chimeric mice with either T-bet-sufficient or T-bet-deficient B cells before and during STm infection. Chimeras were infected with 10^5 STm or remained uninfected as controls. At the specified time points, mice were sacrificed and splenic B cell numbers were quantified by flow cytometry ***A.*** Representative flow cytometry plots showing recirculating follicular and MZ B cell staining of splenocytes from T-bet$^{+/+BCELL}$ and T-bet$^{-/-BCELL}$ mice. Numbers denote MZ or recirculating B2 cells as a proportion of total splenocytes. ***B. I*** Total number of splenic recirculating B cells in T-bet$^{+/+BCELL}$ and T-bet$^{-/-BCELL}$ spleens before and during infection with STm. ***II*** Total number of splenic MZ B cells in T-bet$^{+/+BCELL}$ and T-bet$^{-/-BCELL}$ spleens before and during infection with STm. Each point represents one mouse. Data are pooled from 2-3 experiments.

5.2.1.9 B cell-intrinsic T-bet is required for antibody class-switching to IgG2a during STm infection

Staining of spleen sections by immunohistology revealed higher background numbers of splenic IgM^+ and $IgG2b^+$ plasma cells in uninfected T-$bet^{+/+BCELL}$ and T-$bet^{-/-BCELL}$ mice, than would be expected in C57BL6 WT mice (figure 5.15 and 5.16A and B). However, plasma cell numbers increased after infection and no difference in IgM^+ and $IgG2b^+$ plasma cell numbers were observed in T-$bet^{+/+BCELL}$ and T-$bet^{-/-BCELL}$ spleens at either stage of infection (figure 5.15 and 5.16A and B). Staining for $IgG2a^+$ plasma cells revealed that at day 0, T-$bet^{+/+BCELL}$ plasma cell numbers were again higher than expected, however $IgG2a^+$ plasma cells were rare and only sporadic in T-$bet^{-/-BCELL}$ spleens (figure 5.15 and 5.16C BIII). By day 7 p.i, an increase above background numbers occurred in T-$bet^{-/-BCELL}$ mice, however $IgG2a^+$ plasma cell numbers were >4-fold lower when compared to T-$bet^{+/+BCELL}$ mice ($p \leq 0.001$). Strikingly, by D35p.i when GC contribute to plasma cell output, the number of $IgG2a^+$ plasma cells was no higher than background in T-$bet^{-/-BCELL}$ mice and >100 fold lower than in T-$bet^{+/+BCELL}$ mice ($p \leq 0.001$) (figure 5.16 C).

Consistent with these findings, OMP-specific IgM^+ and $IgG2b^+$ antibody titres were similar in the two groups of mice at both stages of infection (figure 5.17A and B), whilst $IgG2a^+$ switched antibody was completely undetectable in T-$bet^{-/-BCELL}$ mice at day 35 pi (figure 5.17C). This was in stark contrast to T-$bet^{+/+BCELL}$ mice, that produced marked IgG2a titres at this point ($p \leq 0.001$). Thus, T-bet expression in B cells is required for optimal switching to IgG2a during the early stages of infection and becomes an absolute requirement during the later stages of the response.

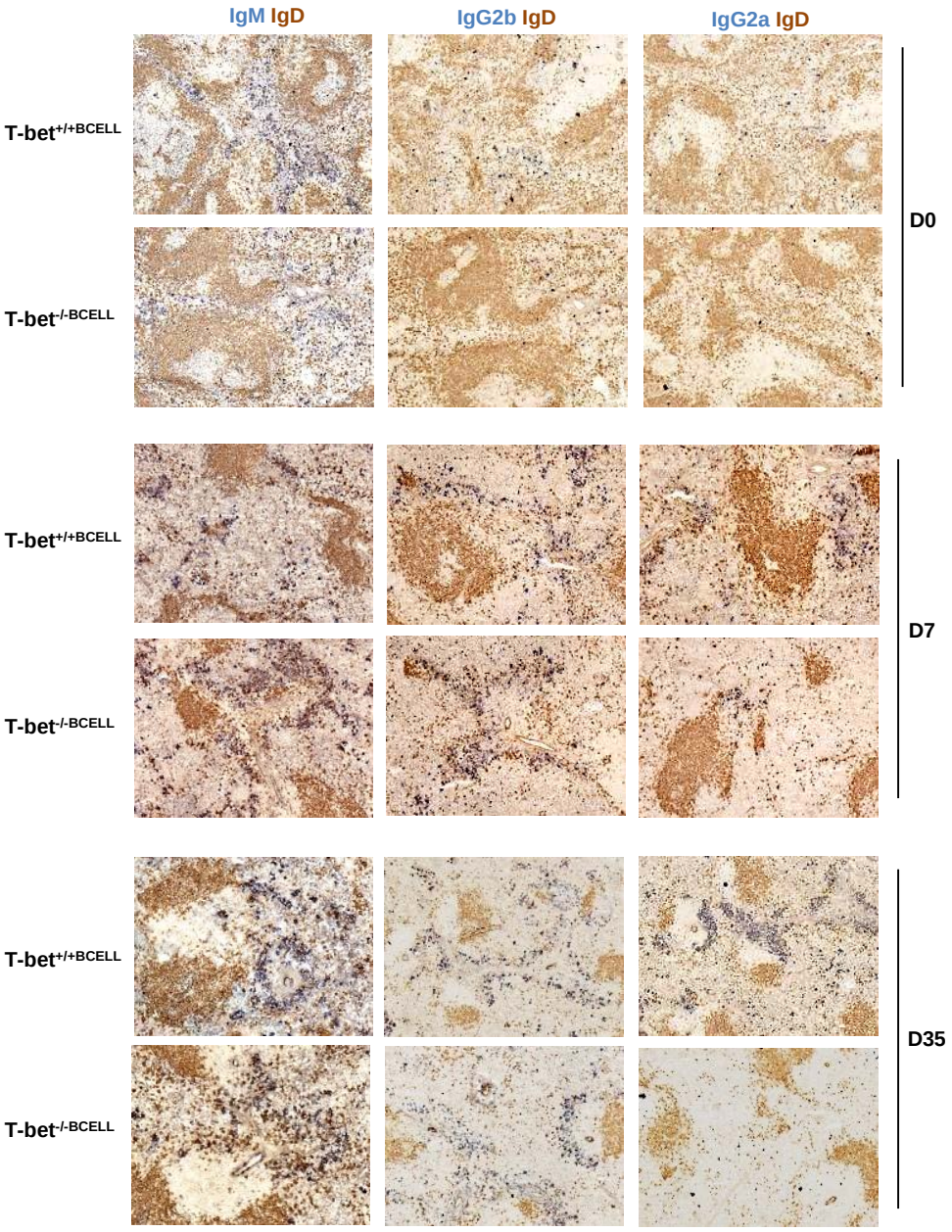

Figure 5.15. Staining of EF plasma cells in chimeric mice with either T-bet-sufficient or T-bet-deficient B cells before and during STm infection. Chimeras were infected with 10^5 STm or remained uninfected as controls. At the specified time points, mice were sacrificed and the spleens were stained for EF plasma cells. Representative photographs from T-bet$^{+/+BCELL}$ and T-bet$^{-/-BCELL}$ spleens stained with ***left panels*** IgM (blue) and IgD (brown) to detect non-switched EF plasma cells, ***middle panels*** IgG2b (blue) and IgD brown and ***right panels*** IgG2a (blue) and IgD (brown) to detect class-switched EF plasma cells. Photographs are representative of at least 7 mice per group at day 7 and 35 p.i and 3 mice at day 0.

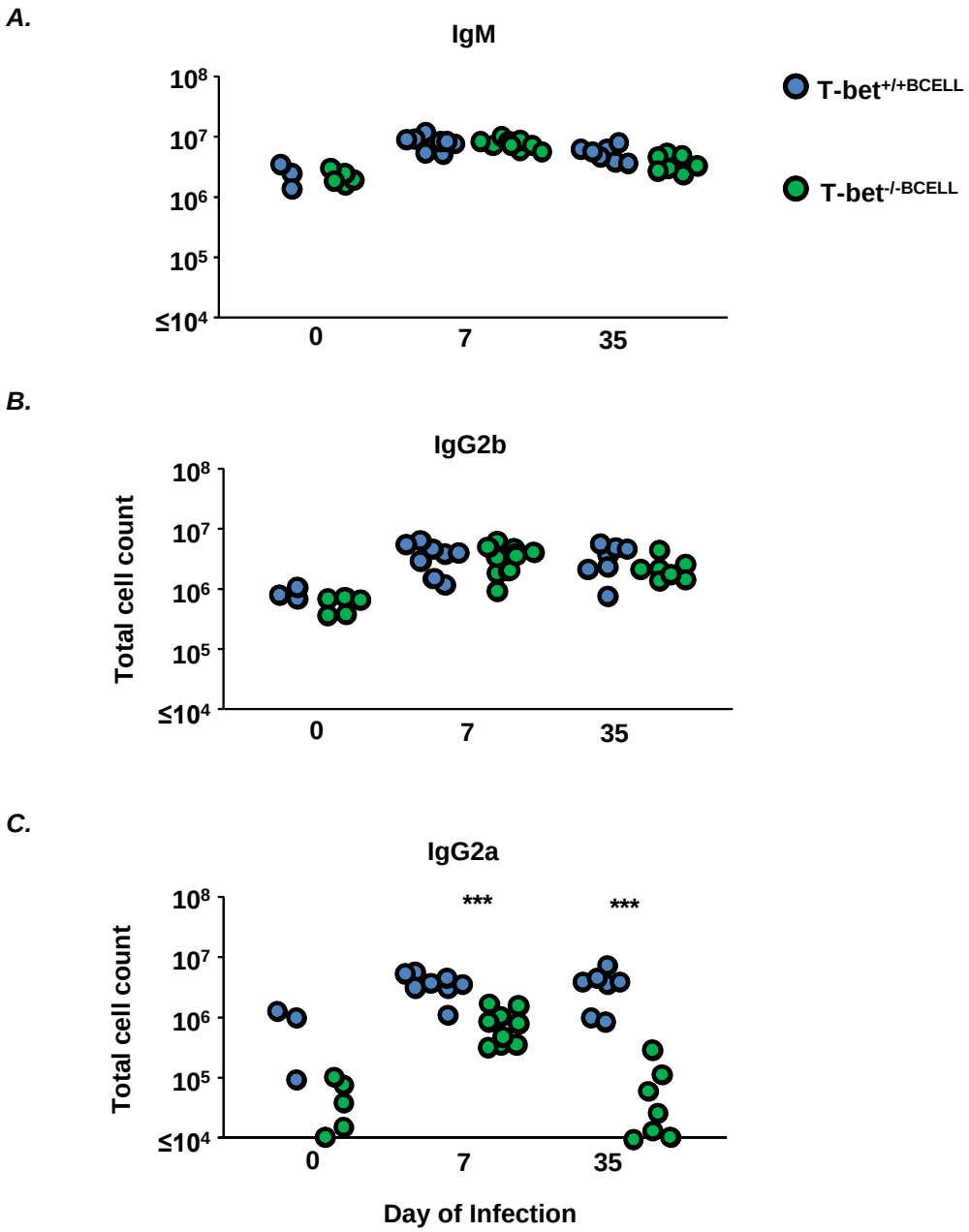

Figure 5.16. EF plasma cell numbers in chimeric mice with either T-bet-sufficient or T-bet-deficient B cells before and during STm infection. Chimeras were infected with 10^5 STm or remained uninfected as controls. At the specified time points, mice were sacrificed and the spleens were stained for EF plasma cells. Total number of splenic ***A,*** IgM^+, ***B,*** $IgG2b^+$ and ***C,*** $IgG2a^+$ plasma cells in T-bet$^{+/+BCELL}$ and T-bet$^{-/-BCELL}$ mice at the specified time points, as quantified by histology. One point represents one mouse. Data are pooled from 2-3 individual experiments. *** $p \leq 0.001$

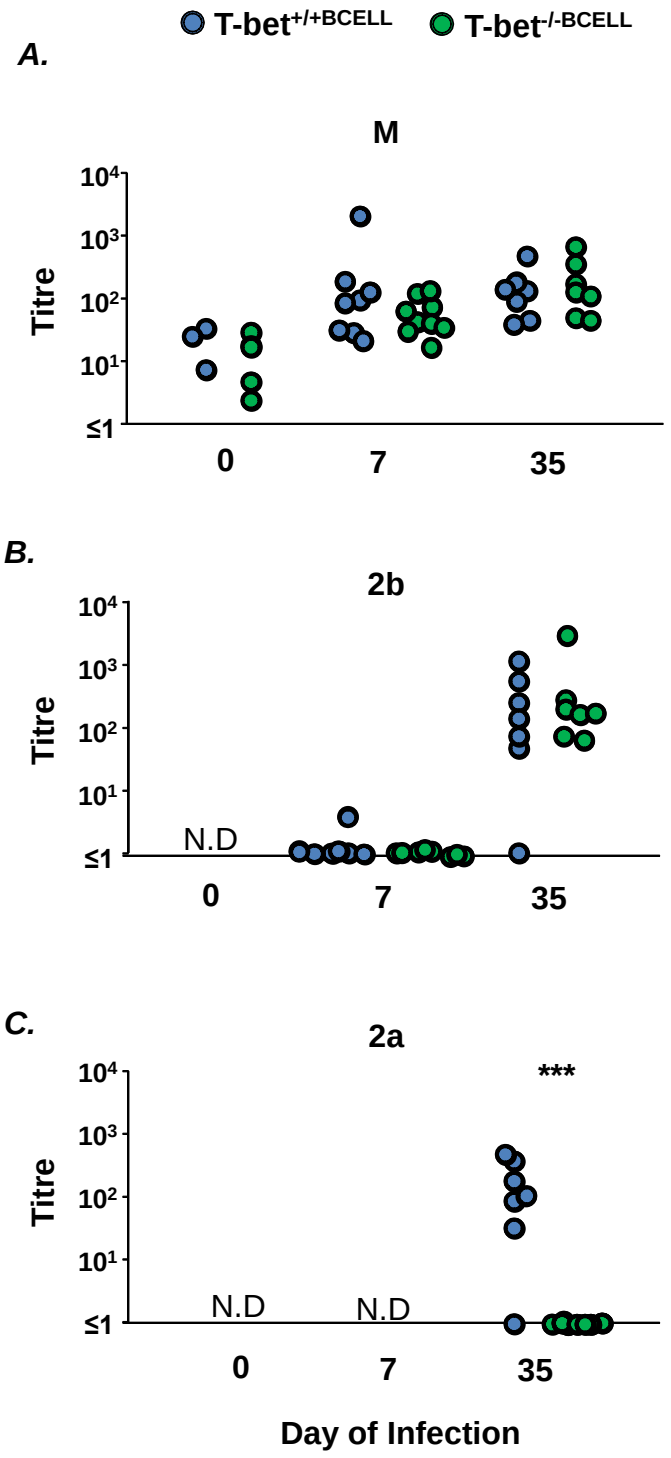

Figure 5.17. OMP-specific antibody titres in chimeric mice with either T-bet-sufficient or T-bet-deficient B cells before and during STm infection. Chimeras were infected with 10^5 STm or remained uninfected as controls. At the specified time points, mice were sacrificed and ***A,*** IgM, ***B,*** IgG2b and ***C,*** IgG2a serum antibody titres were measured by ELISA. One point represents one mouse. Data are pooled from 2-3 individual experiments. *** $p \leq 0.001$

5.2.1.10 Germinal centres and Tfh cells develop normally in T-bet$^{-/-BCELL}$ chimeras

As the IgG2a response was absent in T-bet$^{-/-BCELL}$ chimeras by day 35 p.i, GC and Tfh cell development was assessed. Germinal centres form by day 35 of infection with STm and this coincides with the detection of high titres of switched IgG2a antibody in WT mice (70). Staining of spleen sections for GC revealed T-bet$^{-/-BCELL}$ mice were able to form GC during STm infection (data not shown). Tfh cells, identified by confocal microscopy staining as $CD3^{+}PD1^{+}Bcl\text{-}6^{+}$ cells, were clearly evident within these structures (figure 5.18). Thus, a complete loss of IgG2a by day 35 could not be attributed to a failure to develop the GC or the T cells that support class-switched antibody responses within them. We therefore examined the possibility that the defect in IgG2a class-switching occurred prior to GC entry, during cognate interaction with T cells at the T-B border.

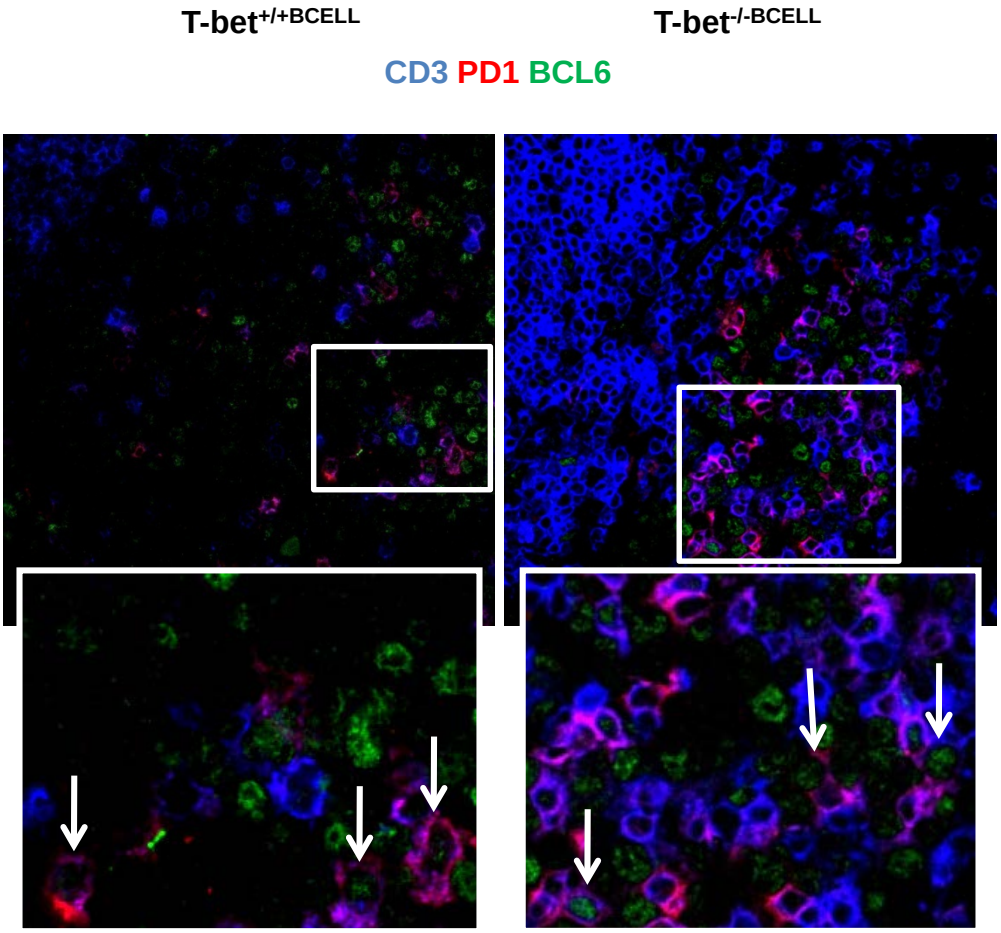

Figure 5.18. Tfh cells in chimeric mice with either T-bet-sufficient or T-bet-deficient B cells during STm infection. Chimeras were infected with 10^5 STm and at day 35 p.i, mice were sacrificed and the spleens stained for Tfh cells by confocal microscopy. Tfh cells were identified as $CD3^+$ (blue) $PD1^+$ (red) $BCL6^+$ (green). The white box shows the enlarged area below and the white arrows on the enlarged image identify Tfh cells. Images are representative of 7 mice per group.

5.2.1.11 Defective IgG2a class-switching in T-bet$^{-/-}$ B cells is reflected in impaired γ2a germline switch transcript production

During T-D antibody responses, germline-switch transcripts are first up-regulated in B cells during their interaction with T cells at the T-B border in secondary lymphoid tissue (56). To address the timing of the IgG2a defect in T-bet$^{-/-BCELL}$ mice, CD19^{+} B220^{+} B cells were sorted by FACS from T cell and B cell chimeric mice and relative γ2a-germline switch transcript mRNA expression was measured as described previously (93). By day 7 of infection, γ2a-germline switch transcripts expression increased nearly 10-fold above background levels in B cells from T-bet$^{+/+TCELL}$ mice and T-bet$^{-/-TCELL}$ mice. Consistent with the plasma cell and antibody data, real-time PCR analysis of CD19^{+} B220^{+} B cells revealed similar mRNA expression levels of γ2a-germline switch transcripts in T-bet$^{+/+TCELL}$ and T-bet$^{-/-TCELL}$ mice at both day 7 and 35 p.i. (figure 5.19A). In the B cell chimeras, T-bet$^{+/+BCELL}$ mice had high background expression of γ2a-germline switch transcripts, whilst expression was absent in B cells from T-bet$^{-/-BCELL}$ mice. By day 7 p.i, γ2a-switch transcript expression had increased in T-bet$^{-/-BCELL}$ mice, however importantly, mRNA expression was significantly lower compared to T-bet$^{+/+BCELL}$ mice ($p \leq 0.01$) (figure 5.19B). At day 35 p.i, when switch transcripts remained detectable in T-bet$^{+/+BCELL}$ mice, they were either undetectable or very weakly expressed in B cells from T-bet$^{-/-BCELL}$ mice ($p \leq 0.001$).

A.

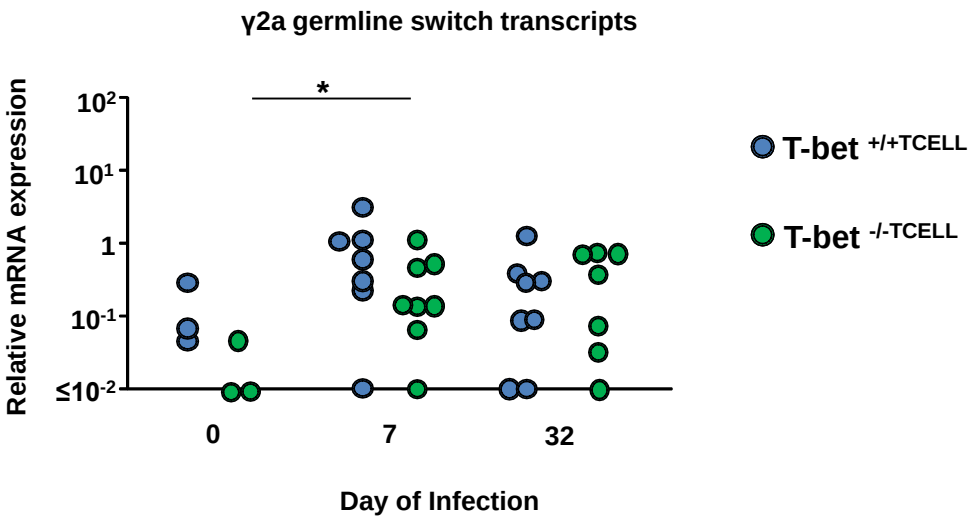

B.

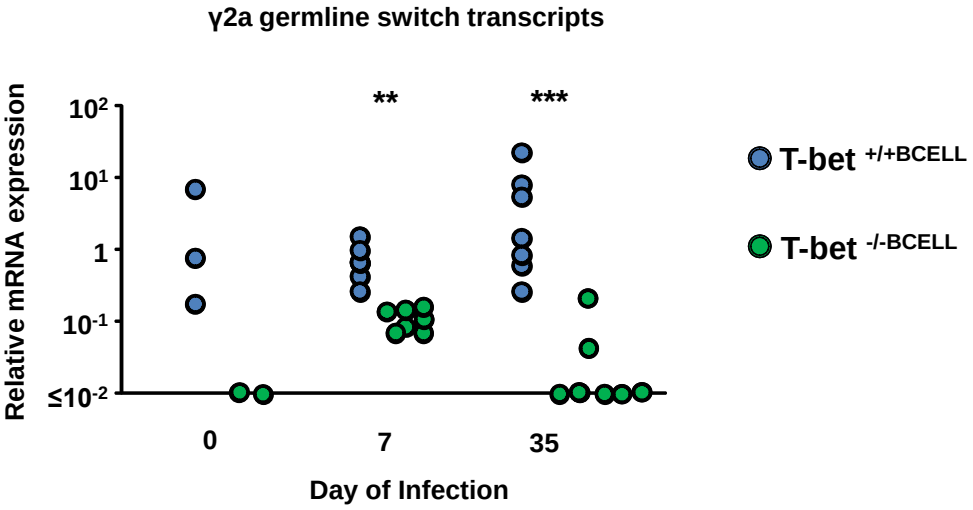

Figure 5.19. γ2a germline-switch transcript mRNA expression in chimeric mice with T-bet-sufficient or T-bet-deficient T cells and T-bet sufficient or T-bet-deficient B cells. Chimeras were infected with 10^5 STm or remained uninfected as controls. At the specified timepoints, $CD19^+$ $B220^+$ B cells were isolated from the spleen by FACS and mRNA gene expression was quantified by RT-PCR. ***A.*** γ2a-germline switch transcript mRNA expression, relative to β-actin, in B cells from $T\text{-}bet^{+/+TCELL}$ and $T\text{-}bet^{-/-TCELL}$ mice. ***B.*** γ2a-germline switch transcript mRNA expression, relative to β-actin, in B cells from $T\text{-}bet^{+/+BCELL}$ and $T\text{-}bet^{-/-BCELL}$ mice. One point represents one mouse. ** $p \leq 0.01$; *** $p \leq 0.001$. Data are pooled from 2 individual experiments.

5.2.1.12 Class-switching to IgG2a during STm infection is not dependent upon normal IFNγ mRNA expression by T cells

The diminution of γ2a germline-switch transcripts in T-bet$^{-/-BCELL}$ mice suggested a defect either during or before initial T-B interaction at the T-B border. As IFNγ can induce IgG2a class switching in B cells (291), we measured expression of mRNA for this cytokine by RT-PCR in T and B cells from both sets of chimeras. In other published data from our group and others (78,79) no IFNγ protein has been detected in T-bet$^{-/-}$ T cells during STm infection. In the T cell chimeras, IFNγ was expressed in T cells from T-bet$^{+/+TCELL}$ chimeras prior to infection, increasing significantly during the infection ($p \leq 0.05$) (figure 5.20A left panel and 5.20B merged). IFNγ expression did not alter significantly between day 0 and 7 in T cells from T-bet$^{-/-TCELL}$ chimeras, although an increased was observed by day 35 p.i ($p \leq 0.05$). Despite this increase, IFNγ expression was markedly lower in T cells from T-bet$^{-/-TCELL}$ chimeras when compared to T-bet$^{+/+TCELL}$ chimeras at day 7 ($p \leq 0.01$) and 35 ($p \leq 0.001$) of infection. In comparison to T cells, IFNγ expression in T-bet sufficient B cells was consistently lower in both T-bet$^{+/+TCELL}$ and T-bet$^{-/-TCELL}$ chimeras (figure 5.20A right panel and 5.20B merged), but no differences were observed between the two groups, showing that a loss of T-bet and reduced IFNγ expression in T cells did not impact upon IFNγ mRNA expression in B cells. Thus, B cells were able to class-switch to IgG2a in the absence of normal IFNγ expression in T cells, but may still require intrinsic IFNγ induction or IFNγ from other sources.

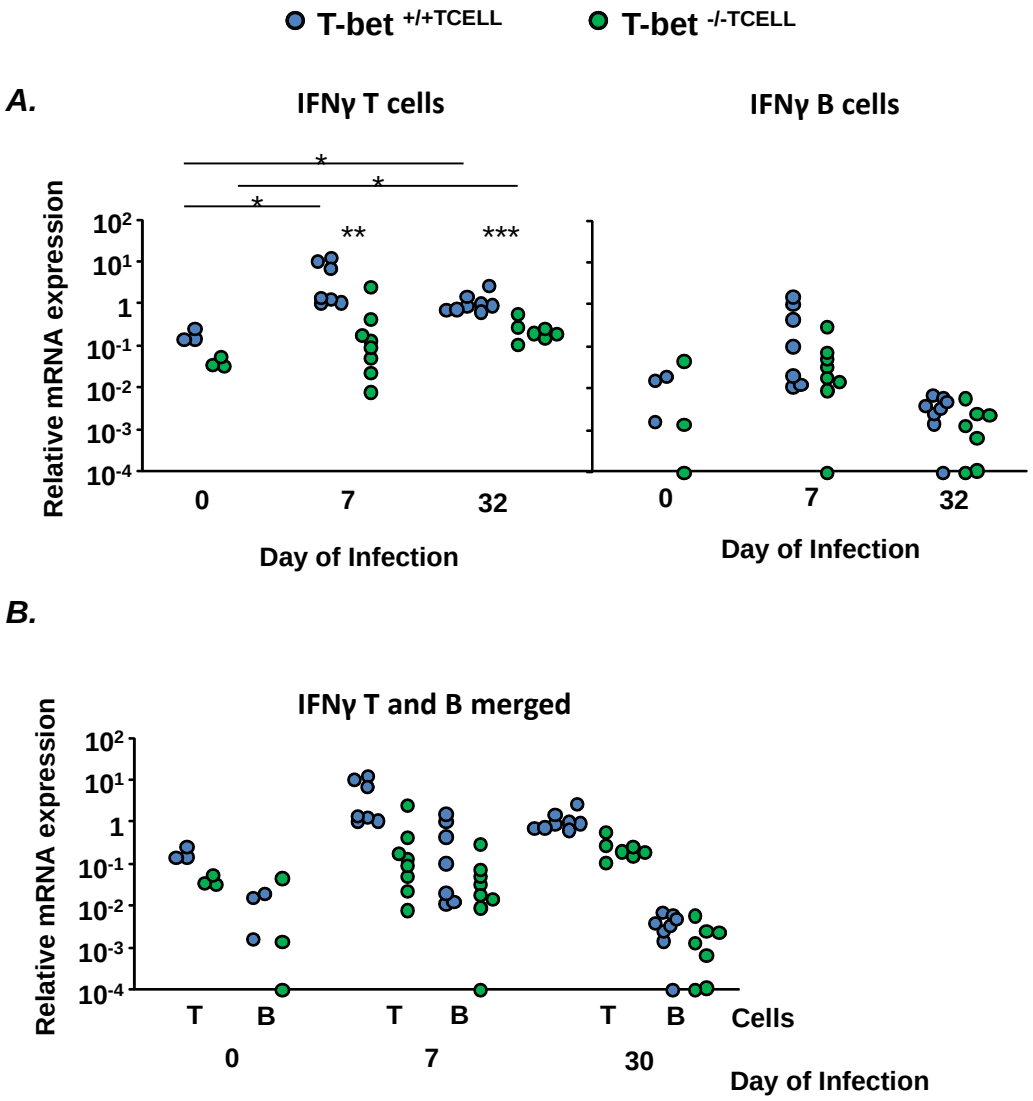

Figure 5.20. IFNγ mRNA expression in chimeric mice with T-bet-sufficient or T-bet-deficient T cells. Chimeras were infected with 10^5 STm or remained uninfected as controls. At the specified time points, $CD19^+$ $B220^+$ B cells and $CD3^+$ T cells were isolated from the spleen by FACS and mRNA gene expression was quantified by RT-PCR. ***A.*** IFNγ mRNA expression, relative to β-actin, in T cells (T) and B cells (B) from T-$bet^{+/+TCELL}$ and T-$bet^{-/-TCELL}$ mice. ***B.*** Merged data from ***A.*** One point represents one mouse. *p ≤ 0.05; **p ≤ 0.01; ***p ≤ 0.001. Data are pooled from 2 individual experiments.

To assess whether a link exists between B cell-intrinsic T-bet and B cell intrinsic IFNγ expression, we measured IFNγ expression in T-bet$^{+/+BCELL}$ and T-bet$^{-/-BCELL}$ chimeras (figure 5.21). The background level of IFNγ expression was high in T cells from these chimeras (figure 5.21 left panel), consistent with the elevated levels of T cell activation shown in figure 5.12. However, throughout infection, the T cells from T-bet$^{+/+BCELL}$ and T-bet$^{-/-BCELL}$ chimeras expressed high levels of IFNγ with no significant differences observed between the two groups (figure 5.21A left panel and 5.21B merged). Again, B-cell expressed IFNγ was consistently lower than that expressed in T cells, but increased above background levels during infection (figure 5.21A right panel and 5.21B merged). A loss of T-bet in B cells had no impact upon B cell-expressed IFNγ, indicating that the absence of IgG2a class switching in T-bet$^{-/-BCELL}$ chimeras is not due to an inability to up-regulate intrinsic IFNγ mRNA expression.

To summarise, T-bet expression in B cells is requisite for optimal IgG2a class-switching during STm infection and this defect appears to occur at the transcriptional level. Germinal centres develop in the absence of T-bet in B cells, which are probably supporting class-switching to other isotypes such as IgG2b, which is T-bet independent. It is unlikely that IFNγ-secretion by T cells is required for the IgG2a response, however IFNγ from other sources may be important. The exact signals that drive T-bet dependent IgG2a class-switching are yet to be identified within this model.

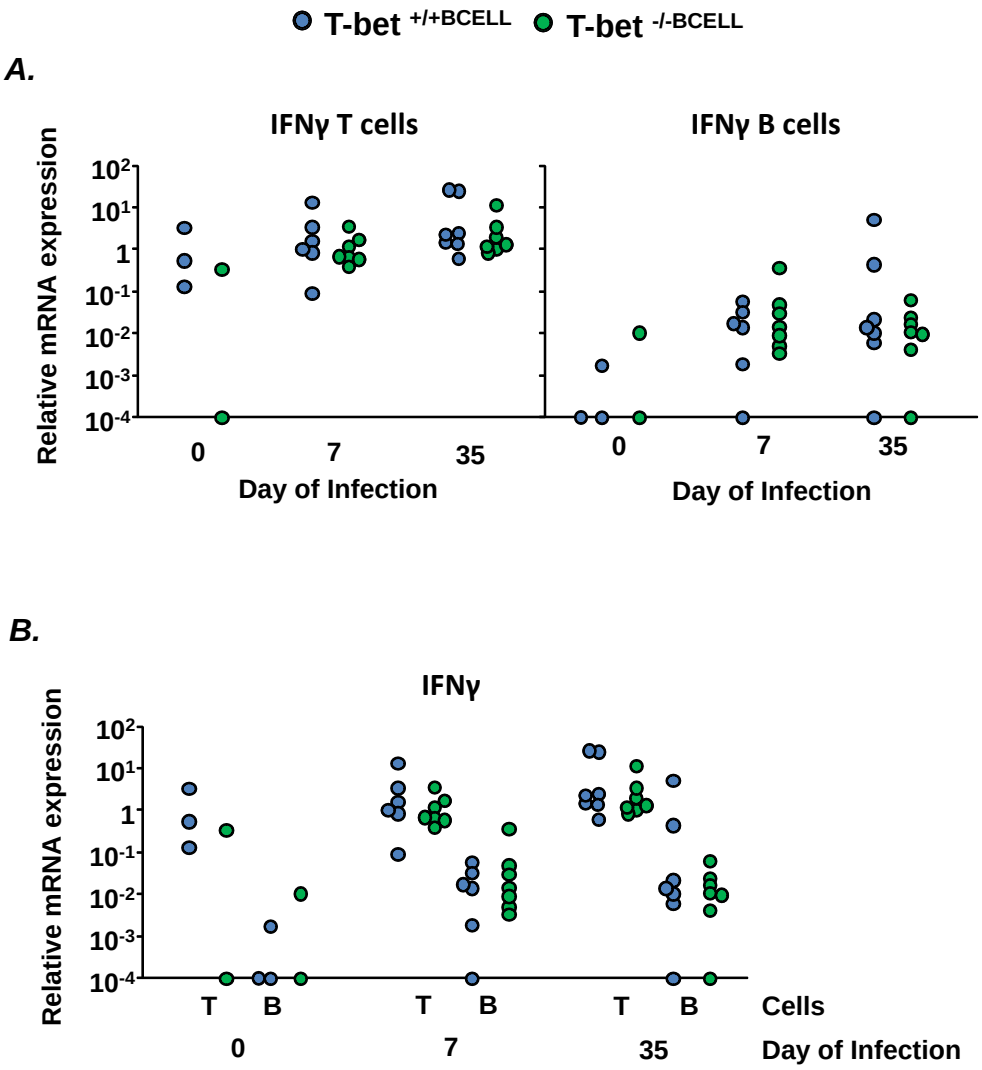

Figure 5.21. IFNγ mRNA expression in chimeric mice with T-bet-sufficient or T-bet-deficient B cells. Chimeras were infected with 10^5 STm or remained uninfected as controls. At the specified time points, $CD19^+$ $B220^+$ B cells and $CD3^+$ T cells were isolated from the spleen by FACS and mRNA gene expression was quantified by RT-PCR. ***A.*** IFNγ mRNA expression, relative to β-actin, in T cells and B cells from T-$bet^{+/+BCELL}$ and T-$bet^{-/-BCELL}$ mice. ***B.*** Merged data from ***A.*** One point represents one mouse. Data are pooled from 2 individual experiments.

During the STm infection studies, IgG1 antibody production was measured in T-bet$^{-/-}$ mice and T-bet$^{-/-BCELL}$ chimeras, to assess for compensatory switching mechanisms. However, no IgG1 was detected, which contrasts with the enhanced production of IgG1 previously reported in T-bet$^{-/-}$ mice (83). We predicted that heightened IgG1 production in T-bet$^{-/-}$ mice may occur only during responses that naturally induce CSR to this subclass. Whilst infection with STm drives a Th1 response with class-switching to IgG2a and IgG2b, immunisation with sFliC from STm drives a Th2 response with dominant switching to IgG1 (239). We therefore investigated the antibody responses to this protein in T-bet$^{-/-}$ mice.

5.2.2 T-bet-mediated control of antibody responses to Th2 antigens

5.2.2.1 Minor defects in early germinal centre development in T-bet$^{-/-}$ mice following immunisation with sFliC

Primary i.p immunisation with sFliC drives a splenic GC response without a concomitant EF plasma cell response, whilst memory responses induce both GC and EF plasma cell development (239). The GC response to sFliC was assessed by histology in WT and T-bet$^{-/-}$ mice following primary sFliC immunisation. The total GC volume per spleen was slightly lower in T-bet$^{-/-}$ mice at day 7 and 14 p.i but these differences were not significant (figure 5.22A). Assessment of GC as a proportion of the total follicle produced a similar result (figure 5.22B). In order to assess the output of the GC, anti-FliC antibody titres were assessed in the two groups of mice.

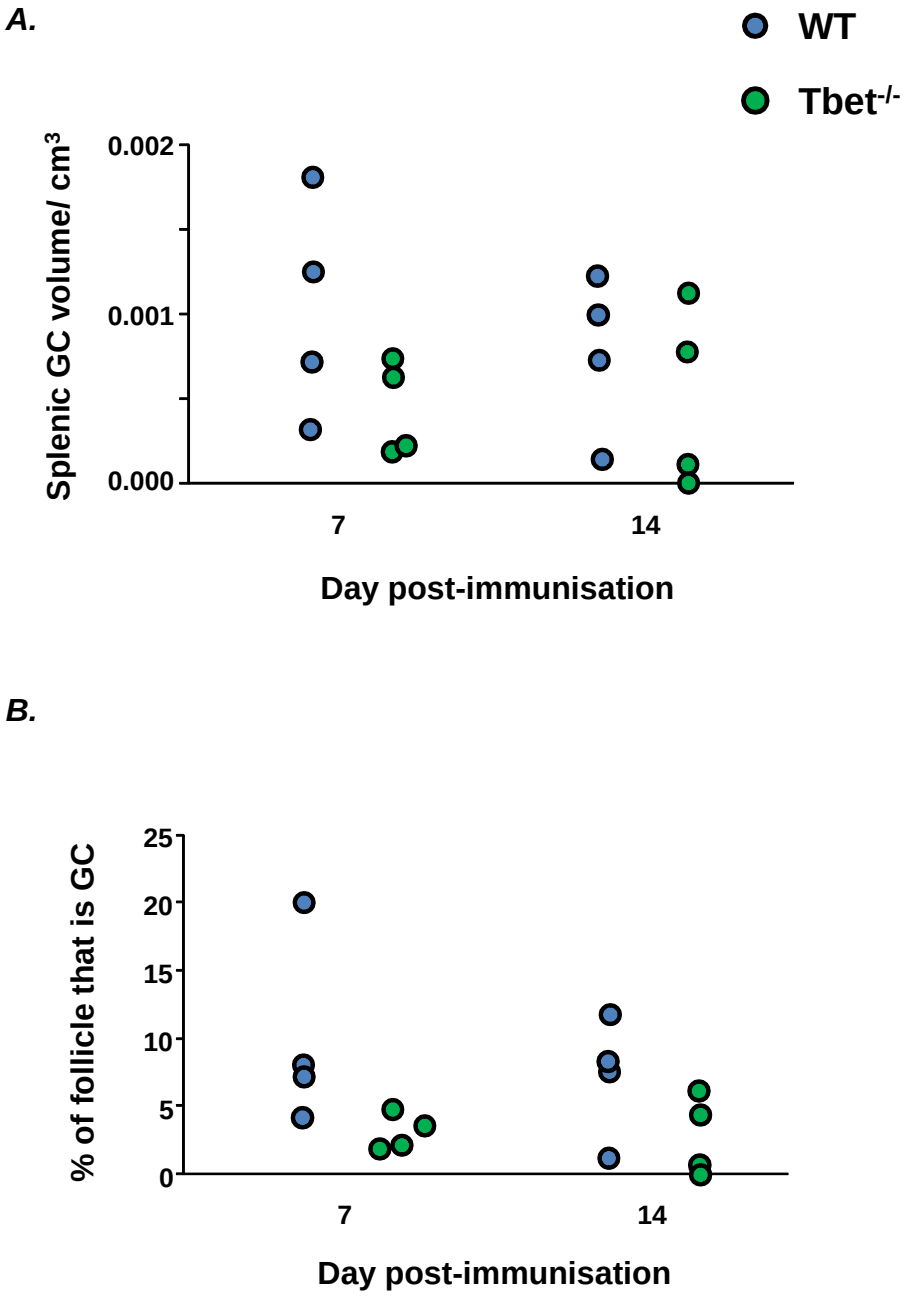

Figure 5.22. Splenic GC volume and size in WT and Tbet$^{-/-}$ mice after primary sFliC immunisation. WT and Tbet$^{-/-}$ mice were immunised with 25µg sFliC. The ***A*****,** total volume of germinal centre per spleen and ***B*****,** proportion of follicle that is germinal centre was quantified by histology at the indicated time points p.i. Data are representative of two experiments giving similar results. One point represents one mouse.

5.2.2.2 Antibody class switching to IgG1 is significantly reduced in T-bet$^{-/-}$ mice following immunisation with sFliC

At day 7 following immunisation with sFliC, the antibody response is dominated by non-switched IgM, whilst high titres of IgG1 are produced by day 14 p.i (239). Assessment of serum anti-FliC antibody by ELISA produced a surprising finding. Whilst IgM production was similar in WT and T-bet$^{-/-}$ mice, class switching to IgG1 was significantly impaired by day 14 p.i ($p \leq 0.05$) (figure 5.23A and B). Furthermore, IgG2b, which is also produced during the sFliC response, was significantly reduced in T-bet$^{-/-}$ mice at day 14 p.i (figure 5.23C) ($p \leq 0.05$). Whilst only produced at low levels following primary immunisation with sFliC, some IgG2a antibody is detectable in the sera of WT mice by day 14 p.i. As expected, no IgG2a antibody was produced by T-bet$^{-/-}$ mice at any point (figure 5.23D). These observations were consistent across a number of similar experiments. Thus, contrary to expectations, T-bet$^{-/-}$ mice were consistently unable to mount optimal antibody responses to an antigen that elicits an IgG1-dominated response. In order to assess this further, the memory response to sFliC was assessed in the two groups of mice.

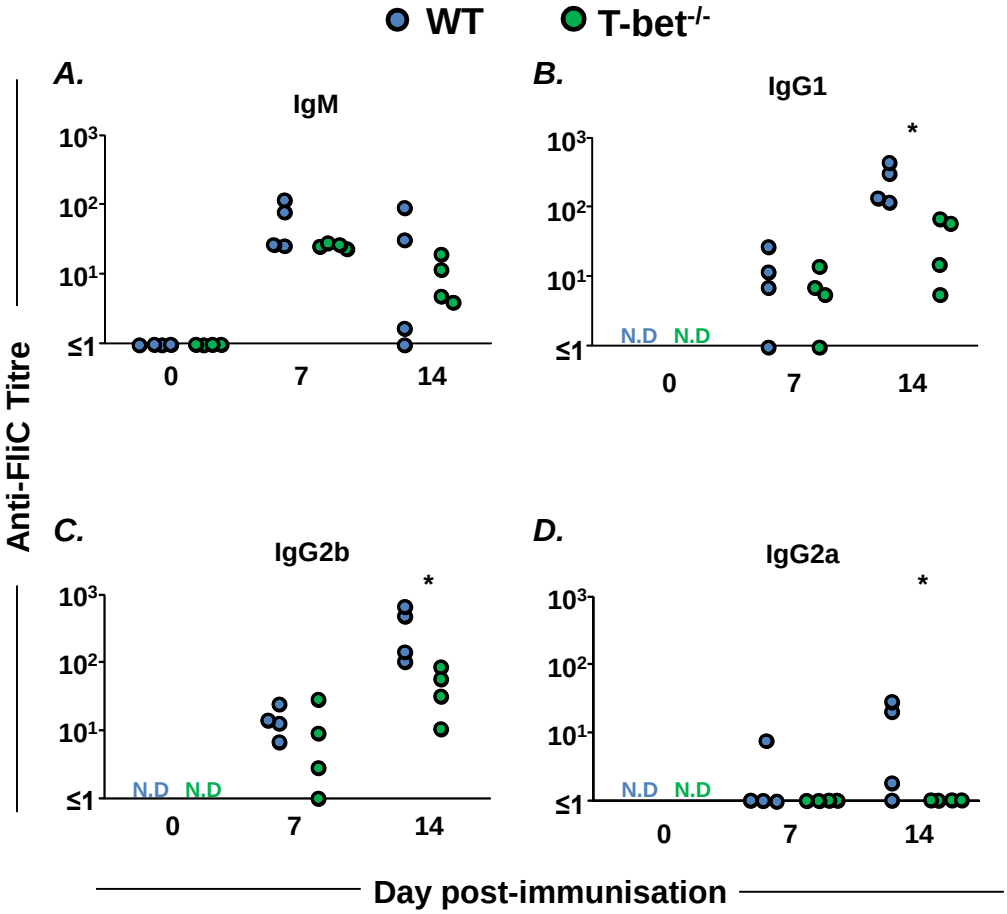

Figure 5.23. FliC-specific antibody titres before after primary sFliC immunisation. WT and T-bet$^{-/-}$ mice were immunised with 25µg of sFliC or remained non-immunised as controls. FliC-specific ***A,*** IgM, ***B,*** IgG1, ***C,*** IgG2b and ***D,*** IgG2a serum antibody was quantified in all mice before and at the times specified p.i. Data are representative of ≥ 2 experiments giving similar findings. One point represents one mouse. * p≤ 0.05.

5.2.2.3 The antibody response to sFliC largely recovers in T-bet$^{-/-}$ mice during the memory response

As mentioned previously, memory responses to sFliC drive a concomitant GC and EF antibody response. Having identified a defect in primary antibody responses to sFliC in T-bet$^{-/-}$ mice, the GC and EF plasma cells response was assessed by histology after two antigen doses. WT and T-bet$^{-/-}$ mice were immunised with sFliC for 35 days and given a secondary sFliC challenge for 4 days. Analysis of spleen sections revealed that the GC volume (figure 5.24 A) and the proportion of follicle occupied by GC (figure 5.24 B) were comparable in WT and T-bet$^{-/-}$ mice. Furthermore, staining of spleen sections with biotinylated sFliC revealed that the total number of FliC^{+} EF plasma cells was similar in WT and T-bet$^{-/-}$ mice (figure 5.25A). Double staining for isotype-specific FliC^{+} cells showed a tendency towards fewer FliC^{+} switched plasma cells in T-bet$^{-/-}$ mice, however these differences were not significant (figure 5.25B I). Furthermore, the majority of the FliC^{+} cells detected in the spleen were also IgG1 (figure 5.25B II). Assessment of FliC-specific serum antibody by ELISA confirmed these results (figure 5.26A-D). Although switched IgG1 and IgG2b antibody titres were lower in T-bet$^{-/-}$ when compared to WT mice, these differences were not as marked as during the primary response. In a second similar experiment, antibody titres were also comparable in WT and T-bet$^{-/-}$ mice (data not shown). As expected, no FliC-specifc IgG2a was produced by T-bet$^{-/-}$ mice.

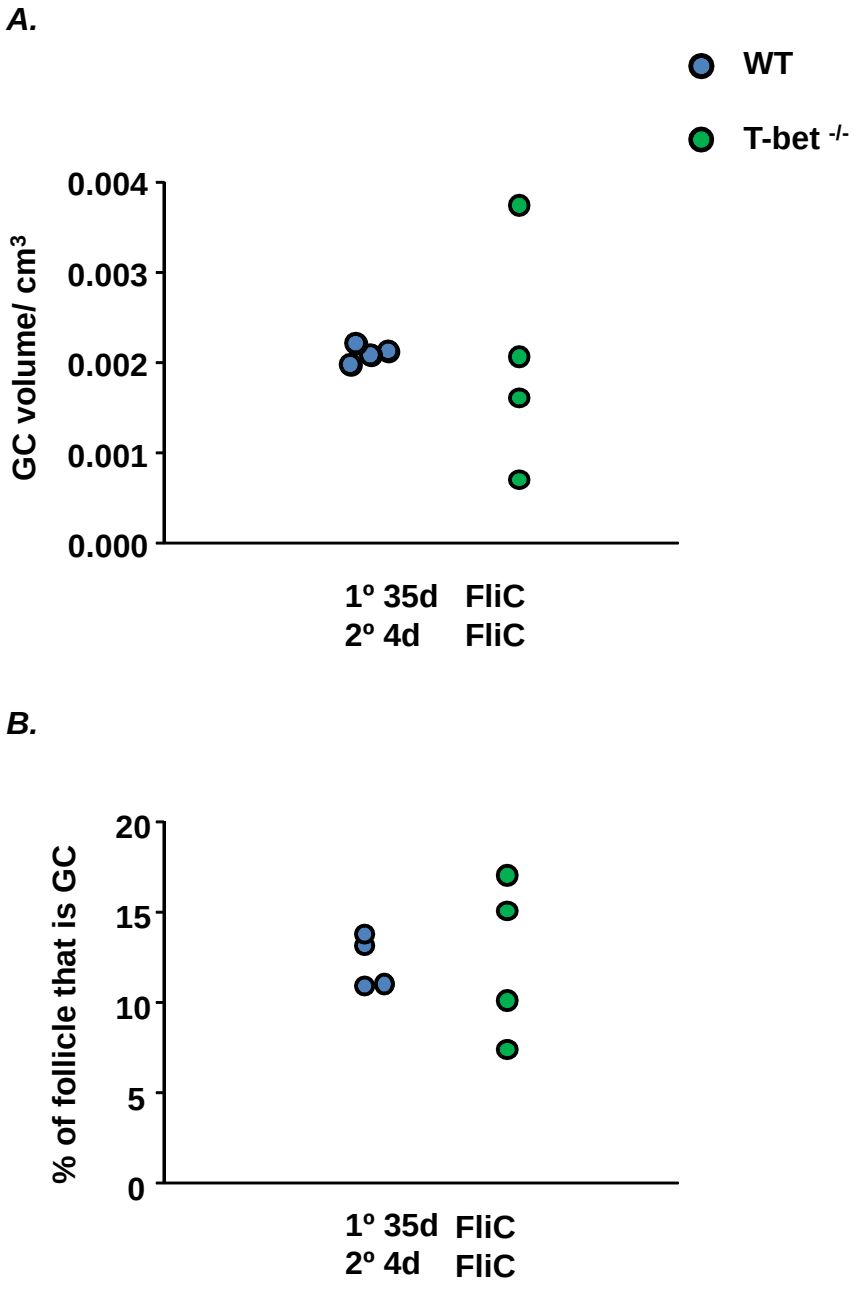

Figure 5.24. Splenic GC volume and size in WT and T-bet$^{-/-}$ mice after secondary sFliC immunisation. WT and T-bet$^{-/-}$ mice were immunised with 25µg sFliC for 35 days and then boosted with 15µg sFliC for a further 4 days. The ***A*,** total volume of GC per spleen and ***B*,** proportion of follicle occupied by GC were quantified by histology after the 4 day secondary immunisation. One point represents one mouse. Data are representative of ≥ 2 experiments giving similar results.

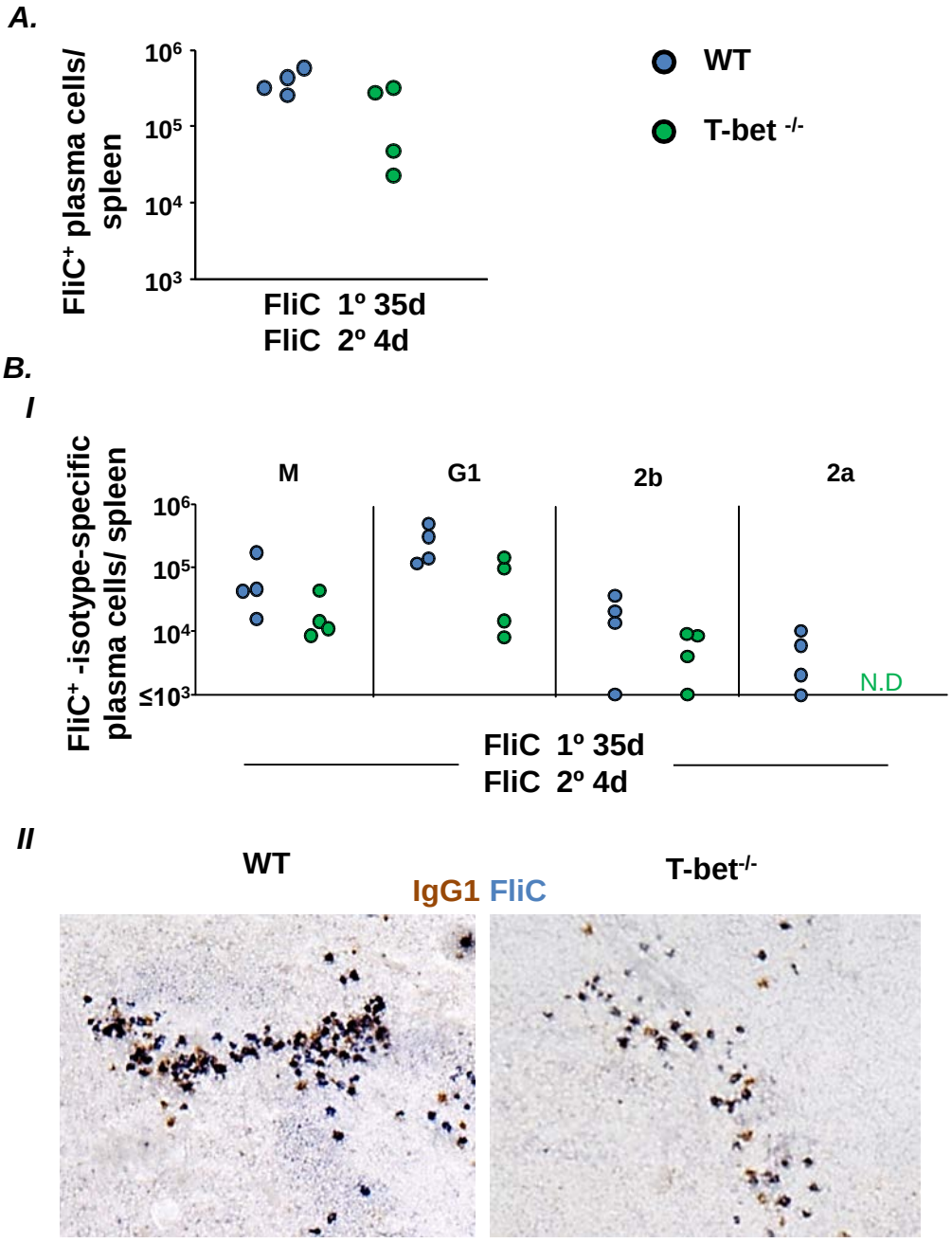

Figure 5.25. FliC-specific plasma cells in WT and T-bet$^{-/-}$ mice after secondary FliC immunisation. WT and Tbet$^{-/-}$ mice were immunised with 25µg soluble flagella protein FliC for 35 days and then boosted with 15µg FliC for a further 4 days. Spleens were stained with biotinylated FliC to detect FliC^{+} plasma cells. ***A.*** Total number of FliC^{+} plasma cells in WT and T-bet$^{-/-}$ mice as quantified by histology. ***B.*** ***I*** Total number of FliC^{+} IgM^{+}/ IgG1^{+} /IgG2b^{+}/IgG2a^{+} double positive plasma cells in the spleens of WT and T-bet$^{-/-}$ mice after secondary immunisation with FliC, as determined by histology. ***II*** Representative spleen sections stained with biotinylated FliC (blue) and IgG1 (brown), showing that the majority of EF FliC^{+} plasma cells in the spleens of WT and T-bet$^{-/-}$ mice are IgG1^{+}. Data are representative of 2 experiments giving similar results. One point represents one mouse.

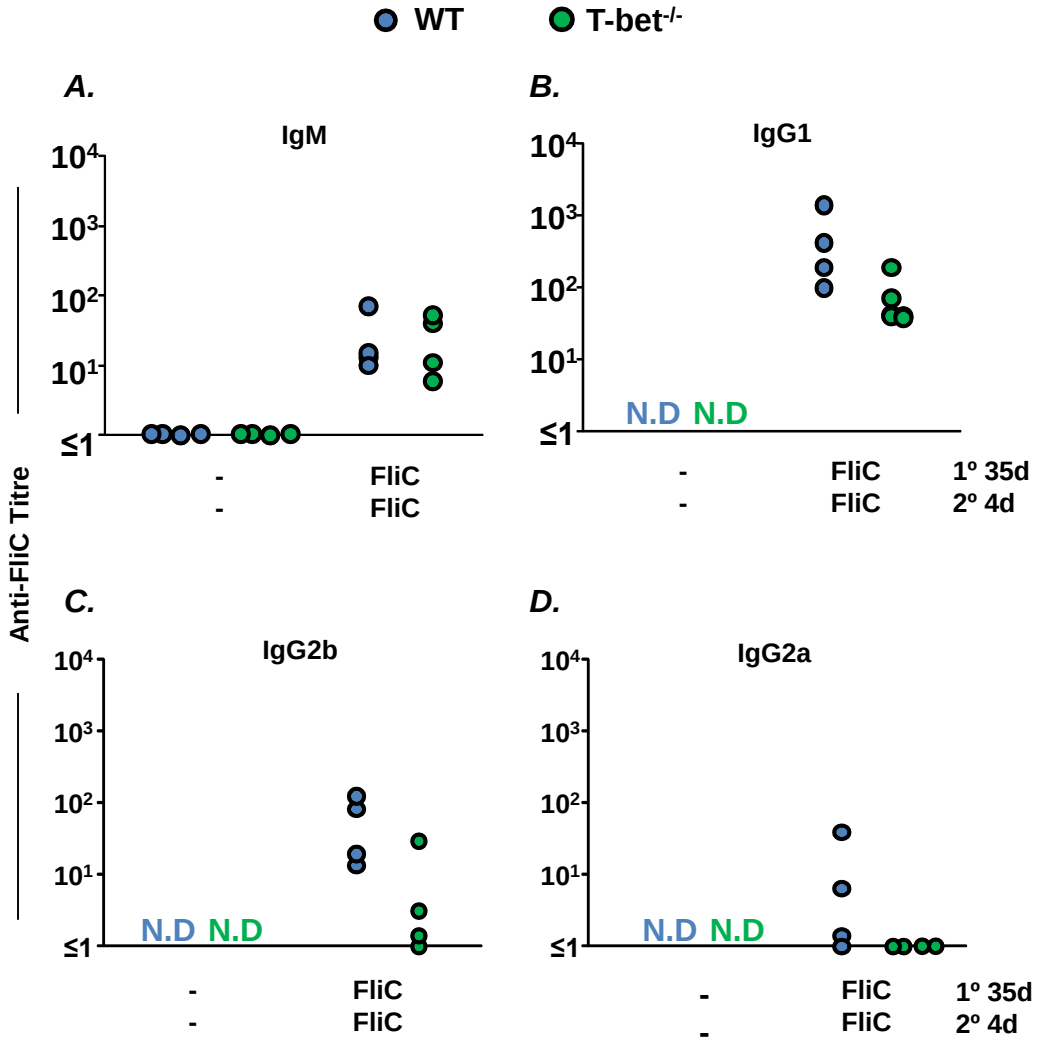

Figure 5.26. FliC-specific antibody titres after secondary sFliC immunisation. WT and T-bet$^{-/-}$ mice were immunised with 25µg of sFliC for 35 days and boosted with 15µg sFliC for 4 days, or remained non-immunised as controls. FliC-specific ***A,*** IgM, ***B,*** IgG1, ***C,*** IgG2b and ***D,*** IgG2a serum antibody was quantified in all mice. One point represents one mouse. Data are representative of 2 experiments giving similar results.

5.2.2.4 Transfer of FliC-specific T cells into T-bet-/- mice rescues antigen-specific antibody production following primary immunisation with sFliC

As defects in antibody production were most marked during the primary response to sFliC, we questioned whether the availability of antigen-specific T cell help may be lacking in T-bet$^{-/-}$ mice. To test this, we transferred antigen-specific T cells from transgenic SM1 mice into WT and T-bet$^{-/-}$ hosts, 24h before sFliC immunisation for 14 days. As a control, a second group of WT and T-bet$^{-/-}$ mice were immunised with sFliC in the absence of SM1 T cell transfer. As expected, the T-bet$^{-/-}$ mice that had not received SM1 T cells produced lower levels of switched IgG1 (figure 5.27B) ($p \leq 0.05$) and IgG2b (figure 5.27C) antigen-specific antibody when compared to WT mice under the same condition. However, following SM1 T cell transfer and immunisation, T-bet$^{-/-}$ mice produced significantly more IgG1 ($p \leq 0.05$) (figure 5.27B) and IgG2b ($p \leq 0.05$) (figure 5.27C) than T-bet$^{-/-}$ mice that had not received SM1 cells. WT mice also produced higher titres of IgG2b following transfer ($p \leq 0.05$). Importantly, in the presence of SM1 T cells, T-bet$^{-/-}$ mice produced similar levels of switched IgG1 and IgG2b antibody to WT mice (figure 5.27B and C). However, the transfer of antigen-specific, T-bet-expressing T cells into T-bet$^{-/-}$ mice, was not sufficient to recover the IgG2a response in T-bet$^{-/-}$ mice (figure 5.27D).

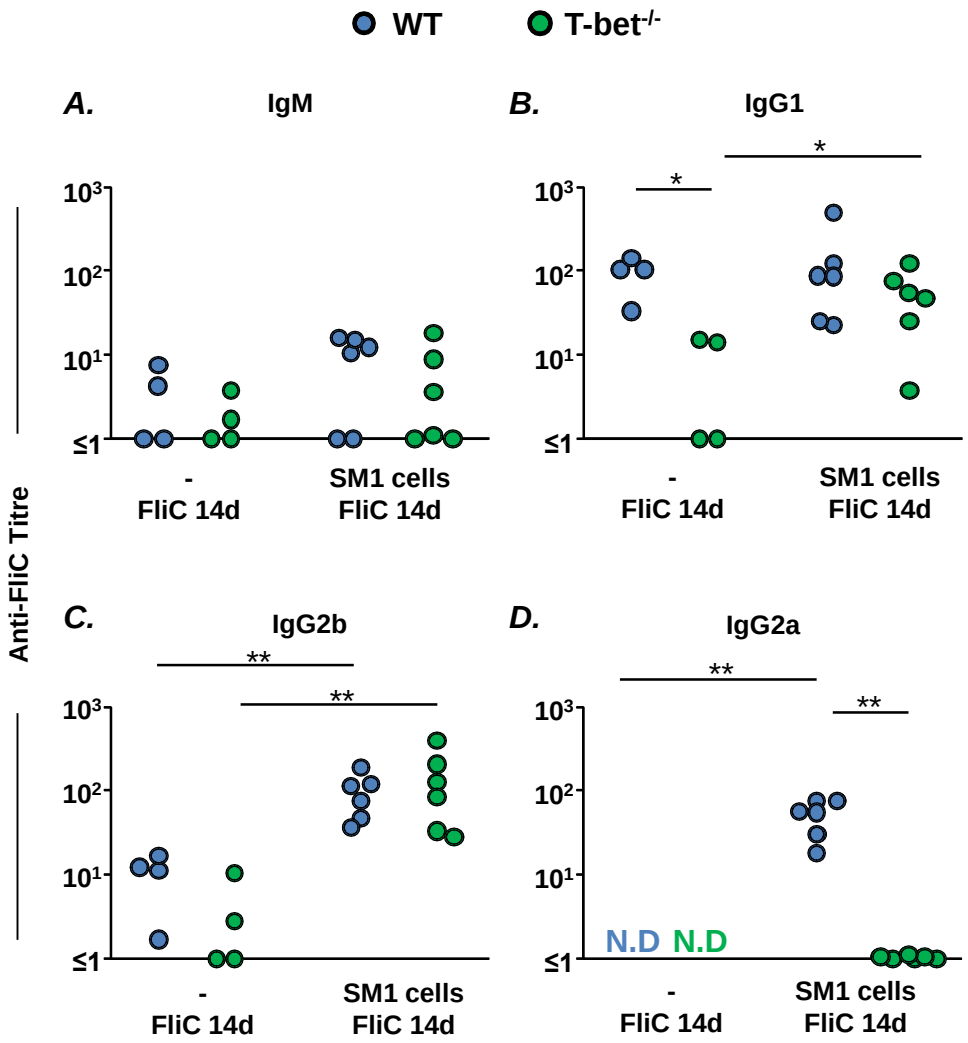

Figure 5.27. FliC-specific antibody titres in WT and T-bet$^{-/-}$ mice following antigen-specific (SM1) T cell transfer and FliC immunisation. WT and T-bet$^{-/-}$ mice were immunised or 14 days with sFliC in the absence or presence of SM1 T cell transfer. Graphs show sFliC-specific ***A,*** IgM, ***B,*** IgG1, ***C,*** IgG2b and ***D,*** IgG2a serum antibody titres under the two conditions. Data are pooled 2 experiments. One point represents one mouse. *p ≤ 0.05; **p ≤ 0.01.

Having observed this defect in IgG1 class switching in T-bet$^{-/-}$ mice, we addressed whether immunisation with a classic Th2 protein antigen would elicit the same effect. Therefore, T-bet$^{-/-}$ mice were immunised with alum-CGG, which drives a concomitant GC and an EF plasma cell response following primary and secondary immunisation.

5.2.2.5 Immunisation with alum-CGG induces discrete effects upon GC and EF responses in T-bet$^{-/-}$ mice

Following primary immunisation with alum-CGG for 8 and 14 days, the splenic GC size and volume was assessed by histology in WT and T-bet$^{-/-}$ mice. Whilst both of these parameters were similar in WT and T-bet$^{-/-}$ mice at day 8 p.i, a significant impairment was observed in GC volume (figure 5.28A) and size (figure 5.28B) in T-bet$^{-/-}$ mice at day 14 p.i ($p \leq 0.05$). As alum-CGG also drives an EF plasma cell response, this B cell differentiation pathway was examined in WT and T-bet$^{-/-}$ mice at each time point. Staining for CGG^{+} plasma cells by immunohistochemistry revealed that the EF plasma cell response was not greatly impacted by T-bet loss. Total numbers of splenic CGG^{+} -specific plasma cells were similar in WT and T-bet$^{-/-}$ mice at both time points studied (figure 5.29A) and the majority of these plasma cells had switched to IgG1 by day 14 p.i (figure 5.29B). As plasma cell class-switching was largely normal in T-bet$^{-/-}$ mice, the antibody response was analysed (figure 5.30A-D). Apart from the expected absence of IgG2a antibody in T-bet$^{-/-}$ sera (figure 5.30D), and a marginal delay in reaching peak IgG1 titres (figure 5.30B), antibody production was similar in WT and T-bet$^{-/-}$ mice after primary alum-CGG immunisation. Thus limited, distinct defects were observed in the development of B cell responses to alum-CGG in T-bet$^{-/-}$ mice.

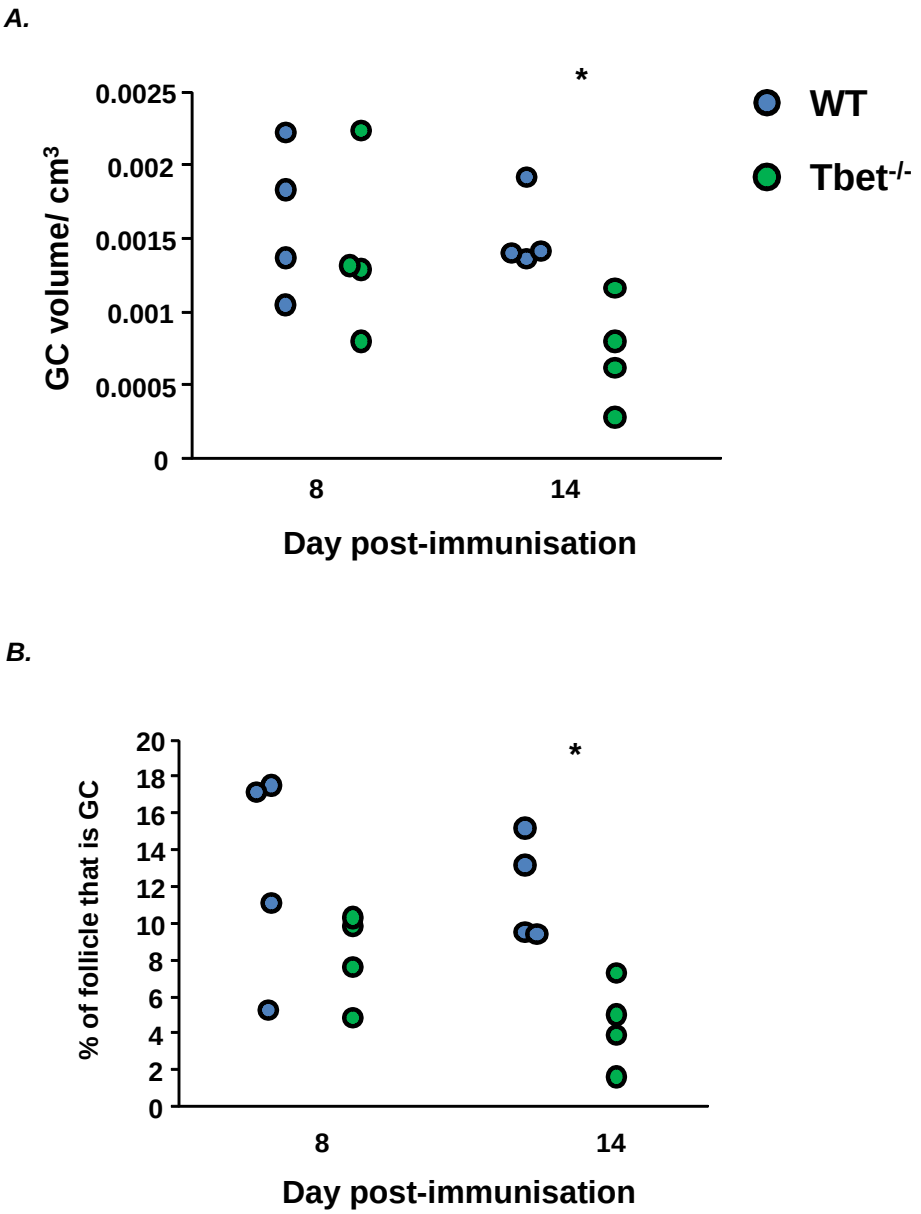

Figure 5.28. Splenic GC volume and size in WT and T-bet$^{-/-}$ mice after alum-CGG immunisation. WT and T-bet$^{-/-}$ mice were immunised with 50µg alum-CGG. The ***A*****,** volume of germinal centre per spleen and ***B*****,** proportion of follicle that is germinal centre was quantified by histology at the indicated time points after immunisation. One point represents one mouse. * $p \leq 0.05$

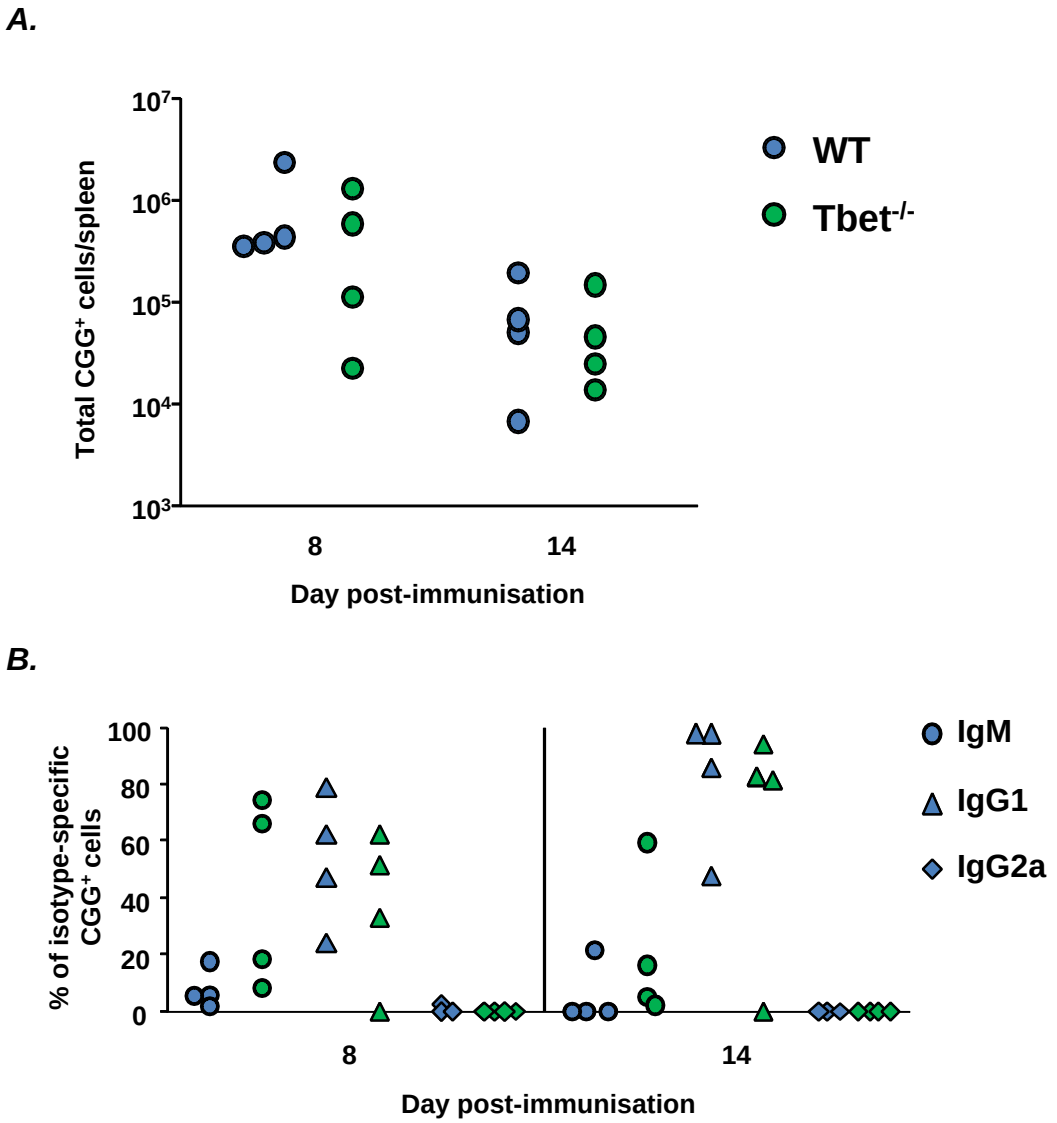

Figure 5.29. Switched and non-switched CGG^+ plasma cells in WT and T-$bet^{-/-}$ mice after alum-CGG immunisation. WT and T-$bet^{-/-}$ mice were immunised with 50µg alum-CGG. The ***A*,** total number of CGG^+ plasma cells and ***B*,** proportion of CGG^+ plasma cells that are IgM^+, $IgG1^+$ and $IgG2a^+$ were quantified by histology at the indicated time points after immunisation. One point represents one mouse.

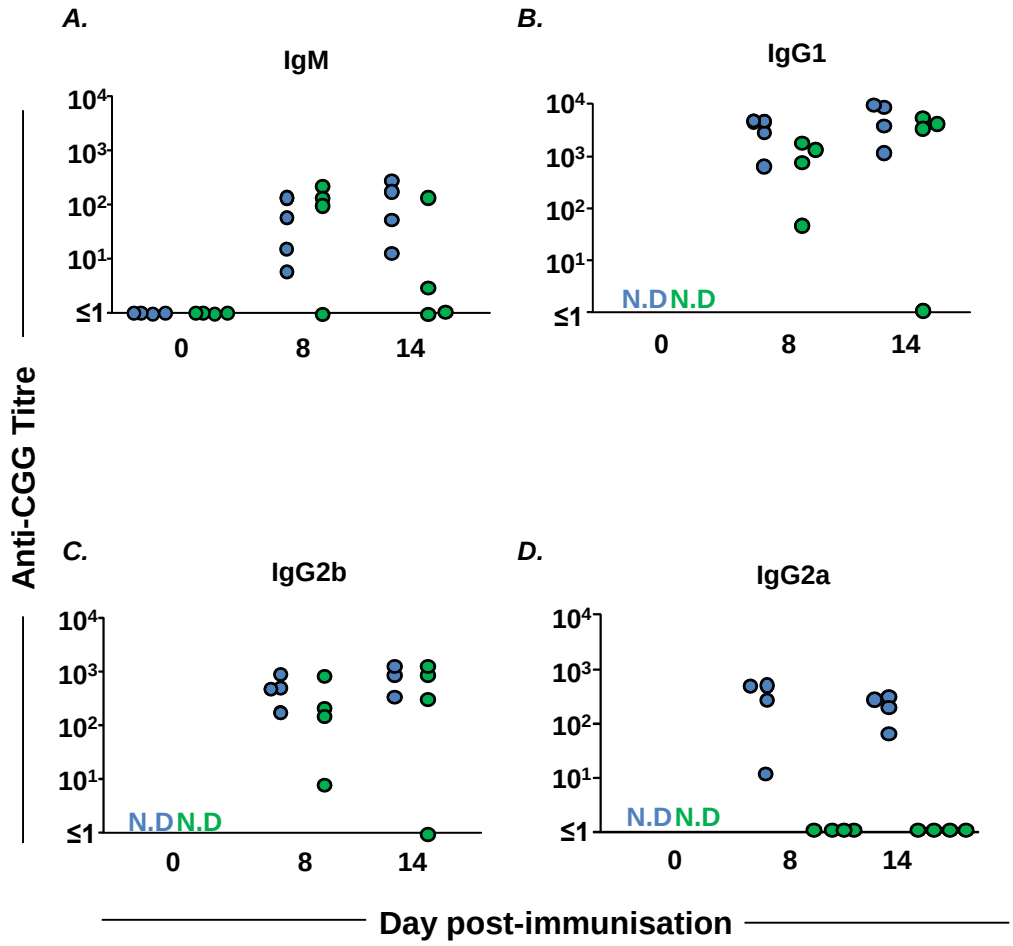

Figure 5.30. CGG-specific antibody titres before after primary alum-CGG immunisation. WT and T-bet$^{-/-}$ mice were immunised with 50µg of alum-CGG or remained non-immunised as controls. CGG-specific ***A,*** IgM, ***B*****,** IgG1, ***C****,* IgG2b and ***D,*** IgG2a serum antibody was quantified in all mice before and at the times specified p.i. One point represents one mouse. Data are representative of ≥ 2 experiments giving similar results.

5.2.2.6 GC development is impaired but class-switching is intact in T-bet-/- mice during the memory response to alum-CGG

To assess whether the defect in GC development was corrected during the memory response, WT and T-bet$^{-/-}$ mice were immunised with alum-CGG for 35days and boosted with soluble NP-CGG for a further 4 days. Assessment of GC in the spleen by histology revealed that GC development was still markedly impaired in T-bet$^{-/-}$ mice, with both the total splenic GC volume (figure 5.31A) and the proportion of follicle occupied by GC (figure 5.31B) being reduced below that of WT mice ($p \leq 0.05$). Despite this, the number of CGG^{+} plasma cells was similar in the spleens WT and T-bet$^{-/-}$ mice after the second immunisation (figure 5.32A) and the ability to class-switch to IgG1 was not compromised in T-bet$^{-/-}$ mice (figure 5.32B). Consistent with a defect in the initiation of the immune response, the total number of NP-specific plasma cells in the spleen was significantly lower in T-bet$^{-/-}$ mice when compared to WT mice (figure 5.32A). Despite the vast majority of NP-specific cells being IgM^{+} at this early stage, a small proportion of these cells had switched to IgG1 in WT mice (figure 5.32C), however an IgG1 switched response to NP was almost completely absent in T-bet$^{-/-}$ mice, consistent with a delay in the initiation of class-switching. Antibody titres were next assessed by ELISA, showing that despite the near absence of splenic GC, T-bet$^{-/-}$ mice were able to produce comparable titres of class-switched antibody to WT mice, with the obvious exception of IgG2a (figure 5.33A-D). NP-specific IgM was also produced in similar quantities in the two groups (figure 5.33E) and no NP-specific class-switched antibody was detected in either WT or T-bet$^{-/-}$ mice (data not shown).

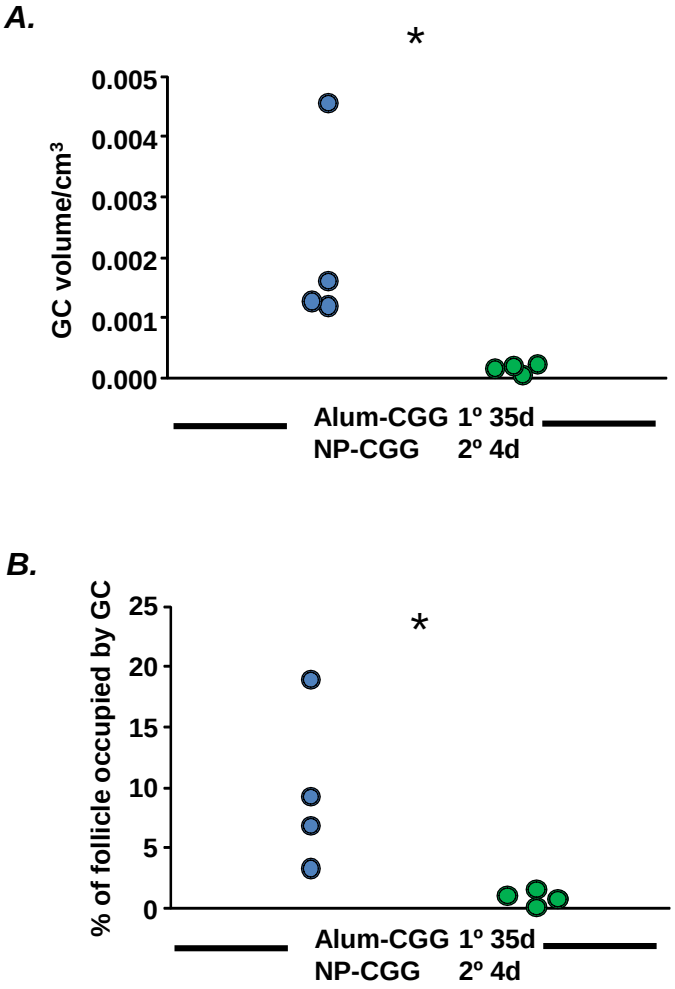

Figure 5.31. Splenic GC size and volume in WT and T-bet$^{-/-}$ mice after alum-CGG immunisation and NP-CGG boost. WT and T-bet$^{-/-}$ mice were immunised with 50µg alum-CGG for 35 days and boosted with 20µg sNP-CGG for 4 days. The ***A*****,** volume of GC per spleen and ***B*****,** proportion of follicle that is GC was quantified by histology. One point represents one mouse. * $p \leq 0.05$

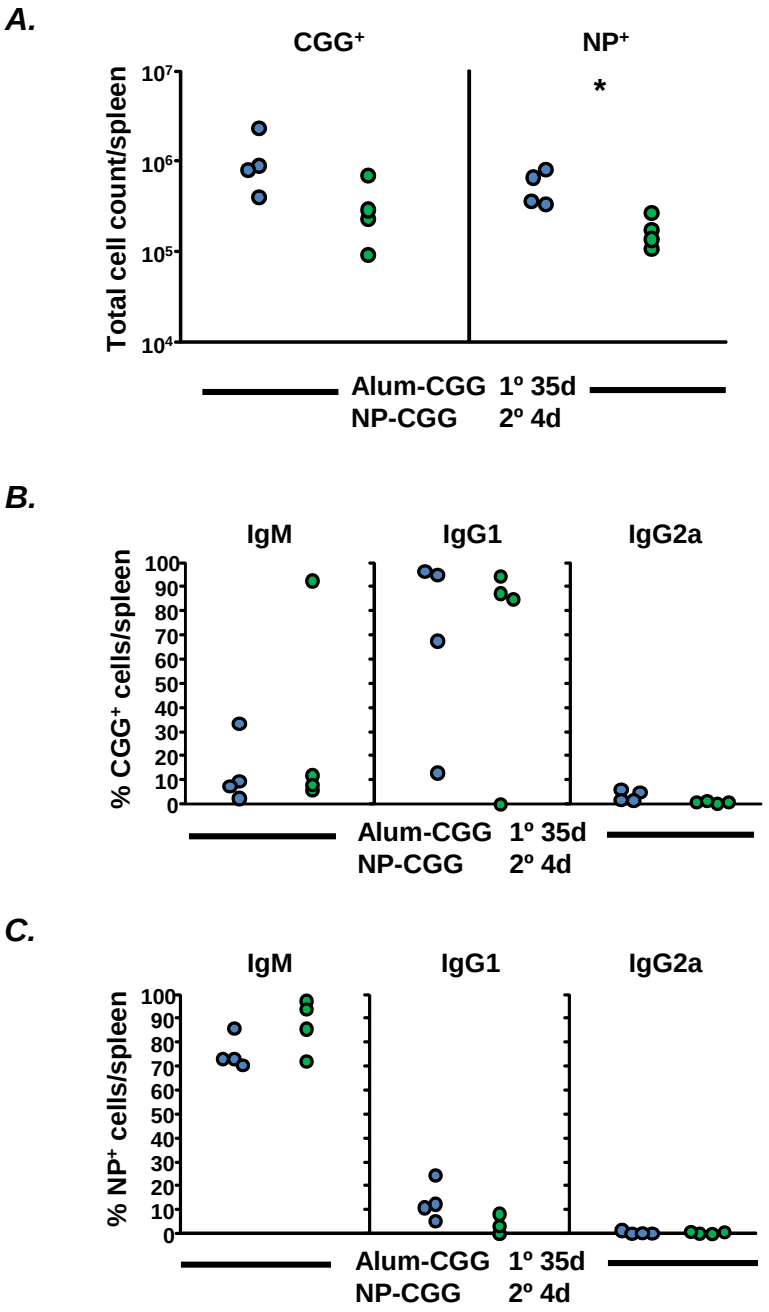

Figure 5.32. CGG and NP specific plasma cells in WT and T-bet$^{-/-}$ spleens after alum-CGG immunisation and NP-CGG boost. WT and T-bet$^{-/-}$ mice were immunised with alum-CGG for 35 days and boosted with sNP-CGG for 4 days. ***A***. Total number of splenic CGG^{+} (left panel) and NP^{+} plasma cells (right panel) as quantified by histology. ***B.*** The proportion of CGG^{+} plasma cells and ***C,*** NP^{+} plasma cells that are IgM (left panel), IgG1 (middle panel) and IgG2a (right panel). One point represents one mouse. Data are represeentative of 2 experiments giving similar results.

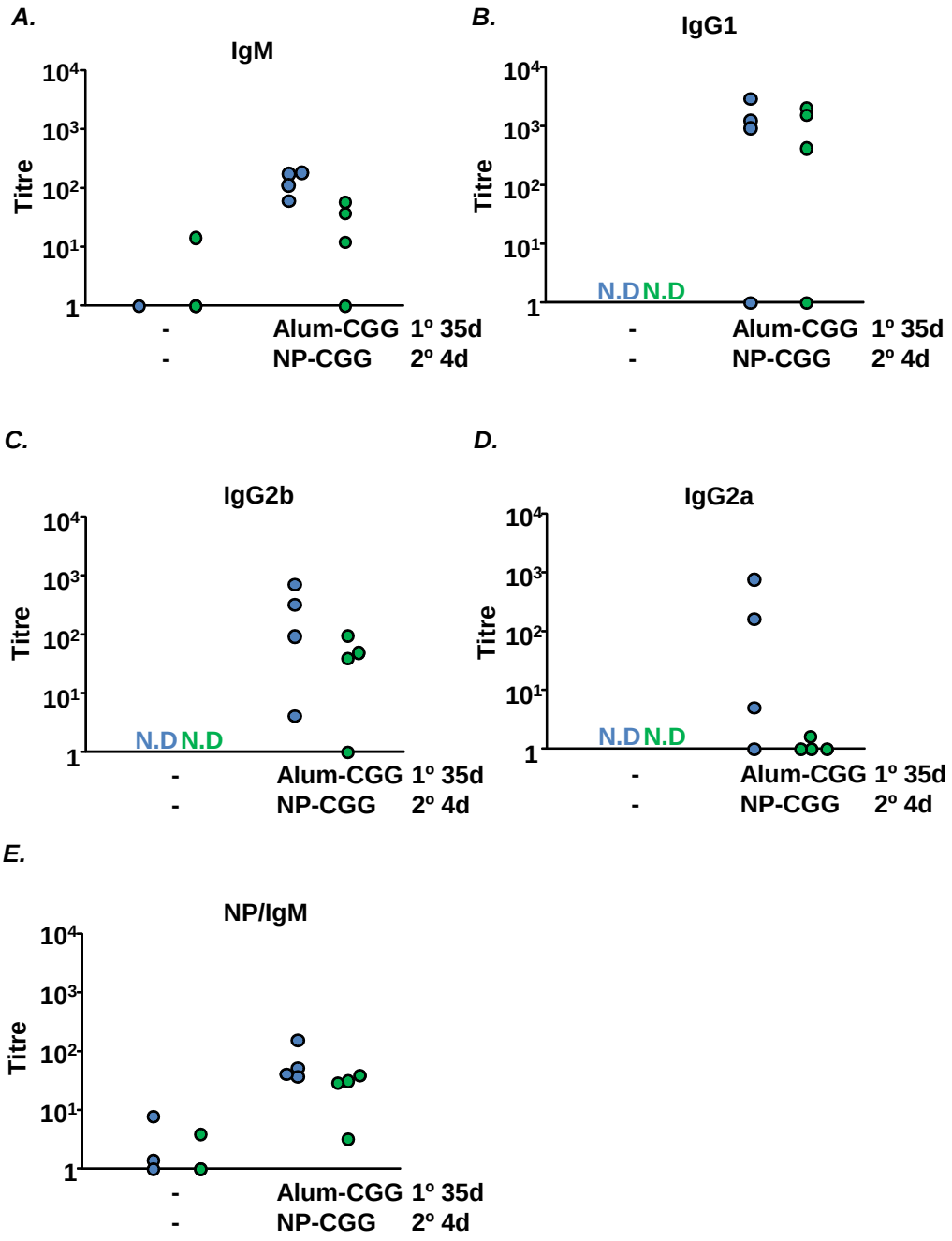

Figure 5.33. Anti-CGG and NP antibody titres in WT and T-bet$^{-/-}$ spleens after alum-CGG immunisation and NP-CGG boost. WT and T-bet$^{-/-}$ mice were immunised with alum-CGG for 35 days and boosted with soluble NP-CGG for 4 days. Anti-CGG serum ***A***, IgM ***B,*** IgG1, ***C,*** IgG2b and ***D,*** IgG2a and ***E,*** anti-NP antibody titres were measured after the four day boost. One point represents one mouse. Data are representative of 2 experiments giving similar results.

Thus, the reduced antibody titres in T-bet$^{-/-}$ mice following immunisation with Th2 antigens are most prominent during the primary response and may be context and/or antigen dependent. The recovery of antibody titres during the memory response to sFliC and following the provision of antigen-specific T cells, suggests a possible defect in the provision of T cell help, which could relate to a delay in T cell priming or subsequent T-B interactions. Overall, the studies carried out in this chapter highlight a role for T-bet in multiple facets of the antibody response, extending beyond the control of Th1 cell differentiation and subsequent antibody class-switching to IgG2a.

5.3 Discussion

The global transcriptional regulator of Th1-differentiation, T-bet, promotes IFNγ secretion by T cells (72) and Ig class switching to IgG2a (83,291-293). *In vitro* studies show that T-bet expression in B cells can be induced by direct antigen stimulation (293) or via indirect mechanisms such as IFNγ (83,293), leading to IgG2a and IgG2b production by B cells. Previously, T-bet$^{-/-}$ mice failed to produce IgG2a-class switched antibody in response to STm infection, however the importance of T and B cell-expressed T-bet for this response was not addressed (79). We postulated that switching to IgG2a during STm infection would require T cell- and B cell-intrinsic T-bet expression, whilst IgG2b production would be T-bet independent.

Here we report that T cell expressed T-bet is dispensable for IgG2a class-switching during STm infection, whilst B cell-intrinsic T-bet is essential for this response. Conversely, T-bet expression is not required for IgG2b production in this model. A second, surprising finding is the selective role of T-bet in the antibody response to Th2 antigens. T-bet$^{-/-}$ mice immunised with sFliC produced lower levels of IgG1 and IgG2b antibody than WT mice, a defect that was corrected upon the provision of antigen specific T cells. This defect may be antigen specific, as immunisation with alum-CGG revealed only modest defects in the B cell response, mainly relating to GC development. These data emphasise the multiple roles of T-bet within the immune system and highlight its involvement in antibody responses on multiple levels.

5.3.1 T-bet-mediated regulation of antibody responses to STm infection

Consistent with a previous report (79) our data confirm that T-bet expressed in T cells is essential for the clearance of STm infection. This failure to clear occurred despite $CD4^+$ T cell activation, as assessed by CD62L loss, which we have previously shown to be a good marker of T cell activation in this model (203). T-$bet^{-/-}$ mice in the current study demonstrated normal levels of T cell activation, however in the T-$bet^{-/-TCELL}$ chimeras, proportions of activated cells were lower than in T-$bet^{+/+TCELL}$ mice. The reason for this discrepancy is unclear, however may relate to an ability of other T-$bet^{+/+}$ cells to regulate T-$bet^{-/-}$ T cells. Despite this difference, T-$bet^{-/-}$ T cells from the chimeras did activate above background levels during infection. Equal activation and proliferation capabilities have previously been demonstrated in antigen-specific, T-bet-deficient T cells during STm infection (79). As such, the failure to clear STm infection has been attributed to a failure of T-$bet^{-/-}$ T cells to secrete high levels of IFNγ (79). Consistent with this, we observed significantly lower levels of IFNγ expression in T cells from T-$bet^{-/-TCELL}$ chimeras when compared to those from T-$bet^{+/+TCELL}$ chimeras, and recently published data from our group shows that T-$bet^{-/-}$ T cells do not secrete IFNγ (78).

As IgG2b production is not defective in T-$bet^{-/-}$ mice, it suggests that switching to this isotype during STm infection is not IFNγ-dependent. Total splenocytes from STm infected T-$bet^{-/-}$ mice produce little or no IFNγ (79), consistent with T-bet-mediated IFNγ production by cells such as NK cells (72) and DC (81). It is likely that CSR to IgG2b can be controlled by alternative mechanisms, such as transforming growth factor (TGF)-β, which has previously been shown to directly regulate IgG2b class switching (296). It is possible that TGF-β is produced during STm infection to regulate the Th1-driven

inflammatory response, especially during the latter stages of infection. This immunomodulatory function of TGF-β has previously been shown to dampen disease in murine EAE (297).

As IFNγ production by T cells is controlled by T-bet (72,76) we predicted that T-bet deficient T cells would be unable to induce IgG2a switching in B cells. IFNγ can up-regulate T-bet in B cells, leading to IgG2a production via a STAT 1 mediated pathway (83,293). However, no defect in $IgG2a^{+}$ plasma cell induction or antibody production was observed in $T\text{-}bet^{-/-TCELL}$ chimeras. These data illustrate that the critical T cell signals supporting class-switching during STm infection do not include T-bet and IFNγ. However, IFNγ produced by a non-T cell may be important for IgG2a switching, as the lack of IgG2a production in $T\text{-}bet^{-/-}$ mice is corrected in $T\text{-}bet^{-/-TCELL}$ chimeras, where a lack of T-bet and subsequent IFNγ production is restricted to the T cell compartment. Establishing a direct link between IFNγ production and IgG2a class switching during STm can be achieved using $IFN\gamma^{-/-}$ mice, a colony that is now established at the The University of Birmingham. The data presented here suggest that T cells may act to 'licence' to IgG2a switching in B cells, by providing other important signals such as CD40-CD40L interaction, rather than by directly instigating the IgG2a CSR transcriptional programme.

Aside from IFNγ, other factors are able to drive IgG2a production by B cells. The $T\text{-}bet^{-/-BCELL}$ chimeras illustrate that IgG2a switching is dependent, almost entirely, upon B cell intrinsic T-bet expression. Type 1 interferons can induce IgG2a switching in B cells (83), however this occurs in a T-bet independent manner. Whilst there may be some T-bet independent IgG2a switching occurring at day 7 of infection, when some IgG2a class-

switching is detectable in T-bet$^{-/-BCELL}$ chimeras, it is unlikely to play a role during the later response.

A pathway that has received some recent attention is the CpG-induced induction of T-bet in B cells (293) and subsequent IgG2a production (293,294). This pathway operates via direct TLR 9 ligation on the B cell, leading to T-bet expression via a MyD88-dependent, STAT-1 independent mechanism. Supporting a TLR-mediated mechanism is previous work in mice with a B cell-intrinsic defect in MyD88. These mice are unable to produce IgG2a during STm infection, whilst IgG2b production is only moderately affected (224). However, a loss of B cell-intrinsic MyD88 also attenuated IFNγ production by T cells and this was held at least partly accountable for the lack of IgG2a switched antibody in these mice (224). In contrast, we observed normal levels of IFNγ expression in T cells from T-bet$^{-/-BCELL}$ chimeras. Although protein levels were not assessed here, the mice were able to effectively clear STm infection, indicating that IFNγ production by T cells is not compromised by T-bet loss in B cells. This does not discount the possibility that IgG2a class switching in our model is controlled by a TLR-MyD88-T-bet pathway, but infers that a loss of MyD88 in B cells negatively affects multiple B cell functions. For example, recent evidence shows that *Salmonella* antigens can induce shedding of CD62L on B cells in a MyD88-dependent, TLR9-independent fashion (298). This shedding directs B cell traffic to the spleen and away from lymph nodes, a mechanism that may allow programming of the T cell response described previously by Barr and colleagues (224). It would be interesting to assess antibody responses in TLR 9-deficient mice during STm infection, to assess for aberrations in IgG2a class-switching. Furthermore, an analysis of STAT 1 phosphorylation in STm-exposed WT B cells may give an indication of the

mechanisms that regulate IgG2a class switching via T-bet. Whilst IFNγ-mediated T-bet induction and IgG2a production operates through STAT 1, the CpG-TLR9 pathway is STAT 1 independent (293).

A second interesting observation made during this work was the induction of a modest, yet apparent, IgG2a plasmablast response by day 7 in T-bet$^{-/-BCELL}$ mice, which had completely disappeared by day 35 p.i. Whilst there may be some T-bet independent mechanisms involved in early switching (83) this also questions whether T-bet in B cells is differentially involved in EF versus GC IgG2a responses. The plasma cells produced at day 7 of infection arise entirely from the EF pathway of growth, and these are likely to be short lived and therefore absent by day 35 p.i, when GC contribute to the plasma cell response. T-bet clearly contributes to EF IgG2a switching early during STm infection, as plasma cell numbers and γ2a-switch transcripts were reduced in T-bet$^{-/-BCELL}$ mice at this point when compared to T-bet$^{+/+}$ B cells. However, the complete absence of IgG2a switching at day 35 p.i suggests a more specific defect in GC IgG2a switching. In the current study T-bet$^{-/-BCELL}$ mice exhibit no obvious deficiency in GC development, and whilst not examined in detail, Tfh cells were present within these structures. This contrasts with work carried out in MyD88$^{-/-BCELL}$ mice, where defects in GC development coincide with defective IgG2a antibody responses (224). It is possible that T-bet is important for switching to IgG2a within the GC, rather than in GC development. On the other hand, the observed absence of γ2a-germline switch transcripts in B cells from T-bet$^{-/-BCELL}$ mice suggests that the defect in class-switching occur at the T-B border, prior to GC entry (56). In order to examine this further, a kinetic series of studies would be required to closely assess the timing of IgG2a switching-loss. An in depth analysis of T-bet expression in WT B cells at each stage of

STm infection would also help to ascertain when T-bet becomes important for class-switching.

Thus, whilst it is clear that T-bet in B cells drives class-switching to IgG2a during STm, the exact signals that facilitate this process have not yet been identified. The PCR data provide some information as to the timing of the defect and we can likely eliminate T-cell-produced IFNγ as a critical mediator of this response. However, further experiments using gene-deficient mice, as well as a closer analysis of the genes that regulate T-bet induction in B cells, will be key to establishing the exact mechanism driving this response.

5.3.2 T-bet mediated control of antibody responses to non-viable protein antigen

The second key finding of this chapter is that a loss of T-bet selectively impairs antibody responses to Th2 antigens, during which IgG1 production is dominant. Previously, an overproduction of Th2-associated switched antibody subclasses has been reported in mice lacking T-bet (83) or IFNγ (299), however our results suggest that the opposite occurs, in an antigen specific manner. Primary immunisation with sFliC resulted in defective switched antibody responses to IgG1 and IgG2b. This defect was not recapitulated to the same degree when mice were immunised with alum-CGG, despite some defects in GC maintenance and a marginal delay in switched plasma cell induction. As expected, no IgG2a was produced at any time in T-bet$^{-/-}$ mice, arguing against suggestions that T-bet is dispensable for IgG2a switching to T-D antigens, but not for IgG2a switching to T-I antigens (291). Of note, the transfer of T-bet-expressing SM1 T cells into T-bet$^{-/-}$ mice was

not sufficient to restore the IgG2a response to sFliC, supporting the B cell-intrinsic control of IgG2a switching observed during STm infection.

The defect in class switching following primary sFliC immunisation was not restricted to IgG1 and the immunisation regimes used here and previously (83,291) show that T-bet$^{-/-}$ mice can produce this subclass of antibody. Moreover, this defect recovered substantially during the memory response, suggesting that readily available T cell help can restore switching, although switched memory B cells with higher affinity for the antigen may also contribute to these heightened responses. Supporting the T cell help hypothesis was the recovery of the antibody response following antigen-specific SM1 T cell transfer and primary sFliC immunisation. It is therefore unlikely that T-bet directly regulates transcription of the IgG1 gene, but rather that it exerts indirect effects on GC responses via an alternative mechanism. One possibility is a defect in T cell priming, due to a loss of T-bet in DC. Transgenic T cells primed with T-bet-deficient DC produce less IFNγ than those primed with WT DC (81). In an arthritis model, antigen-loaded T-bet$^{-/-}$ DC failed to effectively prime T cells *in vivo*, resulting in a lack of IFNγ, IL4 and IL2 production by T cells. This was not due a failure of DC to accumulate in LN or up-regulate expression of the chemokine receptors that facilitate this process (300). Whilst the priming defect of T-bet$^{-/-}$ DC has been linked mainly to defects in initiating Th1 responses, it has been postulated that T-bet regulates the transcription of multiple genes in DC that are required for optimal T cell priming (81). As such, this function of T-bet in DC may not be restricted to the Th1 programme. Arguing against this is recent work form our lab, showing that T cells from T-bet$^{-/-}$ mice immunised with sFliC express similar levels of IL4 mRNA to WT mice at day 4 p.i (78).

An alternative mechanism by which T-bet could regulate antibody responses relates to its proposed role in $CD4^+$ T cell trafficking into inflammatory sites. T-bet has been shown to modulate T cell binding to P-selectin and expression of the chemokine receptor CXCR3 (284). Whilst these molecules and chemokines are largely related to Th1 responses, the dynamics of Th2 responses have not been studied in depth in T-$bet^{-/-}$ mice. It is possible that the migration of T cells is also altered in T-$bet^{-/-}$ mice in response to Th2 antigens, resulting in delayed T-B interactions and sub-optimal antibody responses. This being said, defects in T cell priming or trafficking would be likely to result in impaired antibody production in T-$bet^{-/-}$ mice immunised with alum-CGG as well as sFliC. One difference between the primary response to sFliC and that to alum-CGG, is the parallel induction of an EF and GC plasma cell response in the latter, with the former producing antibody solely via the GC pathway. GC maintenance was impaired in T-bet mice following alum-CGG immunisation and GC were virtually absent following an NP-CGG boost. However, no defects in class-switched antibody production were observed, suggesting that EF responses are sufficient to produce high levels of IgG1 antibody in this system and may be less vulnerable to the loss of T-bet than are GC responses. Aberrant T cell migration within GC could lead to altered GC responses. Indeed, there may also be a role for T-bet in B cell migration to or within the GC. Analysis of chemokines and chemokine receptors in T-$bet^{-/-}$ mice during the various responses may help to dissect some of the mechanisms at play here.

A second consideration, relating to the antigen specificity of the IgG1 defect, is the difference in immune priming mechanisms during sFliC and alum-CGG responses. The understanding of how aluminium adjuvants exert their stimulatory effects upon the

immune system is still incomplete (301), however there is evidence to suggest that it is not TLR mediated (302,303). Whilst, there are probably some shared features in the two responses, such as activation of the inflammasome through NLR (304,305) bacterial flagellin also utilizes TLR5, which is integral for its stimulation of the innate immune system (306). Whilst humoral immunity elicited by flagellin may not rely entirely upon TLR5, mice lacking TLR5 show significant decreases in IgG1 production during the primary response, as do MyD88$^{-/-}$ mice (307). As discussed, T-bet is linked to TLR signalling pathways (293) and an absence of T-bet in DC has also been reported to diminish the adjuvant activity of CpG oligodeoxynucleotides (288). As such, T-bet may be linked to other TLR pathways, such as TLR 5, and enhance the adjuvant activity of proteins that stimulate the immune system in this way. Assessing T-bet expression in DC, for example, stimulated with various TLR agonists, could help to establish a link between T-bet and TLR signalling pathways.

To conclude, a novel role for T-bet in switched antibody responses to IgG1 has been identified here. Whilst this is unlikely to reflect a direct link between T-bet and IgG1-gene transcription, it may indicate a role for T-bet in DC following sFliC immunisation, or in chemokine regulation and migration in T or B cells. Overall, these data emphasise the multifunctional role of T-bet within the immune system and highlight its ability to regulate antibody responses on several different levels.

CHAPTER 6: GENERAL DISCUSSION

The key focus of this thesis was to identify the factors that regulate B cell responses to STm, with particular emphasis on the GC reaction, EF responses and mechanisms of antibody class-switching. Initial experiments assessed the role of CD31 in B cell responses during primary infection with STm and following vaccination, whilst subsequent chapters addressed how cytokines associated with Th2 responses, and the transcription factor T-bet, influence B cell responses in this model. The data presented herein highlight two key points; firstly, EF and GC responses to STm infection are regulated by different mechanisms and secondly, there are some, previously unappreciated similarities in the way that Th1 and Th2 B cell responses are controlled.

A number of the gene-deficient mice studied here, including $IL4^{-/-}$, $IL13^{-/-}$, $IL4R\alpha^{-/-}$ and $IL6^{-/-}$ mice, displayed defects in GC development, yet a concomitant suppression of the EF plasma cell response was not observed. Previous studies have reported differential control of EF and GC plasma cell generation in $IL6^{-/-}$ (121,124) and $IL4R\alpha^{-/-}$ (94) mice. Furthermore, cytokine expression levels vary at different sites within the same tissue (271), indicating that cytokines are influential at discrete microanatomical sites within SLO. Previous data have associated IL4 and IL13 most closely with GC reactions, as opposed to EF class-switching, possibly explaining why the defect reported here was specific to GC development. Mice deficient in either of these cytokines display no defect in the production of early class-switched $IgG1^{+}$ EF plasma cells (93), however GC are smaller in $IL4R\alpha^{-/-}$ mice at a point when B cells are selected in GC by T cells (94). Furthermore, IL4-expressing Tfh cells are commonly found within the GC and are able to facilitate class-

switching (126,260,308), whilst IFNγ expressing Tfh cells are less frequent within this niche. Whilst this may reflect the antigens used in these studies, it cannot be excluded that IL4 is a signature cytokine produced by Tfh cells. Indeed, disruption of the PI3K signalling pathway, which is essential for Tfh function, results in attenuated IL21 and IL4 transcription (117). As such, IL4 may be important for GC B cell selection to a range of TD antigens, whilst being dispensable for the EF plasma cell development. One important feature of the $IL4^{-/-}$ and $IL13^{-/-}$ data presented here, was the lack of a discernible augmentation of the IgG2a or IgG2b response. A reason for this may be that increases in IgG2a production only become apparent during recall responses, as seen in previous studies in $IL4^{-/-}$ and $IL4^{-/-}IL13^{-/-}$ double deficient mice, in response to alum-ppt proteins (91,95).

The marked defect in GC development in IL6 deficient mice probably reflects a different mechanism of action when compared to IL4 and IL13. We considered the possibility that the FDC stromal network within the GC may provide the IL6 required to form effective GC responses to STm, as has been shown previously using model antigens (104). This would explain why GC, but not EF plasma cell responses were defective in $IL6^{-/-}$ mice. Unfortunately, the chimera data presented here did not provide an unequivocal answer regarding the source of IL6 that is important for driving such reactions. Nevertheless, it shows that there is redundancy in the sources of IL6 during this response and our findings support the pleiotropic functions of IL6 within the immune system, as well the fact that numerous cells can produce and respond to IL6 (276). This contrasts with the expression pattern and purported roles of IL4 and IL13, which are less diverse that that of IL6.

IL6$^{-/-}$ mice produced very low titres of class-switched antibody at day 42 p.i, which can probably be explained by the near absence of GC in IL6$^{-/-}$ mice at this time point. When GC did appear in IL6$^{-/-}$ mice, so did high titres of class-switched antibody. This suggests that in this model, IL6 does not control class-switching *per se*, but rather in the absence of IL6, the defect in GC formation indirectly results in a failure to optimise class-switched antibody production. These data emphasise the requisite role of the GC in driving effective class-switched antibody responses to STm, as shown during the original characterisation of this model (70).

Whilst necessary for effective antibody production, the presence of GC structures does not necessarily guarantee the production of class-switched antibody during STm infection, as highlighted by the T-bet$^{-/-BCELL}$ chimeras and CD31$^{-/-}$ mice. Little or no class-switched antibody was produced by CD31$^{-/-}$ mice in response to STm, despite the presence of GC in the spleen throughout infection. However, owing to the abundance of GC in the spleens of uninfected CD31$^{-/-}$ mice, these GC were unlikely to be STm specific. It is unfortunate that circumstances did not allow us to examine the defects in CD31$^{-/-}$ mice further. T-bet$^{-/-BCELL}$ mice were also able to form GC in response to STm infection and Tfh cells could be clearly visualised within these structures, however no IgG2a^{+} class-switching was observed at day 35 p.i. The GC reactions that developed in these mice were probably supporting class-switching to other isotypes, such as IgG2b, which was unaltered in the absence of T-bet. The absence of IgG2a switch transcripts in T-bet$^{-/-BCELL}$ mice suggests that this defect occurred at the T-B border, prior to GC entry (56), but this doesn't rule out the possibility that T-bet in B cells is also required for class-switching to IgG2a within the GC.

There was some early, EF IgG2a class-switching that was independent of T-bet in B cells, however this was lost by day 35 p.i. It is possible that different subsets of B cells respond at discrete stages of STm infection, and class-switching may be differentially regulated in each cell type. Data from our lab shows that the early EF IgM response to STm infection is mediated by B1b cells and is T-I (13). Whilst class-switching during STm is T-D (70), some of the switched cells may arise from B1b cells, in which class-switching could be differentially regulated. For example, type 1 interferons can induce IgG2a class switching in the absence of T-bet (83). Collectively, these data highlight the different signals that control class-switch transcript up-regulation, facilitate GC entry and drive EF reactions during STm infection.

A second interesting finding from the work described in this thesis is that similarities exist in the factors that regulate Th1 and Th2 B cell responses. Cytokines classically associated with Th2 responses influenced GC development during STm infection. Although marginal, a defect in GC size and volume was apparent in $IL4^{-/-}$, $IL13^{-/-}$, $IL4R\alpha^{-/-}$ mice, data that are strengthened by the similar extent of the defect across all groups. This reflects a generic role for IL4 and IL13 in GC reactions to Th1 and Th2 antigens, possible reasons for which are outlined above. Whilst not a signature cytokine of the Th2 response, IL6 is thought to direct T cells towards a Th2 phenotype (100,102,309) and defects in GC formation in $IL6^{-/-}$ mice have been reported following immunisation with model Th2 antigens (103,104). Our finding of impaired GC development in $IL6^{-/-}$ mice during infection with a Th1 antigen, again reflects similarities in GC development and function during Th1 and Th2 responses. Possibly the most surprising finding reported in this context was the selective role of T-bet in optimal IgG1 responses to Th2 antigens. The correction of the IgG1 defect during the

memory response to FliC, and upon provision of antigen specific T cells, suggests a possible defect in the ability of T cells to provide efficient help to B cells. On the other hand, GC development did not recover during the memory response to alum-CGG, despite an ability to produce high titres of class-switched antibody. This could highlight a role for T-bet in the expansion or maintenance of GC reactions and may again reflect differences in the regulation of EF- and GC-derived antibody responses.

5.1 Future Directions

The data presented in this thesis identify several areas that warrant further investigation. For the reasons discussed in chapter 3, the CD31 B cell project was put on hold. Without identifying the reason for our incongruent findings in the original $CD31^{-/-}$ strain and the rederived $PECAM^{-/-}$ strain, further investigation into the mechanisms surrounding our observations were not justified, scientifically, financially or strategically .

5.1.1 T-bet mediated control of antibody class-switching

Two avenues can be pursued with regard to the T-bet data, one concerning the signals that drive B cell intrinsic, T-bet-mediated switching to IgG2a, and the other relating to the role of T-bet in optimal IgG1 antibody responses. Initially, it will be interesting to ascertain whether a link exists between IFNγ, T-bet and IgG2a class-switching during STm infection. A colony of $IFN\gamma^{-/-}$ mice has recently been established by our group at the University of Birmingham, allowing this question to be addressed. Some very preliminary data suggest that early, splenic IgG2a class-switching is dependent upon IFNγ, however

these data require confirmation and extension to later time points, to identify when IFNγ might be involved. If IFNγ is required for IgG2a class-switching, a link between IFNγ and T-bet in B cells would need to be established. Whilst IFNγ and T-bet may both be required for class-switching to IgG2a during STm infection, these signals may be independent of one another. This can be addressed by looking at T-bet expression in B cells in IFNγ$^{-/-}$ mice during infection.

In the absence of a link between T-bet and IFNγ, other factors that control T-bet transcription would need to be considered. Using STm-exposed B cells to measure the expression of transcription factors operating upstream of T-bet, may give some clues as to the mechanism of T-bet induction. For example, IFNγ-mediated T-bet induction and IgG2a production operates through STAT-1, whilst other pathways of T-bet induction in B cells, such as the CpG-TLR9 pathway, are STAT 1 independent (293). If phosphorylation of STAT-1 does not occur in STm-exposed WT cells, this may be indicative of TLR9-mediated IgG2a class-switching. It would be interesting to establish a line of TLR 9$^{-/-}$ mice at The University of Birmingham, in order to assess this possibility further.

It would also be informative to extend the STAT-1 analysis to sFliC-exposed B cells, as the low level of IgG2a produced in this system appears to be independent of T-bet in T cells, and is therefore likely to be controlled by B cell intrinsic T-bet. Assessing the transcription factors in the two models may uncover different pathways of T-bet mediated IgG2a production in response to the same antigen, presented in a different context. The defect in IgG1 and IgG2b class-switching in T-bet$^{-/-}$ mice immunised with Th2 antigen sFliC also warrants further investigation. It will be necessary to establish whether there is a

defect in T-B interaction in the spleen, either at the T-B border, or within GC. It would be informative in this regard, to measure the expression of γ1 and γ2b-germline switch transcripts in purified WT and T-bet$^{-/-}$ B cells, at various time points following primary immunisation with sFliC, in order to gain a clear understanding of when class-switching is initiated in T-bet$^{-/-}$ B cells in this system. The defect in IgG2b production in this system is intriguing, as IgG2b production was not defective in T-bet$^{-/-}$ mice infected with STm. An analysis of chemokines and chemokine receptors in T and B cells in the two models may also be informative, as there may be defects in migration that affect EF plasma cell or GC formation, expansion or function.

5.1.2 IL6-mediated control of antibody class-switching

Although interesting, the defect in GC formation in IL4-, IL13- and IL4Rα-deficient mice did not impact upon class-switched antibody production, and was therefore not pursued here. However, it would be interesting to pursue the IL6 project and determine exactly where IL6 exerts its effects. Firstly, it would be informative to carry out an extensive analysis of the cell populations that up-regulate or acquire the IL6R during STm infection, at a time when GC are forming. This would allow identification of the populations that could respond to IL6 at this time point, and the elimination of others. I would also like to assess the expression of chemokine receptors on pre-GC T and B cells, to in order to identify whether they may be defects in the responsiveness of these cells to chemokine gradients, that prevent their entry into GC. Further characterisation of the Tfh cells, or pre-GC Tfh-cells in IL6$^{-/-}$ spleen during the STm response is also required, in order to further

understand whether productive T-B interactions are taking place, and whether these interactions facilitate EF growth rather than GC entry.

5.3 Summary and final conclusions

This thesis provides evidence that the signalling, adhesion receptor CD31, the cytokines IL4, IL13 and IL6, and the transcription factor T-bet, all have selective roles in regulating facets of the B cell response to STm infection. T-bet in B cells is required for initiating IgG2a switch-transcript induction, a failure of which impacts upon both EF and GC IgG2a class-switching, whilst IgG2b production is independent of T-bet expression. T-bet can also modify Th2 antibody responses, in an antigen specific manner. Following T-B interaction, IL6 arising from either haematopoietic or radiation-resistant cells is required for the formation of GC during STm infection, but is less important for the development of an EF plasma cell response. An absence of IL6 has a negative effect upon all sub-classes of antibody, as does a loss of CD31. Upon entry into the GC, there may be a role for IL4 and IL13 signalling in B cell selection, as evidenced by the smaller, less abundant GC in the absence of these cytokines.

Therefore, B cell immunity to STm infection requires the coordinated actions of multiple signals, each working to optimise a distinct aspect of the B cell response. Furthermore, whilst the existence of ‘typical’ T-D antibody responses to Th1 and Th2 antigens cannot be disputed, this work emphasises that divergence from these simplified concepts is inevitable within the complexities of the immune system.

APPENDIX 1: MEDIA, SOLUTIONS AND BUFFERS

All reagents used were purchased from Sigma-Aldrich (Poole, UK), unless otherwise specified.

Full culture medium	RPMI_1640 10% foetal calf serum (Biosera, E.Sussex UK) 2mM glutamine 100U/ml penicillin 100µg/ml streptomycin
Ammonium Chloride (ACK) red blood cell lysis buffer	1litre (L) dH_2O 8.29g NH_4Cl 1g $KHCO_3$ 37.2mg EDTA (all filter sterilised)
Luria Bertani (L.B) Medium	1L dH_2O 20g Lennox. L Broth base (Invitrogen, Paisley, UK) Autoclaved to sterilise
Phosphate buffered saline (PBS) pH 7.4	1LdH_2O 8.5g NaCl 1.07g Na_2HPO_4 0.39g NaH_2PO_4 Autoclaved to sterilise
Agar plates	1LdH_2O 20g granulated agar (Melford, Ipswich, UK). 20g Lennox. L Broth base Autoclaved to sterilise and pour plated
Fc receptor blocking buffer	2% Bovine serum albumin (BSA)/PBS 16/32 fc blocking antibody (ebioscience Hatfield, UK) diluted 1:50 10%FCS

Tris buffer pH 7.6	1LdH_2O 3.75ml 10.1M HCl (Fisher scientific, Loughborough UK) 3.188g NaCl ((Melford, Ipswich, UK) 6.057g Trizma base
Tris buffer pH 9.2	As above but at pH 9.2. Initially pH 200 ml to give pH 9.2 using HCl (dropwise with 1M or greater) and make up to desired volume with NaCl.
Peroxidase Substrate	15mls Tris buffer pH 7.6 10mg of 3,3 deaminobenzidine tetrahydrochloride (DAB) Two drops of hydrogen peroxide added to filtered solution
Alkaline phosphatase (AP) substrate	10mls Tris buffer pH 9.2 8mgs levimasole 4mgs naphthol-AS-MX-phosphate 10mgs fast blue BB salt Filtered
Enzyme-Linked ImmunoSorbent Assay (ELISA) coating buffer pH 9.6	1 capsule carbonate-bicarbonate dissolved in 100ml dH_2O
ELISA AP substrate	1 Sigma fast p-Nitrophenyl phosphate tablet and 1 Tris buffer tablet/20ml dH_2O
DABCO	90% glycerol 2.5g 1,4-diazabicyclo (2,2,2) octane (DABCO) (Sigma) (for 100mls) 10% PBS

APPENDIX 2: GENERATION OF sFLIC

sFliC was generated by Jessie Hitchcock or Charlotte Cook in conjunction with Dr. Margaret Goodall and has been described (78,239). As this antigen was generated by others, these preparation details have been taken with minor adaptations from the PhD thesis of Dr. Saeeda Bobat (Bobat, S. 2011. Characterising the immune response to Salmonella during a systemic infection. *The University of Birmingham eTheses Repository*).

Protocol

FliC was amplified from SL3261 and ligated into pET22b+ (Merck Chemicals, Nottingham, UK) to create pET22b+ FliC Xho1 containing a C-terminal His-Tag, expressed beta-lactamase conferring ampicillin resistance, and expressed FliC under the control of Isopropyl β-D-Thiogalactopyranoside (IPTG) (Promega, Southampton, UK) induction of the Lac operon through the T7 promoter. This was transformed into chemically competent BL21 DE3. sFliC was then isolated following over-expression in LB medium. Bacteria were incubated overnight at 37°C with aeration, in LB supplemented with ampicillin. The culture was then diluted 1:100 in fresh media and incubated at 37°C until mid-log phase (ODλ600 0.6-0.8). Following this, IPTG was added at a final concentration of 1 mM, to induce sFliC expression. Once induced, culturing was continued for 2.5 hours, after which the cell paste was harvested at 6000 x g for 20 minutes at 4°C.

Protein purification was achieved via a two-step process. Initially, cells were re-suspended in Bugbuster (Merck Chemicals, Nottingham, UK) and agitated at room temperature for 20 min. The cell lysate was centrifuged at 16, 000 x g for 20 minutes at 4ºC to remove cellular debris. The resulting lysate was filtered through a 0.22 µm filter (Millipore, MA, USA) and incubated with Ni-NTA Sepharose (Qiagen, Hilden, Germany) for 45 minutes at room temperature. Flagellin was then purified by Nickle-affinity chromatography using a disposable Polypropylene Column (Qiagen). After the lysate had passed through, the column was washed with five volumes of PBS and the His-tagged protein (sFliC) was eluted in 5 ml PBS containing 100mM Imidazole (Melford Laboratories). Flagellin was then extensively dialysed against PBS under gentle agitation at 4°C. Subsequently, sFliC was filtered and purified to homogeneity by affinity chromatography using an anti-FliC monoclonal antibody in conjunction with Dr Margaret Goodall.

Purified sFliC was further dialysed and protein identity and purity was assessed by Sodium-Dodecyl-Sulphate Polyacrylamide Gel Electrophoresis (SDS-PAGE), revealing the presence of sFliC at the expected molecular weight (56 kDa) and the absence of contaminating protein post affinity chromatography. Protein concentration was determined using the bicinchoninic acid (BCA) assay (Thermo Fisher Scientific, MA, USA) adapted for use in microplates. In brief, 50 µl of the purified protein and diluent were mixed with 200 µl of the BCA working reagent (BCA and copper complex) and incubated at 37°C for 30 minutes, alongside albumin protein standards. Following incubation, the colour change observed upon the simultaneous reduction of copper in the working reagent upon protein binding, and the chelating of BCA by this resulting cuprous ion, was read at 550 - 570 nm using an Emax Precision Microplate reader (Molecular Devices). A standard curve of

absorbance was constructed against known concentrations of the protein standards, which was used to determine the concentration of the protein. LPS contamination was assessed using the Sigma E-TOXATE Kit as per manufacturer's guidelines and shown to be ≤1 Endotoxin Unit EU/300µg. Sterile antigen was stored at -20ºC.

APPENDIX 3: CONJUGATION OF NP TO CGG

NP was conjugated to CGG by Chandra Raykundalia and has been previously described (240).

Buffers

Coupling buffer 0.2M $NaHCo_3/Na_2CO_3$ pH9.0	Prepare 0.2M $NaHCO_3$ Adjust pH with 0.2MNa_2CO_3
0.2M Boratebuffer pH 8.4	6.18g H_3BO_3 9.4g Na_2borate 9gNaCl

Protocol

CGG was dialysed against 0.2M $NaHCo_3/Na_2CO_3$ pH 9.0 and the solution was stirred on ice. NP-OSuc was dissolved in DMF (10mg/ml) and the appropriate amount was added drop-wise to the CGG solution, at a ratio of 1:20 (NP:CGG). The solution was then stirred for 2-3hr. Unbound hapten was removed by extensive dialysis against PBS, consisting of 4 buffer changes over two nights, at 4ºC. The coupling rate was determined by measuring the OD_{430nm} (NP) and the OD_{280nm} (protein), by diluting NP-CGG 1:10 in borate buffer pH 8.4. As NP has some absorption at 280nm, standard curves were produced for NP-OSuc at 430nm and NP-OSuc and CGG at 280nm. The NP concentration in NP-CGG was measured using the OD 430nm, then the NP absorption at 280nm was subtracted from the OD_{280}nm. The solution was then sterile filtered. Sterile antigen was stored at 4ºC.

APPENDIX 4: PREPARATION OF PURIFIED PORINS FROM STM

Purified porins from STm (strain ATCC 14028) were extracted by Dr. Cristina-Gil Cruz and their preparation has been described (13). As I did not make the porins used for immunisations, the preparation details given below are taken with minor adaptations from the PhD thesis of Dr. Saeeda Bobat (Bobat, S. 2011. Characterising the immune response to Salmonella during a systemic infection. *The University of Birmingham eTheses Repository*).

Buffers

All prepared with MilleQ H_2O and filter sterilised with a 0.45 µm filter (Millipore, MA, USA)

Wash Buffer	50 mM Tris.HCl (pH 7.4)
Solubilisation Buffer	50 mM Tris.HCl (pH 7.4) 2% Sodium Dodecyl Suplate (SDS)
Nikaido Solubilisation Buffer	50 mM Tris.HCl (pH 7.4) 1% Sodium Dodecyl Suplate (SDS) 3.25 mM EDTA 0.05% β2-mercaptoethanol
Nikaido Purification Buffer	50 mM Tris.HCl (pH 7.4) 0.5% Sodium Dodecyl Suplate (SDS) 3.25 mM EDTA 200 mM NaCl

Protocol

Purified porins from STm (strain ATCC 14028) were obtained through repeated extraction with SDS. STm was incubated in minimal salts medium (MAM) containing 0.1% yeast extract, 0.5% glucose and 0.1% $MgSO_4$ at 37°C with aeration (200 rpm) until late log phase (ODλ600nm of 1). Cells were then diluted 1:10 in 1.5 L MAM and further incubated until late log phase.

Cells were harvested at 6000 x g for 15 minutes at 4°C and washed in wash buffer, followed by resuspension and disruption using a French pressure cell at 20, 000 psi. Un-broken cells were removed at 6000 x g for 20 minutes at 4°C and the lysate was centrifuged at 30,000 x g for 40 minutes at 4°C. The resulting envelope fraction was re-suspended in 100ml solubilisation buffer and incubated for 2 hours with aeration at 120rpm at 37°C. The soluble inner membrane fraction was then separated from the insoluble outer membrane (OM) by centrifugation at 30, 000 x g for 45 minutes at 4°C. This extraction step was performed twice. Pelleted cells (OM envelope) were re-suspended in Nikaido buffer and incubated for 1 hour at 37°C with aeration (120 rpm) before centrifugation at 30, 000 x g for 1 hour at 20°C. The resulting supernatant contained the OM fraction.

Final purification was by FPLC gel filtration on a Sephacryl S-200 column with Nikaido's purification buffer. Fractions with an O.D at λ280 nm of > 0.2 were pooled and extensively dialysed against PBS containing 0.1% (w/v) SDS. Purity was assessed by SDS-PAGE and protein concentration was assessed using the BCA assay (Thermo Fisher Scientific) (see

appendix 2). The LAL assay showed LPS contamination to be 0.06 EU/480 µg protein. Protein identity was confirmed by trypsin digest and Quadrupole Time of Flight (QTOF) mass spectrometry at the School of Biosciences Functional Proteomics Unit (University of Birmingham). Protein was stored at -80ºC.

APPENDIX 5: PREPARATION OF TOTAL OMP ANTIGEN

Total OMP were prepared by Jessica Hitchcock or Charlotte Cook and has been described (244). As I did not prepare the OMP for ELISA, the preparation details given below are taken, with minor adaptions, from the PhD thesis of Dr. Saeeda Bobat (Bobat, S. 2011. Characterising the immune response to Salmonella during a systemic infection. *The University of Birmingham eTheses Repository*).

Total OMP preparations were prepared by 2% Triton X-100 extraction. Cells were harvested at an ODλ600 nm of 1.0 by centrifugation at 10,000 x g for 10 minutes at 4°C. Cells were then washed in 10 mM Tris-HCl (pH 7.4) under the same conditions and re-suspended in the same buffer containing 2 mM PMSF (Roche). Cells were then disrupted using a French pressure cell at 20,000 psi and harvested at 6,000 x g for 10 minutes at 4°C to remove unbroken cells. The lysate was centrifuged at 30,000 x g for 90 minutes at 4°C. Pelleted cell envelopes were incubated in 10 mM Tris-HCl containing 2% Triton X-100 for 15 minutes at room temperature, followed by centrifugation at 30,000 x g as before. The soluble OMP were then washed extensively in 10 mM Tris-HCl. The total OMP preparation was re-suspended in this buffer and protein concentration was determined using the BCA assay (see appendix 2). The antigen was stored at -20°C until further use.

Reference List

1. Braff, M. H., M. Zaiou, J. Fierer, V. Nizet, and R. L. Gallo. 2005. Keratinocyte production of cathelicidin provides direct activity against bacterial skin pathogens. *Infect. Immun.* 73: 6771-6781.

2. Gallo, R. L., M. Murakami, T. Ohtake, and M. Zaiou. 2002. Biology and clinical relevance of naturally occurring antimicrobial peptides. *J. Allergy Clin. Immunol.* 110: 823-831.

3. Janeway, C. A., and R. Medzhitov. 2002. Innate immune recognition. *Annual Review of Immunology* 20: 197-216.

4. Aderem, A., and D. M. Underhill. 1999. Mechanisms of phagocytosis in macrophages. *Annu. Rev. Immunol.* 17: 593-623.

5. Soehnlein, O., and L. Lindbom. 2010. Phagocyte partnership during the onset and resolution of inflammation. *Nat. Rev. Immunol.* 10: 427-439.

6. Bogdan, C., M. Rollinghoff, and A. Diefenbach. 2000. Reactive oxygen and reactive nitrogen intermediates in innate and specific immunity. *Curr. Opin. Immunol.* 12: 64-76.

7. Medzhitov, R., and C. A. Janeway, Jr. 1997. Innate immunity: impact on the adaptive immune response. *Curr. Opin. Immunol.* 9: 4-9.

8. Pasare, C., and R. Medzhitov. 2004. Toll-like receptors: linking innate and adaptive immunity. *Microbes. Infect.* 6: 1382-1387.

9. Banchereau, J., and R. M. Steinman. 1998. Dendritic cells and the control of immunity. *Nature* 392: 245-252.

10. Carroll, M. C. 2008. Complement and humoral immunity. *Vaccine* 26 Suppl 8: I28-I33.

11. Haury, M., A. Sundblad, A. Grandien, C. Barreau, A. Coutinho, and A. Nobrega. 1997. The repertoire of serum IgM in normal mice is largely independent of external antigenic contact. *Eur. J. Immunol.* 27: 1557-1563.

12. Alugupalli, K. R., J. M. Leong, R. T. Woodland, M. Muramatsu, T. Honjo, and R. M. Gerstein. 2004. B1b lymphocytes confer T cell-independent long-lasting immunity. *Immunity.* 21: 379-390.

13. Gil-Cruz, C., S. Bobat, J. L. Marshall, R. A. Kingsley, E. A. Ross, I. R. Henderson, D. L. Leyton, R. E. Coughlan, M. Khan, K. T. Jensen, C. D. Buckley, G. Dougan, I. C. MacLennan, C. Lopez-Macias, and A. F. Cunningham. 2009. The porin OmpD

from nontyphoidal Salmonella is a key target for a protective B1b cell antibody response. *Proc. Natl. Acad. Sci. U. S. A* 106: 9803-9808.

14. Haas, K. M., J. C. Poe, D. A. Steeber, and T. F. Tedder. 2005. B-1a and B-1b cells exhibit distinct developmental requirements and have unique functional roles in innate and adaptive immunity to S. pneumoniae. *Immunity.* 23: 7-18.

15. Alt, F. W., T. K. Blackwell, R. A. DePinho, M. G. Reth, and G. D. Yancopoulos. 1986. Regulation of genome rearrangement events during lymphocyte differentiation. *Immunol. Rev.* 89: 5-30.

16. Freitas, A. A., and B. Rocha. 2000. Population Biology of Lymphocytes: the Flight for Survival. *Annual Review of Immunology* 18: 83-111.

17. Mebius, R. E., and G. Kraal. 2005. Structure and function of the spleen. *Nat. Rev. Immunol.* 5: 606-616.

18. Forster, R., A. Schubel, D. Breitfeld, E. Kremmer, I. Renner-Muller, E. Wolf, and M. Lipp. 1999. CCR7 coordinates the primary immune response by establishing functional microenvironments in secondary lymphoid organs. *Cell* 99: 23-33.

19. Luther, S. A., H. L. Tang, P. L. Hyman, A. G. Farr, and J. G. Cyster. 2000. Coexpression of the chemokines ELC and SLC by T zone stromal cells and deletion of the ELC gene in the plt/plt mouse. *Proc. Natl. Acad. Sci. U. S. A* 97: 12694-12699.

20. Nakano, H., S. Mori, H. Yonekawa, H. Nariuchi, A. Matsuzawa, and T. Kakiuchi. 1998. A novel mutant gene involved in T-lymphocyte-specific homing into peripheral lymphoid organs on mouse chromosome 4. *Blood* 91: 2886-2895.

21. Forster, R., A. E. Mattis, E. Kremmer, E. Wolf, G. Brem, and M. Lipp. 1996. A putative chemokine receptor, BLR1, directs B cell migration to defined lymphoid organs and specific anatomic compartments of the spleen. *Cell* 87: 1037-1047.

22. Gunn, M. D., V. N. Ngo, K. M. Ansel, E. H. Ekland, J. G. Cyster, and L. T. Williams. 1998. A B-cell-homing chemokine made in lymphoid follicles activates Burkitt's lymphoma receptor-1. *Nature* 391: 799-803.

23. Legler, D. F., M. Loetscher, R. S. Roos, I. Clark-Lewis, M. Baggiolini, and B. Moser. 1998. B cell-attracting chemokine 1, a human CXC chemokine expressed in lymphoid tissues, selectively attracts B lymphocytes via BLR1/CXCR5. *J. Exp. Med.* 187: 655-660.

24. Ebisuno, Y., T. Tanaka, N. Kanemitsu, H. Kanda, K. Yamaguchi, T. Kaisho, S. Akira, and M. Miyasaka. 2003. Cutting edge: the B cell chemokine CXC chemokine ligand 13/B lymphocyte chemoattractant is expressed in the high endothelial venules of lymph nodes and Peyer's patches and affects B cell trafficking across high endothelial venules. *J. Immunol.* 171: 1642-1646.

25. Cyster, J. G., S. B. Hartley, and C. C. Goodnow. 1994. Competition for follicular niches excludes self-reactive cells from the recirculating B-cell repertoire. *Nature* 371: 389-395.

26. MacLennan, I. C., K. M. Toellner, A. F. Cunningham, K. Serre, D. M. Sze, E. Zuniga, M. C. Cook, and C. G. Vinuesa. 2003. Extrafollicular antibody responses. *Immunol. Rev.* 194: 8-18.

27. Rogers, P. R., C. Dubey, and S. L. Swain. 2000. Qualitative changes accompany memory T cell generation: faster, more effective responses at lower doses of antigen. *J. Immunol.* 164: 2338-2346.

28. Hardy, R. R., and K. Hayakawa. 1991. A developmental switch in B lymphopoiesis. *Proc. Natl. Acad. Sci. U. S. A* 88: 11550-11554.

29. Martin, F., and J. F. Kearney. 2002. Marginal-zone B cells. *Nat. Rev. Immunol.* 2: 323-335.

30. LeBien, T. W., and T. F. Tedder. 2008. B lymphocytes: how they develop and function. *Blood* 112: 1570-1580.

31. Nagasawa, T. 2006. Microenvironmental niches in the bone marrow required for B-cell development. *Nat. Rev. Immunol.* 6: 107-116.

32. Brack, C., M. Hirama, R. Lenhard-Schuller, and S. Tonegawa. 1978. A complete immunoglobulin gene is created by somatic recombination. *Cell* 15: 1-14.

33. Hardy, R. R., C. E. Carmack, S. A. Shinton, J. D. Kemp, and K. Hayakawa. 1991. Resolution and characterization of pro-B and pre-pro-B cell stages in normal mouse bone marrow. *J. Exp. Med.* 173: 1213-1225.

34. Melchers, F. 2005. The pre-B-cell receptor: selector of fitting immunoglobulin heavy chains for the B-cell repertoire. *Nat. Rev. Immunol.* 5: 578-584.

35. Goodnow, C. C., S. Adelstein, and A. Basten. 1990. The need for central and peripheral tolerance in the B cell repertoire. *Science* 248: 1373-1379.

36. Kasaian, M. T., H. Ikematsu, and P. Casali. 1992. Identification and analysis of a novel human surface CD5- B lymphocyte subset producing natural antibodies. *J. Immunol.* 148: 2690-2702.

37. Le Pottier, L., V. Devauchelle, J. O. Pers, C. Jamin, and P. Youinou. 2007. The mosaic of B-cell subsets (with special emphasis on primary Sjogren's syndrome). *Autoimmun. Rev.* 6: 149-154.

38. Hardy, R. R., and K. Hayakawa. 2001. B cell development pathways. *Annu. Rev. Immunol.* 19: 595-621.

39. Rakhmanov, M., B. Keller, S. Gutenberger, C. Foerster, M. Hoenig, G. Driessen, B. M. van der, J. J. van Dongen, E. Wiech, M. Visentini, I. Quinti, A. Prasse, N.

Voelxen, U. Salzer, S. Goldacker, P. Fisch, H. Eibel, K. Schwarz, H. H. Peter, and K. Warnatz. 2009. Circulating CD21low B cells in common variable immunodeficiency resemble tissue homing, innate-like B cells. *Proc. Natl. Acad. Sci. U. S. A* 106: 13451-13456.

40. Carroll, M. C. 2004. The complement system in B cell regulation. *Mol. Immunol.* 41: 141-146.

41. Ghosn, E. E., Y. Yang, J. Tung, L. A. Herzenberg, and L. A. Herzenberg. 2008. CD11b expression distinguishes sequential stages of peritoneal B-1 development. *Proc. Natl. Acad. Sci. U. S. A* 105: 5195-5200.

42. Griffin, D. O., N. E. Holodick, and T. L. Rothstein. 2011. Human B1 cells in umbilical cord and adult peripheral blood express the novel phenotype CD20+ CD27+ CD43+ CD70-. *J. Exp. Med.* 208: 67-80.

43. Montecino-Rodriguez, E., H. Leathers, and K. Dorshkind. 2006. Identification of a B-1 B cell-specified progenitor. *Nat. Immunol.* 7: 293-301.

44. Hayakawa, K., R. R. Hardy, A. M. Stall, L. A. Herzenberg, and L. A. Herzenberg. 1986. Immunoglobulin-bearing B cells reconstitute and maintain the murine Ly-1 B cell lineage. *Eur. J. Immunol.* 16: 1313-1316.

45. Duber, S., M. Hafner, M. Krey, S. Lienenklaus, B. Roy, E. Hobeika, M. Reth, T. Buch, A. Waisman, K. Kretschmer, and S. Weiss. 2009. Induction of B-cell development in adult mice reveals the ability of bone marrow to produce B-1a cells. *Blood* 114: 4960-4967.

46. Possee, R. D., G. C. Schild, and N. J. Dimmock. 1982. Studies on the mechanism of neutralization of influenza virus by antibody: evidence that neutralizing antibody (anti-haemagglutinin) inactivates influenza virus in vivo by inhibiting virion transcriptase activity. *J. Gen. Virol.* 58: 373-386.

47. Robbins, F. C., and J. B. Robbins. 1986. Current status and prospects for some improved and new bacterial vaccines. *Annu. Rev. Public Health* 7: 105-125.

48. Swanson, J. A., and A. D. Hoppe. 2004. The coordination of signaling during Fc receptor-mediated phagocytosis. *J. Leukoc. Biol.* 76: 1093-1103.

49. Leibson, P. J. 1997. Signal transduction during natural killer cell activation: inside the mind of a killer. *Immunity.* 6: 655-661.

50. Noelle, R. J., and E. C. Snow. 1991. T helper cell-dependent B cell activation. *FASEB J.* 5: 2770-2776.

51. Carrasco, Y. R., and F. D. Batista. 2006. B cell recognition of membrane-bound antigen: an exquisite way of sensing ligands. *Curr. Opin. Immunol.* 18: 286-291.

52. Depoil, D., S. Fleire, B. L. Treanor, M. Weber, N. E. Harwood, K. L. Marchbank, V. L. Tybulewicz, and F. D. Batista. 2008. CD19 is essential for B cell activation by promoting B cell receptor-antigen microcluster formation in response to membrane-bound ligand. *Nat. Immunol.* 9: 63-72.

53. Reth, M. 1989. Antigen receptor tail clue. *Nature* 338: 383-384.

54. Harwood, N. E., and F. D. Batista. 2010. Early events in B cell activation. *Annu. Rev. Immunol.* 28: 185-210.

55. Kawabe, T., T. Naka, K. Yoshida, T. Tanaka, H. Fujiwara, S. Suematsu, N. Yoshida, T. Kishimoto, and H. Kikutani. 1994. The immune responses in CD40-deficient mice: impaired immunoglobulin class switching and germinal center formation. *Immunity.* 1: 167-178.

56. Toellner, K. M., S. A. Luther, D. M. Sze, R. K. Choy, D. R. Taylor, I. C. MacLennan, and H. Acha-Orbea. 1998. T helper 1 (Th1) and Th2 characteristics start to develop during T cell priming and are associated with an immediate ability to induce immunoglobulin class switching. *J. Exp. Med.* 187: 1193-1204.

57. Banchereau, J., F. Bazan, D. Blanchard, F. Briere, J. P. Galizzi, C. Vankooten, Y. J. Liu, F. Rousset, and S. Saeland. 1994. The Cd40 Antigen and Its Ligand. *Annual Review of Immunology* 12: 881-922.

58. MacLennan, I. C. 2005. Germinal centers still hold secrets. *Immunity.* 22: 656-657.

59. Germain, R. N. 1994. MHC-dependent antigen processing and peptide presentation: providing ligands for T lymphocyte activation. *Cell* 76: 287-299.

60. Ingulli, E., A. Mondino, A. Khoruts, and M. K. Jenkins. 1997. In vivo detection of dendritic cell antigen presentation to CD4(+) T cells. *J. Exp. Med.* 185: 2133-2141.

61. Luther, S. A., A. Gulbranson-Judge, H. Acha-Orbea, and I. C. MacLennan. 1997. Viral superantigen drives extrafollicular and follicular B cell differentiation leading to virus-specific antibody production. *J. Exp. Med.* 185: 551-562.

62. Kaiko, G. E., J. C. Horvat, K. W. Beagley, and P. M. Hansbro. 2008. Immunological decision-making: how does the immune system decide to mount a helper T-cell response? *Immunology* 123: 326-338.

63. Cella, M., D. Scheidegger, K. Palmer-Lehmann, P. Lane, A. Lanzavecchia, and G. Alber. 1996. Ligation of CD40 on dendritic cells triggers production of high levels of interleukin-12 and enhances T cell stimulatory capacity: T-T help via APC activation. *J. Exp. Med.* 184: 747-752.

64. Koch, F., U. Stanzl, P. Jennewein, K. Janke, C. Heufler, E. Kampgen, N. Romani, and G. Schuler. 1996. High level IL-12 production by murine dendritic cells: upregulation via MHC class II and CD40 molecules and downregulation by IL-4 and IL-10. *J. Exp. Med.* 184: 741-746.

65. Mosmann, T. R., H. Cherwinski, M. W. Bond, M. A. Giedlin, and R. L. Coffman. 1986. Two types of murine helper T cell clone. I. Definition according to profiles of lymphokine activities and secreted proteins. *J. Immunol.* 136: 2348-2357.

66. Mosmann, T. R., and R. L. Coffman. 1989. TH1 and TH2 cells: different patterns of lymphokine secretion lead to different functional properties. *Annu. Rev. Immunol.* 7: 145-173.

67. Baecher-Allan, C., J. A. Brown, G. J. Freeman, and D. A. Hafler. 2001. CD4+CD25high regulatory cells in human peripheral blood. *J. Immunol.* 167: 1245-1253.

68. Fontenot, J. D., M. A. Gavin, and A. Y. Rudensky. 2003. Foxp3 programs the development and function of CD4+CD25+ regulatory T cells. *Nat. Immunol.* 4: 330-336.

69. Jelley-Gibbs, D. M., T. M. Strutt, K. K. McKinstry, and S. L. Swain. 2008. Influencing the fates of CD4 T cells on the path to memory: lessons from influenza. *Immunol. Cell Biol.* 86: 343-352.

70. Cunningham, A. F., F. Gaspal, K. Serre, E. Mohr, I. R. Henderson, A. Scott-Tucker, S. M. Kenny, M. Khan, K. M. Toellner, P. J. Lane, and I. C. MacLennan. 2007. Salmonella induces a switched antibody response without germinal centers that impedes the extracellular spread of infection. *J. Immunol.* 178: 6200-6207.

71. Szabo, S. J., B. M. Sullivan, C. Stemmann, A. R. Satoskar, B. P. Sleckman, and L. H. Glimcher. 2002. Distinct effects of T-bet in TH1 lineage commitment and IFN-gamma production in CD4 and CD8 T cells. *Science* 295: 338-342.

72. Szabo, S. J., S. T. Kim, G. L. Costa, X. Zhang, C. G. Fathman, and L. H. Glimcher. 2000. A novel transcription factor, T-bet, directs Th1 lineage commitment. *Cell* 100: 655-669.

73. Hwang, E. S., S. J. Szabo, P. L. Schwartzberg, and L. H. Glimcher. 2005. T helper cell fate specified by kinase-mediated interaction of T-bet with GATA-3. *Science* 307: 430-433.

74. Lighvani, A. A., D. M. Frucht, D. Jankovic, H. Yamane, J. Aliberti, B. D. Hissong, B. V. Nguyen, M. Gadina, A. Sher, W. E. Paul, and J. J. O'Shea. 2001. T-bet is rapidly induced by interferon-gamma in lymphoid and myeloid cells. *Proc. Natl. Acad. Sci. U. S. A* 98: 15137-15142.

75. Kisseleva, T., S. Bhattacharya, J. Braunstein, and C. W. Schindler. 2002. Signaling through the JAK/STAT pathway, recent advances and future challenges. *Gene* 285: 1-24.

76. Mullen, A. C., F. A. High, A. S. Hutchins, H. W. Lee, A. V. Villarino, D. M. Livingston, A. L. Kung, N. Cereb, T. P. Yao, S. Y. Yang, and S. L. Reiner. 2001.

Role of T-bet in commitment of TH1 cells before IL-12-dependent selection. *Science* 292: 1907-1910.

77. Sugimoto, N., M. Nakahira, H. J. Ahn, M. Micallef, T. Hamaoka, M. Kurimoto, and H. Fujiwara. 2003. Differential requirements for JAK2 and TYK2 in T cell proliferation and IFN-gamma production induced by IL-12 alone or together with IL-18. *Eur. J. Immunol.* 33: 243-251.

78. Bobat, S., A. Flores-Langarica, J. Hitchcock, J. L. Marshall, R. A. Kingsley, M. Goodall, C. Gil-Cruz, K. Serre, D. L. Leyton, S. E. Letran, F. Gaspal, R. Chester, J. L. Chamberlain, G. Dougan, C. Lopez-Macias, I. R. Henderson, J. Alexander, I. C. MacLennan, and A. F. Cunningham. 2011. Soluble flagellin, FliC, induces an Ag-specific Th2 response, yet promotes T-bet-regulated Th1 clearance of Salmonella typhimurium infection. *Eur. J. Immunol.* 41: 1606-1618.

79. Ravindran, R., J. Foley, T. Stoklasek, L. H. Glimcher, and S. J. McSorley. 2005. Expression of T-bet by CD4 T cells is essential for resistance to Salmonella infection. *J. Immunol.* 175: 4603-4610.

80. Neurath, M. F., B. Weigmann, S. Finotto, J. Glickman, E. Nieuwenhuis, H. Iijima, A. Mizoguchi, E. Mizoguchi, J. Mudter, P. R. Galle, A. Bhan, F. Autschbach, B. M. Sullivan, S. J. Szabo, L. H. Glimcher, and R. S. Blumberg. 2002. The transcription factor T-bet regulates mucosal T cell activation in experimental colitis and Crohn's disease. *J. Exp. Med.* 195: 1129-1143.

81. Lugo-Villarino, G., R. Maldonado-Lopez, R. Possemato, C. Penaranda, and L. H. Glimcher. 2003. T-bet is required for optimal production of IFN-gamma and antigen-specific T cell activation by dendritic cells. *Proc. Natl. Acad. Sci. U. S. A* 100: 7749-7754.

82. Snapper, C. M., C. Peschel, and W. E. Paul. 1988. IFN-gamma stimulates IgG2a secretion by murine B cells stimulated with bacterial lipopolysaccharide. *J. Immunol.* 140: 2121-2127.

83. Peng, S. L., S. J. Szabo, and L. H. Glimcher. 2002. T-bet regulates IgG class switching and pathogenic autoantibody production. *Proc. Natl. Acad. Sci. U. S. A* 99: 5545-5550.

84. Cunningham, A. F., and K. M. Toellner. 2003. Rapid development of Th2 activity during T cell priming. *Clin. Dev. Immunol.* 10: 1-6.

85. Glimcher, L. H., and K. M. Murphy. 2000. Lineage commitment in the immune system: the T helper lymphocyte grows up. *Genes Dev.* 14: 1693-1711.

86. Snapper, C. M., F. D. Finkelman, and W. E. Paul. 1988. Regulation of IgG1 and IgE production by interleukin 4. *Immunol. Rev.* 102: 51-75.

87. Swain, S. L., A. D. Weinberg, M. English, and G. Huston. 1990. IL-4 directs the development of Th2-like helper effectors. *J. Immunol.* 145: 3796-3806.

88. Flowers, L. O., H. M. Johnson, M. G. Mujtaba, M. R. Ellis, S. M. Haider, and P. S. Subramaniam. 2004. Characterization of a peptide inhibitor of Janus kinase 2 that mimics suppressor of cytokine signaling 1 function. *J. Immunol.* 172: 7510-7518.

89. Nawijn, M. C., G. M. Dingjan, R. Ferreira, B. N. Lambrecht, A. Karis, F. Grosveld, H. Savelkoul, and R. W. Hendriks. 2001. Enforced expression of GATA-3 in transgenic mice inhibits Th1 differentiation and induces the formation of a T1/ST2-expressing Th2-committed T cell compartment in vivo. *J. Immunol.* 167: 724-732.

90. Mohrs, M., B. Ledermann, G. Kohler, A. Dorfmuller, A. Gessner, and F. Brombacher. 1999. Differences between IL-4- and IL-4 receptor alpha-deficient mice in chronic leishmaniasis reveal a protective role for IL-13 receptor signaling. *J. Immunol.* 162: 7302-7308.

91. McKenzie, G. J., P. G. Fallon, C. L. Emson, R. K. Grencis, and A. N. McKenzie. 1999. Simultaneous disruption of interleukin (IL)-4 and IL-13 defines individual roles in T helper cell type 2-mediated responses. *J. Exp. Med.* 189: 1565-1572.

92. McKenzie, G. J., C. L. Emson, S. E. Bell, S. Anderson, P. Fallon, G. Zurawski, R. Murray, R. Grencis, and A. N. McKenzie. 1998. Impaired development of Th2 cells in IL-13-deficient mice. *Immunity.* 9: 423-432.

93. Cunningham, A. F., P. G. Fallon, M. Khan, S. Vacheron, H. Acha-Orbea, I. C. MacLennan, A. N. McKenzie, and K. M. Toellner. 2002. Th2 activities induced during virgin T cell priming in the absence of IL-4, IL-13, and B cells. *J. Immunol.* 169: 2900-2906.

94. Cunningham, A. F., K. Serre, K. M. Toellner, M. Khan, J. Alexander, F. Brombacher, and I. C. MacLennan. 2004. Pinpointing IL-4-independent acquisition and IL-4-influenced maintenance of Th2 activity by CD4 T cells. *Eur. J. Immunol.* 34: 686-694.

95. Kopf, M., G. Le Gros, M. Bachmann, M. C. Lamers, H. Bluethmann, and G. Kohler. 1993. Disruption of the murine IL-4 gene blocks Th2 cytokine responses. *Nature* 362: 245-248.

96. Brewer, J. M., M. Conacher, C. A. Hunter, M. Mohrs, F. Brombacher, and J. Alexander. 1999. Aluminium hydroxide adjuvant initiates strong antigen-specific Th2 responses in the absence of IL-4- or IL-13-mediated signaling. *J. Immunol.* 163: 6448-6454.

97. Dodge, I. L., M. W. Carr, M. Cernadas, and M. B. Brenner. 2003. IL-6 production by pulmonary dendritic cells impedes Th1 immune responses. *J. Immunol.* 170: 4457-4464.

98. Romano, C. C., M. J. Mendes-Giannini, A. J. Duarte, and G. Benard. 2005. The role of interleukin-10 in the differential expression of interleukin-12p70 and its beta2 receptor on patients with active or treated paracoccidioidomycosis and healthy infected subjects. *Clin. Immunol.* 114: 86-94.

99. Taga, T., and T. Kishimoto. 1992. Role of a two-chain IL-6 receptor system in immune and hematopoietic cell regulation. *Crit Rev. Immunol.* 11: 265-280.

100. Diehl, S., C. W. Chow, L. Weiss, A. Palmetshofer, T. Twardzik, L. Rounds, E. Serfling, R. J. Davis, J. Anguita, and M. Rincon. 2002. Induction of NFATc2 expression by interleukin 6 promotes T helper type 2 differentiation. *J. Exp. Med.* 196: 39-49.

101. Yang, Y., J. Ochando, A. Yopp, J. S. Bromberg, and Y. Ding. 2005. IL-6 plays a unique role in initiating c-Maf expression during early stage of CD4 T cell activation. *J. Immunol.* 174: 2720-2729.

102. Diehl, S., J. Anguita, A. Hoffmeyer, T. Zapton, J. N. Ihle, E. Fikrig, and M. Rincon. 2000. Inhibition of Th1 differentiation by IL-6 is mediated by SOCS1. *Immunity.* 13: 805-815.

103. Kopf, M., S. Herren, M. V. Wiles, M. B. Pepys, and M. H. Kosco-Vilbois. 1998. Interleukin 6 influences germinal center development and antibody production via a contribution of C3 complement component. *J. Exp. Med.* 188: 1895-1906.

104. Wu, Y., M. E. El Shikh, R. M. El Sayed, A. M. Best, A. K. Szakal, and J. G. Tew. 2009. IL-6 produced by immune complex-activated follicular dendritic cells promotes germinal center reactions, IgG responses and somatic hypermutation. *Int. Immunol.* 21: 745-756.

105. Nurieva, R. I., Y. Chung, D. Hwang, X. O. Yang, H. S. Kang, L. Ma, Y. H. Wang, S. S. Watowich, A. M. Jetten, Q. Tian, and C. Dong. 2008. Generation of T follicular helper cells is mediated by interleukin-21 but independent of T helper 1, 2, or 17 cell lineages. *Immunity.* 29: 138-149.

106. Yu, D., and C. G. Vinuesa. 2010. The elusive identity of T follicular helper cells. *Trends Immunol.* 31: 377-383.

107. Lee, S. K., R. J. Rigby, D. Zotos, L. M. Tsai, S. Kawamoto, J. L. Marshall, R. R. Ramiscal, T. D. Chan, D. Gatto, R. Brink, D. Yu, S. Fagarasan, D. M. Tarlinton, A. F. Cunningham, and C. G. Vinuesa. 2011. B cell priming for extrafollicular antibody responses requires Bcl-6 expression by T cells. *J. Exp. Med.* 208: 1377-1388.

108. Rolf, J., K. Fairfax, and M. Turner. 2010. Signaling pathways in T follicular helper cells. *J. Immunol.* 184: 6563-6568.

109. Qi, H., J. L. Cannons, F. Klauschen, P. L. Schwartzberg, and R. N. Germain. 2008. SAP-controlled T-B cell interactions underlie germinal centre formation. *Nature* 455: 764-769.

110. Johnston, R. J., A. C. Poholek, D. DiToro, I. Yusuf, D. Eto, B. Barnett, A. L. Dent, J. Craft, and S. Crotty. 2009. Bcl6 and Blimp-1 are reciprocal and antagonistic regulators of T follicular helper cell differentiation. *Science* 325: 1006-1010.

111. Nurieva, R. I., Y. Chung, G. J. Martinez, X. O. Yang, S. Tanaka, T. D. Matskevitch, Y. H. Wang, and C. Dong. 2009. Bcl6 mediates the development of T follicular helper cells. *Science* 325: 1001-1005.

112. Yu, D., S. Rao, L. M. Tsai, S. K. Lee, Y. He, E. L. Sutcliffe, M. Srivastava, M. Linterman, L. Zheng, N. Simpson, J. I. Ellyard, I. A. Parish, C. S. Ma, Q. J. Li, C. R. Parish, C. R. Mackay, and C. G. Vinuesa. 2009. The transcriptional repressor Bcl-6 directs T follicular helper cell lineage commitment. *Immunity.* 31: 457-468.

113. Breitfeld, D., L. Ohl, E. Kremmer, J. Ellwart, F. Sallusto, M. Lipp, and R. Forster. 2000. Follicular B helper T cells express CXC chemokine receptor 5, localize to B cell follicles, and support immunoglobulin production. *J. Exp. Med.* 192: 1545-1552.

114. Kim, C. H., L. S. Rott, I. Clark-Lewis, D. J. Campbell, L. Wu, and E. C. Butcher. 2001. Subspecialization of CXCR5+ T cells: B helper activity is focused in a germinal center-localized subset of CXCR5+ T cells. *J. Exp. Med.* 193: 1373-1381.

115. Schaerli, P., K. Willimann, A. B. Lang, M. Lipp, P. Loetscher, and B. Moser. 2000. CXC chemokine receptor 5 expression defines follicular homing T cells with B cell helper function. *J. Exp. Med.* 192: 1553-1562.

116. Haynes, N. M., C. D. Allen, R. Lesley, K. M. Ansel, N. Killeen, and J. G. Cyster. 2007. Role of CXCR5 and CCR7 in follicular Th cell positioning and appearance of a programmed cell death gene-1high germinal center-associated subpopulation. *J. Immunol.* 179: 5099-5108.

117. Gigoux, M., J. Shang, Y. Pak, M. Xu, J. Choe, T. W. Mak, and W. K. Suh. 2009. Inducible costimulator promotes helper T-cell differentiation through phosphoinositide 3-kinase. *Proc. Natl. Acad. Sci. U. S. A* 106: 20371-20376.

118. Rolf, J., S. E. Bell, D. Kovesdi, M. L. Janas, D. R. Soond, L. M. Webb, S. Santinelli, T. Saunders, B. Hebeis, N. Killeen, K. Okkenhaug, and M. Turner. 2010. Phosphoinositide 3-kinase activity in T cells regulates the magnitude of the germinal center reaction. *J. Immunol.* 185: 4042-4052.

119. McCausland, M. M., I. Yusuf, H. Tran, N. Ono, Y. Yanagi, and S. Crotty. 2007. SAP regulation of follicular helper CD4 T cell development and humoral immunity is independent of SLAM and Fyn kinase. *J. Immunol.* 178: 817-828.

120. Linterman, M. A., L. Beaton, D. Yu, R. R. Ramiscal, M. Srivastava, J. J. Hogan, N. K. Verma, M. J. Smyth, R. J. Rigby, and C. G. Vinuesa. 2010. IL-21 acts directly on B cells to regulate Bcl-6 expression and germinal center responses. *J. Exp. Med.* 207: 353-363.

121. Poholek, A. C., K. Hansen, S. G. Hernandez, D. Eto, A. Chandele, J. S. Weinstein, X. Dong, J. M. Odegard, S. M. Kaech, A. L. Dent, S. Crotty, and J. Craft. 2010. In vivo regulation of Bcl6 and T follicular helper cell development. *J. Immunol.* 185: 313-326.

122. Eddahri, F., S. Denanglaire, F. Bureau, R. Spolski, W. J. Leonard, O. Leo, and F. Andris. 2009. Interleukin-6/STAT3 signaling regulates the ability of naive T cells to acquire B-cell help capacities. *Blood* 113: 2426-2433.

123. Wei, L., A. Laurence, K. M. Elias, and J. J. O'Shea. 2007. IL-21 is produced by Th17 cells and drives IL-17 production in a STAT3-dependent manner. *J. Biol. Chem.* 282: 34605-34610.

124. Eto, D., C. Lao, D. DiToro, B. Barnett, T. C. Escobar, R. Kageyama, I. Yusuf, and S. Crotty. 2011. IL-21 and IL-6 are critical for different aspects of B cell immunity and redundantly induce optimal follicular helper CD4 T cell (Tfh) differentiation. *PLoS. One.* 6: e17739.

125. Ma, C. S., S. Suryani, D. T. Avery, A. Chan, R. Nanan, B. Santner-Nanan, E. K. Deenick, and S. G. Tangye. 2009. Early commitment of naive human CD4(+) T cells to the T follicular helper (T(FH)) cell lineage is induced by IL-12. *Immunol. Cell Biol.* 87: 590-600.

126. Reinhardt, R. L., H. E. Liang, and R. M. Locksley. 2009. Cytokine-secreting follicular T cells shape the antibody repertoire. *Nat. Immunol.* 10: 385-393.

127. Onizuka, T., M. Moriyama, T. Yamochi, T. Kuroda, A. Kazama, N. Kanazawa, K. Sato, T. Kato, H. Ota, and S. Mori. 1995. BCL-6 gene product, a 92- to 98-kD nuclear phosphoprotein, is highly expressed in germinal center B cells and their neoplastic counterparts. *Blood* 86: 28-37.

128. Dent, A. L., A. L. Shaffer, X. Yu, D. Allman, and L. M. Staudt. 1997. Control of inflammation, cytokine expression, and germinal center formation by BCL-6. *Science* 276: 589-592.

129. Shaffer, A. L., X. Yu, Y. He, J. Boldrick, E. P. Chan, and L. M. Staudt. 2000. BCL-6 represses genes that function in lymphocyte differentiation, inflammation, and cell cycle control. *Immunity.* 13: 199-212.

130. Shaffer, A. L., K. I. Lin, T. C. Kuo, X. Yu, E. M. Hurt, A. Rosenwald, J. M. Giltnane, L. Yang, H. Zhao, K. Calame, and L. M. Staudt. 2002. Blimp-1 orchestrates plasma cell differentiation by extinguishing the mature B cell gene expression program. *Immunity.* 17: 51-62.

131. Gatto, D., D. Paus, A. Basten, C. R. Mackay, and R. Brink. 2009. Guidance of B cells by the orphan G protein-coupled receptor EBI2 shapes humoral immune responses. *Immunity.* 31: 259-269.

132. MacLennan, I. C. 1994. Germinal centers. *Annu. Rev. Immunol.* 12: 117-139.

133. Allen, C. D., K. M. Ansel, C. Low, R. Lesley, H. Tamamura, N. Fujii, and J. G. Cyster. 2004. Germinal center dark and light zone organization is mediated by CXCR4 and CXCR5. *Nat. Immunol.* 5: 943-952.

134. Caron, G., S. Le Gallou, T. Lamy, K. Tarte, and T. Fest. 2009. CXCR4 expression functionally discriminates centroblasts versus centrocytes within human germinal center B cells. *J. Immunol.* 182: 7595-7602.

135. Kelsoe, G. 1996. Life and death in germinal centers (redux). *Immunity.* 4: 107-111.

136. Liu, Y. J., J. Zhang, P. J. Lane, E. Y. Chan, and I. C. MacLennan. 1991. Sites of specific B cell activation in primary and secondary responses to T cell-dependent and T cell-independent antigens. *Eur. J. Immunol.* 21: 2951-2962.

137. Figge, M. T., A. Garin, M. Gunzer, M. Kosco-Vilbois, K. M. Toellner, and M. Meyer-Hermann. 2008. Deriving a germinal center lymphocyte migration model from two-photon data. *J. Exp. Med.* 205: 3019-3029.

138. Hauser, A. E., T. Junt, T. R. Mempel, M. W. Sneddon, S. H. Kleinstein, S. E. Henrickson, U. H. von Andrian, M. J. Shlomchik, and A. M. Haberman. 2007. Definition of germinal-center B cell migration in vivo reveals predominant intrazonal circulation patterns. *Immunity.* 26: 655-667.

139. Hauser, A. E., M. J. Shlomchik, and A. M. Haberman. 2007. In vivo imaging studies shed light on germinal-centre development. *Nat. Rev. Immunol.* 7: 499-504.

140. Meyer-Hermann, M. E., and P. K. Maini. 2005. Cutting edge: back to "one-way" germinal centers. *J. Immunol.* 174: 2489-2493.

141. Muramatsu, M., K. Kinoshita, S. Fagarasan, S. Yamada, Y. Shinkai, and T. Honjo. 2000. Class switch recombination and hypermutation require activation-induced cytidine deaminase (AID), a potential RNA editing enzyme. *Cell* 102: 553-563.

142. Revy, P., T. Muto, Y. Levy, F. Geissmann, A. Plebani, O. Sanal, N. Catalan, M. Forveille, R. Dufourcq-Labelouse, A. Gennery, I. Tezcan, F. Ersoy, H. Kayserili, A. G. Ugazio, N. Brousse, M. Muramatsu, L. D. Notarangelo, K. Kinoshita, T. Honjo, A. Fischer, and A. Durandy. 2000. Activation-induced cytidine deaminase (AID) deficiency causes the autosomal recessive form of the Hyper-IgM syndrome (HIGM2). *Cell* 102: 565-575.

143. Vinuesa, C. G., I. Sanz, and M. C. Cook. 2009. Dysregulation of germinal centres in autoimmune disease. *Nature Reviews Immunology* 9: 845-857.

144. Kosco-Vilbois, M. H. 2003. Are follicular dendritic cells really good for nothing? *Nat. Rev. Immunol.* 3: 764-769.

145. Qin, D., J. Wu, M. C. Carroll, G. F. Burton, A. K. Szakal, and J. G. Tew. 1998. Evidence for an important interaction between a complement-derived CD21 ligand on follicular dendritic cells and CD21 on B cells in the initiation of IgG responses. *J. Immunol.* 161: 4549-4554.

146. Liu, Y. J., D. E. Joshua, G. T. Williams, C. A. Smith, J. Gordon, and I. C. MacLennan. 1989. Mechanism of antigen-driven selection in germinal centres. *Nature* 342: 929-931.

147. Allen, C. D., T. Okada, H. L. Tang, and J. G. Cyster. 2007. Imaging of germinal center selection events during affinity maturation. *Science* 315: 528-531.

148. Hargreaves, D. C., P. L. Hyman, T. T. Lu, V. N. Ngo, A. Bidgol, G. Suzuki, Y. R. Zou, D. R. Littman, and J. G. Cyster. 2001. A coordinated change in chemokine responsiveness guides plasma cell movements. *J. Exp. Med.* 194: 45-56.

149. Garcia, D., V, A. Gulbranson-Judge, M. Khan, P. O'Leary, M. Cascalho, M. Wabl, G. G. Klaus, M. J. Owen, and I. C. MacLennan. 1999. Dendritic cells associated with plasmablast survival. *Eur. J. Immunol.* 29: 3712-3721.

150. Odegard, J. M., B. R. Marks, L. D. DiPlacido, A. C. Poholek, D. H. Kono, C. Dong, R. A. Flavell, and J. Craft. 2008. ICOS-dependent extrafollicular helper T cells elicit IgG production via IL-21 in systemic autoimmunity. *J. Exp. Med.* 205: 2873-2886.

151. Ho, F., J. E. Lortan, I. C. MacLennan, and M. Khan. 1986. Distinct short-lived and long-lived antibody-producing cell populations. *Eur. J. Immunol.* 16: 1297-1301.

152. Matsumoto, M., S. F. Lo, C. J. Carruthers, J. Min, S. Mariathasan, G. Huang, D. R. Plas, S. M. Martin, R. S. Geha, M. H. Nahm, and D. D. Chaplin. 1996. Affinity maturation without germinal centres in lymphotoxin-alpha-deficient mice. *Nature* 382: 462-466.

153. Wang, Y., G. Huang, J. Wang, H. Molina, D. D. Chaplin, and Y. X. Fu. 2000. Antigen persistence is required for somatic mutation and affinity maturation of immunoglobulin. *Eur. J. Immunol.* 30: 2226-2234.

154. Manz, R. A., A. Thiel, and A. Radbruch. 1997. Lifetime of plasma cells in the bone marrow. *Nature* 388: 133-134.

155. Sze, D. M., K. M. Toellner, D. Garcia, V, D. R. Taylor, and I. C. MacLennan. 2000. Intrinsic constraint on plasmablast growth and extrinsic limits of plasma cell survival. *J. Exp. Med.* 192: 813-821.

156. Bowman, E. P., N. A. Kuklin, K. R. Youngman, N. H. Lazarus, E. J. Kunkel, J. Pan, H. B. Greenberg, and E. C. Butcher. 2002. The intestinal chemokine thymus-expressed chemokine (CCL25) attracts IgA antibody-secreting cells. *J. Exp. Med.* 195: 269-275.

157. Fikrig, E., S. W. Barthold, M. Chen, I. S. Grewal, J. Craft, and R. A. Flavell. 1996. Protective antibodies in murine Lyme disease arise independently of CD40 ligand. *J. Immunol.* 157: 1-3.

158. de Vinuesa, C. G., M. C. Cook, J. Ball, M. Drew, Y. Sunners, M. Cascalho, M. Wabl, G. G. Klaus, and I. C. MacLennan. 2000. Germinal centers without T cells. *J. Exp. Med.* 191: 485-494.

159. Song, H., and J. Cerny. 2003. Functional heterogeneity of marginal zone B cells revealed by their ability to generate both early antibody-forming cells and germinal centers with hypermutation and memory in response to a T-dependent antigen. *J. Exp. Med.* 198: 1923-1935.

160. Montecino-Rodriguez, E., and K. Dorshkind. 2006. New perspectives in B-1 B cell development and function. *Trends Immunol.* 27: 428-433.

161. Bos, N. A., H. Kimura, C. G. Meeuwsen, H. De Visser, M. P. Hazenberg, B. S. Wostmann, J. R. Pleasants, R. Benner, and D. M. Marcus. 1989. Serum immunoglobulin levels and naturally occurring antibodies against carbohydrate antigens in germ-free BALB/c mice fed chemically defined ultrafiltered diet. *Eur. J. Immunol.* 19: 2335-2339.

162. Engel, P., L. J. Zhou, D. C. Ord, S. Sato, B. Koller, and T. F. Tedder. 1995. Abnormal B lymphocyte development, activation, and differentiation in mice that lack or overexpress the CD19 signal transduction molecule. *Immunity.* 3: 39-50.

163. Masmoudi, H., T. Mota-Santos, F. Huetz, A. Coutinho, and P. A. Cazenave. 1990. All T15 Id-positive antibodies (but not the majority of VHT15+ antibodies) are produced by peritoneal CD5+ B lymphocytes. *Int. Immunol.* 2: 515-520.

164. Kroese, F. G., E. C. Butcher, A. M. Stall, P. A. Lalor, S. Adams, and L. A. Herzenberg. 1989. Many of the IgA producing plasma cells in murine gut are derived from self-replenishing precursors in the peritoneal cavity. *Int. Immunol.* 1: 75-84.

165. Garcia, D., V, P. O'Leary, D. M. Sze, K. M. Toellner, and I. C. MacLennan. 1999. T-independent type 2 antigens induce B cell proliferation in multiple splenic sites, but exponential growth is confined to extrafollicular foci. *Eur. J. Immunol.* 29: 1314-1323.

166. Kruschinski, C., M. Zidan, A. S. Debertin, S. von Horsten, and R. Pabst. 2004. Age-dependent development of the splenic marginal zone in human infants is associated with different causes of death. *Hum. Pathol.* 35: 113-121.

167. Alugupalli, K. R., R. M. Gerstein, J. Chen, E. Szomolanyi-Tsuda, R. T. Woodland, and J. M. Leong. 2003. The resolution of relapsing fever borreliosis requires IgM and is concurrent with expansion of B1b lymphocytes. *J. Immunol.* 170: 3819-3827.

168. Pillai, S., A. Cariappa, and S. T. Moran. 2005. Marginal zone B cells. *Annu. Rev. Immunol.* 23: 161-196.

169. Martin, F., A. M. Oliver, and J. F. Kearney. 2001. Marginal zone and B1 B cells unite in the early response against T-independent blood-borne particulate antigens. *Immunity.* 14: 617-629.

170. Hsu, M. C., K. M. Toellner, C. G. Vinuesa, and I. C. MacLennan. 2006. B cell clones that sustain long-term plasmablast growth in T-independent extrafollicular antibody responses. *Proc. Natl. Acad. Sci. U. S. A* 103: 5905-5910.

171. Newman, P. J. 1999. Switched at birth: a new family for PECAM-1. *J. Clin. Invest* 103: 5-9.

172. Pritchard, N. R., and K. G. Smith. 2003. B cell inhibitory receptors and autoimmunity. *Immunology* 108: 263-273.

173. Otipoby, K. L., K. B. Andersson, K. E. Draves, S. J. Klaus, A. G. Farr, J. D. Kerner, R. M. Perlmutter, C. L. Law, and E. A. Clark. 1996. CD22 regulates thymus-independent responses and the lifespan of B cells. *Nature* 384: 634-637.

174. Ujike, A., K. Takeda, A. Nakamura, S. Ebihara, K. Akiyama, and T. Takai. 2002. Impaired dendritic cell maturation and increased T(H)2 responses in PIR-B(-/-) mice. *Nat. Immunol.* 3: 542-548.

175. Bolland, S., and J. V. Ravetch. 2000. Spontaneous autoimmune disease in Fc(gamma)RIIB-deficient mice results from strain-specific epistasis. *Immunity.* 13: 277-285.

176. Graesser, D., A. Solowiej, M. Bruckner, E. Osterweil, A. Juedes, S. Davis, N. H. Ruddle, B. Engelhardt, and J. A. Madri. 2002. Altered vascular permeability and early onset of experimental autoimmune encephalomyelitis in PECAM-1-deficient mice. *J. Clin. Invest* 109: 383-392.

177. Wong, M. X., J. D. Hayball, P. M. Hogarth, and D. E. Jackson. 2005. The inhibitory co-receptor, PECAM-1 provides a protective effect in suppression of collagen-induced arthritis. *J. Clin. Immunol.* 25: 19-28.

178. Newman, P. J., M. C. Berndt, J. Gorski, G. C. White, S. Lyman, C. Paddock, and W. A. Muller. 1990. PECAM-1 (CD31) cloning and relation to adhesion molecules of the immunoglobulin gene superfamily. *Science* 247: 1219-1222.

179. Simmons, D. L., C. Walker, C. Power, and R. Pigott. 1990. Molecular cloning of CD31, a putative intercellular adhesion molecule closely related to carcinoembryonic antigen. *J. Exp. Med.* 171: 2147-2152.

180. Stockinger, H., S. J. Gadd, R. Eher, O. Majdic, W. Schreiber, W. Kasinrerk, B. Strass, E. Schnabl, and W. Knapp. 1990. Molecular characterization and functional analysis of the leukocyte surface protein CD31. *J. Immunol.* 145: 3889-3897.

181. Jackson, D. E., C. M. Ward, R. Wang, and P. J. Newman. 1997. The protein-tyrosine phosphatase SHP-2 binds platelet/endothelial cell adhesion molecule-1

(PECAM-1) and forms a distinct signaling complex during platelet aggregation. Evidence for a mechanistic link between PECAM-1- and integrin-mediated cellular signaling. *J. Biol. Chem.* 272: 6986-6993.

182. Lu, T. T., M. Barreuther, S. Davis, and J. A. Madri. 1997. Platelet endothelial cell adhesion molecule-1 is phosphorylatable by c-Src, binds Src-Src homology 2 domain, and exhibits immunoreceptor tyrosine-based activation motif-like properties. *J. Biol. Chem.* 272: 14442-14446.

183. DeLisser, H. M., M. Christofidou-Solomidou, R. M. Strieter, M. D. Burdick, C. S. Robinson, R. S. Wexler, J. S. Kerr, C. Garlanda, J. R. Merwin, J. A. Madri, and S. M. Albelda. 1997. Involvement of endothelial PECAM-1/CD31 in angiogenesis. *Am. J. Pathol.* 151: 671-677.

184. Duncan, G. S., D. P. Andrew, H. Takimoto, S. A. Kaufman, H. Yoshida, J. Spellberg, d. l. P. Luis, A. Elia, A. Wakeham, B. Karan-Tamir, W. A. Muller, G. Senaldi, M. M. Zukowski, and T. W. Mak. 1999. Genetic evidence for functional redundancy of Platelet/Endothelial cell adhesion molecule-1 (PECAM-1): CD31-deficient mice reveal PECAM-1-dependent and PECAM-1-independent functions. *J. Immunol.* 162: 3022-3030.

185. Muller, W. A., S. A. Weigl, X. Deng, and D. M. Phillips. 1993. PECAM-1 is required for transendothelial migration of leukocytes. *J. Exp. Med.* 178: 449-460.

186. Thompson, R. D., K. E. Noble, K. Y. Larbi, A. Dewar, G. S. Duncan, T. W. Mak, and S. Nourshargh. 2001. Platelet-endothelial cell adhesion molecule-1 (PECAM-1)-deficient mice demonstrate a transient and cytokine-specific role for PECAM-1 in leukocyte migration through the perivascular basement membrane. *Blood* 97: 1854-1860.

187. Dasgupta, B., E. Dufour, Z. Mamdouh, and W. A. Muller. 2009. A novel and critical role for tyrosine 663 in platelet endothelial cell adhesion molecule-1 trafficking and transendothelial migration. *J. Immunol.* 182: 5041-5051.

188. Bogen, S., J. Pak, M. Garifallou, X. Deng, and W. A. Muller. 1994. Monoclonal antibody to murine PECAM-1 (CD31) blocks acute inflammation in vivo. *J. Exp. Med.* 179: 1059-1064.

189. Dhanjal, T. S., C. Pendaries, E. A. Ross, M. K. Larson, M. B. Protty, C. D. Buckley, and S. P. Watson. 2007. A novel role for PECAM-1 in megakaryocytokinesis and recovery of platelet counts in thrombocytopenic mice. *Blood* 109: 4237-4244.

190. Evans, P. C., E. R. Taylor, and P. J. Kilshaw. 2001. Signaling through CD31 protects endothelial cells from apoptosis. *Transplantation* 71: 457-460.

191. Ferrero, E., D. Belloni, P. Contini, C. Foglieni, M. E. Ferrero, M. Fabbri, A. Poggi, and M. R. Zocchi. 2003. Transendothelial migration leads to protection from

starvation-induced apoptosis in CD34+CD14+ circulating precursors: evidence for PECAM-1 involvement through Akt/PKB activation. *Blood* 101: 186-193.

192. Bergom, C., C. Gao, and P. J. Newman. 2005. Mechanisms of PECAM-1-mediated cytoprotection and implications for cancer cell survival. *Leuk. Lymphoma* 46: 1409-1421.

193. Bergom, C., R. Goel, C. Paddock, C. Gao, D. K. Newman, S. Matsuyama, and P. J. Newman. 2006. The cell-adhesion and signaling molecule PECAM-1 is a molecular mediator of resistance to genotoxic chemotherapy. *Cancer Biol. Ther.* 5: 1699-1707.

194. Tanaka, Y., S. M. Albelda, K. J. Horgan, G. A. Vanseventer, Y. Shimizu, W. Newman, J. Hallam, P. J. Newman, C. A. Buck, and S. Shaw. 1992. Cd31 Expressed on Distinctive T-Cell Subsets Is A Preferential Amplifier of Beta-1 Integrin-Mediated Adhesion. *Journal of Experimental Medicine* 176: 245-253.

195. Reedquist, K. A., E. Ross, E. A. Koop, R. M. Wolthuis, F. J. Zwartkruis, Y. van Kooyk, M. Salmon, C. D. Buckley, and J. L. Bos. 2000. The small GTPase, Rap1, mediates CD31-induced integrin adhesion. *J. Cell Biol.* 148: 1151-1158.

196. Gao, C., W. Sun, M. Christofidou-Solomidou, M. Sawada, D. K. Newman, C. Bergom, S. M. Albelda, S. Matsuyama, and P. J. Newman. 2003. PECAM-1 functions as a specific and potent inhibitor of mitochondrial-dependent apoptosis. *Blood* 102: 169-179.

197. Ma, L., C. Mauro, G. H. Cornish, J. G. Chai, D. Coe, H. Fu, D. Patton, K. Okkenhaug, G. Franzoso, J. Dyson, S. Nourshargh, and F. M. Marelli-Berg. 2010. Ig gene-like molecule CD31 plays a nonredundant role in the regulation of T-cell immunity and tolerance. *Proc. Natl. Acad. Sci. U. S. A* 107: 19461-19466.

198. Newton-Nash, D. K., and P. J. Newman. 1999. A new role for platelet-endothelial cell adhesion molecule-1 (CD31): inhibition of TCR-mediated signal transduction. *J. Immunol.* 163: 682-688.

199. Henshall, T. L., K. L. Jones, R. Wilkinson, and D. E. Jackson. 2001. Src homology 2 domain-containing protein-tyrosine phosphatases, SHP-1 and SHP-2, are required for platelet endothelial cell adhesion molecule-1/CD31-mediated inhibitory signaling. *J. Immunol.* 166: 3098-3106.

200. Wong, M. X., D. Roberts, P. A. Bartley, and D. E. Jackson. 2002. Absence of platelet endothelial cell adhesion molecule-1 (CD31) leads to increased severity of local and systemic IgE-mediated anaphylaxis and modulation of mast cell activation. *J. Immunol.* 168: 6455-6462.

201. Maas, M., M. Stapleton, C. Bergom, D. L. Mattson, D. K. Newman, and P. J. Newman. 2005. Endothelial cell PECAM-1 confers protection against endotoxic shock. *Am. J. Physiol Heart Circ. Physiol* 288: H159-H164.

202. Wilkinson, R., A. B. Lyons, D. Roberts, M. X. Wong, P. A. Bartley, and D. E. Jackson. 2002. Platelet endothelial cell adhesion molecule-1 (PECAM-1/CD31) acts as a regulator of B-cell development, B-cell antigen receptor (BCR)-mediated activation, and autoimmune disease. *Blood* 100: 184-193.

203. Ross, E. A., R. E. Coughlan, A. Flores-Langarica, S. Bobat, J. L. Marshall, K. Hussain, J. Charlesworth, N. Abhyankar, J. Hitchcock, C. Gil, C. Lopez-Macias, I. R. Henderson, M. Khan, S. P. Watson, I. C. MacLennan, C. D. Buckley, and A. F. Cunningham. 2011. CD31 Is Required on CD4+ T Cells To Promote T Cell Survival during Salmonella Infection. *J. Immunol.*

204. Moon, J. J., and S. J. McSorley. 2009. Tracking the dynamics of salmonella specific T cell responses. *Curr. Top. Microbiol. Immunol.* 334: 179-198.

205. Mastroeni, P., and M. Sheppard. 2004. Salmonella infections in the mouse model: host resistance factors and in vivo dynamics of bacterial spread and distribution in the tissues. *Microbes. Infect.* 6: 398-405.

206. Mastroeni, P., and N. Menager. 2003. Development of acquired immunity to Salmonella. *J. Med. Microbiol.* 52: 453-459.

207. Mastroeni, P. 2002. Immunity to systemic Salmonella infections. *Curr. Mol. Med.* 2: 393-406.

208. Jones, B. D., N. Ghori, and S. Falkow. 1994. Salmonella typhimurium initiates murine infection by penetrating and destroying the specialized epithelial M cells of the Peyer's patches. *J. Exp. Med.* 180: 15-23.

209. Rescigno, M., M. Urbano, B. Valzasina, M. Francolini, G. Rotta, R. Bonasio, F. Granucci, J. P. Kraehenbuhl, and P. Ricciardi-Castagnoli. 2001. Dendritic cells express tight junction proteins and penetrate gut epithelial monolayers to sample bacteria. *Nat. Immunol.* 2: 361-367.

210. Gewirtz, A. T., P. O. Simon, Jr., C. K. Schmitt, L. J. Taylor, C. H. Hagedorn, A. D. O'Brien, A. S. Neish, and J. L. Madara. 2001. Salmonella typhimurium translocates flagellin across intestinal epithelia, inducing a proinflammatory response. *J. Clin. Invest* 107: 99-109.

211. Wick, M. J. 2004. Living in the danger zone: innate immunity to Salmonella. *Curr. Opin. Microbiol.* 7: 51-57.

212. Vidal, S. M., D. Malo, K. Vogan, E. Skamene, and P. Gros. 1993. Natural resistance to infection with intracellular parasites: isolation of a candidate for Bcg. *Cell* 73: 469-485.

213. Vidal, S., P. Gros, and E. Skamene. 1995. Natural resistance to infection with intracellular parasites: molecular genetics identifies Nramp1 as the Bcg/Ity/Lsh locus. *J. Leukoc. Biol.* 58: 382-390.

214. Kirby, A. C., U. Yrlid, and M. J. Wick. 2002. The innate immune response differs in primary and secondary Salmonella infection. *J. Immunol.* 169: 4450-4459.

215. Hess, J., C. Ladel, D. Miko, and S. H. Kaufmann. 1996. Salmonella typhimurium aroA- infection in gene-targeted immunodeficient mice: major role of CD4+ TCR-alpha beta cells and IFN-gamma in bacterial clearance independent of intracellular location. *J. Immunol.* 156: 3321-3326.

216. Gaspal, F., V. Bekiaris, M. Y. Kim, D. R. Withers, S. Bobat, I. C. MacLennan, G. Anderson, P. J. Lane, and A. F. Cunningham. 2008. Critical synergy of CD30 and OX40 signals in CD4 T cell homeostasis and Th1 immunity to Salmonella. *J. Immunol.* 180: 2824-2829.

217. Hess, J., C. Ladel, D. Miko, and S. H. Kaufmann. 1996. Salmonella typhimurium aroA- infection in gene-targeted immunodeficient mice: major role of CD4+ TCR-alpha beta cells and IFN-gamma in bacterial clearance independent of intracellular location. *J. Immunol.* 156: 3321-3326.

218. Cleary, A. M., W. Tu, A. Enright, T. Giffon, R. Dewaal-Malefyt, K. Gutierrez, and D. B. Lewis. 2003. Impaired accumulation and function of memory CD4 T cells in human IL-12 receptor beta 1 deficiency. *J. Immunol.* 170: 597-603.

219. Jouanguy, E., R. Doffinger, S. Dupuis, A. Pallier, F. Altare, and J. L. Casanova. 1999. IL-12 and IFN-gamma in host defense against mycobacteria and salmonella in mice and men. *Curr. Opin. Immunol.* 11: 346-351.

220. McSorley, S. J., and M. K. Jenkins. 2000. Antibody is required for protection against virulent but not attenuated Salmonella enterica serovar typhimurium. *Infect. Immun.* 68: 3344-3348.

221. Mittrucker, H. W., B. Raupach, A. Kohler, and S. H. Kaufmann. 2000. Cutting edge: role of B lymphocytes in protective immunity against Salmonella typhimurium infection. *J. Immunol.* 164: 1648-1652.

222. Guzman, C. A., S. Borsutzky, M. Griot-Wenk, I. C. Metcalfe, J. Pearman, A. Collioud, D. Favre, and G. Dietrich. 2006. Vaccines against typhoid fever. *Vaccine* 24: 3804-3811.

223. Klugman, K. P., H. J. Koornhof, J. B. Robbins, and N. N. Le Cam. 1996. Immunogenicity, efficacy and serological correlate of protection of Salmonella typhi Vi capsular polysaccharide vaccine three years after immunization. *Vaccine* 14: 435-438.

224. Barr, T. A., S. Brown, P. Mastroeni, and D. Gray. 2009. B cell intrinsic MyD88 signals drive IFN-gamma production from T cells and control switching to IgG2c. *J. Immunol.* 183: 1005-1012.

225. MacLennan, C. A., E. N. Gondwe, C. L. Msefula, R. A. Kingsley, N. R. Thomson, S. A. White, M. Goodall, D. J. Pickard, S. M. Graham, G. Dougan, C. A. Hart, M.

E. Molyneux, and M. T. Drayson. 2008. The neglected role of antibody in protection against bacteremia caused by nontyphoidal strains of Salmonella in African children. *J. Clin. Invest* 118: 1553-1562.

226. Mastroeni, P., C. Simmons, R. Fowler, C. E. Hormaeche, and G. Dougan. 2000. Igh-6(-/-) (B-cell-deficient) mice fail to mount solid acquired resistance to oral challenge with virulent Salmonella enterica serovar typhimurium and show impaired Th1 T-cell responses to Salmonella antigens. *Infect. Immun.* 68: 46-53.

227. Mastroeni, P., B. Villarreal-Ramos, and C. E. Hormaeche. 1993. Adoptive transfer of immunity to oral challenge with virulent salmonellae in innately susceptible BALB/c mice requires both immune serum and T cells. *Infect. Immun.* 61: 3981-3984.

228. Barr, T. A., S. Brown, P. Mastroeni, and D. Gray. 2010. TLR and B cell receptor signals to B cells differentially program primary and memory Th1 responses to Salmonella enterica. *J. Immunol.* 185: 2783-2789.

229. Santos, R. L., S. P. Zhang, R. M. Tsolis, R. A. Kingsley, L. G. Adams, and A. J. Baumler. 2001. Animal models of Salmonella infections: enteritis versus typhoid fever. *Microbes and Infection* 3: 1335-1344.

230. O'Callaghan, D., D. Maskell, F. Y. Liew, C. S. Easmon, and G. Dougan. 1988. Characterization of aromatic- and purine-dependent Salmonella typhimurium: attention, persistence, and ability to induce protective immunity in BALB/c mice. *Infect. Immun.* 56: 419-423.

231. Hormaeche, C. E., H. S. Joysey, L. Desilva, M. Izhar, and B. A. Stocker. 1991. Immunity conferred by Aro- Salmonella live vaccines. *Microb. Pathog.* 10: 149-158.

232. Cascalho, M., A. Ma, S. Lee, L. Masat, and M. Wabl. 1996. A quasi-monoclonal mouse. *Science* 272: 1649-1652.

233. Mombaerts, P., A. R. Clarke, M. A. Rudnicki, J. Iacomini, S. Itohara, J. J. Lafaille, L. Wang, Y. Ichikawa, R. Jaenisch, M. L. Hooper, and . 1992. Mutations in T-cell antigen receptor genes alpha and beta block thymocyte development at different stages. *Nature* 360: 225-231.

234. Kopf, M., H. Baumann, G. Freer, M. Freudenberg, M. Lamers, T. Kishimoto, R. Zinkernagel, H. Bluethmann, and G. Kohler. 1994. Impaired immune and acute-phase responses in interleukin-6-deficient mice. *Nature* 368: 339-342.

235. Kuhn, R., K. Rajewsky, and W. Muller. 1991. Generation and analysis of interleukin-4 deficient mice. *Science* 254: 707-710.

236. McSorley, S. J., S. Asch, M. Costalonga, R. L. Reinhardt, and M. K. Jenkins. 2002. Tracking salmonella-specific CD4 T cells in vivo reveals a local mucosal response to a disseminated infection. *Immunity.* 16: 365-377.

237. Soriano, P. 1999. Generalized lacZ expression with the ROSA26 Cre reporter strain. *Nat. Genet.* 21: 70-71.

238. Hoiseth, S. K., and B. A. Stocker. 1981. Aromatic-dependent Salmonella typhimurium are non-virulent and effective as live vaccines. *Nature* 291: 238-239.

239. Cunningham, A. F., M. Khan, J. Ball, K. M. Toellner, K. Serre, E. Mohr, and I. C. MacLennan. 2004. Responses to the soluble flagellar protein FliC are Th2, while those to FliC on Salmonella are Th1. *Eur. J. Immunol.* 34: 2986-2995.

240. Nossal, G. J., and M. Karvelas. 1990. Soluble antigen abrogates the appearance of anti-protein IgG1-forming cell precursors during primary immunization. *Proc. Natl. Acad. Sci. U. S. A* 87: 1615-1619.

241. Fillatreau, S., C. H. Sweenie, M. J. McGeachy, D. Gray, and S. M. Anderton. 2002. B cells regulate autoimmunity by provision of IL-10. *Nat. Immunol.* 3: 944-950.

242. Maas, H. J., and F. W. Orthel. 1976. Histo-morphometric analysis applied to spleens of Marek's disease virus inoculated chickens. *Avian Pathol.* 5: 195-200.

243. Flores-Langarica, A., J. L. Marshall, S. Bobat, E. Mohr, J. Hitchcock, E. A. Ross, R. E. Coughlan, M. Khan, N. Van Rooijen, I. R. Henderson, I. C. MacLennan, and A. F. Cunningham. 2011. T Zone Localized Monocyte-Derived Dendritic Cells Promote Th1 Priming to Salmonella. *Eur. J. Immunol.*

244. Henderson, I. R., M. Meehan, and P. Owen. 1997. Antigen 43, a phase-variable bipartite outer membrane protein, determines colony morphology and autoaggregation in Escherichia coli K-12. *FEMS Microbiol. Lett.* 149: 115-120.

245. Wong, M. X., J. D. Hayball, and D. E. Jackson. 2008. PECAM-1-regulated signalling thresholds control tolerance in anergic transgenic B-cells. *Mol. Immunol.* 45: 1767-1781.

246. Watt, S. M., J. Williamson, H. Genevier, J. Fawcett, D. L. Simmons, A. Hatzfeld, S. A. Nesbitt, and D. R. Coombe. 1993. The heparin binding PECAM-1 adhesion molecule is expressed by CD34+ hematopoietic precursor cells with early myeloid and B-lymphoid cell phenotypes. *Blood* 82: 2649-2663.

247. Newman, D. K., C. Hamilton, and P. J. Newman. 2001. Inhibition of antigen-receptor signaling by platelet endothelial cell adhesion molecule-1 (CD31) requires functional ITIMs, SHP-2, and p56(lck). *Blood* 97: 2351-2357.

248. Wong, M. X., and D. E. Jackson. 2004. Regulation of B cell activation by PECAM-1: implications for the development of autoimmune disorders. *Curr. Pharm. Des* 10: 155-161.

249. O'Brien, C. D., G. Cao, A. Makrigiannakis, and H. M. DeLisser. 2004. Role of immunoreceptor tyrosine-based inhibitory motifs of PECAM-1 in PECAM-1-dependent cell migration. *Am. J. Physiol Cell Physiol* 287: C1103-C1113.

250. Pillai, S., A. Cariappa, and S. T. Moran. 2005. Marginal zone B cells. *Annu. Rev. Immunol.* 23: 161-196.

251. Eisenberg, R. A., S. Y. Craven, R. W. Warren, and P. L. Cohen. 1987. Stochastic control of anti-Sm autoantibodies in MRL/Mp-lpr/lpr mice. *J. Clin. Invest* 80: 691-697.

252. Robosky, L. C., D. F. Wells, L. A. Egnash, M. L. Manning, M. D. Reily, and D. G. Robertson. 2005. Metabonomic identification of two distinct phenotypes in Sprague-Dawley (Crl:CD(SD)) rats. *Toxicol. Sci.* 87: 277-284.

253. Rohde, C. M., D. F. Wells, L. C. Robosky, M. L. Manning, C. B. Clifford, M. D. Reily, and D. G. Robertson. 2007. Metabonomic evaluation of Schaedler altered microflora rats. *Chem. Res. Toxicol.* 20: 1388-1392.

254. Holmes, E., and J. Nicholson. 2005. Variation in gut microbiota strongly influences individual rodent phenotypes. *Toxicol. Sci.* 87: 1-2.

255. Gerlai, R. 2001. Gene targeting: technical confounds and potential solutions in behavioral brain research. *Behav. Brain Res.* 125: 13-21.

256. Seong, E., T. L. Saunders, C. L. Stewart, and M. Burmeister. 2004. To knockout in 129 or in C57BL/6: that is the question. *Trends Genet.* 20: 59-62.

257. Hospital, F. 2001. Size of donor chromosome segments around introgressed loci and reduction of linkage drag in marker-assisted backcross programs. *Genetics* 158: 1363-1379.

258. Serre, K., E. Mohr, K. M. Toellner, A. F. Cunningham, S. Granjeaud, R. Bird, and I. C. MacLennan. 2008. Molecular differences between the divergent responses of ovalbumin-specific CD4 T cells to alum-precipitated ovalbumin compared to ovalbumin expressed by Salmonella. *Mol. Immunol.* 45: 3558-3566.

259. Fazilleau, N., M. D. Eisenbraun, L. Malherbe, J. N. Ebright, R. R. Pogue-Caley, L. J. McHeyzer-Williams, and M. G. McHeyzer-Williams. 2007. Lymphoid reservoirs of antigen-specific memory T helper cells. *Nat. Immunol.* 8: 753-761.

260. King, I. L., and M. Mohrs. 2009. IL-4-producing CD4+ T cells in reactive lymph nodes during helminth infection are T follicular helper cells. *J. Exp. Med.* 206: 1001-1007.

261. Vogelzang, A., H. M. McGuire, D. Yu, J. Sprent, C. R. Mackay, and C. King. 2008. A fundamental role for interleukin-21 in the generation of T follicular helper cells. *Immunity.* 29: 127-137.

262. Ramsay, A. J., A. J. Husband, I. A. Ramshaw, S. Bao, K. I. Matthaei, G. Koehler, and M. Kopf. 1994. The role of interleukin-6 in mucosal IgA antibody responses in vivo. *Science* 264: 561-563.

263. Bromander, A. K., L. Ekman, M. Kopf, J. G. Nedrud, and N. Y. Lycke. 1996. IL-6-deficient mice exhibit normal mucosal IgA responses to local immunizations and Helicobacter felis infection. *J. Immunol.* 156: 4290-4297.

264. Everest, P., J. Allen, A. Papakonstantinopoulou, P. Mastroeni, M. Roberts, and G. Dougan. 1997. Salmonella typhimurium infections in mice deficient in interleukin-4 production: role of IL-4 in infection-associated pathology. *J. Immunol.* 159: 1820-1827.

265. Hirano, T., K. Yasukawa, H. Harada, T. Taga, Y. Watanabe, T. Matsuda, S. Kashiwamura, K. Nakajima, K. Koyama, A. Iwamatsu, and . 1986. Complementary DNA for a novel human interleukin (BSF-2) that induces B lymphocytes to produce immunoglobulin. *Nature* 324: 73-76.

266. Jego, G., R. Bataille, and C. Pellat-Deceunynck. 2001. Interleukin-6 is a growth factor for nonmalignant human plasmablasts. *Blood* 97: 1817-1822.

267. Dienz, O., S. M. Eaton, J. P. Bond, W. Neveu, D. Moquin, R. Noubade, E. M. Briso, C. Charland, W. J. Leonard, G. Ciliberto, C. Teuscher, L. Haynes, and M. Rincon. 2009. The induction of antibody production by IL-6 is indirectly mediated by IL-21 produced by CD4+ T cells. *J. Exp. Med.* 206: 69-78.

268. Romani, L., A. Mencacci, E. Cenci, R. Spaccapelo, C. Toniatti, P. Puccetti, F. Bistoni, and V. Poli. 1996. Impaired neutrophil response and CD4+ T helper cell 1 development in interleukin 6-deficient mice infected with Candida albicans. *J. Exp. Med.* 183: 1345-1355.

269. Eckmann, L., and M. F. Kagnoff. 2001. Cytokines in host defense against Salmonella. *Microbes. Infect.* 3: 1191-1200.

270. Heyman, B., E. J. Wiersma, and T. Kinoshita. 1990. In vivo inhibition of the antibody response by a complement receptor-specific monoclonal antibody. *J. Exp. Med.* 172: 665-668.

271. Mohr, E., K. Serre, R. A. Manz, A. F. Cunningham, M. Khan, D. L. Hardie, R. Bird, and I. C. MacLennan. 2009. Dendritic cells and monocyte/macrophages that create the IL-6/APRIL-rich lymph node microenvironments where plasmablasts mature. *J. Immunol.* 182: 2113-2123.

272. Jabara, H., D. Laouini, E. Tsitsikov, E. Mizoguchi, A. Bhan, E. Castigli, F. Dedeoglu, V. Pivniouk, S. Brodeur, and R. Geha. 2002. The binding site for TRAF2 and TRAF3 but not for TRAF6 is essential for CD40-mediated immunoglobulin class switching. *Immunity.* 17: 265-276.

273. Schrader, C. E., E. K. Linehan, S. N. Mochegova, R. T. Woodland, and J. Stavnezer. 2005. Inducible DNA breaks in Ig S regions are dependent on AID and UNG. *J. Exp. Med.* 202: 561-568.

274. Xu, J., T. M. Foy, J. D. Laman, E. A. Elliott, J. J. Dunn, T. J. Waldschmidt, J. Elsemore, R. J. Noelle, and R. A. Flavell. 1994. Mice deficient for the CD40 ligand. *Immunity.* 1: 423-431.

275. Walker, L. S., A. Gulbranson-Judge, S. Flynn, T. Brocker, C. Raykundalia, M. Goodall, R. Forster, M. Lipp, and P. Lane. 1999. Compromised OX40 function in CD28-deficient mice is linked with failure to develop CXC chemokine receptor 5-positive CD4 cells and germinal centers. *J. Exp. Med.* 190: 1115-1122.

276. Dienz, O., and M. Rincon. 2009. The effects of IL-6 on CD4 T cell responses. *Clin. Immunol.* 130: 27-33.

277. Van Snick, J., S. Cayphas, A. Vink, C. Uyttenhove, P. G. Coulie, M. R. Rubira, and R. J. Simpson. 1986. Purification and NH2-terminal amino acid sequence of a T-cell-derived lymphokine with growth factor activity for B-cell hybridomas. *Proc. Natl. Acad. Sci. U. S. A* 83: 9679-9683.

278. Burdin, N., L. Galibert, P. Garrone, I. Durand, J. Banchereau, and F. Rousset. 1996. Inability to produce IL-6 is a functional feature of human germinal center B lymphocytes. *J. Immunol.* 156: 4107-4113.

279. Corbel, C., and F. Melchers. 1984. The synergism of accessory cells and of soluble alpha-factors derived from them in the activation of B cells to proliferation. *Immunol. Rev.* 78: 51-74.

280. Adams, E. F., B. Rafferty, and M. C. White. 1991. Interleukin 6 is secreted by breast fibroblasts and stimulates 17 beta-oestradiol oxidoreductase activity of MCF-7 cells: possible paracrine regulation of breast 17 beta-oestradiol levels. *Int. J. Cancer* 49: 118-121.

281. Heinrich, P. C., I. Behrmann, S. Haan, H. M. Hermanns, G. Muller-Newen, and F. Schaper. 2003. Principles of interleukin (IL)-6-type cytokine signalling and its regulation. *Biochem. J.* 374: 1-20.

282. Arai, T., K. Hiromatsu, H. Nishimura, Y. Kimura, N. Kobayashi, H. Ishida, Y. Nimura, and Y. Yoshikai. 1995. Effects of in vivo administration of anti-IL-10 monoclonal antibody on the host defence mechanism against murine Salmonella infection. *Immunology* 85: 381-388.

283. Sullivan, B. M., O. Jobe, V. Lazarevic, K. Vasquez, R. Bronson, L. H. Glimcher, and I. Kramnik. 2005. Increased susceptibility of mice lacking T-bet to infection with Mycobacterium tuberculosis correlates with increased IL-10 and decreased IFN-gamma production. *J. Immunol.* 175: 4593-4602.

284. Lord, G. M., R. M. Rao, H. Choe, B. M. Sullivan, A. H. Lichtman, F. W. Luscinskas, and L. H. Glimcher. 2005. T-bet is required for optimal proinflammatory CD4+ T-cell trafficking. *Blood* 106: 3432-3439.

285. Koch, M. A., G. Tucker-Heard, N. R. Perdue, J. R. Killebrew, K. B. Urdahl, and D. J. Campbell. 2009. The transcription factor T-bet controls regulatory T cell homeostasis and function during type 1 inflammation. *Nat. Immunol.* 10: 595-602.

286. Alcaide, P., T. G. Jones, G. M. Lord, L. H. Glimcher, J. Hallgren, Y. Arinobu, K. Akashi, A. M. Paterson, M. A. Gurish, and F. W. Luscinskas. 2007. Dendritic cell expression of the transcription factor T-bet regulates mast cell progenitor homing to mucosal tissue. *J. Exp. Med.* 204: 431-439.

287. Taqueti, V. R., N. Grabie, R. Colvin, H. Pang, P. Jarolim, A. D. Luster, L. H. Glimcher, and A. H. Lichtman. 2006. T-bet controls pathogenicity of CTLs in the heart by separable effects on migration and effector activity. *J. Immunol.* 177: 5890-5901.

288. Lugo-Villarino, G., S. Ito, D. M. Klinman, and L. H. Glimcher. 2005. The adjuvant activity of CpG DNA requires T-bet expression in dendritic cells. *Proc. Natl. Acad. Sci. U. S. A* 102: 13248-13253.

289. Sullivan, B. M., A. Juedes, S. J. Szabo, M. von Herrath, and L. H. Glimcher. 2003. Antigen-driven effector CD8 T cell function regulated by T-bet. *Proc. Natl. Acad. Sci. U. S. A* 100: 15818-15823.

290. Townsend, M. J., A. S. Weinmann, J. L. Matsuda, R. Salomon, P. J. Farnham, C. A. Biron, L. Gapin, and L. H. Glimcher. 2004. T-bet regulates the terminal maturation and homeostasis of NK and Valpha14i NKT cells. *Immunity.* 20: 477-494.

291. Gerth, A. J., L. Lin, and S. L. Peng. 2003. T-bet regulates T-independent IgG2a class switching. *Int. Immunol.* 15: 937-944.

292. Mohr, E., A. F. Cunningham, K. M. Toellner, S. Bobat, R. E. Coughlan, R. A. Bird, I. C. MacLennan, and K. Serre. 2010. IFN-{gamma} produced by CD8 T cells induces T-bet-dependent and -independent class switching in B cells in responses to alum-precipitated protein vaccine. *Proc. Natl. Acad. Sci. U. S. A* 107: 17292-17297.

293. Liu, N., N. Ohnishi, L. Ni, S. Akira, and K. B. Bacon. 2003. CpG directly induces T-bet expression and inhibits IgG1 and IgE switching in B cells. *Nat. Immunol.* 4: 687-693.

294. Lin, L., A. J. Gerth, and S. L. Peng. 2004. CpG DNA redirects class-switching towards "Th1-like" Ig isotype production via TLR9 and MyD88. *Eur. J. Immunol.* 34: 1483-1487.

295. Fazilleau, N., L. J. McHeyzer-Williams, H. Rosen, and M. G. McHeyzer-Williams. 2009. The function of follicular helper T cells is regulated by the strength of T cell antigen receptor binding. *Nat. Immunol.* 10: 375-384.

296. Seo, G. Y., S. R. Park, and P. H. Kim. 2009. Analyses of TGF-beta1-inducible Ig germ-line gamma2b promoter activity: involvement of Smads and NF-kappaB. *Eur. J. Immunol.* 39: 1157-1166.

297. Huss, D. J., R. C. Winger, G. M. Cox, M. Guerau-de-Arellano, Y. Yang, M. K. Racke, and A. E. Lovett-Racke. 2011. TGF-beta signaling via smad4 drives IL-10 production in effector Th1 cells and reduces T cell trafficking in EAE. *Eur. J. Immunol.*

298. Morrison, V. L., T. A. Barr, S. Brown, and D. Gray. 2010. TLR-mediated loss of CD62L focuses B cell traffic to the spleen during Salmonella typhimurium infection. *J. Immunol.* 185: 2737-2746.

299. Wang, Z. E., S. L. Reiner, S. Zheng, D. K. Dalton, and R. M. Locksley. 1994. CD4+ effector cells default to the Th2 pathway in interferon gamma-deficient mice infected with Leishmania major. *J. Exp. Med.* 179: 1367-1371.

300. Wang, J., J. W. Fathman, G. Lugo-Villarino, L. Scimone, U. von Andrian, D. M. Dorfman, and L. H. Glimcher. 2006. Transcription factor T-bet regulates inflammatory arthritis through its function in dendritic cells. *J. Clin. Invest* 116: 414-421.

301. Marrack, P., A. S. McKee, and M. W. Munks. 2009. Towards an understanding of the adjuvant action of aluminium. *Nat. Rev. Immunol.* 9: 287-293.

302. Gavin, A. L., K. Hoebe, B. Duong, T. Ota, C. Martin, B. Beutler, and D. Nemazee. 2006. Adjuvant-enhanced antibody responses in the absence of toll-like receptor signaling. *Science* 314: 1936-1938.

303. Schnare, M., G. M. Barton, A. C. Holt, K. Takeda, S. Akira, and R. Medzhitov. 2001. Toll-like receptors control activation of adaptive immune responses. *Nat. Immunol.* 2: 947-950.

304. Eisenbarth, S. C., O. R. Colegio, W. O'Connor, F. S. Sutterwala, and R. A. Flavell. 2008. Crucial role for the Nalp3 inflammasome in the immunostimulatory properties of aluminium adjuvants. *Nature* 453: 1122-1126.

305. Franchi, L., A. Amer, M. Body-Malapel, T. D. Kanneganti, N. Ozoren, R. Jagirdar, N. Inohara, P. Vandenabeele, J. Bertin, A. Coyle, E. P. Grant, and G. Nunez. 2006. Cytosolic flagellin requires Ipaf for activation of caspase-1 and interleukin 1beta in salmonella-infected macrophages. *Nat. Immunol.* 7: 576-582.

306. Hayashi, F., K. D. Smith, A. Ozinsky, T. R. Hawn, E. C. Yi, D. R. Goodlett, J. K. Eng, S. Akira, D. M. Underhill, and A. Aderem. 2001. The innate immune response to bacterial flagellin is mediated by Toll-like receptor 5. *Nature* 410: 1099-1103.

307. Sanders, C. J., L. Franchi, F. Yarovinsky, S. Uematsu, S. Akira, G. Nunez, and A. T. Gewirtz. 2009. Induction of adaptive immunity by flagellin does not require robust activation of innate immunity. *Eur. J. Immunol.* 39: 359-371.

308. Zaretsky, A. G., J. J. Taylor, I. L. King, F. A. Marshall, M. Mohrs, and E. J. Pearce. 2009. T follicular helper cells differentiate from Th2 cells in response to helminth antigens. *J. Exp. Med.* 206: 991-999.

309. Yang, Y., J. Ochando, A. Yopp, J. S. Bromberg, and Y. Ding. 2005. IL-6 plays a unique role in initiating c-Maf expression during early stage of CD4 T cell activation. *J. Immunol.* 174: 2720-2729.